SQUAMISH-LILLOOET REGIONAL DISTRICT

Quantitative Landslide Hazard and Risk Assessment – Reid Road Area, Electoral Area C

Final
January 26, 2023

BGC Project No.: 1358010

Prepared by BGC Engineering Inc. for:
Squamish-Lillooet Regional District

BGC ENGINEERING INC. 500-980 Howe Street, Vancouver, BC Canada V6Z 0C8
Tel: 604.684.5900 Fax: 604.684.5909

TABLE OF REVISIONS

ISSUE	DATE	REV	REMARKS
DRAFT	November 30, 2022	A	Original Issue
FINAL	January 26, 2023	1	Final report incorporating SLRD review comments.

LIMITATIONS

BGC Engineering Inc. (BGC) prepared this document for the account of Squamish-Lillooet Regional District. The material in it reflects the judgment of BGC staff in light of the information available to BGC at the time of document preparation. Any use which a third party makes of this document or any reliance on decisions to be based on it is the responsibility of such third parties. BGC accepts no responsibility for damages, if any, suffered by any third party as a result of decisions made or actions based on this document.

As a mutual protection to our client, the public, and ourselves all documents and drawings are submitted for the confidential information of our client for a specific project. Authorization for any use and/or publication of this document or any data, statements, conclusions or abstracts from or regarding our documents and drawings, through any form of print or electronic media, including without limitation, posting or reproduction of same on any website, is reserved pending BGC's written approval. A record copy of this document is on file at BGC. That copy takes precedence over any other copy or reproduction of this document.

SUMMARY

BGC Engineering Inc. (BGC) was retained by the Squamish-Lillooet Regional District (SLRD) to assess steep creek hazards and risks for residential buildings at the outlet of Jason and Mungye creek watersheds at Reid Road, north of Pemberton BC. Reid Road is the main access road for the Ivey Lake subdivision. The road ascends westerly from Pemberton Portage Road and crosses the fans of Jason and Mungye creeks (the study creeks) before terminating at Linda Road southwest of Ivey Lake. This study was prompted by an emergency evacuation order for eight properties and evacuation alert for four properties on Jason Creek fan (SLRD, February 24, 2022) following a series of hydrogeomorphic events in November to December 2021 that resulted in washout of the culvert at Reid Road, overland flooding, and sedimentation. At the time of writing, one property remains on evacuation order. The evacuation order and alert have been rescinded for other affected areas.

The purpose of this assessment is to inform short- and long-term risk management decision-making in the Reid Road area by the SLRD and other key stakeholders (e.g., Ministry of Transportation and Infrastructure (MoTI), Ministry of Forests (MoF), Ministry of Emergency Management and Climate Readiness (EMCR), and Red Cross). BGC evaluated clearwater floods, debris floods, and debris flows including those triggered by rock slope failures in the study (Jason and Mungye) watersheds. Landslides (debris slides, rock slides) were only considered in the hazard assessment if they contributed to the frequency and magnitude of debris flows and debris floods on Jason and Mungye creeks. Other hazards with the potential to impact Reid Road area residential development and infrastructure that originate outside of the study creek watersheds were outside of the present scope.

The Jason and Mungye creek watersheds are deeply incised and parallel to the Owl Creek fault that trends NW-SE. Bedrock exposed in the creek channel and ravine sidewalls of both creeks is heavily altered (clayey). This weak, altered rock increases instability affecting the creek channel within the lower watershed areas and contributes to potential debris-flow volume and runout. BGC recognizes that clay-rich debris flows may have the potential to runout farther than coarser debris flows. Outside of the channel areas, the rock is hard and coarsely jointed forming blocky talus material.

Using a combination of desktop and field observations, BGC classified the study creeks as:

- **Jason Creek:** susceptible to debris flows with two triggering mechanisms:
  - Precipitation-triggered debris flows that originate in the watershed in response to periods of high rainfall and antecedent moisture conditions[1].
  - Rock slide-triggered debris flows that originate in the watershed in response to partial or full failure of unstable rock masses.
- **Mungye Creek:** susceptible to a continuum of processes from flood to debris flow.

[1] Antecedent moisture condition refers to how wet or saturated the soil is prior to a period of heavy rainfall.

BGC observed two locations of unstable rock masses with the potential to trigger large debris flows on the east side of Jason Creek. These areas show signs of recent movement (open cracks and displacement observed in InSAR analysis between May 2017 and June 2022). Debris flows that originate from either precipitation- or rock slide-triggering can travel downslope and impact the developed areas of the fan in a matter of seconds to minutes with little to no time to move out of harms' way. Debris flows can also occur in a series of pulses that each take seconds to minutes but collectively persist over an hour or more. Debris floods generally occur over longer durations than debris flows and have lower intensity. As a result, debris floods are less likely to result to an injury or loss of life to someone in a building but can cause injuries to individuals outside of buildings. Inundation (flooding) and bank erosion are the dominant drivers of hazard and risk from debris floods.

Based on the information collected and reviewed to date, BGC interprets that rock slide-triggered debris flows on Jason Creek are relatively rare and historically have occurred at return periods[2] greater than approximately 1,000-years. Additional monitoring would be needed to assess if the future probability of rock slide-triggered debris flows is increased/increasing above historic rates.

A core component of a hazard assessment is to determine how often (frequency) and what size (magnitude) a hazard may be. This is expressed with a frequency-magnitude (F-M) relationship. BGC used a combination of historical records, aerial imagery interpretation, field observations, radiocarbon dating of samples collected from test pits and natural exposures, and empirical techniques, to develop best estimate F-M relationships for each creek (Table E-1-1).

Table E-1-1. Summary of best estimate F-M relationships for each study creek.

Representative Return Period (years)	Jason Creek			Mungye Creek		
	Process	Sediment volume (m^3)	Peak Discharge (m^3/s)	Process	Sediment volume (m^3)	Peak Discharge (m^3/s)
20	Debris flow	4,000	100	Flood	-	2
50		8,000	170	Debris flood (Type 1)	2,500	3
200		13,000	250	Debris flood (Type 2)	7,500	9
500		19,000	340	Debris flow	14,000	260
2,000		55,000	790		24,000	410

Notes:
1. Debris flood types after Church & Jakob (2020).
2. Sediment volumes reported are those arriving at the fan apex. BGC rounded sediment volumes to the nearest 1,000 m^3 for debris flows and the nearest 100 m^3 for debris floods.
3. BGC rounded peak discharges to nearest 1 m^3/s for floods and debris floods, and to the and nearest 10 m^3/s for debris flows.

The F-M relationship informs development of representative hazard scenarios for numerical modelling. Hazard scenarios also consider how infrastructure on the creeks, namely culverts, are likely to perform in response to the hazard. There are five culverts along the two study creeks.

[2] Return period is a way to communicate the probability of an event occurring in a given year (annual exceedance probability) and does not indicate that an event will recur at regular or set intervals.

Mungye Creek is conveyed below Reid Road in a culvert before joining Jason Creek. Jason Creek is conveyed below Reid Road in a culvert and passes through three additional culvert crossings downstream of the confluence with Mungye (residential driveway, Pemberton Portage Road, and CN Rail). These culverts are undersized to convey debris floods and debris flows and are likely to block leading to overland flooding along Reid Road.

BGC used the numerical modelling programs DAN-3D to model rock slope failure in the Jason Creek watershed and HEC-RAS to model floods, debris floods, and debris flows on both Jason and Mungye creeks. BGC used the model results coupled with interpretation of field evidence and analyses to develop a composite hazard map for the study area that the SLRD can use to inform land-use planning and risk management. The highest hazard areas are on Jason Creek from the fan apex downstream to and eastward along Reid Road and within the Mungye Creek channel.

BGC assessed life-safety risk to individuals in inhabited buildings associated with steep creek hazards in the study watersheds. The results indicate that that five properties on the Jason Creek fan have annual probability of death of an individual (PDI) greater than 1:10,000, a threshold adopted by multiple jurisdictions in Canada and internationally for risk tolerance from natural hazards. These are:

- 1781 Reid Road
- 1782 Reid Road
- 1788 Reid Road
- 1794 Reid Road
- 1802 Reid Road.

The property at the fan apex (1781 Reid Road, PID 1608908) has PDI >1:1,000 and BGC assessed that it is at **imminent risk** from debris flows during periods of high rainfall. Debris flows could impact the other properties listed with little warning during periods of high rainfall or in response to a rock slide, but BGC assessed that the probability and expected consequences of such impacts are lower than at 1781 Reid Road. Debris flows could also impact other properties on and downstream of Jason Creek fan, but BGC assessed the risks to be within levels normally considered tolerable for existing development in other jurisdictions. BGC did not identify any properties on Mungye Creek fan where PDI exceeded 1:10,000 for inhabited buildings. BGC did not assess risk to individuals outside of buildings. BGC expects economic damage associated with inundation, erosion, and debris deposition to residential development and infrastructure (road, rail, culverts) on both Jason and Mungye Creeks and surrounding areas. Given the gradient of Reid Road and existing culvert capacities at the creek crossings on both study creeks, BGC expects culvert blockage and significant flow concentration along the road surface towards downstream areas.

To reduce risk from debris flows on Jason Creek, BGC recommends a phased approach:

- **Phase 1:** Construction of flow diversion berms on individual properties (1781, 1782, 1788, 1794, 1802 Reid Road).
- **Phase 2:** Channel excavation and bridge construction at Reid Road crossing.

BGC estimated cost for Phase 1 at $2.1 Million including capital and operations and maintenance (O&M) costs over a 75-year service life. Of this, $380,000 is for the construction of a geosynthetic reinforced soil (GRS) wall to protect the home at 1781 Reid Road, the property with the highest estimated life safety risk. BGC estimated cost for Phase 2 at $ 5.7 Million (inclusive of O&M over 75-year service life). These cost estimates are conceptual-level (-50% to +100%) and for the purpose of identifying a preferred risk management approach and to support funding applications.

On Mungye Creek, BGC recommends replacement of the Reid Road culvert with a box culvert designed with sufficient capacity to convey the 200-year debris flood to reduce damage to Reid Road and economic risk to residential development. BGC estimated the cost for this replacement to be $1.1 Million (inclusive of O&M over 75-year service life). As for Jason Creek, this cost estimate is conceptual-level.

The proposed phased approach for Jason Creek facilitates construction of mitigation measures over two phases as design, funding, and permitting allow. Future phases of design require stakeholder engagement and refinement of the mitigation designs at both creeks. Finally, BGC recommends that SLRD review applicable land-use policies to reduce risk to future development or redevelopment within the study area, informed by the composite hazard map provided with this assessment.

TABLE OF CONTENTS

LIST OF TABLES

LIST OF FIGURES

LIST OF APPENDICES

LIST OF DRAWINGS

ACKNOWLEDGEMENT

This report was completed after the untimely passing of Dr. Matthias Jakob, P.Geo., P.L.Eng., one of the leading international experts in steep creek hazards and risk. Dr. Jakob was engaged in the hazard and risk assessment and conceptual mitigation options assessment throughout the project, including as part of field work. The project team is grateful for his contributions and acknowledges that the findings presented herein and report benefitted from his contribution and review.

1. INTRODUCTION

1.1. General

The Ivey Lake subdivision is located 4 km northwest of the Village of Pemberton, BC. It is accessed by Reid Road, which joins Pemberton Portage Road about 4 km north of Mt Currie (Drawing 01). The road ascends westerly from Pemberton Portage Road up and across the Jason Creek fan and then descends across the Mungye Creek fan and terminates at Linda Road southwest of Ivey Lake. Linda Road and McKenzie Basin Forest Service Road to the west provide a 4WD access route for the community; however, BGC understands from conversations with the Squamish-Lillooet Regional District (SLRD) and residents that this access is seasonal as snow cover and steep road conditions prevent safe and reliable egress in the winter months.

Jason and Mungye creeks are susceptible to a range of steep creek hazards (flood, debris flood and debris flow) (Baumann, October 1997; Cordilleran, December 13, 2021) and rock slope failures (Piteau & Associates (Piteau), 1981; PK Read, 2016). In November and December 2021, Jason Creek experienced three hydrogeomorphic events which impacted several properties and road crossings through debris flow and debris flooding, and localized bank erosion (Frontera 2021; Cordilleran, December 13, 2021). In response to the events, the SLRD issued an evacuation order for eight properties in connection with an assessed “imminent” debris-flow risk with destructive potential for life and property (Cordilleran, December 13, 2021). The evacuation order for the eight affected properties, along with an evacuation alert for an additional four properties[3] dated February 24, 2022 is shown in Figure 1-1.

To inform risk management decision-making for the area, SLRD requested a quantitative assessment of hazards and risk from landslides (including rock slides & debris flows), debris floods, and floods affecting the Reid Road area with a focus on the Mungye and Jason creek watersheds (SLRD, May 11, 2022). BGC understands that SLRD decisions on possible re-occupancy of the affected properties will be informed by the outcomes of the present detailed hazard/risk assessment of said hazards (SLRD, May 11, 2022).

In response to BGC’s draft report and risk assessment update letter (November 25, 2022), the SLRD updated the evacuation order as shown in Figure 1-2. At the time of writing, only one property located at the fan apex (1781 Reid Road) remains on evacuation order.

[3] The four affected properties are located on three parcels.

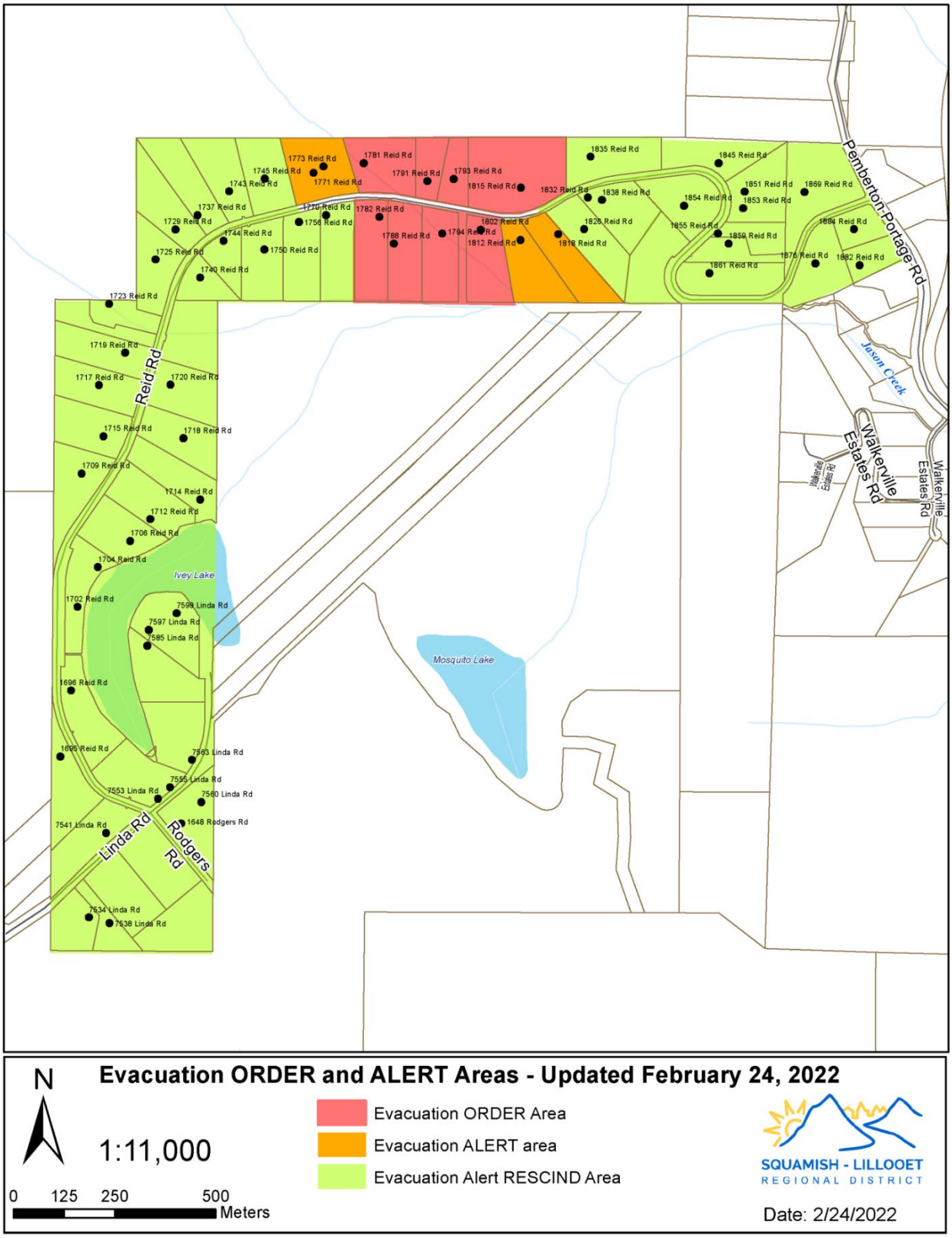

Figure 1-1. Evacuation order and alert for Reid Road as of February 24, 2022.

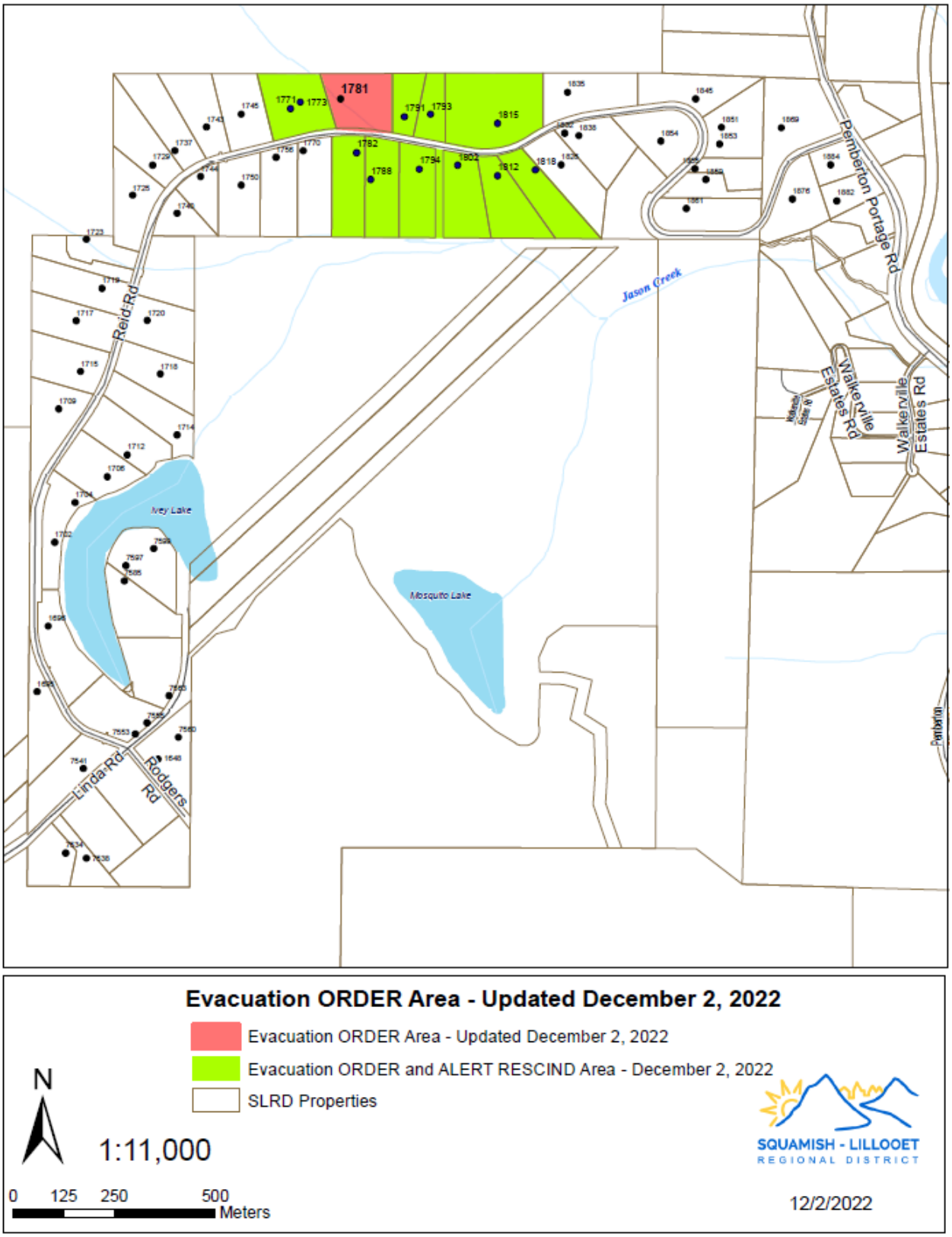

Figure 1-2. Evacuation order for Reid Road as of December 2, 2022.

1.2. Scope of Work

BGC's scope of work is outlined in the proposed work plan (BGC, June 6, 2022). The project was carried out under the terms of professional services agreement between SLRD and BGC dated July 19, 2022.

The scope of work includes:

- Steep creek geohazard assessment for Jason and Mungye creeks, including:
  - Desktop analysis to assess site conditions including acquisition of lidar topography and inSAR[4] analysis over the study area
  - Field study to assist in geohazard characterization and reconstruction of historic debris floods/flows including dendrochronology, stratigraphic analysis of test pits and radiocarbon dating of samples from test pits.
  - Frequency-magnitude (F-M) analysis of rock slope failure and steep creek processes
  - Numerical modelling of dominant processes on the study creeks
  - Development of a composite hazard map for the study area
- Risk assessment, including:
  - Quantitative life-loss risk assessment (QRA) based on the hazard assessment results and existing development layout.
  - Qualitative assessment of potential impacts to buildings and infrastructure in the study area
- Conceptual mitigation design, including:
  - Development of mitigation design basis and objectives
  - Development of conceptual design options and options analysis
  - Estimation of life-cycle costs of the preferred mitigation system (capital and operations and maintenance (O&M) costs over the expected service life).

The purpose of this assessment is to inform short- and long-term risk management decision-making in the Reid Road area by the SLRD and other key stakeholders (e.g., Ministry of Transportation and Infrastructure (MoTI), Ministry of Forests (MoF), Ministry of Emergency Management and Climate Readiness (EMCR), and Red Cross).

BGC evaluated clearwater floods, debris floods, and debris flows including those triggered by rock slope failures in the study (Jason and Mungye) watersheds. Landslides (debris slides, rock slides) were only considered in the hazard assessment if they contributed to the frequency and magnitude of debris flows and debris floods on Jason and Mungye creeks. BGC did not assess additional geohazards that could threaten the study area (e.g., snow avalanches and earthquakes). Moreover, BGC did not consider rock fall and rock slide hazards outside of the study creek watersheds including immediately east of Jason Creek above Lot 5 Reid Road. This area has been the subject of multiple studies (Baumann Engineering, October 1997, Blunden, 1981; Piteau, 1981) and was the subject of the 1982 restrictive covenant #T59223 based on the potential for rock fall and rock slide hazards originating from the slope. BGC understands that this

[4] InSAR (Interferometic Synthetic Aperture Radar) is a technique to map ground deformation using radar images of the Earth collected from satellites.

restrictive covenant has been modified in response to a more recent study (P.K. Read Engineering Ltd. (P.K. Read), March 3, 2016). As this hazard is out of scope, this report has not been reviewed by BGC.

The study scope was informed by and followed guidance by Engineers and Geoscientists of British Columbia (EGBC, 2017) guidelines for flood map preparation, EGBC professional practice guidelines for Legislated Flood Assessments in a Changing Climate in BC (EGBC, 2018) and Landslide Assessments in British Columbia (EGBC, 2022). BGC also reviewed the BC Ministry of Transportation and Infrastructure (MoTI) Subdivision Preliminary Layout Review – Natural Hazard Risk directive (MoTI, 2015).

1.3. Study Team

The study team that contributed to this scope of work includes experts in the fields of hazard, risk, and mitigation design from BGC and Cordilleran Geoscience (Cordilleran) as summarized in Table 1-1.

Table 1-1. Study team. Professional designations are for practice in British Columbia.

Project Role	Team Member
Project Manager	Lauren Hutchinson, M.Sc., P.Eng.
Technical Leads	Matthias Jakob, Ph.D., P.Geo., P.L.Eng.; Lauren Hutchinson, M.Sc., P.Eng.
Technical Reviewers	Alex Strouth, M.A.Sc., P.Eng. (Mitigation) Kris Holm, M.Sc., P.Geo. (Overall, risk) Michael Porter, M.Eng., P.Eng., LEG (Corporate)
Project Geoscientists / Engineers	Andrew Mitchell, Ph.D., P.Eng. Celeste Melliship, B.A., ADP Hazel Wong, M.Eng., P.Geo. Hilary Shirra, B.A.Sc., EIT Jeanine Engelbrecht, Ph.D. Kathleen Horita, M.Sc., P.Eng. Matthieu Sturzenegger, Ph.D., P.Geo. Pierre Friele, M.Sc., P.Geo., L.Eng. (Cordilleran Geoscience) Sophia Zubrycky, M.A.Sc., P.Eng.

1.4. Related Documents and Studies

The following documents provide additional information relevant to the Reid Road area QRA:

- Cordilleran (December 13, 2021) summarizes the Jason Creek hazards and presents findings from Cordilleran's site visits completed as part of the emergency response work in December 2021.
- Emergency Response Support - Jason Creek (Reid Road) Assessment (BGC, February 18, 2022) summarizes the third-party review completed by BGC of the Cordilleran (December 13, 2021) report.

In support of the present assessment, BGC compiled and reviewed previous reports that pertain to the hazards and risks on Reid Road from 1974 to present. A summary of key findings and BGC

comments on these previous reports are summarized in Appendix A. Appendix A also provides a list of additional data sources compiled in support of this assessment (e.g., air photos).

1.5. Report Outline

This report is organized into the following sections:

- *Section 2 Steep Creek Hazards*
  Overview of steep creek hazards (debris floods and debris flows) and how they differ from floods. Detailed descriptions of these hazard types are provided in Appendix B.
- *Section 3 Study Area*
  Description of the study area including the geomorphology, existing development, forestry activities and history, wildfire history, climate, and previous reports. The characterization is informed by field observations (Appendix C) and includes a summary of existing infrastructure on the study creeks (Appendix D).
- *Section 4 Hazard Assessment*
  Results of the hazard assessment for Jason and Mungye creeks. Additional details and methods to support are provided in Appendices E, F, and G. Results of the composite hazard mapping informed by numerical flow modelling (Appendix H) are also presented. Hazard mapping methods are outlined in Appendix I.
- *Section 5 Risk Assessment*
  Results of the quantitative risk assessment. Additional details on the methods are included in Appendix J.
- *Section 6 Conceptual Mitigation Design*
  Conceptual mitigation options for consideration at Jason and Mungye creeks to reduce risk from debris flows and debris floods. Conceptual-level (-50% to +100%) cost estimates for preferred options are presented with additional detail in Appendix K.
- *Section 7 Summary and Recommendations*
  Summary of key findings, recommendations for next steps, and report limitations.

Photographs of the study creeks collected by BGC and Cordilleran as part of the field work are included in the Photographs Attachment.

2. STEEP CREEK HAZARDS

2.1. Introduction

Steep creek or hydrogeomorphic hazards are natural hazards that involve a mixture of water and debris or sediment (Figure 2-1). These hazards typically occur on creeks and steep rivers with small watersheds (usually less than 100 km^2) in mountainous terrain, usually after intense or long rainfall events, sometimes aided by snowmelt and worsened by forest fires.

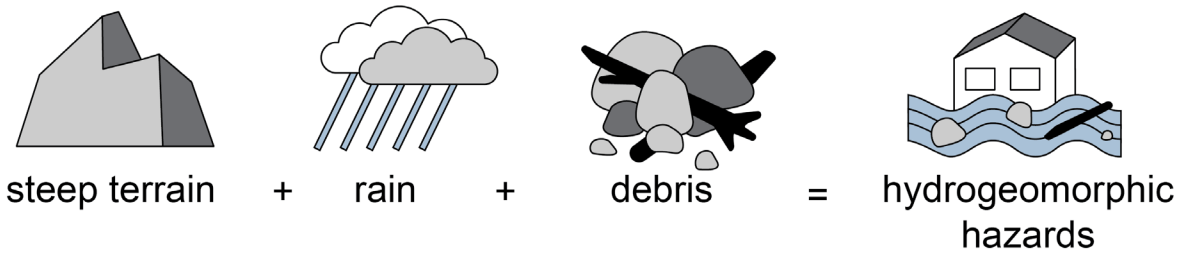

Figure 2-1. Illustration of steep creek hazards.

Steep creek hazards span a continuum of processes from clearwater floods (flood) to debris flows (Figure 2-2).

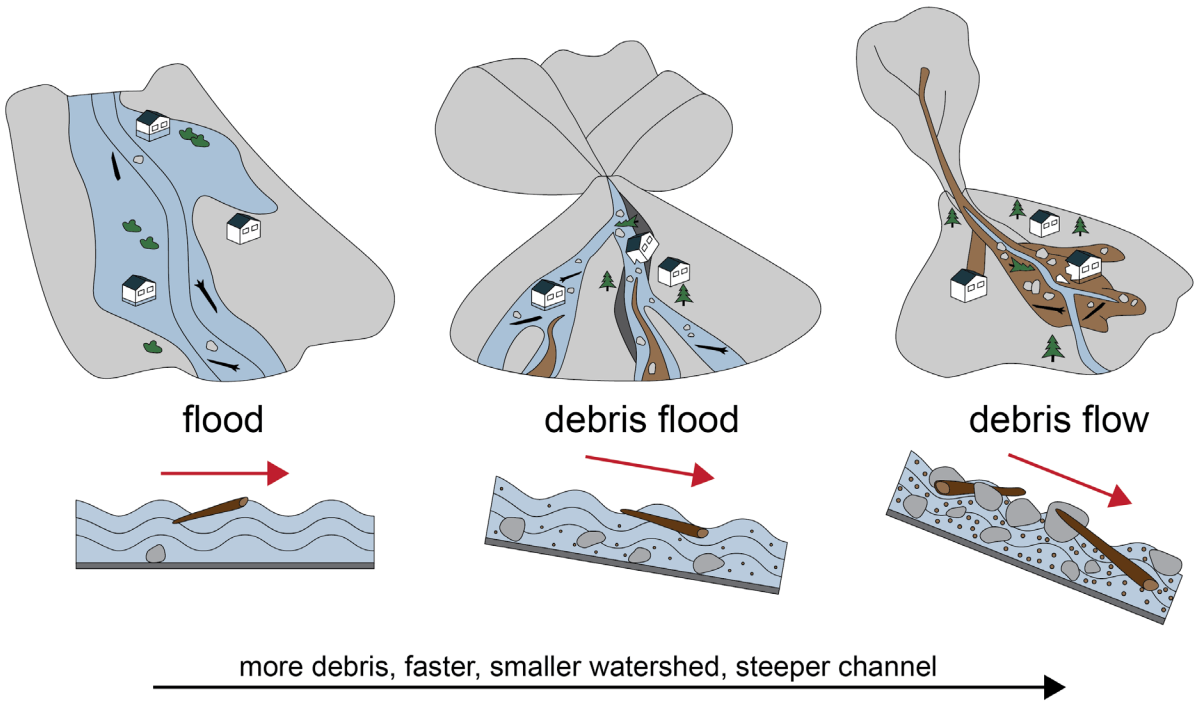

Figure 2-2. Simplified illustration summarizing the hazards associated with each hydrogeomorphic process.

Steep creek hazards are often communicated as a function of return period to indicate the frequency that events of a certain size are expected to occur (e.g., 2-year return period). Importantly, return period is an indication of the probability that an event will occur in any given year, and is not a set recurrence interval (i.e., if a 10-year return period event occurs, that does not indicate it will not happen again for nine years, and instead the probability it could occur again the following year is 1/10).

The following two sections describe some general characteristics about debris floods and debris flows and how they differ from floods. More detail on and the implications of these processes are provided in Appendix B.

2.2. Debris Floods

Debris floods occur when large volumes of water in a creek or river entrain the gravel, cobbles, and boulders on the channel bed; this is known as “full bed mobilization” along with woody debris. Debris floods can occur from different mechanisms. BGC has adopted the definitions of three different sub-types of debris floods per Church and Jakob (2020):

- Type 1 – Debris floods that are generated from rainfall- or snowmelt-runoff resulting in sufficient water depth to result in full bed mobilization.
- Type 2 – Debris floods that are generated from diluted debris flows (e.g., a debris flow that runs into a main channel in the upper watershed).
- Type 3 – Debris floods that are generated from natural (e.g., landslide dam, glacial lake outbursts, moraine dam outbursts) or artificial dam (e.g., water retention or tailings dam) breaches.

Sediment and woody debris become entrained in debris floods leading to an increase in the volume of organic and mineral debris flowing down a channel as compared with floods, and an ensuing increase in peak discharge. Debris floods typically contain up to 20% debris concentration by volume.

The effects of debris floods can range from relatively harmless to catastrophic depending on their magnitude and duration. Inundation (flooding) and bank erosion are the dominant drivers of hazard and risk from debris floods. While relatively rare, injuries and/or fatalities can occur when people try to escape these events (e.g., are impacted while outside of buildings).

2.3. Debris Flows

Debris flows have higher sediment concentrations than debris floods and can approach consistencies similar to wet concrete as they have approximately 50% debris concentration by volume. Debris flows are typically faster than debris floods and have substantially higher velocities and flow depths, resulting in higher peak discharges and impact forces. They are particularly threatening to life and properties due to these characteristics, including to individuals within buildings. In general, the velocity and flow depth of debris flows are highest at the fan apex (where the creek emerges from the watershed) and decrease with distance away from the apex laterally and downstream. Local characteristics on the fan can redirect and channelize flows such that the

velocity, flow depth, or both, are high enough to result in significant damage or life loss at locations distant from the fan apex.

Debris flows occur as two-phased flow with a coarse boulder front followed by a muddy afterflow (sometimes referred to as hyper-concentrated flow) (Figure 2-3). The coarse front has higher impact forces because of the boulder and woody debris content and presents the highest risk to life safety. The muddy afterflow is lower intensity and the ability to transport boulders and woody debris decreases as flow depths decrease as the flow runs over the fan surface. In general, muddy afterflows result in lower safety risk to individuals in buildings but can have flow depths and velocities high enough to present a safety risk to individuals outside of buildings and result in economic damages associated with flooding, sedimentation, and erosion. The coarse front typically occurs over seconds to minutes while the muddy afterflow can occur over minutes to an hour. Debris-flows can occur as a single pulse or series of pulses that collectively occur over a series of hours with each individual pulse being of lower duration.

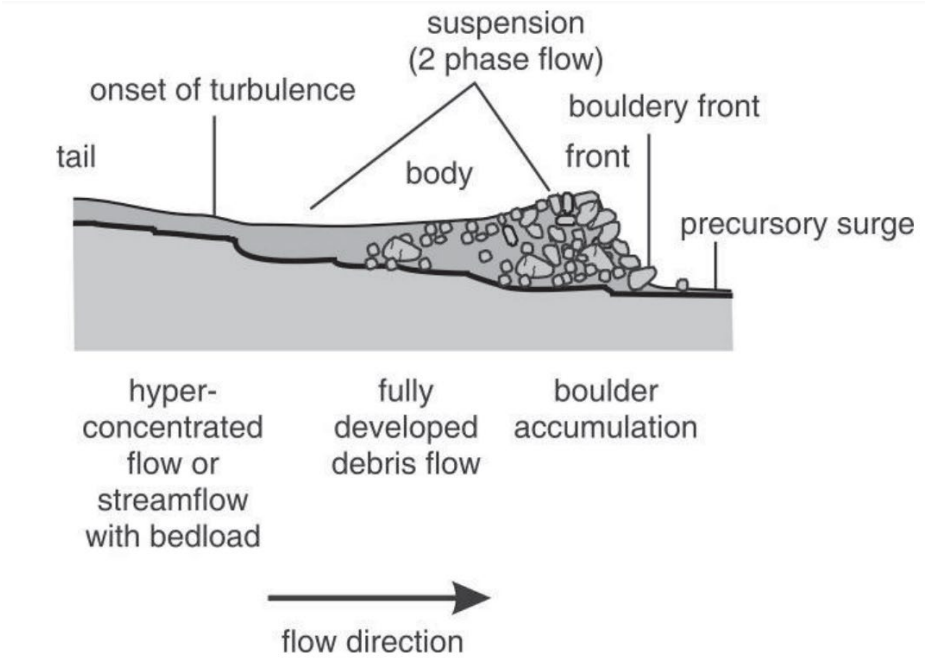

Figure 2-3. Schematic of two-phased debris-flow behaviour (Pierson, 1986).

2.4. Comparing Steep Creek Processes

Individual steep creeks can be subject to a range of process types and experience different peak discharges depending on the process, even within the same return period class. Figure 2-3 demonstrates this concept with an example cross-section of a steep creek, including representative flood depths for the peak discharge ("Q") of the following processes:

- Q_2: Clearwater flow with 2-year return period
- Q_{200}: Clearwater flow with 200-year return period (i.e., a clearwater flood)
- $Q_{max\ debris\ flood\ (full\ bed\ mobilization)}$: Type 1 debris flood generated by full bed mobilization
- $Q_{max\ debris\ flood\ (outburst\ flood)}$: Type 3 debris flood generated by an outburst flood
- $Q_{max\ debris\ flow}$: Debris flow.

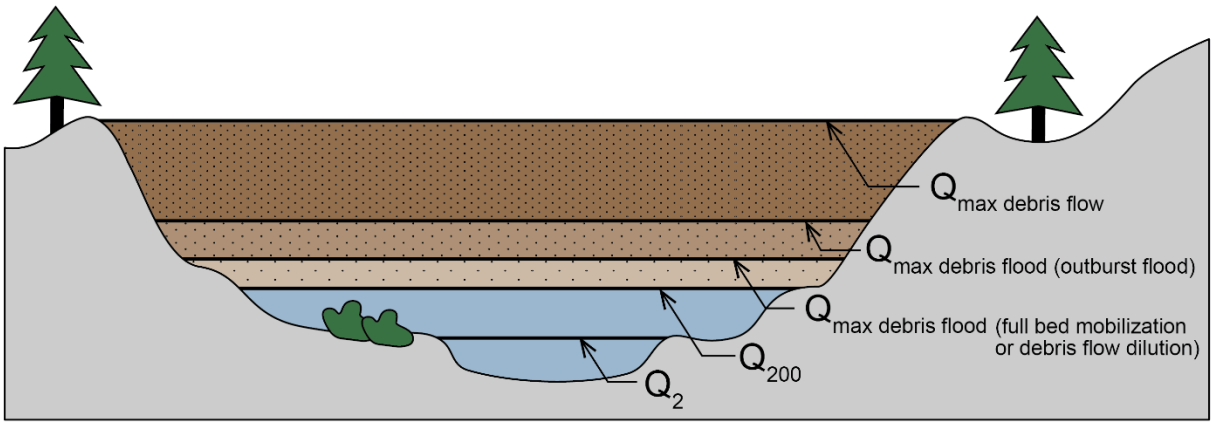

Figure 2-4. Conceptual steep creek channel cross-section showing peak discharge levels for different events. Note that for some outburst floods or debris flows the discharge may exceed what is shown here.

This difference in peak discharge is one of the reasons that process-type identification is critical for steep creeks. For example, if a culvert is designed to accommodate a 200-year clearwater flood, but the creek experiences a debris flow with a much larger peak discharge, the culvert would likely be damaged or destroyed.

Floods and debris floods tend to occur over a series of hours to days while debris flows occur in a matter of seconds to minutes. For floods, event duration influences the potential impacts. A longer duration is more likely to saturate protective dikes, increasing the likelihood for piping and dike failure prior to, or instead of, the structure being overtopped. For debris floods, the duration of the event will also affect the total volume of sediment transported and the amount of bank erosion occurring. For debris flows, the short duration of the events makes it very unlikely that sufficient warning could occur between the debris flow being triggered and reaching an area at risk. Similarly, it is unlikely that a person could outrun a debris flow. This short duration increases the risk of injury or life loss associated with debris flows.

2.5. Impacts of Forestry on Watersheds

The relationship between forest harvesting activities, including opening of cutblocks and road construction, and landslide activity within watersheds is well-documented in many studies and across several scales (e.g., Guthrie, 2002; Guthrie, 2022; Jakob, 2000; Jordan, 2002; Millard 1999). Jordan (2002) found that landslide frequencies were increased by roughly 10 times by forest development in the Arrow and Kootenay Lake Forest Districts of BC with 95% of development-related landslides being the result of roads or skid trails. On older roads, road-fill failures were the most common cause of failure while on newer roads, drainage concentration and diversion by roads was found to be the most common cause (Jordan, 2001). Jordan (2001) and Grainger (2001, 2004) also identify the influence of “gentle-over-steep” situations where a road is constructed on gentle sloping, low-hazard terrain and landslides occur on steeper terrain below. Jakob (2000) similarly found that landslide activity was 9 times higher than in undisturbed forest on the west coast of Vancouver Island, BC. Moreover, Jakob (2000) found that failures in logged terrain occurred in gentler slopes than in natural terrain. The most common failure mechanisms were debris slides and debris flows initiating from road fill failures. These studies

illustrate the importance of sound forestry management practices to limit increased landslide activity.

Although not discussed at depth in this report, it is also important to emphasize the effects of forest harvesting activities on water quality. The construction and presence of roads lead to high erosion and sedimentation, which affects fish-bearing water bodies or where drainages are used as domestic water resources. BGC understands that some landowners in the study area have water intakes on the study creeks.

2.6. Wildfire Effects on Watersheds

Wildfires impact the hydrology and stability of a slope through loss of vegetation and modification of soil properties. During a fire, hydrophobic compounds accumulate below the soil surface, causing an increase of water repellency and reducing water storage capacity of the soil (Shakesby & Doerr, 2006). The removal of soil-mantling vegetation and litter reduces evapotranspiration and infiltration rates in the soil and changes the soil moisture dynamics (Rengers et al., 2020; Moody and Martin, 2001), as well as causing reduction in root strength, thus reducing the apparent cohesion of the soil (Rengers et al., 2020). There is also an increase of precipitation reaching the ground surface through loss of vegetative canopy (Rengers et al., 2020; Parise and Cannon, 2012). Figure 2-4 outlines some of the effects of wildfires on slope hydrology and stability.

As a result, burned slopes are often more susceptible to debris flows, debris floods, floods, and other slope hazards. The largest events are most often triggered by the first major storm following the wildfire event and the hazard remains elevated in the first 2 years following a fire (Cannon & Gartner, 2005; De Graff et al., 2015; Staley et al., 2020). Landscape recovery is usually reached after 5 to 10 years, depending upon the rate of vegetation regrowth in the fire area (Bartels et al., 2016).

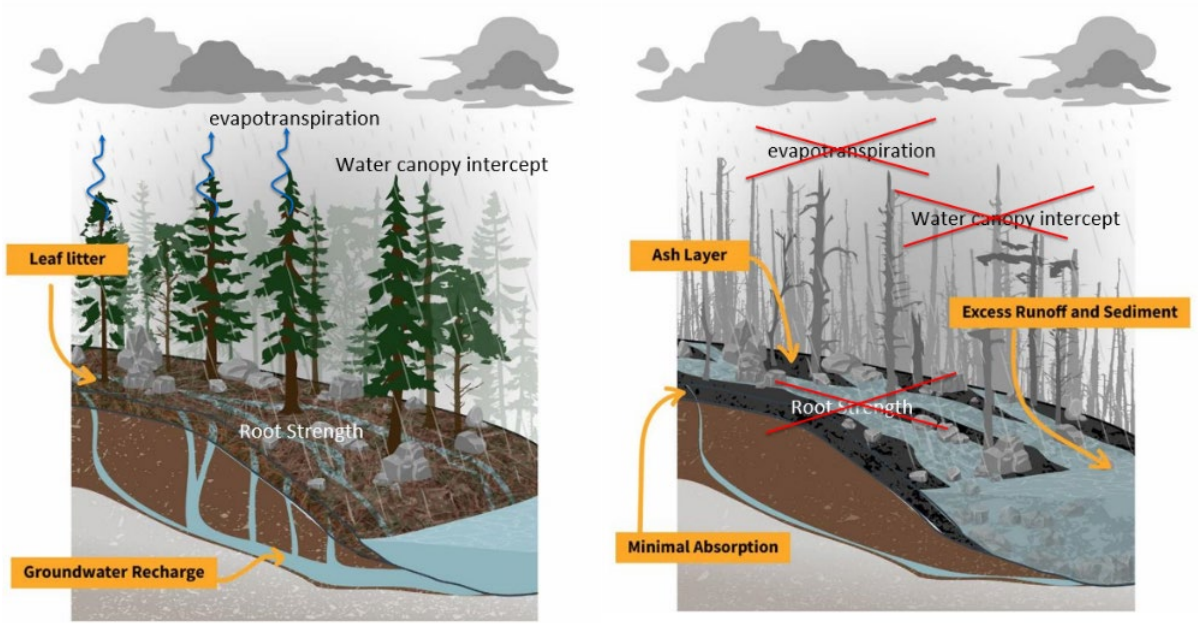

Figure 2-5. Schematic showing hydrology on a slope in unburned conditions (left) and the potential effects of wildfires on slope hydrology, which influences slope stability (right). Figure adapted from United States Geological Survey (2020).

3. STUDY AREA

This section describes the physical setting of the Jason and Mungye creek watersheds. Observations of the study area are supported by data compiled by BGC and Cordilleran and previous assessments provided by SLRD (Appendix A) as well as from field work completed by BGC (Lauren Hutchinson, Matthias Jakob, Sophia Zubrycky) and Cordilleran (Pierre Friele) on July 20-22; 26-27, September 10, September 16, 2022, and October 19, 2022. The field traverse and observation points are shown in Appendix C. Representative photographs of the study area are provided in the Photographs Attachment.

3.1. First Nations

Jason and Mungye creeks are within the traditional and unceded territory of the Lil'wat Nation.

3.2. Watershed and Fan Characterization

3.2.1. Physical Setting

The Jason and Mungye creek watersheds are underlain by marine sedimentary and volcanic rocks of the Lower Cretaceous Gambier Group (Riddell, 1992; Schiarizza & Church, 1996). The Owl Creek fault trends NW-SE, and the deeply incised channels of Jason and Mungye Creeks are parallel to it.

The bedrock exposed in the creek channel and ravine sidewalls is heavily altered (clayey) with grey and cream to orange colours. Outside of the channel areas, the rock is generally hard and coarsely jointed forming blocky talus material. However, there are locations outside the channels, especially lower in the watersheds, where altered rock exists. These occurrences of altered rock are not mapped in detail, yet their presence is important, as these weak rocks condition the instability affecting the creek channels within the lower watershed areas.

Cross cutting the NW-SE alignment of Owl fault and Jason and Mungye Creeks are near vertical joints oriented NE-SW. In Jason Creek especially, the intersection of the NW-SE fault trend and the NE-SW joints control rock slope instabilities in the bluffs on the east side of Jason Creek.

The study area has been glaciated numerous times over the last 2-3 million years, and this has shaped landscape morphology and surficial deposits. With the highest elevations in the study area about 1,435 m, the entire watershed was ice-covered. Ridge crests are scoured rock outcrops. On mid and lower slopes, till veneers and blankets are common. In the valley bottoms, there are various sediments resulting from glacier outwash deposition and from blockage of valley drainage by glaciers. For example, along the lower Birkenhead River near Jason Creek, the lowest sediments exposed along the river banks are lacustrine from when Lillooet Valley glacier blocked the Birkenhead River outlet. These sediments are overlain by bouldery outwash gravels forming the relict fan of Owl Creek. This terrace stands at 260 m elevation, 20 m above the Birkenhead River floodplain and is onlapped by the lower Jason Creek fan (Figure 3-1).

In the post glacial period, these glacial forms and deposits have been modified by landslide and steep creek processes to produce rockfall talus, incised ravines, colluvial and fluvial fans, and floodplains.

Jason and Mungye creeks drain the southeast facing slope above Birkenhead River near its mouth. They have similar basin morphometries (Table 3-1) with basin sizes of approximately 1.2 - 1.8 km^2 and watershed steepness[5] of 0.74-0.85 m/m, suggesting debris flow as the process affecting the fan apices. The long profiles of both watersheds above the fan apices are convex, with steeper terrain within the lower watersheds between approximately 450-500 m and 940-1,100 m elevation, breaking to moderate terrain above (Figure 3-1). It is the lower watershed areas that present the greatest hazard to fan areas, and this is the zone where field work was confined (Appendix C).

Available topographic maps and GIS flow routing based on lidar data show that Jason Creek flows from a small lake at 1,375 m elevation. Anecdotal observation from a resident indicated that the lake may feed Mungye Creek. Close examination of the lidar slope contours indicates that creek avulsion in a localised flat area below the lake outlet could allow for water to flow from the lake to Mungye Creek. We have mapped the lake as part of Jason Creek. Inclusion of the lake subbasin in one or the other watersheds does not change the basin morphometric analysis.

[5] Watershed steepness is also referred to as Melton Ratio, the ratio of watershed relief divided by the square root of watershed area (Melton, 1957). It is one means of assessing the dominant steep creek process type of a watershed.

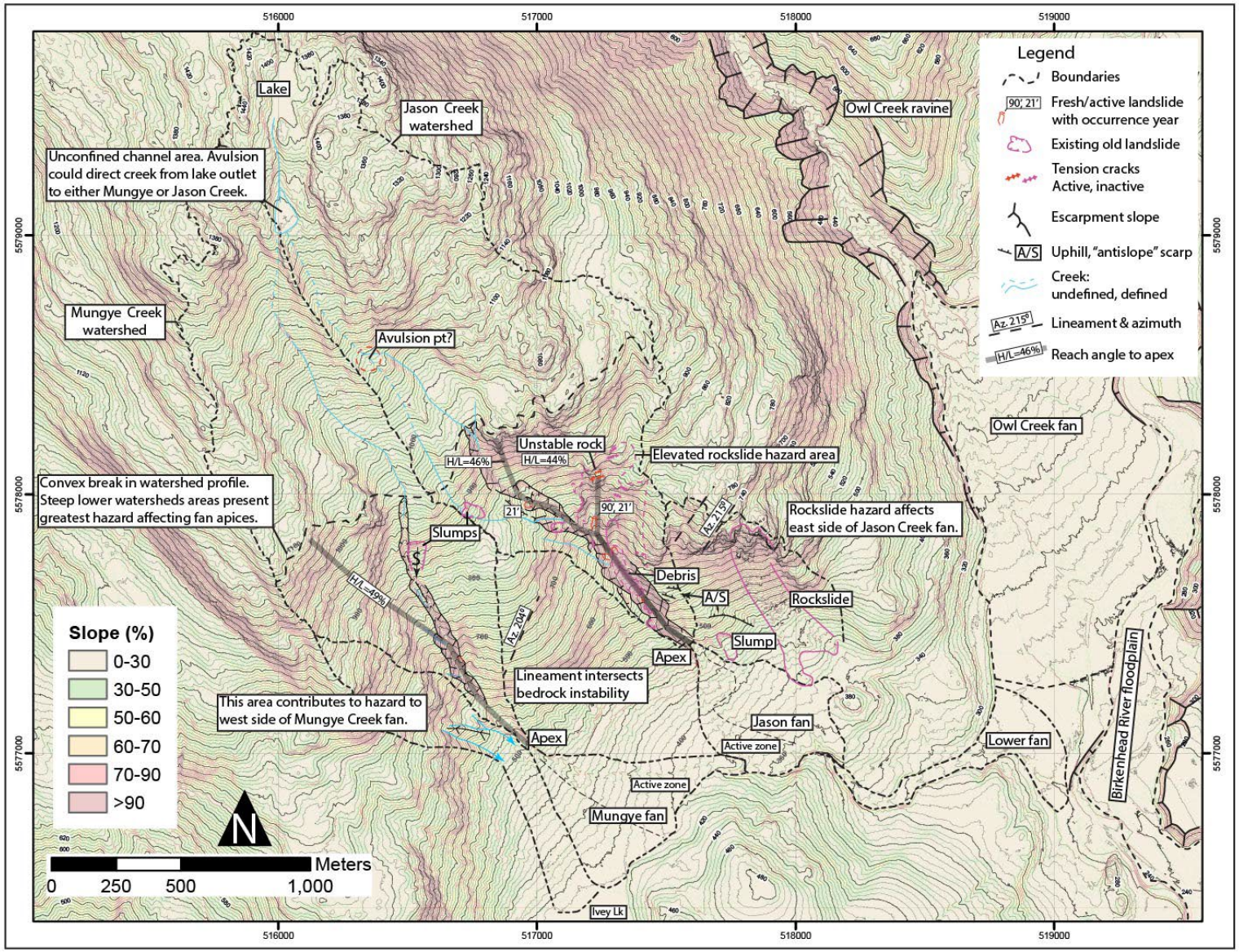

Figure 3-1. Topographic map of study area showing slope shading and geomorphic features. This map complements Drawing 03.

3.2.1.1. Jason Creek

The confined reach between the fan apex at 450 m elevation and the break in slope at 970 m elevation (Figure 3-1) presents the greatest landslide risk affecting Jason Creek. In this bedrock ravine, the west (right) sidewall is 10-60 m tall, while the east (left) sidewall rises 10-300 m above the channel. On the channel floor and the lower slopes of both sidewalls, bedrock is highly altered fault gouge material (Photo 25); while higher on the ravine sidewalls bedrock is typically hard and coarsely jointed.

This condition of hard brittle rock underlain by very soft, altered bedrock allows for deep seated instability of the ravine sidewalls. On the west (right) sidewall there are several bedrock linears, or uphill facing scarps aligned parallel to the ravine crest. These suggest slope deformation. Numerous spoon-shaped scallops indicate past slump instabilities (Figure 3-1, Drawing 03). BGC identified several fresh slumps in the field.

On the east (left) sidewall, there is one site approximately 100 m above the channel floor, where the brittle cap rock is slowly toppling at rates detectable by repeat pass satellite imagery (Section 4.2). BGC assessed that this site could release a rapid landslide in the range of 15,000-50,000 m^3. In addition, there are gaps in several bluff lines that suggest that large rock collapses have occurred in the past. On lidar imagery, these gaps are flanked downslope by colluvial aprons that are likely deposits derived from former collapse(s). The floor of the ravine is typically very narrow and V-sided, but between 550-600 m elevation the valley flat widens to about 50 m, and this area accommodates colluvial infill 3-5 m thick and represents midslope storage of landslide debris. At several sites (Figure 3-1, Drawing 03, Photos 13, 14) fresh tension cracks indicate that this landslide debris is unstable with the potential for collapse, or creep, feeding debris to the channel.

The existence of sidewall instabilities, including creep, in weak bedrock and in old landslide debris means that there may be a high debris recharge rate along the channel. Localised creep of sidewalls feeds debris directly to the channel, and also forces the channel to the opposite side, causing undermining and further instability.

From the apex at 450 m elevation, the Jason Creek fan has a 560 m radius sweeping over a 60^0 arc and has an area of 0.26 km^2. The fan surface has a concave profile, with gradients of 22% near the apex, 16% in the middle reach along Reid Road, and 12% near the toe. The downslope margin of the fan body is confined by a bedrock outcrop. Where the combined flow of Mungye and Jason Creeks flows along the toe abutting the rock to the south, it has incised a ravine in sediment up to 15 m deep. During BGC field traverses, no exposures suitable for stratigraphic analysis were observed. It is likely that much of this sediment thickness is till, with a capping of Jason fan colluvium. At the fan toe ravine crest, at 355 m elevation, it is likely that <5 m thickness is fan material. At the surface, subrounded 1-2 m diameter boulders of granitic lithology support this interpretation. The lower fan below 380 m elevation is persistently wet from seepage, and seepage gullies deepen as they steepen to join the confined mainstem.

The historic creek channel flows down the west side of the fan, where it is incised 1-2 m in the fan surface, but splays where freeboard is locally zero. Old channel-like depressions exist at the

fan apex and these trend SE to the central and east sectors of the fan. Debris blockage at the apex could force an avulsion south-eastward on the fan surface.

Reid Road climbs the fan from east to west and intersects Jason Creek. This configuration allows for Reid Road to capture flood water and debris, channeling flow downslope and off the east edge of the fan into a small gully. This possibility creates another potential damage corridor on the east side of the rock knoll that bounds Jason Creek fan on the SE (Drawing 03).

A conspicuous feature of Jason Creek fan is the scattered distribution of megablocks (large angular boulders, e.g. Photo 19), 3-8 m diameter across the surface downslope to about 380 m elevation. They are mostly in the central fan sector aligned with the creek axis upstream of the fan apex. These megablocks represent the surface expression of historic rock slide-triggered debris-flow deposits (Figure 3-1).

3.2.1.2. Mungye Creek

Like Jason Creek, the lower watershed presents the greatest hazard affecting the fan (Figure 3-1). The ravine channel is narrower and less deep than Jason Creek. BGC only identified one bank instability that appeared fresh during field traverses. This instability was extant in 1997 (Baumann, 1997). The west side of the watershed has the greatest hazard with 400 m relief from the channel to the bluff crest at 1,100 m elevation. However, in the western bluffs, no deep-seated instability has been noted, and the outcrops visited appear vulnerable to fragmental rockfall only. On the left bank between 820-880 m elevation BGC identified a slump in bedrock approximately 50 m wide by approximately 75 m long and up to about 5 m thick, representing a prehistoric point source volume of up to 20,000 m^3. BGC did not identify any other point source scars during field visits. In comparison to Jason Creek, the debris-flow hazard on Mungye Creek appears to be lower (see Section 4.3).

From the apex at 500 m elevation, the Mungye.Creek fan has a 635 m radius sweeping over a 63˚ arc and has an area of 0.27 km^2. The fan surface has a concave profile, with gradients of 22% near the apex, 16% in the middle reach along Reid Road, and 12% near the toe. The Mungye Creek channel follows the eastern fan margin and is generally well confined from the apex down to Reid Road. Below the road, the active channel area widens to 50 m and up to 75 m at the fan toe.

The downslope margin of the fan body is confined by a bedrock outcrop. On the west side of the distal margin the fan elevation at 415 m forms a barrier sill impounding Ivey Lake (which drains over a rock sill on the west side of the lake), and approximately 100 m of the shoreline is formed by the fan toe. Moving east on the distal margin the fan surface slopes gently down to merge with Jason Creek fan. There is no evident outflow channel from Ivey Lake, but seepage through the sill feeds persistently wet ground, until the confluence of Mungye Creek where a defined channel exists. There is an apparent topographic bulking of the fan on the west margin where it abuts the rock knoll to dam Ivey Lake (Figure 3-1). This higher relief area forces creek activity to the eastern margin.

3.2.2. Steep Creek Process Classification

Watershed and fan characteristics of Jason and Mungye creeks are summarized in Table 3-1.

Table 3-1. Watershed and fan characteristics of Jason and Mungye creeks.

Characteristic		Jason Creek	Mungye Creek
Watershed area (km^2)		1.78	1.22
Maximum watershed elevation (m)		1440	1440
Minimum watershed elevation (m)		450	500
Watershed relief (m)		990	940
Melton Ratio (km/km)[1]		0.75	0.86
Average channel gradient of mainstem above fan apex (%)		39	32
Fan area (km^2)[2]		0.19	0.22
Average gradient at fan apex (%)		23	20
Average fan gradient (%)	Above Reid Road	16	16
	Below Reid Road	12 (4 on lower fan)[3]	12

Notes:

1. Melton ratio is the ratio of watershed relief divided by the square root of watershed area (Melton, 1957).
2. Upper fan areas are reported in table. Combined upper and lower fan areas are measured at 0.26 km^2 for Jason Creek and 0.27 km^2 for Mungye Creek.
3. The lower Jason Creek fan is shown on Drawing 01.

Based on watershed stream length and Melton ratio (Wilford et al., 2004) Jason and Mungye creeks would both be classified as debris-flow prone (Figure 3-2). This preliminary classification does not account for the continuum of processes that a watershed may be subject to at different return periods. Based on review of aerial imagery, watershed and fan characteristics, and field observations BGC classifies the dominant process types on Jason and Mungye creeks by return period as summarized in Table 3-2.

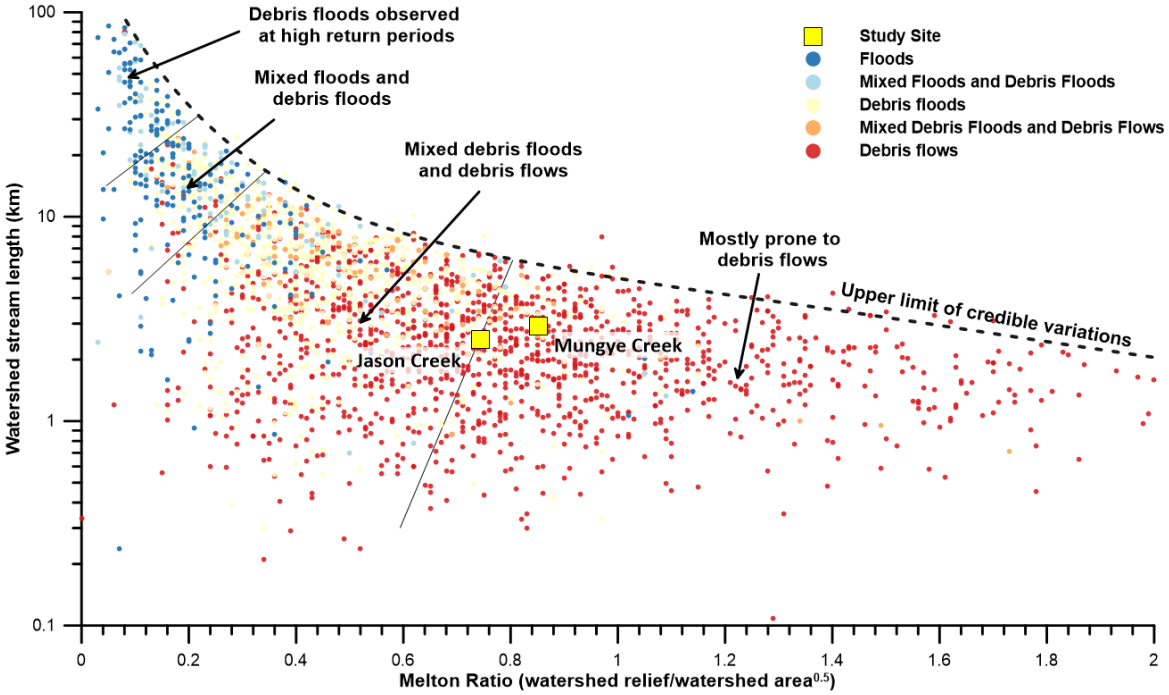

Figure 3-2. Classification of Jason and Mungye creeks with respect to hydrogeomorphic processes, based on stream length[6] and Melton Ratio.

Table 3-2. Dominant steep creek process type(s) on Jason and Mungye creeks.

Return Period Range (years)	Representative Return Period (years)[1]	Jason Creek	Mungye Creek
10 to 30	20	Debris flow	Flood
30 to 100	50	Debris flow	Debris flood (Type 1)[3]
100 to 300	200	Debris flow	Debris flood (Type 2)[3]
300 to 1,000	500	Debris flow	Debris flow
1,000 to 3,000	2,000	Debris flow	Debris flow

Notes:

1. BGC uses a representative return period to represent the return period ranges used in the risk assessment. The representative return periods approximate the geomean of the return period range.
2. Consistent with EGBC guidelines for Class 2 (medium to large subdivisions of 6 to 50 single-family lots), BGC considered return periods up to the 1,000 to 3,000-year range. The EGBC guidelines specify return periods up to 2,500 years and data collection over 1,500-years (EGBC, September 29, 2022).
3. BGC adopted the debris flood categories presented in Church & Jakob (2020). Debris flood types are introduced in Section 2.2 and described in detail in Appendix B.

In addition to watershed ruggedness (Melton ratio) estimates, travel angles and probable reach provide insight on hazards. The travel angle is the slope from the crest to the toe of a landslide. Travel angles have been recorded for many types of landslides and regressions developed to predict landslide reach by landslide volume (e.g., Corominas, 1996). For landslides equal to 2,000 m^3 in volume, and considering the “all debris flows” regression, Corominas (1996) predicts

[6] Stream length is measured upstream along the stream extending farthest from the debris fan apex.

a travel angle of 0.44 m/m. Larger volume landslides would have smaller angles, meaning they would travel farther.

This technique can be applied to evaluate the potential reach from a landslide source to a specific point of concern, like a fan apex or buildings. Considering the fan apices, a collapse of the unstable rock mass at 800 m elevation in Jason Creek has a reach angle of 0.44 m/m to the fan apex, and a collapse from the highest bluffs in the lower watershed have a reach of 0.46 m/m to the fan. Similarly, in Mungye Creek, a collapse from the highest bluffs in the lower watershed have a reach of 0.49 m/m to the fan.

This simple analysis of travel angles and reach indicates that debris flows initiating above 800 m elevation and with volumes larger than about 2,000 m^3 will reach the fan apices and travel beyond and onto fan surfaces. Smaller debris flows starting lower in the watersheds would also affect fan areas. Section 4.4 describes numerical modelling used to quantify debris-flow runout onto fan surfaces, across a range of scenarios.

3.3. Existing Development

3.3.1. Buildings

Reid Road is populated with residential properties and vacation rental cabins at Ivey Lake Lodge. The residential properties are a combination of full-time occupation primary residences and secondary properties. BGC assessed which building(s) on a property contain livable space (shown as “Building-Inhabited” on Drawing 02) and which are other building types (e.g., shed, garage, outbuilding, shown as “Building-Other” on Drawing 02) that do not contain livable space. BGC’s categorization is based on field observations collected in July 2022 where access to the property was provided by the landowner(s). For other properties, BGC assessed building use based on the site layout, building size, and information available on BC Assessment Authority online portal. This categorization is not meant to communicate the current occupancy or whether the buildings are primary or secondary residences.

There are thirteen parcels that intersect the Jason Creek fan, nine parcels that intersect the Mungye Creek fan, and seven that intersect the lower fan. A subset of these properties have inhabited building(s) within the fan area (Drawing 02). Inhabited building construction type varies across the two fans from modular tiny home to custom-built multi-story. In support of the risk assessment (Section 5), BGC visited all properties where landowner permission was provided and assessed building construction type, number of stories, height of lowest point of water ingress (usually door jam or windows) on the upslope side of the building, and any relevant observations of damage from the Nov 2021 events (Figures D-1 to D-15 in Appendix D). BGC was denied permission to access 1793 and 1788 Reid Road on the Jason Creek fan and did not receive permission to access 1709, 1717, 1718, or 1714 Reid Road.

3.3.2. Culverts

Along the study creeks, there are five culvert crossings within the study area. Jason Creek crosses Reid Road, a culvert below a residential driveway, Pemberton Portage Road, and the CN Rail line. Mungye Creek crosses Reid Road upstream of the confluence with Jason Creek

(Drawing 02). Photos and dimensions of these culverts are summarized in Figures D-16 to D-20 in Appendix D. BGC estimated the capacity[7] of the culverts below public roads and the CN Rail line using a publicly available software created and distributed by the U.S. Department of Transportation Federal Highway Administration (FHWA, 2022) called HY-8 version 7.70.2.0 (Table 3-3). These estimates are preliminary, for the purposes of comparison with anticipated flows on the creeks, and should not be relied upon for design.

Table 3-3. Summary of culvert dimensions and capacity estimates.

Creek	Crossing	Existing Culvert Dimensions	Cover Depth[2] (m)	Estimated Capacity (m^3/s)[3]	
				Top of culvert[4]	Overtop road
Jason Creek	Reid Road	1600 mm CSP[1]	1.1	4	6
	Pemberton Portage Road	1300 mm CSP	3	2	6
	CN Railway	(a) Main: 1100 mm CSP (b) North: 1150 mm CSP (c) Middle: 1250 mm CSP (d) South: 950 mm CSP	2.3 (above main culvert)	10	12
Mungye Creek	Reid Road	1500 (vertical) x 1350 mm (horizontal) CSP	1.8	3	6

Notes:
1. CSP stands for corrugated steel pipe culvert.
2. Cover depth is measured as the distance between the top of the inlet pipe and the top of the road/railway structure.
3. All capacity estimates are rounded to the nearest whole number.
4. Discharge when headwater level reaches top of inlet pipe.

3.3.3. Adhoc/Orphan Berms

Cordilleran (December 13, 2021) identified an engineered berm on the left (north) bank of Jason Creek on the Lower Fan (Drawing 02). The berm parallels the creek and based on lidar collected in July 2022 measures approximately 180 m long with variable height above natural grade ranging from 0.5 m to 1.7 m and an approximately 5 m wide crest width. BGC did not visit this berm to evaluate construction material and condition as it does not influence life safety risk on the study creeks. While this berm provides creek capacity to confine the combined flows of Mungye and Jason Creeks along lower Jason Creek, there is a scenario, whereby a Jason Creek avulsion along Reid Road can bypass the head of this feature and affect properties on lower Jason Creek fan.

Orphan berms are constructed linear features built to train flood or debris flows, or created as a by-product of creek cleaning activities, that have not been “engineered”. Specifically, they are not designed to any formal standard (e.g., impact and/or scour resilience, or crest height) by a Qualified Professional and are not under jurisdictional authority, meaning there is typically no

[7] Capacity indicates how much flow (discharge) a culvert can convey. Depending on the managing authority, capacity can be based on the peak discharge for water to reach the top of the culvert, or the peak discharge for water, and sediment, if applicable, to overtop the crossing (road, rail, etc.).

management plan in place government their monitoring and maintenance. These features are important because they train/control flows and may transfer risks.

As outlined in Cordilleran (December 13, 2021), emergency works completed during the November/December 2021 events created non-engineered berms along the left (east) bank of Jason Creek from the fan apex downstream to Reid Road. These berms are formed from material excavated from the channel. They are not engineered or fully continuous and avulsion is likely during future events at the upstream side (e.g., Photos 5, 6).

Following the 2021 events, homeowners completed remedial works on their own properties. On 1794 Reid Road, there is a berm and channel that approximately parallels Reid Road approximately 30 m south of the road. It measures approximately 45 m long and 1 m high with a 0.5 m crest width. The berm appears to be constructed of material sourced on site and to the best of BGC's knowledge, this berm is not engineered. It does not include erosion protection and BGC expects that it would have limited resistance to high velocity flows.

Reid Road was constructed as a slight through-cut (approximately 0.5 1 m deep) for the approximately 75 m distance east of the crossing of Jason Creek. This through-cut extends across the north end of lot 1782 Reid Road and would serve to redirect shallow flows down Reid Road.

3.4. Forestry Activity and History

Mungye and Jason Creeks are forested. The Ivey Lake Local Resource Use Plan outlines age class and species distribution over the watershed areas (Ivey Lake Planning Team, May 16, 2001). Approximately 85% of the watersheds is mature (>100-year-old) growth with large old growth (>250 years) along Jason Creek from the headwaters to the approximate location of the fan apex. There is no known landslide activity attributed to past logging activity.

Baumann Engineering (1997) was a detailed terrain stability assessment conducted to support proposed logging activities within Jason and Mungye Creek watersheds. The report identified the potential for logging activities within and around the creek ravines to directly impact properties on Jason and Mungye Creek fans.

Since 1997, there is one active logging block in the Mungye Creek watershed with starting harvest date in 2016, based on a provincial forest tenure database (Government of British Columbia, 2022). An adjacent block has a harvest date of 2022, but the block is not located directly within the Mungye Creek watershed and forestry roads supporting the block are not mapped within the watershed. However, there is a retired[8] forestry road in the lower part of the Mungye Creek watershed at approximately 830 m elevation. There are no active or retired logging blocks in the Jason Creek watershed. There are 2 active cut blocks located at the lower fan. Active and retired forest cut blocks as well as forestry roads in the study creek area and proximity are shown in Figure 3-3.

[8] Retired is the 'life cycle status code' available in iMapBC. A specific definition is not provided. BGC interprets this to mean that no future logging activities are anticipated in the cut block. BGC notes that retired does not necessarily indicate deactivated.

In Mungye Creek watershed, at 575 m elevation just above the fan apex there is an old logging road and landing built during first pass logging in the 1900s. This road crosses at a point of low freeboard on the channel, and it is possible that a debris flow could avulse right at the road crossing. However, there is a tributary creek flowing parallel to Mungye Creek, and the incised channel would redirect any avulsion back towards the fan apex. As described in Section 2.5, logging activities have the potential to increase the likelihood of slope failures, debris floods, debris flows, and flow avulsions in watersheds. The effects of logging on steep creek processes are further discussed in Appendix B.

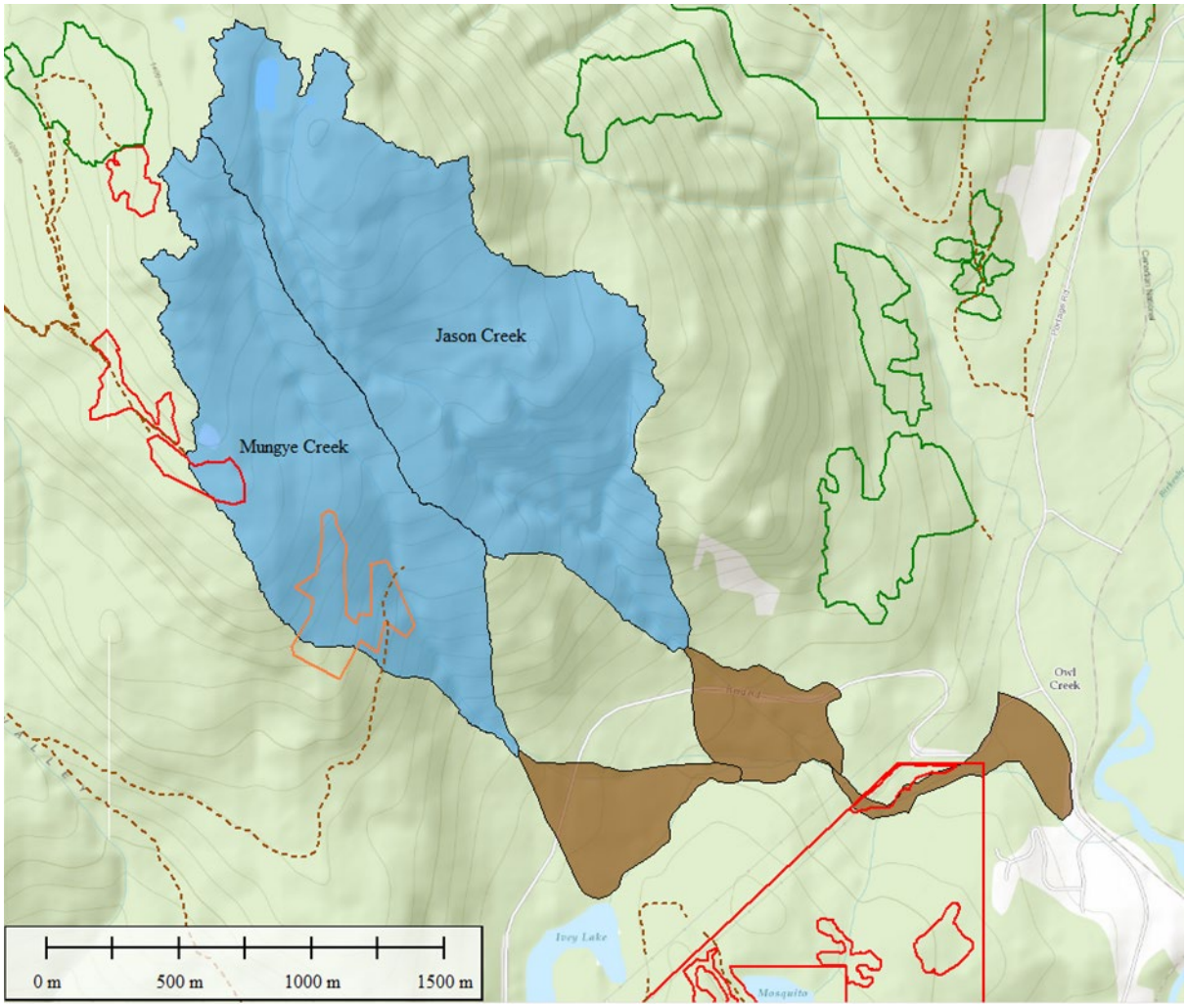

Figure 3-3. Active (red), retired (green), and orange (unknown) cut blocks and forestry roads (dashed brown) in the study area. The Jason and Mungye Creeks watersheds (blue) and fans (brown) are also shown. Map source: Global Mapper.

3.5. Wildfire History

The BC Wildfire Service (2022) has recorded no wildfire activity in Jason and Mungye creeks watersheds over the period of 1920 to 2021. BGC reviewed the wildfire history in a 30 km radius buffer zone around the site to gain insight into the regional fire frequency. Within this area, 110 historical fires were recorded between 1920 and 2021 with burned areas ranging between

0.001 km^2 to 47 km^2. The influence of wildfires on watersheds is introduced in in Section 2.6 and discussed in detail in Appendix B. The frequency and magnitude of post-fire debris flows in the study watersheds are discussed in Section 4.

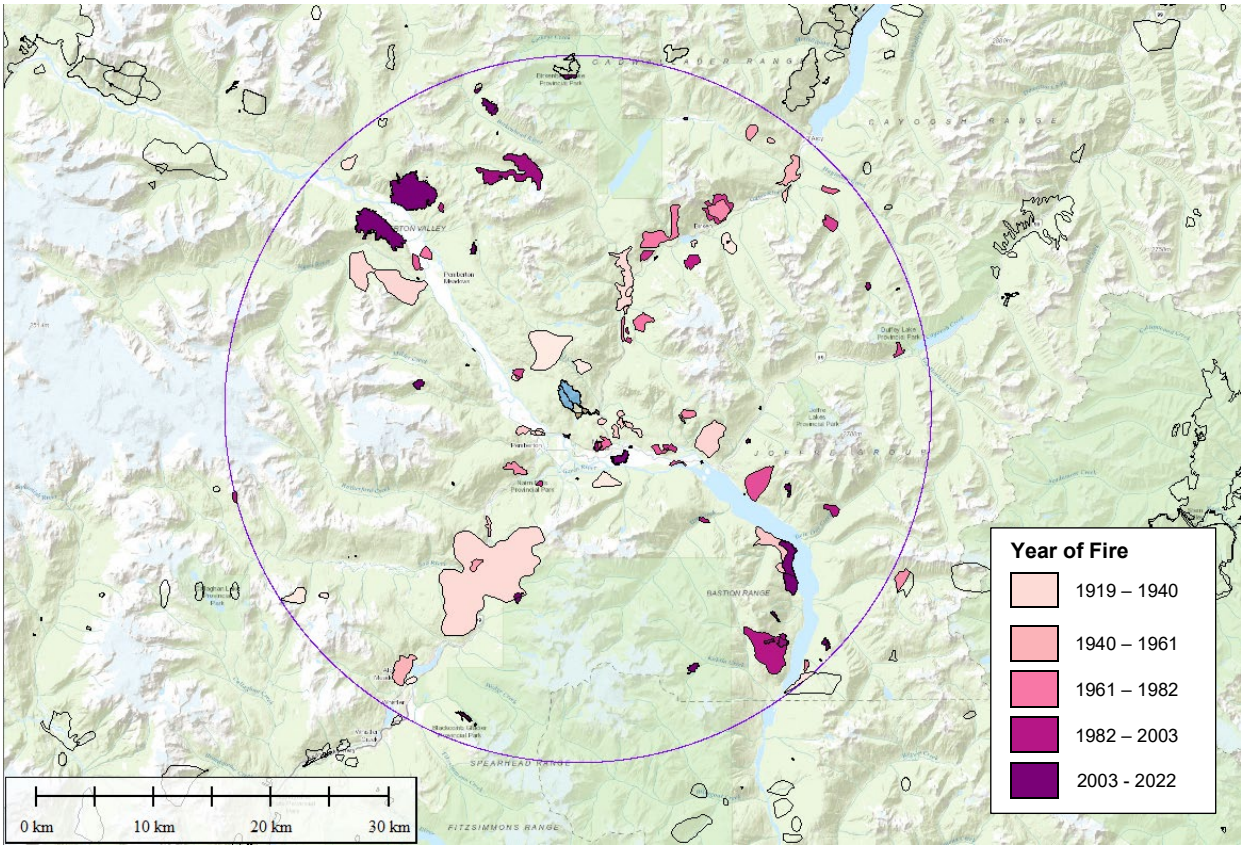

Figure 3-4. Historical fire perimeters (filled, see legend) in the area reviewed (purple), which is a 30 km buffer zone around the site. Historical fire perimeters which are outside of the buffer are outlined in black. The Jason and Mungye Creeks watersheds (blue) and fans (brown) are also shown.

3.6. Climate

BGC reviewed climate data for the area surrounding Reid Road. The closest station providing historical climate normals (1981 to 2010) is the Whistler weather station (1100875), located approximately 28.5 km southwest of the study site (Figure 3-5). Monthly precipitation is highest in the winter (November to January), and lowest in the summer (July to August) (Figure 3-5). On average, temperatures vary from -2.5°C in the winter to 16.5°C in the summer.

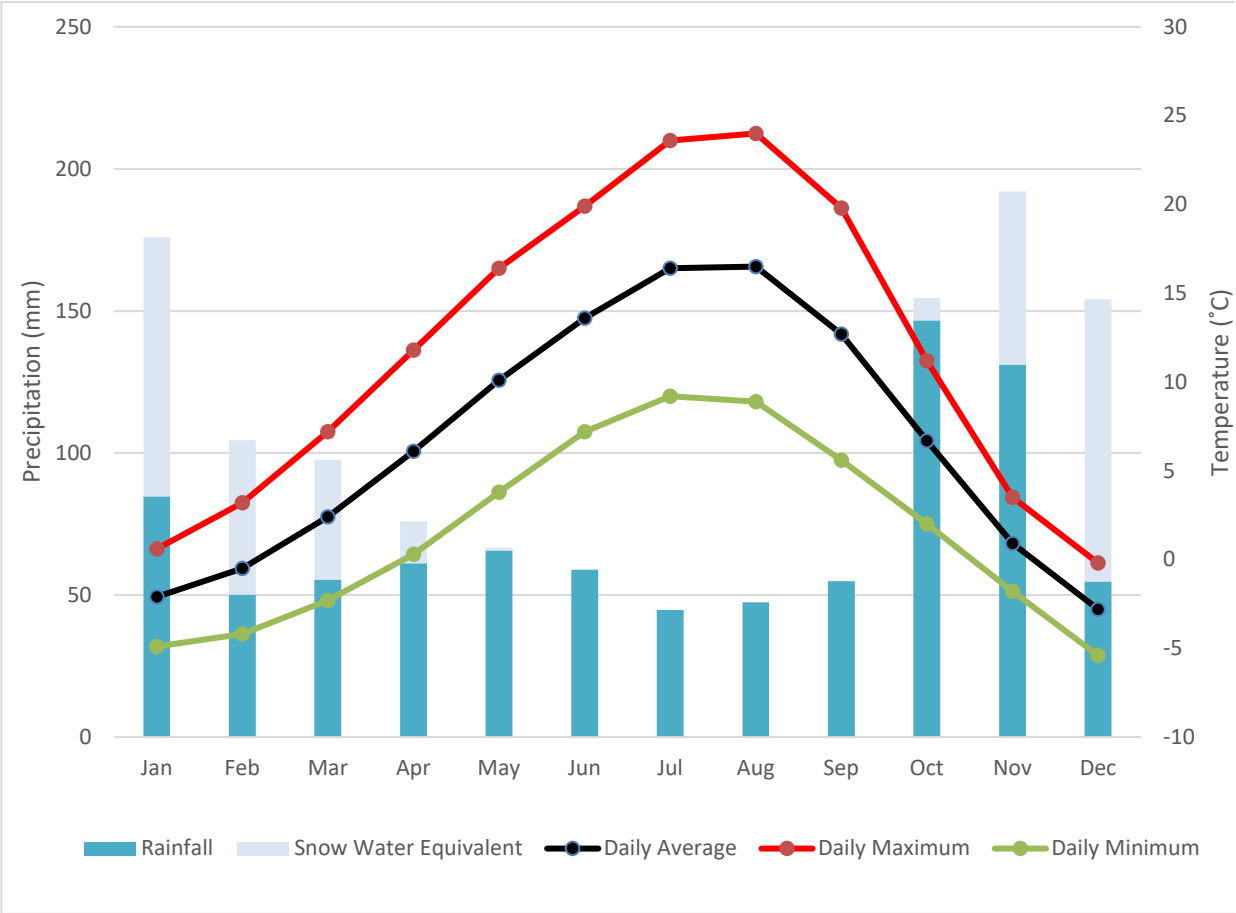

Figure 3-5. Climate normals at the Whistler climate station for 1981 to 2010.

BGC assessed the applicability of the Whistler weather station to the Reid Road study area by comparing historical intensity-duration-frequency (IDF) relationships from the Pemberton Station[9] (1086083) to that at the Whistler Station. This showed that, compared to the Whistler Station, the Pemberton area historically experienced 40 - 50% higher rainfall intensity for shorter-duration storms (6 hours or less) and 30 – 50% higher rainfall intensity for higher return period storms (20 years or more).

BGC used a precipitation model (Simonovic et al., 2015) to estimate climate-change adjusted rainfall intensity at Reid Road in support of F-M relationship development (Section 4.3). To evaluate the applicability of the precipitation model for Reid Road, BGC compared historical IDFs at four existing gauged weather stations with the gridded storm dataset from the precipitation model at those same locations. BGC assessed the following weather stations. Their location relative to the Reid Road study area is listed:

- Pemberton station, located 6 km to the southwest
- Whistler station, located 28.5 km to the southwest
- Daisy Lake Dam station, located 50 km to the southwest

[9] The Pemberton station has published IDF data based on the period of 1969 to 1984 but does not have the most recent climate normal (1981 to 2010).

- Lillooet station, located 68 km to the northeast.

BGC compared the station data to values from the precipitation model at the location of the weather stations. BGC found that on average, the station data was very close to the modeled values, and therefore no additional adjustment factor needed to be applied.

The critical months for debris-flood and debris-flow initiation are typically September to December; however, the potential for debris flows in other months of the year cannot be ruled out. In those months, antecedent moisture conditions (i.e., how much rain or snowmelt has occurred prior to a potentially debris-flow initiating storm) and high intensity and prolonged rain coincide. Particularly dangerous are situations in which a relatively thin (< 0.5 m) layer of wet snow exists followed by rapid rise in freezing level and heavy and prolonged precipitation, typical for atmospheric rivers originating in the subtropics or tropics and affecting the BC Coast, or sequences of standard north Pacific cyclones. Rainfall is still high in January, but some of it may be absorbed by accumulated snow at higher elevation that acts as a sponge delaying or hindering transfer of rainwater into the underlying forest soils. With climate change, however, the debris-flow prone season is likely to prolong with debris flows becoming more likely in all winter months as snow depth decreases in conjunction with heavier and more frequent heavy rain (Jakob and Owen, 2021). BGC considered climate change impacts on the frequency and magnitude of steep creek hazard processes on Jason and Mungye creeks as part of the hazard assessment (Section 4).

3.7. Previous Hazard and Risk Assessments

The watershed and fan complexes of Jason and Mungye creeks have been studied at various levels of detail by numerous firms and practitioners. BGC reviewed previous reports provided by the SLRD dating from 1974 to present (summary list and tabulation of key findings and BGC comments on each are provided in Appendix A). Previous reports may be grouped into four categories: 1) those produced to support the subdivision application and approval process (Blunden 1981; Piteau 1981); 2) those conducted for forest planning (Baumann Engineering, 1997); 3) higher level regional geohazard screening to support SLRD permit approvals process (Baumann Engineering, 1993; BGC, 2020); and 4) site-specific reports conducted to support subdivision or building permit application (see Appendix A). Hazard and risk conclusions from Baumann Engineering (1997) were incorporated into the local resource use plan report (Ivey Lake Planning Team, May 16, 2001).

Instabilities in the watershed have been identified by various parties since approximately 1981. The initial subdivision approval process only identified rockfall as a hazard meriting concern (Piteau, 1981), and resulted in MoTI delimiting a rockfall covenant area. BGC notes that Blunden (1981) recognized the ravine sidewall instabilities within Jason Creek, active landslide source areas, and recent debris "spreads" affecting Jason Creek fan, yet these observations were not carried through the subdivision process as conditions affecting any lots, and nor were they cited by any subsequent site-specific reports (with the exception of Baumann Engineering, 2003) conducted to support building permits. Debris-flow hazards are not specifically mentioned or described until 1997 by Baumann Engineering (1997, 2003) who describe and quantify such hazards based on air photo analysis and detailed field checking. The Baumann (1997) study

identified the initiation site of the 1990 debris flow (also noted as being an unstable area by Blunden 1981), and described the existence of sagging bedrock slopes above. Baumann (1997) outlined the high landslide hazard and potential risks affecting Jason Creek fan and the buildings situated on it. They also pointed out the inadequacy of the existing culvert on Jason Creek at Reid Road. SNC Lavalin (July 27, 1998) provided a design for a flood training berm at 1791 Reid Road, but the structure was never built.

Previous reports should be evaluated with consideration of the professional standards at the time in which they were written and the data to which previous practitioners had access (i.e., an expectation to complete air photo analysis, detailed terrain mapping of site and upslope areas, channel assessments, test pitting, stratigraphic analysis, radiometric dating and dendrochronology). Nowadays, there are additional tools, such as high-resolution topography (lidar), change detection methods (InSAR, lidar) and numerical modelling. That said, terrain mapping, channel assessments, and absolute dating techniques have existed since subdivision development but were mostly not applied in past studies with the exception of Baumann (1997) who used dendrochronologic indicators.

4. HAZARD ASSESSMENT

4.1. Introduction

Hazard assessment is the process of identifying and evaluating hazards in an area of interest. The results of a hazard assessment inform subsequent evaluation of the risks associated with the hazards and design of risk-control measures, if required.

In this study we consider steep creeks hazards with the potential to impact downstream developed areas and infrastructure and the potential influence for rock slope instability in the study watersheds. This section summarizes historical hazard events, results of the frequency-magnitude (F-M) analysis for each creek, and numerical modelling of hazard scenarios. The assessment methods applied are summarized in Figure 4-1. Additional details on the methods applied are provided in Appendices E through I.

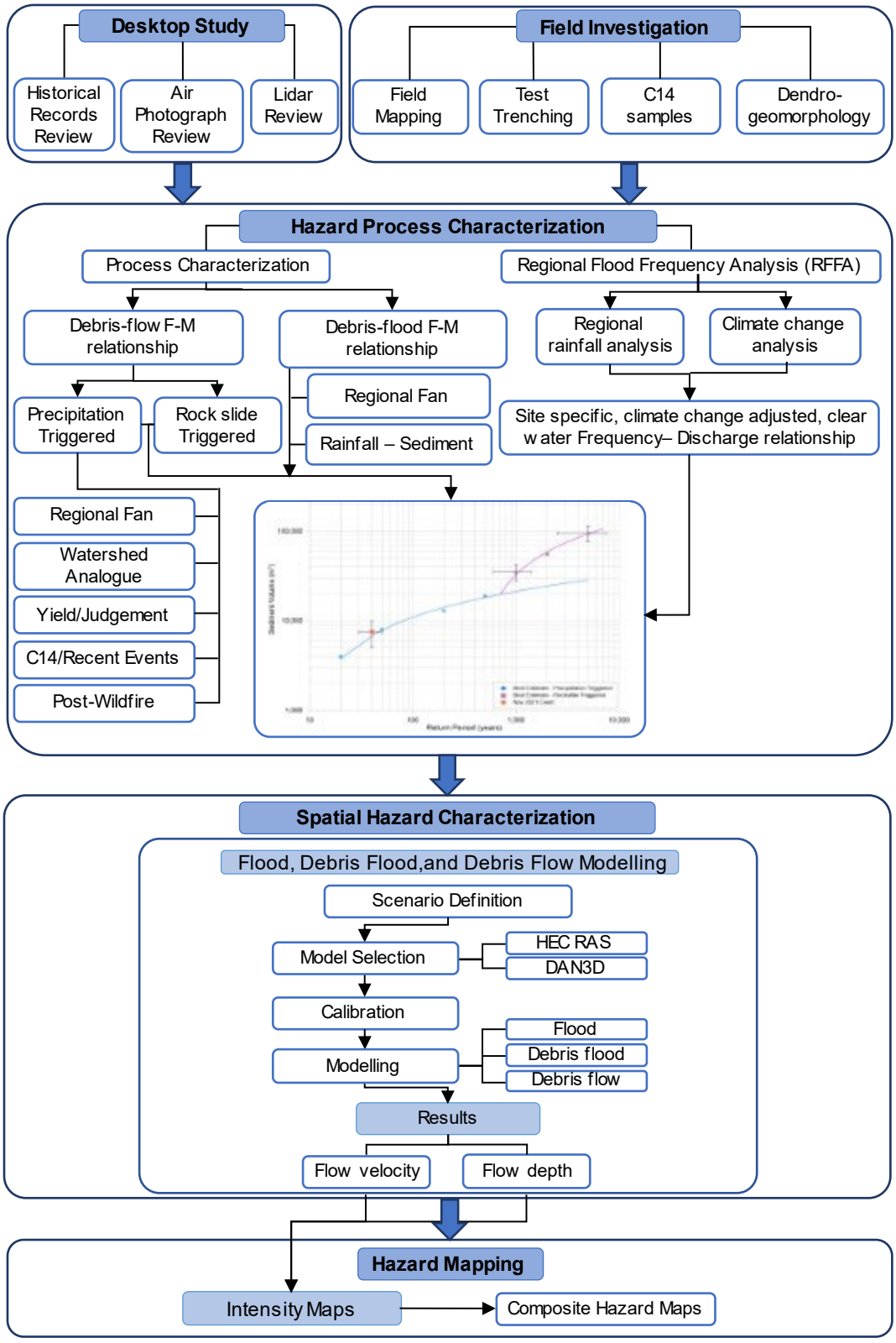

Figure 4-1. Steep creek assessment workflow (modified from Jakob et al., 2022) at Jason and Mungye Creeks.

4.2. Rock Slope Stability - InSAR Analysis

BGC contracted TRE Altamira (TRE) to complete Interferometric Synthetic Aperture Radar (InSAR) analysis of ground displacement over the study area. The objective of this analysis was to identify locations of movement and movement rates over the period of available data. TRE analyzed Sentinel-1 satellite imagery from May 2017 to June 2022. Displacement in four directions (one-dimensional (1D) line of sight ascending and descending, and two-dimensional (2D) vertical and east-west) was reported. The technique results in maps that show ground displacement at individual locations that can be queried to determine movement rates and directions over time.

TRE provided results in a summary PowerPoint that is included as Appendix E and vector shapefiles showing measurement locations and the deformation history over the time series. The data is also accessible through a web-map service for data visualization and interrogation. BGC reviewed the InSAR data to assess displacement at the locations of rock slope instability identified during field traverses and evident in lidar (Drawing 03). The measured displacement on the southern rock mass was 3.1 mm/year vertically downwards with a component of movement towards the east at a rate of 2 mm/year (Figures E-3 and E-4 in Appendix E).

This analysis supports BGC's field observations and geomorphic mapping to confirm that, over the period of observation, there is displacement of this rock mass. Additional analyses or monitoring in the future would be required to evaluate if the displacement is increasing over time to a threshold that could indicate failure of the unstable rock mass(es) is likely.

In the event of partial or full failure of these rock masses, BGC expects that the failed volume would travel downslope entraining (picking up) additional material from the unstable slopes immediately below and then along the Jason Creek channel further entraining material before depositing on the fan surface.

The InSAR analysis suggests there may be ongoing deformation of the cliff above the rock slide covenant area east of Jason Creek. This area was not included in BGC's scope, and no follow up detailed displacement analysis was conducted by BGC at this site. At the request of the SLRD, BGC could analyze displacement in this location and summarize as a memo under separate cover. BGC also recommends that the SLRD review whether updating of past assessments for this area are warranted with the benefit of the lidar acquired in 2022.

4.3. Site History

The geomorphological history of a site can be assessed through anecdotal observations, historical records, air photo and satellite imagery interpretation, and field observations, namely stratigraphic analysis, radiocarbon dating, and dendrochronology. The following sections summarize the key findings from each of these methods.

4.3.1. Anecdotal & Historical Records

Baumann (1997) compiled the following anecdotal observations:

"*Evidence was found for at least four [historical] debris flow events, the oldest dating to about 1900 A.D. Evidence for this event comes from a scarred cedar tree that was logged in the 1920's. An event 40 to 50 years ago [~1952±5 yrs] was aged approximately by the age of hemlock and cedar trees growing on a debris levee. According to Dr. Raymond Rogers, a debris flow reached the lower portion of the fan sometime around 1970. Successional brush along the lower channel, visible on the air photos, provides evidence of this event. Local residents described a small debris flow that deposited on Reid Road in 1990.*"

4.3.2. Aerial Imagery Interpretation

BGC reviewed air photos from 1946 to 2016, satellite imagery from 2019, and a high-resolution orthophoto acquired in July 2022. A high-level review of GeoBC imagery from 1981, 1986, 1994, 2005 and 2016 was also undertaken. As no evidence of historic debris floods or debris flows were present in these images, they were not examined further. A detailed summary is provided in Appendix G and observations are shown on Drawing 06.

Over the record of aerial imagery reviewed (76 years), BGC did not identify any evidence of historic debris floods or debris flows large enough to be evident on aerial imagery (Brardinoni et al., 2003) except for the November/December 2021 debris flows on Jason Creek.

4.3.3. Stratigraphic Analysis and Radiocarbon Dating

Cordilleran and BGC excavated 11 test pits and examined two natural exposures on Jason Creek fan and four test pits on Mungye Creek fan (Drawing 07).

Test pit logs and radiocarbon dating results from Beta Analytics are included in Appendix D. Lab results present radiocarbon ages as conventional 14C and calibrated calendar years before 1950. In our results, we have presented dates as calibrated calendar years before 2022.

4.3.4. Dendrogeomorphology

BGC collected 20 tree core samples and six tree slice samples during field visits in July and September 2022 (Drawing 07). BGC estimated the age of historical debris flows using evidence of impacts to the tree and tree ring dating. Based on the samples collected, BGC estimated that debris flows have occurred approximately every 12 to 17 years on Jason Creek. The debris flows were of sufficient size to impact trees adjacent to the channel, but not of sufficient intensity to knock the trees down or leave any appreciable evidence in aerial imagery (Section 4.2.2.). BGC did not collect dendrogeomorphology samples from the Mungye Creek watershed. As a result, BGC did not estimate a historic debris-flow frequency from dendrogeomorphology on Mungye Creek. A detailed description of dendrogeomorphology analysis results is included in Appendix G.

4.3.5. Summary

BGC has reconstructed the site history at Jason and Mungye Creek using a combination of historic records, aerial imagery, and field investigations. The combination of these methods indicates the following:

- Jason Creek
    - Small debris flows that were mainly contained within the channel have occurred approximately every 12 to 17 years.
    - The 1990 and 2021 debris flows originated from the same location. Tension cracks above the headscarp of these failures indicate the potential for future instability.
    - Debris flows have followed the modern channel on the west side of the fan for approximately 1,200 years with evidence of debris flows or debris floods resulting from debris flow dilution approximately every 100 to 500 years.
    - In the central section of the fan, there is evidence of at least two and possibly three large debris flows (deposit thickness of 0.25 -2 m) in the last 2,000 to 3,000 years BGC interprets these events to be the result of rock slope failures (rock slides) impacting saturated fault-gouge rich material that transitions into debris flows in the channel. These are large point source events with volumes >10,000 m^3, ranging up to 35,000 – 75,000 m^3 (Section 4.3).
    - No evidence of debris flow runout below approximately elevation 380 m was observed. Two test pits below this elevation yield radiocarbon ages of 4,000 - 8,000 years BP.
- Mungye Creek
    - No historic debris floods or debris flows large enough to leave a signature on aerial imagery were observed from 1946 to 2021 (75 years).
    - A small slump on the left bank at 650 m elevation was noted in 1997, and this feature appears little changed since then.
    - A debris-flow occurred approximately 1,200 years ago and deposited material approximately 1.2 to 1.5 m deep in the east side of the fan, above and below Reid Road, as observed in two of four excavated test pits.

4.4. Frequency-Magnitude (F-M) Analysis

F-M analysis of steep creek hazards answers the following questions:

- How frequently have steep creek hazards occurred in the past and frequently will they occur in the future?
- When they occur, how much sediment and water volume will be transported and what will be the likely peak discharge (volume and peak discharge are referred to collectively as “magnitude”)?
- How will the answers to the two questions above change with continued climate change?

The answers to these questions are presented in the form of a frequency-magnitude (F-M) pairs for specific return periods on each creek. Estimating the most realistic F--M relationships is important, as it influences the outcome of numerical modelling, informs risk assessments, and is a fundamental design input for potential mitigation measures.

4.4.1. Methods

BGC and Cordilleran used a suite of techniques to assess the F-M relationships for Jason and Mungye creeks informed by industry practice and ongoing research. By doing so, we increase the overall confidence in the results as individual techniques have considerable uncertainty and

limitations. The use of model ensembles is done routinely for weather forecasts, hurricane prediction, El Niño Southern Oscillation (ENSO) forecasts, and climate change models. The assessment methodology applied to develop the F-M relationships is shown schematically on Figure 4-1 and Figure 4-2 and described in detail in Appendix G along with a description of the associated uncertainty and limitations.

4.4.2. Climate Change Considerations

Jakob and Owen (2021) found that the North Shore Mountains are expected to experience a three-fold (300% increase) increase in shallow landslide frequency associated with climate change assuming the Relative Concentration Path (RCP) of 8.5. Shallow landslides, when they occur on slopes upstream of creeks, can directly trigger debris flows or impound the creek leading to debris flows when the water breaches the landslide deposit. The authors predicted this increase in frequency would be accompanied by an increase of 50% in average expected landslide volume.

Jakob and Owen's (2021) work examined regional debris-flow frequency and magnitude. Their findings cannot be directly translated to individual creeks as they do not account for sediment supply limitations[10], as more frequent debris flows can result in lesser magnitudes due to the time required for sediment to build up in the channel between events. What can be said, however, is that debris-flow frequency will increase in conjunction with higher rainfall intensities and higher antecedent conditions. For Jason Creek, where active instability of ravine sidewalls feeds debris to the channel, the presence of slopes containing abundant fault-gouge suggests that the creek is quasi-sediment supply unlimited and may not require long periods of time to 'recharge' (Jakob et al., 2005; Jakob, 2021). For this reason, in response to climate change, more frequent debris flows with similar, or larger sizes, may be expected on Jason Creek. Mungye Creek has a similar watershed size and geology; however, BGC observed less evidence of instability in the watershed. For this reason, more frequent debris floods and debris flows on Mungye Creek may result in lesser magnitudes in response to climate change. However, the response of larger deep-seated landslide events on either creek is harder to predict.

With continued summer heating and drying, the chance of wildfires increases, especially with proposed urbanization as this increases the possibility of human-caused fires (cigarette butts, campfires, barbeque fires, arson). Wildfires in the Jason or Mungye creek watersheds could be followed by post-wildfire debris flows in the few years immediately following the fire. BGC reviewed post-wildfire potential on the study creeks as part of the F-M analysis.

BGC made the following adjustments to the F-M considering climate change effects:

- Integration of climate-adjusted rainfall totals as part of rainfall-runoff analysis (Appendix F). Climate-adjusted totals are for the end of century (2100) with an estimated increase from historic conditions of 16 to 23% (return period dependent) (Simonovic et al., 2015).

[10] Sediment supply limitation refers to the amount of sediment within a creek system that can be mobilized during a debris flood or debris flow. In a sediment-supply limited watershed, the amount of available sediment is lower following a debris flood or debris flow and requires time to 'recharge' to a pre-event volume. In a quasi-sediment supply or fully sediment-supply unlimited creek, there is sufficient available material within a channel to have an event the same size, or larger, in the near-term following a debris flood or debris flow.

- Assessment of post-fire debris-flow frequency and magnitude on Jason and Mungye creeks given increases in air temperature that enhance drying (natural and human-caused fires) and development in the areas around Reid Road (human-caused fires).

The relative effects of these factors are captured in Table 4-3. Notably, the influence of fires is short term (<10 years). Reconstruction of long-term terms from stratigraphy and other methods incorporates these short-term trends to provide long-term historic averages.

Table 4-1. Summary of climate change effects on debris flood and debris flow F-M relationships.

Effect	F-M impact	Confidence
Increases in extreme rainfall frequency	Moves the F-M curve to the left (more frequent events of the same or higher magnitude)	Very High
Increases in extreme rainfall intensity	Moves the F-M curve upwards (larger events at the same return period)	Very High
Increase in wildfire burn severity	Addition of post-fire F-M	High

4.4.3. F-M Relationships

4.4.3.1. Jason Creek

BGC identified two debris-flow triggering mechanisms in the Jason Creek watershed:

- **Precipitation-triggered debris flows** that originate in the watershed in response to periods of high rainfall and antecedent moisture conditions[11].
- **Rock slide-triggered debris flows** that originate in the watershed in response to partial or full failure of unstable rock masses.

Debris flows that originate from either precipitation- or rock slide-triggering can travel downslope and impact the developed areas of the fan and downstream in a matter of seconds to minutes with little to no time to move out of harms' way. Debris flows can also occur in a series of pulses that each take seconds to minutes but collectively persist over an hour or more (e.g., Neff Creek in 2015; Lau, 2017; Westrek, 2016).

BGC's best estimate F-M relationship for debris flows on Jason Creek is outlined in Table 4-2 and shown in Figure 4-2. Based on the information collected and reviewed, BGC interprets that rock slide-triggered debris flows are relatively rare and historically have occurred at return periods greater than approximately 1,000-years with observed deposit thicknesses on properties ranging from 0.5 - 2 m. In absence of additional monitoring, BGC cannot assess if the future probability of rock slide-triggered debris flows is increased/increasing above historic rates.

BGC assessed post-wildfire debris flows as part of this analysis using empirical relationships developed in California (Gartner et al., 2014) and applied elsewhere in BC (e.g., Lytton, Sicamous, Britannia Beach). The empirical relationships predicted sediment volumes comparable

[11] Antecedent moisture condition refers to how wet or saturated the soil is prior to a period of heavy rainfall.

to or lower than the best estimates presented in Table 4-2. As such, the post-wildfire F-M relationships are not presented separately but instead are included within the ranges presented. This does not imply that a wildfire would have no effect on F-M in the watershed should it occur. BGC recommends that if a fire occurs in one of the study creek watersheds, a site-specific post-wildfire debris-flow assessment be undertaken.

Table 4-2. Best estimate F-M relationship for Jason Creek

Representative Return Period (years)	Process Type	Sediment Volume (m^3)		Peak Discharge (m^3/s)	
		Range	Best Estimate	Range	Best Estimate
20	Precipitation-triggered debris flow	1,000 – 8,000	4,000	30 - 170	100
50		5,000 – 10,000	8,000	110 - 200	170
200		7,000 – 15,000	13,000	150 - 280	250
500		7,000 – 27,000	19,000	150 - 450	340
2,000	Rock slide-triggered debris flow	35,000 – 75,000	55,000	550 - 1020	790

Notes:
1. Return period ranges are shown in Table 3-2 and represented by a single return period here.
2. Best estimates are a weighted average of constituent techniques (described in Appendix G).
3. BGC rounded sediment volumes to the nearest 1,000 m^3.
4. BGC rounded peak discharges to the nearest 10 m^3.

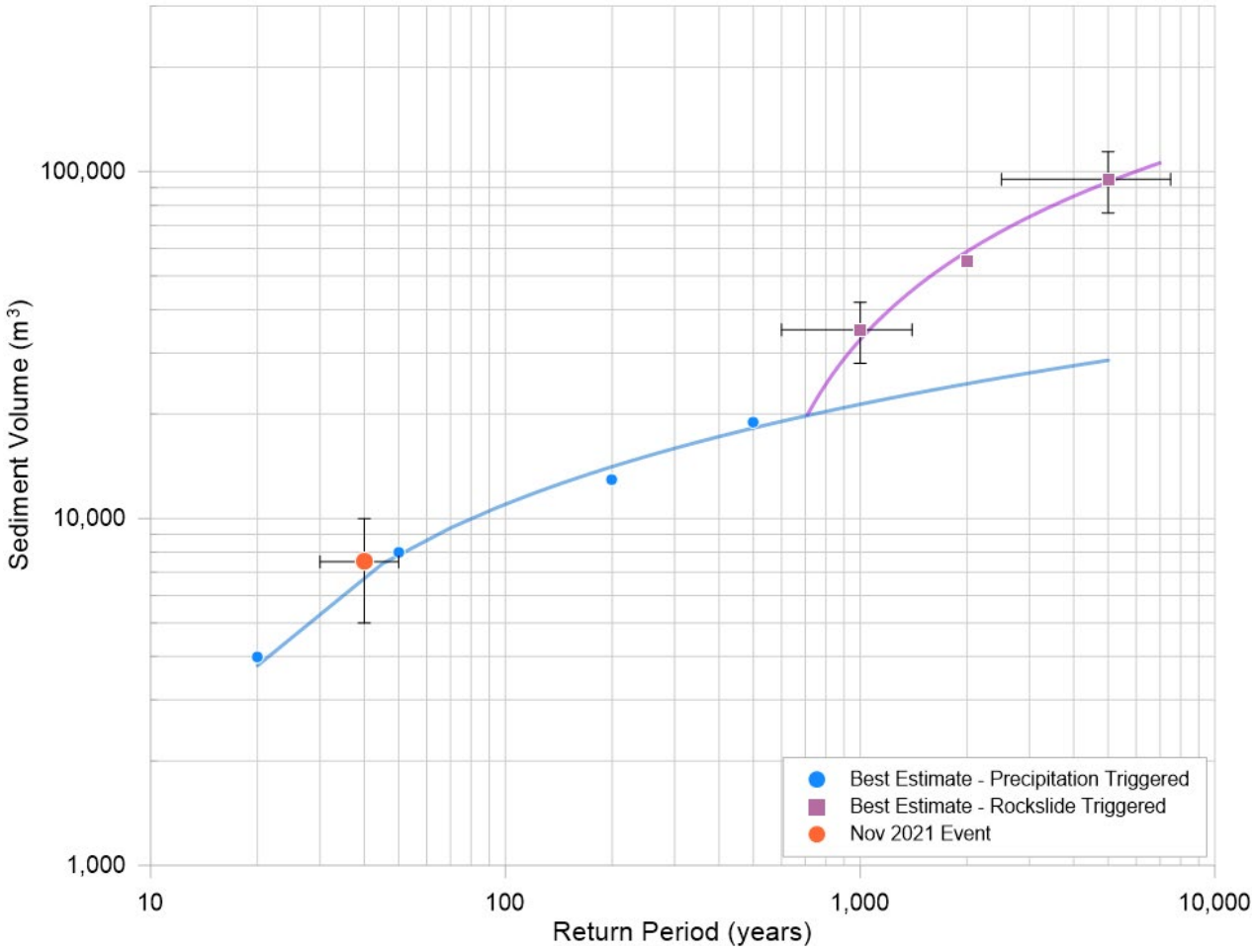

Figure 4-2. Best estimate frequency-magnitude relationship for Jason Creek.

4.4.3.2. Mungye Creek

BGC characterized Mungye Creek as susceptible to range of steep creek process types (Section 3.2.2). At lower return periods, BGC has interpreted that Mungye Creek is susceptible to flood and debris flood hazards, while at higher return periods, Mungye Creek is susceptible to debris flows. BGC's best estimate F-M relationship for Mungye Creek is outlined in Table 4-3 and shown in Figure 4-2. As with Jason Creek, BGC considered post-wildfire debris flows on Mungye Creek and the predicted sediment volumes are within the ranges presented.

Table 4-3. Best estimate F-M relationship for Mungye Creek

Representative Return Period (years)	Process Type[1]	Peak Discharge (m^3/s)			Sediment Volume (m^3)	
		Climate-adjusted[2]	Bulking Factor[3]	Best Estimate[4]	Range	Best Estimate
20	Flood	2.1	1.0	2.1	-	-
50	Debris Flood (Type 1)	3.0	1.1	3.3	-	2,500
200	Debris Flood (Type 2)	4.6	2.0	9.2	3,000 – 16,000	7,500
500	Debris Flow	-	-	260	4,000 – 22,000	14,000
2,000		-	-	410	5,000 – 41,000	24,000

Notes:

1. BGC adopted the debris flood categories presented in Church & Jakob (2020). Debris flood types are introduced in Section 2.2 and described in detail in Appendix B.
2. Climate-adjusted peak discharge is the instantaneous peak discharge for the end of century (2050-2100) based on RCP 8.5.
3. Bulking factor selection is described in Appendix G. BGC assigned a bulking factor of 2 for the 200-year return period to account for higher sediment concentration associated with debris flow dilution immediately upstream of the fan apex.
4. Best estimate of peak discharge for debris floods is the bulked peak instantaneous discharge rounded to one decimal place and for debris flows is calculated as described in Appendix G and rounded to the nearest 10 m^3.
5. Best estimates of sediment volumes are based on a weighted average of constituent techniques as described in Appendix G and rounded to nearest 500 m^3 for debris floods and nearest 1,000 m^3 for debris flows.

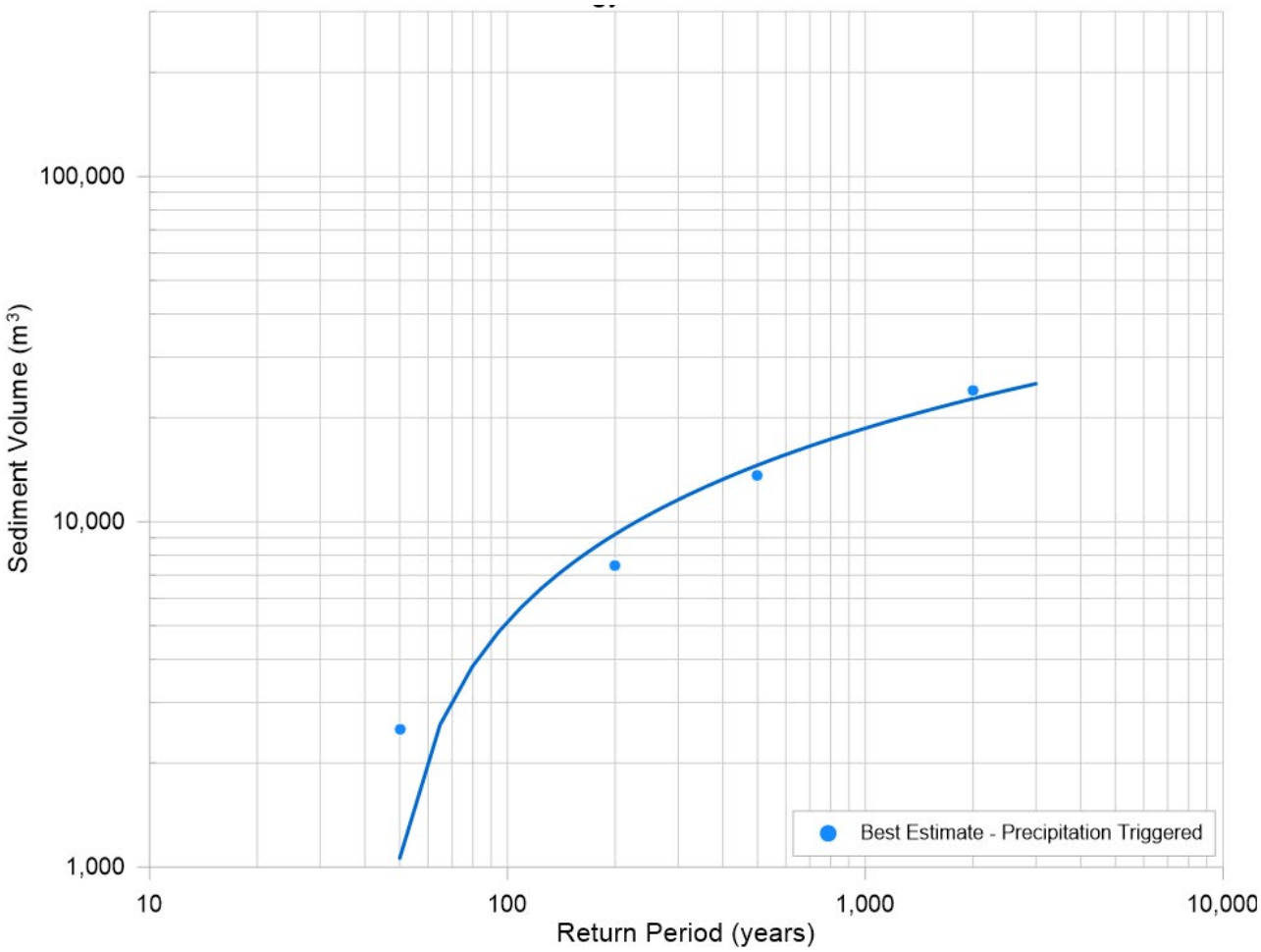

Figure 4-3. Best estimate frequency-magnitude relationship for Mungye Creek.

4.4.4. Uncertainties and Limitations of Frequency-Magnitude Relationships

With flood frequency analysis (FFA), annual flood peaks provide extreme values from which to extrapolate peak flows at various return intervals up to about twice the record length. Where streams are continuously gauged a good data set emerges allowing statistical FFA

In landslide studies there is not a convenient data set to use for prediction. Landslides are stochastic, appearing random in their occurrence; while we do understand forcing mechanisms, the link between the driver and the event is multifactorial (antecedent moisture conditions, rain-on-snow; short duration precipitation) and uncertain, and this makes estimation of F-M curves more challenging. Reconstruction using stratigraphic evidence is challenging because fans are architecturally complex; they are built by depositional events, and subsequently partially eroded by the creek that feeds them. Thus, it is difficult to correlate units from one test pit to another. Further radiocarbon dating provides bracketing ages, rather than direct and absolute ages, for landslide deposits; this further makes correlation difficult. While confidence in the understanding of the stratigraphy will increase with the amount of effort invested in subsurface investigation, expert judgement is always required to formulate the F-M model. In this case BGC considered point source volumes in the watershed, channel assessment to predict precipitation-triggered

debris-flow volumes, a regional F-M model based on fan areas (Jakob et al., 2020), fan stratigraphy, and radiocarbon dating.

4.5. Numerical Modelling

Numerical modelling of hazard scenarios based on the F-M relationships developed for each creek answers the following questions:

- When steep creek hazards occur, how far do they spread across the fan?
- How deep and fast is the flow during a steep creek event?
- What impact forces (the product of the flow depth, velocity, and density) are produced during these events?

BGC completed numerical modelling using a combination of DAN3D, used for the analysis of rapid landslide motion across complex 3D terrain, developed at the University of British Columbia, and HEC-RAS 2D (version 6.2), a public domain hydraulic modelling program developed and supported by the United States Army Corps of Engineers. Appendix H describes the numerical modelling methodology.

4.5.1. Hazard Scenarios

Hazard scenarios represent specific events of a particular frequency and magnitude that may impact a site. Hazard scenarios are organized by representative return period. BGC modelled the hazard scenarios summarized in Table 4-4 and Table 4-5.

4.5.1.1. Jason Creek

BGC modelled debris flows on Jason Creek for all the return periods considered. HEC-RAS was used for precipitation-triggered debris flows (representative return periods of 20-, 50-, 200-, 500-years). A combination of HEC-RAS and DAN3D was used for rock slide-triggered debris flows (representative return period of 2,000-years). For all model scenarios, BGC assumed that the culverts along the channel would block with debris during a debris flow as the culverts are undersized relative to anticipated peak discharges (Section 3.3.2), and culverts are not effective at conveying the debris and woody debris mobilized in a debris flow.

All debris-flow modelling in HEC-RAS was completed in two-phases (coarse front and muddy afterflow) to evaluate the flow depth, velocity, and impact intensity of each phase of the flow. Further detail is provided in Appendix H.

Table 4-4. Jason Creek model scenarios.

Representative Return Period (years)	Modelling Software	Process	Scenario Description	Conditional Probability[1] (%)
20	HEC-RAS	Debris flow	Culverts blocked	100
50	HEC-RAS	Debris flow	Culverts blocked	100
200	HEC-RAS	Debris flow	Culverts blocked	100
500	HEC-RAS	Debris flow	Culverts blocked	100
2,000	HEC-RAS	Debris flow	Culverts blocked	100
	DAN3D	Debris flow	Culverts blocked.	- [2]

Notes:

1. Conditional probability is used in the risk assessment when multiple scenarios are included for a single return period. In these instances, the conditional probability is used to combine the result from the sub-scenarios and expresses the assessed likelihood of the sub-scenario. For every return period, the cumulative conditional probability of all sub-scenarios must total 100.
2. BGC did not assign a conditional probability to the DAN3D model results as they informed the F-M relationship, hazard zonation, and risk assessment, but were not directly included.

4.5.1.2. Mungye Creek

BGC modelled flood, debris flood, and debris flows on Mungye Creek using HEC-RAS. For all return periods greater than 20-years, BGC assumed that the culvert at Reid Road would block due to a combination of sediment and woody debris. For the 20-year return period, BGC assigned a 50% probability to culvert blockage as the anticipated peak discharge (Table 4-3) approaches the capacity of the culvert.

Table 4-5. Mungye Creek model scenarios.

Representative Return Period (years)	Modelling Software	Process	Scenario Description	Conditional Probability[1] (%)
20	HEC-RAS	Flood	Culvert blocked	50
			Culvert unblocked	50
50	HEC-RAS	Debris Flood (Type 1)	Culvert blocked	100
200	HEC-RAS	Debris Flood (Type 2)	Culvert blocked	100
500	HEC-RAS	Debris Flow	Culvert blocked	100
2,000	HEC-RAS	Debris Flow	Culvert blocked	100

Notes:
1. Conditional probability is used in the risk assessment when multiple scenarios are included for a single return period. It is used to combine the results from the sub-scenarios and expresses the assessed likelihood of the sub-scenario. For every return period, the cumulative conditional probability of all sub-scenarios must total 100.

4.5.2. Modelling Results

Numerical model results for individual hazard scenarios are included in Appendix H (Figures H-5 to H-15). The results are presented as intensity (flow depth x velocity^2) which is a measure of the destructive potential of flows and informs the risk assessment (Section 5). The intensity is the maximum combined intensity of the coarse front and muddy afterflow. The following subsections outline site-specific observations.

4.5.2.1. Jason Creek

The coarse front of the debris flow deposits in the existing Jason Creek channel and changes the topography such that channel capacity at the apex is reduced and muddy afterflows avulse (leave the channel) east and across the fan surface as well as eastward along Reid Road for all the scenarios considered. Blockage at the culvert at Reid Road further encourages flow onto and downslope along Reid Road.

The property at the fan apex (1781 Reid Road) is impacted by flows for all return periods considered. Debris flows with return periods greater than 20-years impact the property with sufficient intensity to result in structural damage and life safety risk (intensity >3 m^3/s). Properties downstream of Reid Road (1782, 1788, 1794, 1802 Reid Road) are impacted by the muddy afterflow for return periods up to approximately 1,000-years associated with precipitation-triggered debris flows. For rock slide-triggered debris flows, the coarse front is expected to reach the properties with significantly higher impact intensities.

Flow along Reid Road is directed eastward and around a bedrock outcrop that directs flow downstream and into properties on the Lower Fan.

4.5.2.2. Mungye Creek

Flow on Mungye Creek is contained within the confined channel upstream of Reid Road for return periods up to 200-years. At higher return periods, flow overtops the channel banks on both sides of the channel with greater runout extents on the west side. Blockage of the culvert at Reid Road directs flow onto the road, eastward and downstream into properties. There are localized topographic lows along the Mungye Creek channel downstream of Reid Road where flow avulses at return periods greater than 50-years.

4.5.3. Auxiliary Hazard Scenarios

It is not possible to model all potential hazard scenarios at a given site given the random nature of natural processes and uncertainties associated with flow behavior. As a result, auxiliary hazards not identified in the numerical results are possible on the study creeks. The probability and estimated frequency of such events is not easily assigned and therefore BGC did not assign return periods for them. Auxiliary hazards on the study creeks include:

- Earthquake-triggered rock slides could be larger than the volumes assessed as part of the present study in response to a sufficiently large earthquake.
- Changes to the channels over time, in particular aggradation in the reach of Jason Creek upstream of Reid Road where the channel is deepened and widened from its natural condition, would reduce the channel capacity and increase the likelihood of flow avulsion.
- Interaction of steep creek hazards with observed instability outside of the study creek watershed and fan areas, for example, erosion at the toe of the landslide mapped immediately east of Jason Creek fan apex could result in additional sediment mobilization and/or additional slumping of the landslide mass.

4.5.4. Uncertainties and Limitations of Numerical Modelling

BGC numerically modelled floods, debris floods, and debris flows on the study creeks. All numerical modelling is subject to uncertainty and limitations that can be categorized according to the random nature of natural processes, model inputs, and model limitations. A summary of the uncertainties and limitations of modelling at Jason and Mungye creeks is provided in Appendix H. Importantly, modelling is based on the current topography and the influence of future modifications in the study creek watersheds and fan areas (e.g., associated with mitigation) should be reviewed to determine if there is a resultant change in the hazard and risk.

4.6. Composite Hazard Map

BGC presents the results of the hazard assessment in the form of a “composite hazard map.” A composite hazard map defines hazard levels based on a combination of hazard likelihood and destructive potential (intensity) (Drawing 08). In other words, for any location in the study area, it describes how often and how intense a debris flood or debris flow could be. By combining both hazard frequency and intensity for multiple hazard scenarios, such maps exemplify true hazard. The warmer the colour, the higher the hazard (i.e., dark reds signify a higher hazard than, for example, yellow).

BGC generated the composite hazard map in Drawing 08 using the methods in Appendix I. The composite hazard map does not provide information on the frequency of debris floods or debris flows at specific locations, nor does it allow interpretation of site-specific impact forces. This information, if required, can be determined from the numerical modelling results for individual hazard scenarios (Section 4.4.1).

The composite hazard map is based on BGC's current understanding of steep creek hazards and topography at the site. The hazard zones are not and cannot be precise and should not be interpreted as such. Debris flows and debris floods are to some extent chaotic processes and their exact behaviour cannot be predicted with accuracy. The composite hazard map does not account for any future mitigation measures designed to deflect or stop debris or provide additional bank armouring. The composite hazard map fails to account for any major fan surface alterations by steep creek processes, bank erosion, or by construction. It also does not account for the presence of structures and their effects on flow. Any future global (i.e., for the entire fans) mitigation measures will, depending on their scale, location, and effectiveness, reduce the hazard. Future mitigation measures warrant re-modelling of floods, debris floods, and debris flows to estimate the effect of hazard reduction cartographically.

4.7. Summary

BGC coordinated InSAR analysis of ground displacement over the study area to identify locations of movement and movement rates over the period of available data. This analysis showed displacement on the interpreted unstable rock masses in the lower Jason Creek watershed (Drawing 03). In the event of partial or full failure of these rock masses, BGC expects that the failed volume would travel downslope entraining (picking up) additional material from the unstable slopes immediately below and then along the Jason Creek channel further entraining material before depositing on the fan surface. Additional analyses or monitoring in the future would be required to evaluate if the displacement is increasing over time to a threshold that could indicate failure of the unstable rock mass(es) is likely.

BGC reviewed historic records and aerial imagery, and completed stratigraphic analysis, radiocarbon dating, and dendrogeomorphology to reconstruct the geomorphological history of the study creeks. BGC determined that small debris flows that remain within the channel or immediately adjacent areas are relatively common on Jason Creek (approximately every 12 to 17 years). Larger debris flows occur less frequently approximately every 100 to 500 years as evidenced by deposits observed along and adjacent to the creek channel along the western edge of the fan. Debris flows sufficiently large to move boulders at the scale observed in the central sector of the fan (3 - 5 m diameter) have occurred two to possibly three times in the past 3,000 years. BGC believes that debris flows of this magnitude have historically been triggered by rock slides in the watershed, while the smaller debris flows are triggered by precipitation. On Mungye Creek, BGC did not observe any debris floods or debris flows sufficiently large to leave a signature on air photos over a 75-year period. A destructive debris flow occurred approximately 1,200 years ago affecting the east side of the fan.

Using a model ensemble approach, BGC developed F-M relationships for Jason and Mungye creeks that informed selection of hazard scenarios to evaluate using numerical modelling. The model ensemble approach increases confidence in the best estimate by integrating multiple techniques. Numerical modelling was completed using HEC-RAS and DAN3D (rock slide-triggered debris flows). Modelling of debris flows in HEC-RAS included a coarse front followed by a muddy afterflow.

The model results indicate that the property at the fan apex on Jason Creek (1781 Reid Rd) is impacted by the coarse front for all scenarios considered and properties downstream of Reid Road are impacted by lower intensity muddy afterflows associated with precipitation-triggered flows. Rock slide triggered-debris flows impact the property at the apex and multiple located downstream of Reid Road. On Mungye Creek, flow is well confined in the channel upstream of Reid Road for lower return periods and avulses at higher return periods. Blockage of the culvert at Reid Road results in flow running eastward and downslope into neighbouring properties.

The numerical modelling results informed development of a composite hazard map (Drawing 08). Future mitigation measures will require re-modelling of floods, debris floods, and debris flows to estimate the effect of hazard reduction cartographically

5. RISK ASSESSMENT

5.1. Introduction

Risk is a measure of the probability and severity of an adverse effect to health, property, or the environment, and is estimated by the product of hazard probability (or likelihood) and consequences (Australian Geomechanics Society (AGS), 2007).

The risk assessment is based on the results of the hazard assessment (Section 4) and considers the range of hazard scenarios defined in Section 4. BGC assessed life safety risk[12] associated with steep creek processes on Jason and Mungye creeks. BGC completed the risk assessment for individuals in inhabited[13] buildings. It does not include economic risk or risk to people outside of buildings

5.2. Risk Assessment Methods

BGC assessed individual life safety risk, which is the chance that a specific person will be killed by the hazard, expressed as the annual Probability of Death of an Individual (PDI). Individual risk typically applies to the individual most at risk, corresponding to a person spending the greatest proportion of time at home, such as a young child, stay-at-home person, or an elderly person.

Assessing individual life safety risk requires answering the following questions across the hazard scenarios considered:

- What is the probability of debris flows or debris floods impacting an occupied building, and at what intensities[14]?
- What is the probability that a person is within a building at the time of impact?
- What is the probability that life-loss occurs given impact to an occupied building?

BGC calculated individual risk with Equation 5-1. Figure 5-1 shows how each variable in relates to the questions posed above.

$$PDI_j = \sum_{i=1}^{n} h_i S_{i,j} T_{i,j} V_{i,j} \qquad \text{Equation 5-1}$$

Where:

- PDI_j is the annual probability of death of an individual from the geohazard at building (j) (years^{-1})
- h_i is the annual probability of a geohazard scenario (i) occurring (years^{-1})
- $S_{i,j}$ is the conditional probability that geohazard scenario (i) reaches building (j) (i.e., spatial probability of impact)

[12] Life safety risk considers the potential for a hazard event to result in loss of life for one or more individuals.

[13] Inhabited buildings refer to those with habitable space (as compared with auxiliary buildings such as sheds, garages, etc.). BGC classified buildings into inhabited or non-inhabited based on site observations collected in July 2022 supplemented with interpretation where access to properties was not provided.

[14] Intensity refers to the destructive potential of a geohazard.

- $T_{i,j}$ is the conditional probability a person occupies building (j) during geohazard scenario (i) (i.e., temporal probability)
- $V_{i,j}$ is the conditional probability of fatality at building (j) given impact by the estimated geohazard scenario (i) intensity (i.e., vulnerability)
- n is the total number of geohazard scenarios considered.

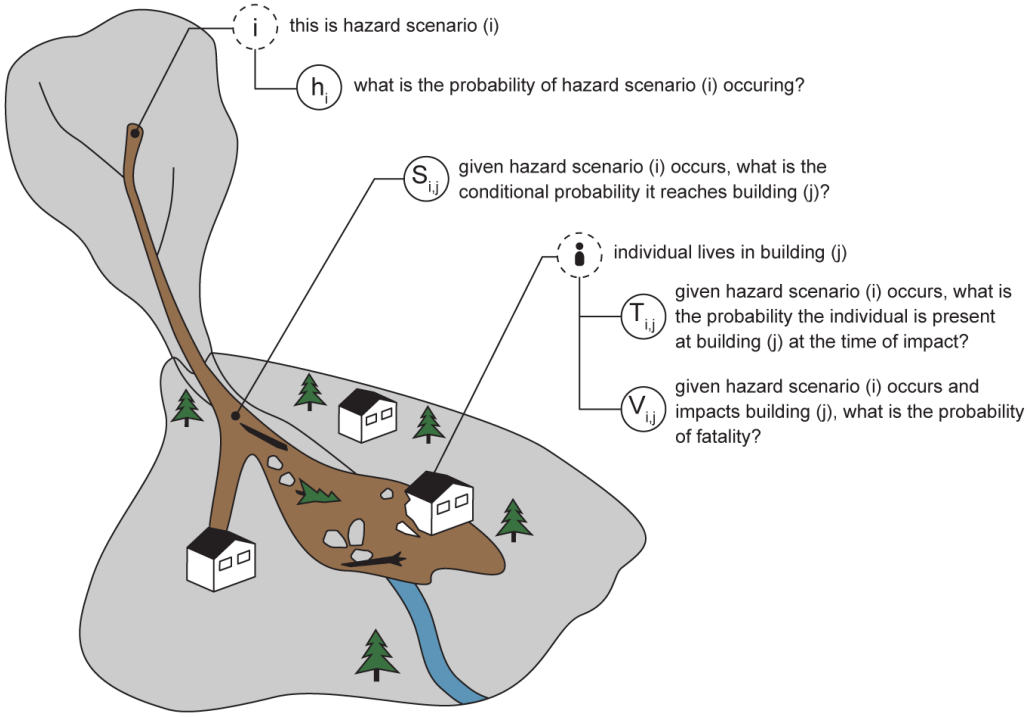

Figure 5-1. Individual risk calculation variables.

BGC estimated the variables in Equation 5-1 and Figure 5-1 based on:

- Frequency-magnitude analysis (n, h_i) (Section 4)
- Numerical modelling results ($S_{i,j}, V_{i,j}$) (Section 4)
- Duration a building is occupied in a given day based on primary building use ($T_{i,j}$)
- Vulnerability criteria developed for debris floods and debris flows ($V_{i,j}$)
- Expert judgement.

Appendix J provides further detail on the risk assessment methods and assumptions.

5.3. Risk Assessment Results

BGC presents individual life safety risk results on Drawing 09 and summarizes the results in Table 5-1.

Table 5-1. Life safety (PDI) to inhabited buildings from debris floods and debris flows on Mungye Creek, and debris flows on Jason Creek.

Risk Level (PDI Range)	Area	Address	Parcel ID
>1:1,000	Jason Creek Fan	1781 Reid Road	1608908
1:1,000 to 1:10,000	Jason Creek Fan	1782 Reid Road	1609084
		1788 Reid Road	1609076
		1794 Reid Road	1609068
		1802 Reid Road	1585134
<1:10,000	Mungye Creek Fan	1712 Reid Road	1609181
		1714 Reid Road	1609173
		1718 Reid Road	1609157
		1719 Reid Road	3108554
		1720 Reid Road	1609149
		No address on BC Assessment Portal	1609131
	Jason Creek Fan and adjacent areas	1770 Reid Road	1609092
		1771, 1773 Reid Road	1608916
		1791 Reid Road	30102065
		1793 Reid Road	30102073
		1812 Reid Road	1609050
		1815 Reid Road	1608886
		1854 Reid Road	1609009
	Lower Fan	1876 Reid Road	23969539
		1 Walkerville Road	23969610
		7669 Pemberton Portage Road	23969555
		7701 Pemberton Portage Road	26459442
		7703 Pemberton Portage Road	26459451
		1882 Pemberton Portage Road	26092085
		1884 Pemberton Portage Road	26092077

Many jurisdictions in Canada and internationally use a risk tolerance threshold of PDI < 1:10,000 for existing development (e.g., District of North Vancouver, Town of Canmore, Cowichan Valley Regional District, District of Squamish). To put 1:10,000 PDI into perspective, an individual's annual risk of life loss depends on several factors including their age, occupation, general state of health, and other environmental factors. Statistics Canada (2009) reports the average Canadian mortality rates by cause. Between 2000 and 2009, the age-standardized risk of loss of life by all causes was approximately 1:200 per year, the average risk from accidental causes was

about 1:4,000 per year, and the average risk from automobile accidents was about 1:13,000 per year.

As outlined in BGC's risk assessment update letter (November 25, 2022), BGC has assessed that 1781 Reid Road (PID 1608908) is at **imminent risk** from debris flows during periods of high rainfall. All properties highlighted in red and orange in Table 5-1 on Jason Creek fan are within the hazard area of the coarse front of rock slide-triggered debris flows. The historic frequency of such events is low enough that BGC has not classified the risk from rock slide-triggered debris flows as "imminent"; however the debris-flow risk at these properties exceeds levels normally considered tolerable for existing development in other jurisdictions in Canada (PDI > 1:10,000). Debris flows could impact the properties highlighted in orange in Table 5-1 with little warning during periods of high rainfall, but BGC assessed that the probability and expected consequences of such impacts are lower than at 1781 Reid Road. Debris flows could also impact the properties not highlighted in Table 5-1, but BGC assessed the risks to be within levels normally considered tolerable for existing development in other jurisdictions.

In jurisdictions with land use or zoning bylaws and that have adopted risk tolerance criteria, new development or redevelopment is not permitted without mitigation works to reduce risk below a risk tolerance threshold (e.g., PDI less than 1:10,000). For existing development, where risk exceeds the threshold, the risk levels would be disclosed on public record and may be included, for example, in a covenant. In some instances, weather and/or slope stability monitoring have been carried out as a temporary means of managing risk until more permanent solutions can be implemented. Further, in some jurisdictions, mitigation works to reduce risk to within tolerable levels would be required as part of building permit applications. Finally, understanding the risk levels provides a basis for prioritization of available resources for risk management and mitigation. This is often a requirement for grant applications that could support funding and implementation of management or mitigation activities.

BGC calculated risk at inhabited buildings. A person(s) outside of a building on other locations on the properties can be at risk of injury or fatality during a debris flow due to the depth, speed, or force of the flow. This can influence the ability of individuals at risk to safely evacuate during an event.

Economic damages associated with flooding, sedimentation, and erosion are expected. BGC has not completed a quantitative assessment of economic damages as part of this scope, but can make the following comments on potential economic damages given the occurrence of debris floods or debris flows on Jason and Mungye creeks:

- Blockage and damage to the Reid Road and downstream crossing locations is expected. Associated damages to the road and rail infrastructure at and downstream or downslope along road grade are expected. The extent of damages is likely to increase with the size of the events.
- Building and property damages associated with flooding, sedimentation, and erosion are expected on both fans. The extent of damage is based on the flooding extents, flow depth, and velocities (Section 4.5.2).

- Access along Reid Road is likely to be compromised by Jason Creek and similarly by Mungye Creek for higher return period events. If access is compromised, costs associated with road repair and emergency management can be expected.

5.4. Limitations of Risk Assessment

BGC's risk assessment is based on the current understanding of steep creek hazards at the site, topography, layout of structures on the fan, and assumed building occupancy. Any changes to the fan surface (e.g., sedimentation and erosion from a debris flow, construction of mitigation measures, etc.), triggering conditions (e.g., forest fire, removal of vegetation in the watershed, large slope failure), or the location(s) and occupancy of buildings may change the risk. Assessment of risk levels could also change with additional monitoring or repeat evaluation of the unstable rock slopes in the watershed.

6. CONCEPTUAL MITIGATION DESIGN

6.1. Introduction

Informed by the results of the risk assessment (Section 5), BGC developed conceptual mitigation options to reduce risk from debris flows on Jason Creek and debris floods and debris flows on Mungye Creek as outlined in the following sections.

6.2. Jason Creek

BGC estimated that life safety risk from debris flows on Jason Creek for select properties up- and downstream of Reid Road exceeds levels normally considered tolerable in other jurisdictions in Canada. BGC has developed and evaluated conceptual mitigation options that reduce life-safety risk on the fan and downstream areas.

6.2.1. Design Considerations

BGC defined a list of mitigation design considerations for Jason Creek (Table 6-1). The considerations outlined were the basis for developing mitigation options and for choosing the preferred approach.

Table 6-1. Jason Creek mitigation design considerations

Item		Description
1	Geohazard process	Mitigation designs address debris flows on Jason Creek. The design will also improve channel conveyance for clearwater flows.
2	Design objective	The primary design objective is to minimize debris-flow life loss risk for residents on the Jason Creek fan. The secondary objectives are to maintain access for all residents along Reid Road and to minimize debris-flow economic losses.
3	Elements at risk	Elements at risk include: • Residential development (safety and economic risk) • Roads and associated infrastructure (i.e., culverts) (access and economic risk) • Railroad (mostly economic risk)
4	Risk transfer avoidance	Mitigation measures should not increase life loss risk and, wherever possible, economic risk at existing buildings and infrastructure.
5	Conceptual design level	BGC developed conceptual-level designs. The intent of this design stage was to identify technically feasible options for further review and consideration.
6	Maintenance	All proposed mitigation measures require routine maintenance, and the designs assume this maintenance will occur as needed. BGC expects maintenance and restoration of channels, berms, and erosion protection following debris flows, and possibly following debris floods or high clearwater flows.

Item		Description
7	Impact to existing development	The proposed mitigation measures require land acquisition and construction on private property. To the extent possible, BGC has aimed to reduce footprints of measures and minimize impacts to existing buildings. At this design stage, BGC has assumed that land acquisition and landowner permissions for construction will be feasible.
8	Topography	The layout of mitigation measures is based on topography from a lidar-derived digital elevation model (DEM) collected in July 2022.
9	Construction materials	Where possible, the designs make use of existing on-site materials and features, including the reuse of excavated fan material for berm construction. As such, BGC has assumed that the fan is composed of sand and gravel material suitable for reuse as berm fill. BGC aimed to achieve a cut/fill balance with material excavated from the channel to minimize the amount of non-native material required to be transported to site.

The five properties where risk exceeds PDI of 1:10,000 (Section 5) have a combined total property value of approximately $6 Million based on land assessment values accessed through the BC Assessment Portal (as of July 1, 2021). BGC compared the estimated costs of mitigation options to this combined total to evaluate if the mitigation options presented a favourable investment in comparison with acquiring the properties as a risk reduction strategy.

At this design stage, BGC has not considered environmental impacts or a detailed cost-benefit assessment for the mitigation options.

6.2.2. Options Assessment

Risk management techniques can include engineered structures (i.e., structural mitigations) and non-structural mitigation (e.g., warning systems). Structural mitigations can be in the watershed, main channel, or on the fan surface. A “mitigation chain” combines multiple techniques to achieve the design objectives and can be constructed in a phased approach over time as funding and permitting allow.

BGC evaluated a range of techniques for Jason Creek (Table 6-2). For each, BGC compared the advantages and disadvantages including technical, economic, social, and environmental factors before determining whether to reject or select it as a feasible technique for additional review.

BGC identified four techniques from Table 6-2 for additional review:

1. Construct flow diversion berms on properties where PDI>1:10,000 (1781, 1782, 1788, 1794, and 1802 Reid Road) to protect these individual buildings (Option 5).
2. Excavate channel and construct clear-span bridge at Reid Road to convey debris flows downstream from fan apex past Reid Road (Option 6).
3. Implement a near-real time monitoring system to identify displacement on rock slopes in the watershed (Option 12).
4. Develop and apply relevant policies to reduce risk to future development (Option 13).

Of these, only Option 6 (excavate channel and construct clear-span bridge) achieves all the risk reduction objectives without additional measures, namely reducing life safety risk, maintaining access on Reid Road, and reducing economic losses. Option 5 (flow diversion berms on individual

properties) reduces life safety risk but does not maintain access or manage economic damage from debris flows to areas not protected by the berms. Option 12 (near real-time monitoring system) has the potential to reduce life-safety risk from rock slide-triggered debris flows if there is an effective early warning system in place. Option 13 (develop and apply relevant policies) is applicable to future development or redevelopment. It does not address risk to existing infrastructure. BGC provides additional details on each of these techniques in the following sections.

Table 6-2. Summary of mitigation techniques considered on Jason Creek. Options selected for further assessment are highlighted in light blue.

Option No.	Approach	Description	Advantages	Disadvantages	Decision
1	No additional mitigation	Do not implement any additional risk reduction measures.	No additional cost.	Does not reduce risk.	**Rejected:** Does not achieve risk reduction objectives.
2	Source zone stabilization	Install rock anchors or soil stabilization to decrease the likelihood of debris flows.	If effective, reduces risk to downstream areas without requiring construction on the fan.	Too many potential sources to stabilize. Not economical. Unlikely to be effective.	**Rejected:** Not technically or economically feasible.
3	Debris retention and/or flood attenuation at fan apex	Construct a basin to retain debris and attenuate discharge to reduce the size and intensity of debris flows downstream. Requires favorable topography and large open area near the fan apex.	Where feasible, such structures can protect the entire fan.	High capital and operations and maintenance (O&M) costs. Requires a large footprint to construct. Only feasible where there is space for upstream storage.	**Rejected:** Not technically or economically feasible given the fan is developed up to the apex and there is insufficient storage in the channel upstream of the apex.
4	Diversion	Divert and channelize Jason Creek along the upstream side of Reid Road	If feasible, reduces the need for a bridge to safely convey debris flows below the road.	Insufficient space to convey flows. Requires a 90° turn in the flow at the road, increasing overtopping potential of the road. Transfers risk to properties east of the channel.	**Rejected:** Not technically feasible given there is insufficient space for a channel on the upstream side of Reid Road, there is no clear downstream deposition location, and it transfers risk.
5		Construct berms on individual properties to divert flow away from individual buildings.	Lower capital and O&M costs than other alternatives. Homeowners can construct with appropriate permissions and engineering review. Low visual impact if located on the upstream side of driveways or integrated into a landscape feature.	Does not preserve access via Reid Road in isolation. Only reduces risk to individual properties. Possible risk transfer (to be addressed in preliminary and detailed design). May be cost-prohibitive if costs are funded by individual homeowners.	**Selected for further review:** BGC recommends installation of berms on properties where PDI>1:10,000 (1781, 1782, 1788, 1794, 1802) in advance of additional improvements at the Reid Road crossing.
6	Improve conveyance	Replace the Jason Creek culvert with a clear-span bridge. Excavate the channel upstream, at, and downstream of the crossing to achieve the required channel capacity and promote debris conveyance. Berm(s) that parallel the east side of Jason Creek might be required (review in preliminary and detailed design).	Achieves all risk reduction objectives. Preserves access along Reid Road for design event and increases resiliency at higher return period events.	High capital and O&M costs; however, may contribute to favourable total costs over full service life by extending service life and reducing maintenance requirements. Requires land acquisition to construct on private properties. Requires significant stakeholder engagement (MoTI, landowner, CN Rail). Possible risk transfer (to be addressed in preliminary and detailed design).	**Selected for further review:** BGC recommends this option be further developed and discussed with MoTI.
7		Replace Reid Road crossing with an armoured swale that allows a debris flow to pass over the road surface at a section designed to withstand the erosion.	Where feasible, armoured swales are a cost-effective option that incurs lower capital cost compared to a bridge or alternate structure.	The road grade at the Reid Road crossing is steep (~11%) and construction of an armoured swale requires substantial regrading along the road to the east and west to maintain a driveable road surface.	**Rejected:** Not technically or economically feasible.
8	Relocate elements at risk	Temporary evacuation of residents from properties where PDI exceeds a threshold or assessed to be at “imminent” risk.	Completely reduces life safety risk to tolerable levels if all residents comply.	Creates significant hardship for affected residents (financial, stress and wellbeing, family disruption). Ineffective if residents do not comply. Funding mechanisms to support affected residents are time limited.	**Rejected:** BGC recognizes this as an effective short-term strategy in response to imminent risk but does not consider it a viable long-term strategy.
9		Acquisition of property/properties most at risk.	Reduces life safety risk to tolerable levels at property(ies) in question. May have a higher benefit-cost ratio in comparison with other mitigation approaches.	Does not reduce risk to properties that are not acquired. Does not preserve access via Reid Road. Likely to cause significant hardship for affected residents.	**Rejected:** Does not achieve overall risk reduction objectives. Consider for further review if other mitigation options are not considered feasible or outside of available funding.

Option No.	Approach	Description	Advantages	Disadvantages	Decision
10		Realign Reid Road downslope of the existing location.	Could decrease the overall road grade to improve driveability. May decrease risk to infrastructure at crossing and decrease risk of losing access for properties west of Jason Creek.	Does not reduce risk to properties on Jason Creek fan. Requires significant stakeholder permissions and grading works.	**Rejected:** Likely not economically or socially feasible. Does not achieve risk reduction objectives.
11	Monitoring and warning systems	Weather-forecast based monitoring system for precipitation-triggered debris flows.	Allows occupation of properties during low-risk periods of the year. Lower capital and O&M costs.	Efficacy depends on the quality of weather forecast data, availability of information on past debris flows and hydroclimatic triggering conditions, operational system to develop and disseminate alerts, and compliance from residents. Systems are inherently designed to be conservative and can lead to multiple 'false warnings' that can result in evacuation fatigue. Funding to develop and maintain such systems is uncertain. Introduces liability concerns. Does not address risk from rock slide-triggered debris flows.	**Rejected:** Weather-based forecast systems are a viable approach in the correct context. At Jason Creek, BGC does not consider it a viable long-term strategy due to the implementation challenges of creating and maintaining an effective early warning and evacuation system (e.g., evacuation fatigue, ownership and operation, liability management, efficacy, funding for system implementation and response when warnings are issued).
12		Rock slope monitoring to evaluate deformation of unstable rock masses. Multiple techniques available for consideration (e.g., InSAR, lidar surveys, GNSS, extensometers). With sufficient data, consider establishing rock deformation-based threshold(s) to support risk-management decision-making.	Increases understanding of rock slope behaviour in the watershed. Lower capital costs than large, engineered structures.	Requires operational support to collect and analyze data collected. Requires a minimum data collection time period to establish seasonal variability in advance of threshold development (~1 year). Does not address risk from precipitation-triggered debris flows.	**Selected for further review:** BGC recommends review of remote-sensing datasets (e.g., lidar and InSAR) at future intervals to evaluate rock slope deformation.
13	Policy approach	Apply land-use and other applicable policies to reduce risk to future developments.	Best practice for geohazard risk management.	Does not reduce risk to existing development. Limited mechanisms to implement without adopted risk tolerance thresholds.	**Selected for further review:** BGC recommends this approach to manage risk to future development or redevelopment on existing properties.

6.2.3. Mitigation Option Details

BGC developed conceptual-level mitigation designs for the techniques selected for further review. BGC based designs on site topography, F-M relationship (Section 4), and numerical modelling results (Section 4). BGC based conceptual mitigation layout and dimensions of engineered structures using the HEC-RAS numerical models developed for hazard analysis with terrain modifications to integrate the proposed mitigations. The following sections provide additional detail on each option. Additional details on the cost estimates are in Appendix K.

6.2.3.1. Construct flow diversion berms on individual properties (Option 5)

Construction of berms on individual properties where PDI>1:10,000 (1781, 1782, 1788, 1794, and 1802 Reid Road) could reduce debris-flow risk at the inhabited buildings on these properties (Figure 6-1).

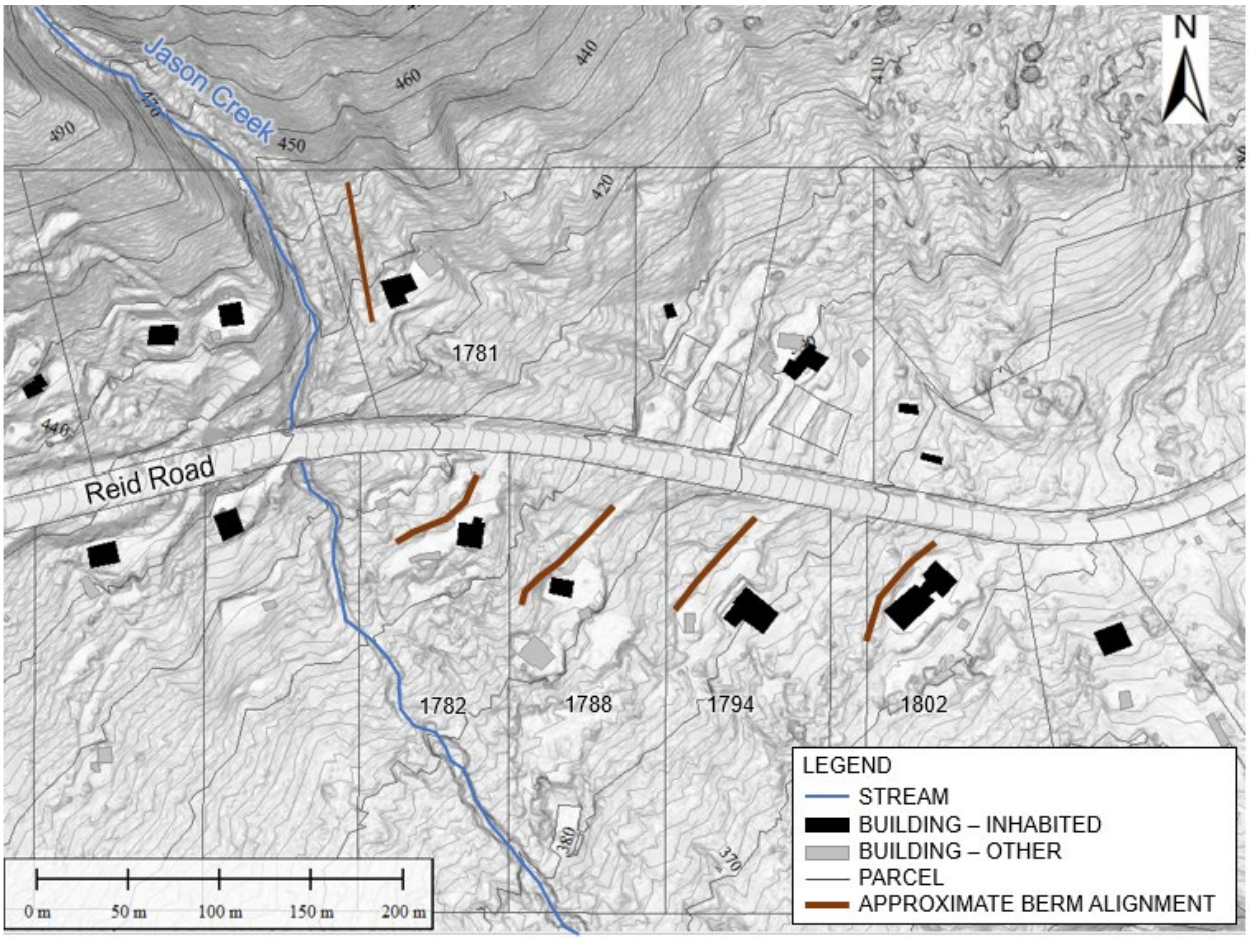

Figure 6-1. Approximate berm alignments at individual properties on Jason Creek fan. Berm alignments shown are for approximate centerlines and do not represent the total footprint required.

A berm oriented parallel to Jason Creek immediately downstream of the fan apex could direct flow away from the inhabited building at 1781 Reid Road (Figure 6-1). BGC estimates a berm height of 3.5 m to 5.5 m tall is required depending on the return period selected for the design

event. Lower return periods (e.g., 200-year as compared with 2,000-year) require a smaller berm; however, residual risk[15] may exceed levels that are considered tolerable. Selection of the design event should be coupled with a residual risk assessment and evaluation of the likely performance of the berm in response to different return periods. BGC based the design height range on a preliminary evaluation of debris-flow superelevation including 0.9 m freeboard (FEMA, 1995; Prochaska et al., 2008). Future phases of design should also include evaluation of debris-flow impact forces and stability assessment. Such analyses will inform the design layout and feasibility given the anticipated high impact forces as the berm is located immediately downstream of the fan apex where flow intensity is highest.

Construction of a berm on the upslope side of the buildings that has two arms oriented downslope from a central point (chevron berm) designed to direct flows around the buildings on each side could also be considered. A chevron berm would likely require removal of the garage structure adjacent of the main inhabited building and/or excavation into the slope to the east of the garage (Drawing 02). Any slope excavation should be coupled with analysis of slope stability in advance of the excavation work. Construction of a berm at 1781 Reid Road may transfer risk to other properties on the fan. The preferred berm alignment (Figure 6-1) may transfer risk to downstream properties and the chevron berm transfers risk to the east. A review of risk transfer is required if this is selected as a preferred approach.

BGC proposes berms at the properties downstream of Reid Road (1782, 1788, 1794, 1802) oriented approximately parallel to the existing property driveways on the upslope side (Figure 6-1). Required berm lengths vary from approximately 40 m to 100 m based on individual site characteristics. Given the orientation of the berms approximately perpendicular to the direction of flow, berm design must account for debris deposition and debris-flow runup on the upstream side. Based on numerical model results and preliminary estimation of debris deposition,[16] BGC estimates berm heights of approximately 2.5 m to 3 m, with height varying locally. Future phases of design require a more detailed assessment of debris deposition, debris-flow runup, and appropriate freeboard.

Multiple construction methods are feasible including erosion-protected earth berms, geosynthetic-reinforced soil (GRS) walls, and concrete or modular retaining (e.g., lock-block) walls. Selection of the appropriate construction method should be informed by debris-flow impact force assessment, local material availability, available funding, and aesthetics. To develop a conceptual level cost estimate for the proposed berms, BGC used a GRS wall for the berm at 1781 Reid Road and erosion protected earth berms at the properties downstream (1782, 188, 1794, 1802). BGC selected a GRS wall at the fan apex as it requires a smaller footprint than an earth berm. For the purposes of cost estimation, the GRS wall is approximately 75 m long, 4.5 m tall above grade with a 4 m crest width and includes erosion protection along the toe. BGC selected the conceptual layout for the approximate requirements of a 500-year precipitation-triggered debris

[15] Residual risk refers to the risk that exists after construction or implementation of mitigation.

[16] BGC estimated debris deposition height using a deposition slope of ½ the fan slope upstream of the berms. With an average gradient of 16% (9°), this is a deposition slope of 8% (4.5°). For an average berm length of 60 m and debris-flow impact at approximately mid-berm, this results in approximately 2.4 m of deposition.

flow as the design event. As outlined above, future phases of design will require assessment of impact loads, debris-flow superelevation, and residual risk to select the appropriate design event and layout. BGC estimates the total capital of the GRS wall to be $330,000 with $50,000 in O&M costs over a 75-year service life (Table 6-3). This cost estimate is subject to change with adjustments in the design event and preferred layout.

BGC used the following average dimensions for the erosion-protected earth berms: 3 m height, 60 m length, 4 m crest width, and 1.5H:1V side slopes. These berms have grouted riprap[17] on the upstream faces. Based on these representative dimensions, and assuming these berms are constructed simultaneously, BGC estimated the total capital of the berms on all properties downstream of Reid Road to be $1.5 Million with an additional $190,000 in O&M costs over a 75-year service life (Table 6-3).

The combined total life-cycle costs for diversion berms on all properties is $2.1 Million (Table 6-3, cost details in Appendix K).

Table 6-3. Estimated costs for flow diversion berms on individual properties.

Component	Capital Cost (-50% to +100%)	O&M Cost (75-year service life)	Total Cost
GRS wall at 1781 Reid Road	$ 330,000	$ 50,000	$ 380,000
Berms on individual properties (1782, 17888, 1794, 1802)	$1.5 Million	$ 190,000	$ 1.7 Million
Total	**$1.9 Million**	**$ 240,000**	**$ 2.1 Million**

Notes:
1. Capital costs include direct and indirect costs.[18]
2. BGC rounded costs to the nearest $10,000 for totals less than $1 Million, and to the nearest $100,000 for costs more than $1 Million.
3. O&M cost estimates are the Net Present Value (NPV) over a 75-year service life with 2% discount rate.

6.2.3.2. Excavate channel and construct clear-span bridge at Reid Road (Option 6)

This mitigation option aims to convey debris flows from the fan apex downstream and past the Reid Road crossing. It includes replacement of the existing Reid Road culvert with a clear-span bridge, channel excavation, and straightening the channel from the fan apex downstream to approximately 100 m downstream of Reid Road (Figure 6-2).

[17] Either grouted riprap or stone pitching are feasible options, but stone pitching is generally more expensive and BGC has not considered it at this stage.

[18] Direct costs refer to material and labour rates. Indirect costs refer to engineering and permitting, mobilization, contractor rates, etc. and are estimated as a proportion of direct costs.

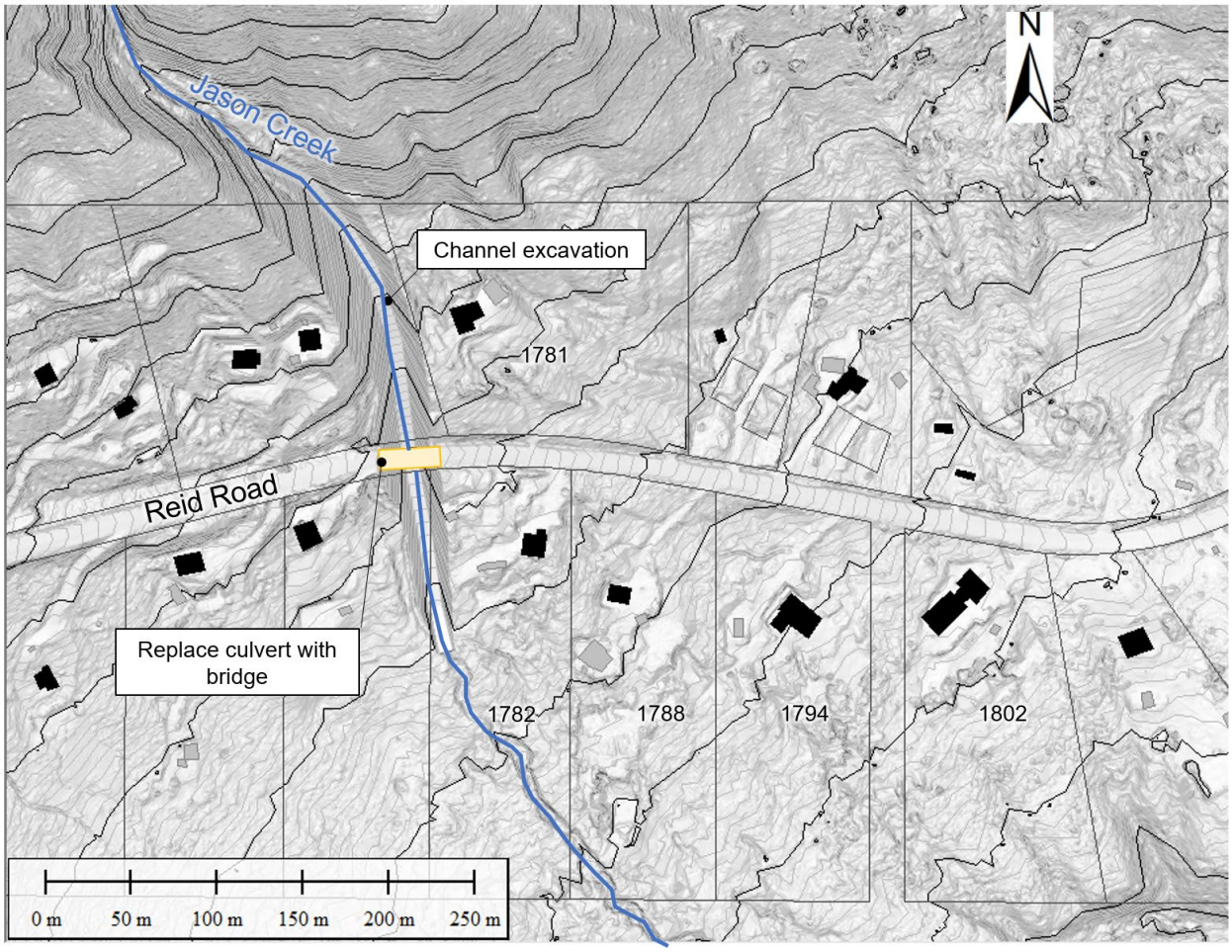

Figure 6-2. Conceptual layout of channel excavation and bridge replacement.

At this conceptual design stage, BGC estimated the dimensions and costs of a bridge designed to convey the peak discharge associated with a 200-year return period debris flow (250 m^3/s, Table 4-2). In consultation with MoTI, future phases of design could involve an update to the design event selection. The existing road grade at the crossing (11% eastward draining) prohibits steepening of the road to elevate the road surface through the crossing and BGC assumed all additional capacity is associated with excavation below the bridge. BGC estimated a height of 2 m from the road surface to the bottom of the lowest bridge girder and included a 2 m freeboard to account for floating logs, flow turbulence, and some natural channel aggradation. To convey the 200-year peak discharge and accounting for the bridge structure height and freeboard, BGC estimates a required bridge span of approximately 32 m and a bridge height of approximately 8 m measured to road surface (corresponding to an elevation of 410 m at the channel bed at midspan). This bridge layout also has sufficient capacity to convey the 500-year debris flow with lower freeboard.

BGC expects the bridge to experience damage during rock slide-triggered debris flows. BGC assumed the road surface will be 8 m wide, consistent with the existing road width. The channel width is 8 m through the crossing with 1.5H:1V abutment slopes and 22% (12°) gradient. It is important for the channel to maintain the natural or steepened gradient through the crossing to

promote conveyance. The bridge abutments also require erosion protection for scour and bank erosion protection. Future phases of design should evaluate the available freeboard on the east side of the bridge with detailed hydraulic modelling given the road grades steeply to the east and freeboard is reduced on that side.

BGC proposes a straightened and excavated channel to increase the channel capacity and tie the crossing into the natural channel (Figure 6-2). Steep, straight, and narrow channels are most effective to promote debris conveyance, however, scour and erosion and more likely in these conditions. In contrast, wider channels have more capacity but are more likely to experience debris deposition that can reduce channel freeboard and cause flow avulsions. Selection of the most effective channel configuration for Jason Creek requires a balance of these two configuration approaches. Channel excavation can also be accompanied with training berms. Given the limited available space on the east side of the channel from the fan apex to the road, BGC favours a channel without an adjacent berm.

The excavated channel is 8 m wide with 1.5H:1V side slopes. BGC selected this relatively steep side slope given the site layout and to minimize the footprint of proposed mitigations. The channel is 24% (13.5°) upstream of Reid Road and 12% (7°) downstream of Reid Road. The steeper slope upstream encourages debris conveyance through the crossing and deposition downstream. This proposed layout requires approximately 39,000 m^3 of material excavation. BGC's preliminary estimate of superelevation at the outside of the channel bend downstream of the fan apex ranges from 0.6 m to 3 m for 200- to 2,000-year debris flows. Future phases of design should include review of superelevation and include appropriate freeboard.

BGC has not included erosion protection along the excavated channel as this would significantly increase the total mitigation cost. BGC expects localized erosion protection on the outside bend at the fan apex and at the bridge crossing to protect the bridge abutments are required. Review of erosion protection requirements should form a component of future design stages. In absence of erosion protection, BGC expects some localized oversteepening of the channel banks during debris flows and periods of high flow; however, the channel is prone to debris deposition and aggradation since it is less than 27% (15°) and will require regular maintenance including channel excavation to maintain capacity. Future phases of design should include the design of access ramps to facilitate debris clearing. Long-term O&M planning should include review of channel condition following periods of high flow. Finally, this approach requires review of downstream infrastructure capacities and relevant asset owner engagement (e.g., MoTI, CN Rail).

BGC estimates the total capital cost of this mitigation chain to be approximately $4.6 Million with an additional $1.1 Million in O&M costs (Table 6-4, Appendix K). Comparison with the total value of the properties where risk is greater than a PDI of 1:10,000 ($6 Million) demonstrates a favourable investment with added economic benefits not quantified herein associated with achieving all the risk reduction objectives, including maintaining road access and reducing damages to properties downstream and east of Jason Creek.

Table 6-4. Estimated cost to excavate channel and construct bridge on Jason Creek.

Component	Capital Cost (-50% to +100%)	O&M Cost (75-year service life)	Total Cost
Bridge replacement at Reid Road	$2.6 Million	$ 190,000	$ 2.8 Million
Channel excavation	$2.0 Million	$ 920,000	$ 2.9 Million
Total	**$4.6 Million**	**$ 1.1 Million**	**$ 5.7 Million**

Notes:
1. Capital costs include direct and indirect costs.
2. BGC rounded costs to the nearest $10,000 for totals less than $1 Million, and to the nearest $100,000 for costs more than $1 Million.
3. O&M cost estimates are the NPV over 75-year service life with 2% discount rate.

6.2.3.3. Rock Slope Monitoring

A near real-time monitoring program and early warning system, combined with a response protocol, is a risk management technique for development where physical mitigation may not be possible or cost prohibitive. It may allow timely evacuation of individuals at risk to a safe location in the event of an imminent rock slide with identifiable precursors to rapid failure (e.g., acceleration of movement).

A key consideration in the development of near real-time monitoring systems is redundancy in both number and types of instruments (Kristensen et al., 2020; Sättele et al., 2016; Sharon & Eberhardt, 2020). Instrument redundancy is necessary to cross-verify instruments, and is particularly useful to minimize false alarms when one instrument may reach threshold levels defined as part of an early warning system. Instrument redundancy is also crucial for back-up in case of malfunction of one of the sensors, particularly during landslide acceleration phases where increased ground disturbance may damage some instruments (Sättele et al., 2016). Ideally, some instruments are also powered by separate and independent sources.

Techniques that would be appropriate to consider at Jason Creek are:

- **GNSS receivers** that measure a position based on the range (distance) to at least four satellites.
    - GNSS provides point measurements at the location of the instruments. The system requires a base station installed on stable ground and rover units installed on identified instabilities. Ideally, the base station is at a location where it can be powered by a local power grid. The rover units are powered by independent batteries. The expected accuracy of the system is approximately 10 mm, and may require local tree clearing to allow clear vision of the sky. Ideally, the GNSS units are installed on poles driven into bedrock to avoid measuring overburden displacements and any potential frost action.
- **Wire Extensometer** that measures displacement across a crack or deformation zone.
    - A wire extensometer consists of a cable anchored at one end and on a spool at the other end. As the cable unravels, distance measurements are recorded by a vibrating wire transducer.

- **Tiltmeter** that measures the change in inclination of a ground surface point.
    - Tiltmeters are used to monitor slope movements where the expected failure mode contains a rotational component (Sharon & Eberhardt, 2020). Tiltmeters are relatively inexpensive and are therefore useful for cross-verification of other instruments. They can be installed on trees or poles driven into bedrock to avoid measuring overburden displacements and any potential frost action.
- **Satellite InSAR** is the same technique used to assess ground deformation from May 2017 to June 2022 (Section 4.2).
    - Satellite InSAR relies on satellite image acquisition which currently varies from 4 to 24 days (Sharon & Eberhardt, 2020) so is not a 'near real-time' monitoring system. There are several limitations with InSAR as a monitoring technique, including the maximum slope velocity that can be tracked (InSAR is best for identifying small (mm-scale) movements), the orientation of slopes, and the presence of vegetation and snow on the ground.
- **Automatic weather station** to correlate deformation measurements with weather parameters, which often have some control on slope stability.
    - Air temperature, solar radiation, rainfall, wind speed, snow depth, and relative humidity are common measurements collected.

As a point of comparison, BGC recently installed a near real-time monitoring system on the Moosehide Landslide, Dawson City, YT that included six GNSS rovers, four wire extensometers, six tiltmeters, and an automatic weather station. Setup, data validation, and development of an understanding of the slope deformation is planned over approximately one year following installation of the monitoring instrument at that site. BGC anticipates that after this period, the monitoring program could be integrated into an early warning system, consisting of pre-defined alert levels associated with an emergency response plan. That system had a capital cost for instruments and installation of $250,000 with an additional $70,000 annually for maintenance and data processing. Over a 75-year service, that amounts to a total life-cycle cost of $2.2 Million.[19]

A near-real time monitoring system provides warning that landslide acceleration is occurring within a day or more lead time. It does not provide warning following a sudden event, such as seismic (e.g., earthquake, nearby blasting) or extreme weather events. In addition, if landslide acceleration is observed, the monitoring system may need to be supplemented with additional instrumentation (e.g., ground-based InSAR) to evaluate landslide motion in support of risk management decisions.

For a near-real time monitoring system to reduce risk, it must be accompanied by an early-warning system with effective operational systems to identify thresholds, issue and disseminate warnings to affected residents, and initiate emergency response actions. The operational implementation challenges of creating and maintaining an effective early warning and evacuation system are similar for weather-based forecast systems and include evacuation fatigue, ownership and

[19] Although instruments likely do not have a 75-year service life, BGC used this value for comparison to the other mitigation options. This is likely an underestimate as instrument replacement and installation would contribute to the total life-cycle costs if planned for a 75-year service life.

operation, liability management, efficacy, and funding for system implementation and response when warnings are issued.

Moreover, a near-real time monitoring system at Jason Creek does not reduce risk from precipitation-triggered debris flows or achieve the other risk reduction objectives (maintain safe access at Reid Road crossing, reduce economic risks). For these reasons, BGC does not recommend this technique for risk management at Reid Road. BGC recommends collecting and/or reviewing more recent publicly available remote-sensing datasets (e.g., lidar or InSAR) at set intervals in the future to study the long-term behaviour of slopes to inform future risk-management decision making.

6.2.3.4. Policy Approach

Development and application of land-use policies can manage risk to future development or redevelopment in the study area including requirements for any future land subdivision. The composite hazard map developed by BGC (Drawing 08) forms a basis for land-use planning. BGC recommends that the SLRD review applicable policies to support long-term risk management in the study area.

6.2.4. Proposed Mitigation

BGC recommends that mitigation at Jason Creek be completed in a phased approach:

- **Phase 1:** Construction of the berms on individual properties (1781, 1782, 1788, 1794, 1802 Reid Road)
- **Phase 2:** Channel excavation and bridge construction at Reid Road crossing.

This approach achieves all risk reduction objectives and allows for phasing to accommodate design, funding, and permitting. BGC recommends the berms be constructed as soon as reasonably practical. With both phases constructed, the berms on individual properties help manage residual risk from channel overtopping. BGC also recommends that SLRD review applicable policies to support long-term risk management in the study area informed by the composite hazard map (Drawing 08).

BGC estimates the total life-cycle costs of the proposed mitigation to be $7.8 Million (Table 6-5).

Table 6-5. Estimated capital cost of proposed mitigation at Jason Creek.

Component	Capital Cost (-50% to +100%)	O&M Cost (75-year service life)	Total Cost
Phase 1: Berms on individual properties			
GRS wall at 1781 Reid Road	$ 330,000	$ 50,000	$ 380,000
Berms on individual properties (1782, 17888, 1794, 1802)	$1.5 Million	$ 190,000	$ 1.7 Million
Subtotal	**$1.8 Million**	**$ 240,000**	**$ 2.1 Million**
Phase 2: Channel excavation and bridge			
Bridge replacement at Reid Road	$2.6 Million	$ 190,000	$ 2.8 Million
Channel excavation	$2.0 Million	$ 920,000	$ 2.9 Million
Subtotal	**$4.6 Million**	**$ 1.1 Million**	**$ 5.7 Million**
Total	**$6.4 Million**	**$ 1.3 Million**	**$ 7.8 Million**

Notes:
1. Capital costs include direct and indirect costs.
2. BGC rounded costs to the nearest $10,000 for totals less than $1 Million, and to the nearest $100,000 for costs more than $1 Million.
3. O&M cost estimates are the NPV over a 75-year service life with 2% discount rate.

6.3. Mungye Creek

BGC determined that life safety risk from debris floods and debris flows on Mungye Creek is within levels normally considered tolerable in other jurisdictions in Canada.[20] For this reason, no additional mitigation is recommended to reduce life safety risk. BGC estimated that the Mungye Creek culvert under Reid Road does not have sufficient capacity to convey the peak discharge for return periods greater than 50-years (Table 3-3). BGC recommends that this culvert is upgraded to reduce overland flooding and economic losses that may result from flood, debris flood and debris flow events on Mungye Creek.

BGC recommends that the Mungye Creek culvert be replaced with a box culvert sized to convey the peak discharge associated with a 200-year return period debris flood (9.2 m^3/s, Table 4-3). BGC determined that a culvert sized approximately 2.5 m by 2.1 m has sufficient capacity for this design discharge. Future phases of design should include a culvert sizing analysis and the design of erosion protection. BGC recommends that this culvert be installed with the same or similar gradient as the natural channel through the reach to encourage debris conveyance rather than deposition within the culvert. As with Jason Creek, BGC also recommends that SLRD review applicable policies to support long-term risk management in the study area informed by the composite hazard map (Drawing 08).

[20] BGC notes that the level of field investigation was lower at Mungye Creek than at Jason Creek (four test pits and two radiocarbon dates). For that reason, there is greater uncertainty in the F-M relationship, resultant modelling, and risk assessment at Mungye Creek than at Jason Creek.

BGC estimates the capital costs of this replacement to be approximately $1 Million (Appendix K). The schedule of the replacement could align with the expected end of service life of the existing culvert. BGC does not have confirmation of the design life remaining on this culvert at this time.

Table 6-6. Estimated capital cost of proposed mitigation at Mungye Creek.

Component	Capital Cost (-50% to +100%)	O&M Cost (75-year service life)	Total Cost
Box culvert at Reid Road	$ 1.0 Million	$ 50,000	$ 1.1 Million

Notes:
1. Capital costs include direct and indirect costs.
2. BGC rounded costs to the nearest $10,000 for totals less than $1 Million, and to the nearest $100,000 for costs more than $1 Million.
3. O&M cost estimates are the NPV over a 75-year service life with 2% discount rate.

6.4. Recommended Future Work

BGC recommends the SLRD consider the following to inform the next stages of the mitigation design:

- Engage MoTI to discuss the proposed replacement of the Jason Creek culvert under Reid Road with a bridge and proposed replacement of the Mungye Creek culvert under Reid Road with a box culvert. Review remaining design life of culvert at Mungye Creek to inform timing of potential culvert replacement.
- Engage a Qualified Environmental Professional to review riparian and aquatic life requirements/restrictions for proposed in-stream works.
- Engage an Engineering Firm to complete preliminary design of mitigation measures once the preferred design(s) are selected.
- Engage the SLRD Board, community members, and other stakeholders to inform selection of the preferred mitigation system.
- Research relevant funding mechanisms to develop a mitigation budget estimate.
- Evaluate available policy mechanisms to reduce risk for future development or redevelopment on the study creek fans.

7. SUMMARY AND RECOMMENDATIONS

7.1. Summary

At the request of Squamish-Lillooet Regional District (SLRD), BGC Engineering Inc. (BGC) completed an assessment of steep creek hazards on Jason and Mungye creeks in the Reid Road area of Electoral Area C. Other hazards with the potential to impact Reid Road area residential development and infrastructure that originate outside of the study creek watersheds were outside of the present scope. This study was prompted by an emergency evacuation order for eight properties and evacuation alert for four properties on Jason Creek fan following a series of hydrogeomorphic events in November to December 2021 that resulted in washout of the culvert at Reid Road, overland flooding, and sedimentation.

BGC classified Jason Creek as debris-flow prone for all return periods considered (20-, 50-, 200-, 500-, and 2000-year) with debris flows triggered by precipitation for the 20- to 500-year return periods and triggered by rock slide(s) for the 2,000-year return period. BGC identified unstable rock masses on the east (left) side of the Jason Creek watershed valley wall with the potential to trigger debris flows in lidar and field observations. InSAR analysis of the period spanning May 2017 to June 2022 indicates displacement of these rock slopes. The bedrock exposed in the creek channel and ravine sidewalls of Jason Creek is heavily altered (clayey). This weak, altered rock increases instability affecting the creek channel within the lower watershed areas and contributes to debris-flow and volume and runout. BGC recognizes that clay-rich debris flows may have the potential to runout farther than coarser-grained debris flows.

BGC classified Mungye Creek as susceptible to a continuum of processes from floods to debris flows. BGC assessed that in comparison with Jason Creek, the debris-flow hazard on Mungye Creek appears to be significantly lower.

Using a combination of historical records, aerial imagery interpretation, field observations, radiocarbon dating of samples collected from test pits and natural exposures, and empirical techniques, BGC developed best estimate F-M relationships for each creek (Table 7-1).

Table 7-1. Summary of best estimate F-M relationships for each study creek.

Representative Return Period (years)	Jason Creek			Mungye Creek		
	Process	Sediment volume (m^3)	Peak Discharge (m^3/s)	Process	Sediment volume (m^3)	Peak Discharge (m^3/s)
20	Debris flow	4,000	100	Flood	-	2
50		8,000	170	Debris flood (Type 1)	2,500	3
200		13,000	250	Debris flood (Type 2)	7,500	9
500		19,000	340	Debris flow	14,000	260
2,000		55,000	790		24,000	410

Notes:
1. Debris flood types after Church & Jakob (2020).
2. Sediment volumes reported are those arriving at the fan apex. BGC rounded sediment volumes to the nearest 1,000 m^3 for debris flows and the nearest 100 m^3 for debris floods.
3. BGC rounded peak discharges to the nearest 1 m^3/s for floods and debris floods, and to the nearest 10 m^3/s for debris flows.

BGC used the F-M relationships to define and numerically model steep creek hazard scenarios across a range of magnitudes. BGC used the numerical modelling programs DAN-3D to model rock slope failure in the Jason Creek watershed and HEC-RAS to model floods, debris floods, and debris flows on both Jason and Mungye creeks. The model results indicate that the debris flow coarse front impacts the property at the fan apex on Jason Creek for all scenarios considered, and lower intensity muddy afterflows associated with precipitation-triggered flows impact properties downstream of Reid Road. Rock slide triggered-debris flows impact the property at the apex and multiple located downstream of Reid Road. On Mungye Creek, flow is well confined in the channel upstream of Reid Road for lower return periods and avulses at higher return periods. Blockage of the culvert on Mungye Creek at Reid Road results in flow running eastward and downslope into neighbouring properties.

BGC assessed life-safety risk to individuals in inhabited buildings associated with steep creek hazards in the study watersheds and determined that five properties on the Jason Creek have annual PDI greater than 1:10,000, a threshold adopted by multiple jurisdictions in Canada and internationally for risk tolerance from natural hazards. These are:

- 1781 Reid Road
- 1782 Reid Road
- 1788 Reid Road
- 1794 Reid Road
- 1802 Reid Road.

The property at the fan apex (1781 Reid Road, PID 1608908) has PDI >1:1,000 and BGC assessed that it is at **imminent risk** from debris flows during periods of high rainfall. Debris flows could impact the other properties listed with little warning during periods of high rainfall, but BGC assessed that the probability and expected consequences of such impacts are lower than at 1781 Reid Road. Debris flows could also impact other properties on and downstream of Jason Creek fan, but BGC assessed the risks to be within levels normally considered tolerable for existing

development in other jurisdictions. BGC did not identify any properties on Mungye Creek fan where PDI exceeded 1:10,000 for inhabited buildings. BGC did not assess risk to individuals outside of buildings. BGC expects economic damage associated with inundation, erosion, and debris deposition to residential development and infrastructure (road, rail, culverts) on both Jason and Mungye Creeks and surrounding areas. Given the gradient of Reid Road and existing culvert capacities at the creek crossings on both study creeks, BGC expects culvert blockage and significant flow concentration along the road surface towards downstream areas.

To reduce risk from debris flows on Jason Creek, BGC recommends a phased approach:

- **Phase 1:** Construction of flow diversion berms on individual properties (1781, 1782, 1788, 1794, 1802 Reid Road)
- **Phase 2:** Channel excavation and bridge construction at Reid Road crossing.

On Mungye Creek, BGC recommends replacement of the Reid Road culvert with a box culvert designed with sufficient capacity to convey the 200-year debris flood to reduce damage to Reid Road and economic risk to residential development. Further, BGC recommends that SLRD review applicable land-use policies to reduce risk to future development or redevelopment within the study area informed by BGC's composite hazard map (Drawing 08).

BGC developed conceptual-level (-50% to +100%) cost estimates for the proposed mitigation which cost approximately $7.8 Million on Jason Creek and $1 Million on Mungye Creek including O&M costs over a 75-year service. The phased approach proposed on Jason Creek facilitates construction of mitigation measures over two phases as funding and permitting allow. Future phases of design require further work to engage stakeholders and refine the mitigation designs.

7.2. Recommendations

BGC outlines recommendations specific to mitigation design in Section 6.4. As a summary, and in addition to those, BGC recommends that the SLRD:

- Review Jason and Mungye creek channel conditions following debris flows, debris floods, or high clearwater flows to evaluate if any changes warrant a re-assessment of the hazard and risk.
- Engage a Qualified Professional to review publicly available remote-sensing (e.g., lidar and InSAR) datasets, if and when new versions become available and consider new data collection at set future intervals. BGC recommends the area of interest include the Jason and Mungye creek watersheds as well as the rockfall area east of Jason Creek.
- Communicate the findings of this report with residents of the Reid Road area.
- Engage with stakeholders and review funding sources to identify preferred risk management approach(es).
- Adopt appropriate policies to manage risk to future development or re-development within the study area.
- Review risk tolerance criteria and engage with SLRD Council and Board on applicability and adoption within the SLRD.
- Develop a regionally-consistent decision-making framework for management of risks associated with natural hazards in excess of established thresholds and/or emergent ("imminent") risks within the SLRD. BGC recommends that this framework include a

methodology to characterize, and where possible quantify, the negative impacts of risk management approaches on affected parties to facilitate cost – benefit comparison.

- Review past assessments of the rockfall area east of Jason Creek to evaluate if an update with the benefit of lidar collected in 2022 is warranted.

7.3. Limitations

BGC based this risk assessment on the current number of dwellings and observed geomorphological conditions in the Jason and Mungye creek watersheds. Estimated risk levels assume constant conditions. Debris fans and the processes in their watersheds are dynamic. Hazard and risk will change to some degree when floods, debris floods, or debris flows aggrade or erode existing channels, or avulse to create new channels. Similarly, any human-made alterations of the landscape through fill placements, cut slopes, or ditching may change the distribution and intensity of debris-flood and debris-flow hazards and thus change the risk profile on the fans and surrounding areas. Modifications to development also change the risk by changing the number and location of persons exposed to hazard. As such, to assure consistency of this report with current conditions, BGC recommends an update to the risk assessment following debris flows or changes to the existing development. Any landscape alterations should require permits from the SLRD and review from professionals with appropriate training in light of this risk assessment.

Deformation of the unstable rock masses in the Jason watershed is not yet sufficiently characterized for a full understanding of movement rates and to assess if the future probability of rock slide-triggered debris flows is increased/increasing above historic rates. BGC recommends additional monitoring of the rock slope through assessment of remote-sensing datasets (e.g., lidar and InSAR) or installation of monitoring equipment (Section 6.2.3.3) to better constrain rock slope behaviour and evaluate risk management approaches in response.

Finally, BGC recognizes that development along Reid Road is subject to additional hazards outside of the scope of this assessment including rock fall and rock slide (e.g., 1982 restrictive covenant #T59223), slump, earthquake, and snow avalanche hazards. In light of the acquisition of detailed lidar topography and orthophoto (20 cm) as part of this assessment, BGC recommends a review of past studies of hazards within the lidar acquisition area to evaluate if the additional topographic data highlights new information or interpretation.

8. CLOSURE

We trust the above satisfies your requirements at this time. Should you have any questions or comments, please do not hesitate to contact us.

Yours sincerely,

BGC ENGINEERING INC.
per:

Lauren Hutchinson, M.Sc., P.Eng.
Senior Geotechnical Engineer

Pierre Friele, M.Sc., P.Geo., L.Eng.
Cordilleran Geoscience

Sophia Zubrycky, M.A.Sc., P.Eng.
Geotechnical Engineer

Reviewed by:

Kris Holm, M.Sc., P.Geo.
Principal Geoscientist

Alex Strouth, M.A.Sc., P.Eng.
Senior Geological Engineer

EGBC Permit To Practice: 1000944

LCH/KH/mjp/mm

REFERENCES

Bartels, S., Chen, H., Wulder, M., & White, J. (2016) Trends in post-disturbance recovery rates of Canada's forests following wildfire and harvest. *Forest Ecology and Management, 361*(1), 194-207. https://doi.org/10.1016/j.foreco.2015.11.015

Baumann Engineering (1994, November 30). *Terrain stability analysis of the Mt Currie-D'arcy corridor in southwestern British Columbia* [Report]. Prepared for Squamish Lillooet Regional District.

Baumann Engineering (1997, October). *Detailed Terrain Mapping with Slope Stability, Potential Erosion and Sediment Delivery Interpretations* [Report]. Prepared for Ministry of Forests.

Baumann Engineering (2003, September 16). *Proposed Subdivision of Lot 14, 1723 Reid Road, Ivey Lake, BC* [Report]. Prepared for Peter and Nicole Jean.

BC Wildfire Service (BCWS). (2022). *Fire Perimeters – Historical* [dataset]. Retrieved from https://open.canada.ca/data/en/dataset/22c7cb44-1463-48f7-8e47-88857f207702.

BC Met Portal. (n.d.) BC Met Portal [Web page]. Retrieved from MetPortal v2.2.3 (shinyapps.io).

BC Ministry of Transportation and Infrastructure (MOTI). (April, 2019). *Supplement to TAC Geometric Design Guide*.

BGC Engineering Inc. (2020). Squamish-Lillooet Regional District Geohazard Risk Prioritization [Report]. Prepared for SLRD.

BGC Engineering Inc. (2022, February 18). *Emergency Response Support, Jason Creek (Reid Road) Assessment* [Report]. Prepared for Squamish-Lillooet Regional District.

BGC Engineering Inc. (2022, May 20). *FBC Detailed Flood Mapping Study - Hummingbird Creek* [Report]. Prepared for Fraser Basin Council.

BGC Engineering Inc. (2022, June 6). *Detailed Quantitative Landslide Hazard and Risk Assessment – Reid Road Area, Electoral Area C* [Proposal and Cost Estimate]. Prepared for Squamish-Lillooet Regional District.

BGC Engineering Inc. (2022, November 25). *Jason Creek Debris-Flow Risk Assessment, Reid Road Area, Electoral Area C – Rev 1* [Letter Report]. Prepared for Squamish-Lillooet Regional District.

Blunden, R.H. (1981, November 5). RE: *Templar Holdings Ltd. Subdivision near Pemberton, BC* [Report]. Prepared for Rodgers & Associates.

Bovis, M., & Jakob, M. (1999). The role of debris-supply conditions in predicting debris flow activity. *Earth Surface Processes and Landforms, 24,* 1039-1054.

Bovis, M., & Jakob, M. (2000). The July 29, 1998 debris-flow and landslide dam at Capricorn Creek, Mount Meager Volcanic Complex, southern Coast Mountains, British Columbia. *Canadian Journal of Earth Sciences, 37*, 1321-1334.

Brardinoni, F., Slaymaker, O., & Hassan, MA. (2003). Landslide inventory in a rugged forested watershed: a comparison between air-photo and field survey data. *Geomorphology, 54,* 179-196. https://doi.org/10.1016/S0169-555X(02)00355-0

British Columbia Ministry of Transportation, Communications and Highways (1979, June 26). *RE: Subdivision Proposal in District Lots 2679 & 4100, Lillooet District* [Letter]. Prepared for Capilano Highlands Limited.

Cannon, S.H. & Gartner, J.E. (2005). Wildfire-related debris flow from a hazards perspective. In M. Jakob, & O. Hungr (Eds.), *Debris flow hazards and related phenomena* (pp. 363-385). Springer, Berlin, Heidelberg. https://doi.org/10.1007/3-540-27129-5_15

Church, M. & Jakob, M. (2020). What is a debris flood? *Water Resources Research*, *56(8).* https://doi.org/10.1029/2020WR027144

Cordilleran Geoscience Terrain Specialists (Cordilleran). (2021, December 13). [Report]. Prepared for Squamish-Lillooet Regional District.

Corominas, J. (1996). The angle of reach as a mobility index for small and large landslides. *Canadian Geotechnical Journal*, *33*, 260-271.

De Graff, J., Cannon, S. & Gartner, J. (2015). The Timing of Susceptibility to Post-Fire Debris Flows in the Western United States. *Environmental & Engineering Geoscience, 21*, 277-292. https://doi.org/10.2113/gseegeosci.21.4.277.

Engineers and Geoscientists BC (EGBC). (2017). *Professional Practice Guidelines - Flood Mapping in BC.* Version 1.0.

Engineers and Geoscientists BC (EGBC). (2018). *Professional Practice Guidelines - Legislated Flood Assessments in a Changing Climate in BC*. Version 2.1.

Engineers and Geoscientists BC (EGBC). (2022). *Professional Practice Guidelines - Landslide Assessments in BC.*

FEMA. (1995). *Engineering Principles and Practices for Retrofitting Flood Prone Residential Buildings:* FEMA 259, Federal Emergency Management Agency. Retrieved from http://www.fema.gov/library/viewRecord.do?id51645

Frontera Geotechnical, 2021. Preliminary Debris Flow and Flood Assessment, 1770 Reid Road, Squamish-Lillooet Regional District, BC [Report]. Prepared for Squamish-Lillooet Regional District.

Gartner Lee Limited (1998, June). *Water Quality and Quantity Inventory for Ivey Lake LRUP* [Report]. Prepared for the Ministry of the Environment, Lands and Parks.

Gartner, J., Cannon, S., & Santi, P. (2014). Empirical models for predicting volumes of sediment deposited by debris flows and sediment-laden floods in the transverse ranges of Southern California. *Engineering Geology, 178,* 45-56. https://doi.org/10.1016/j.enggeo.2014.04.008

Grainger, B. (2004). *Terrain stability field assessments in "Gentle over Steep" terrain of the southern interior of British Columbia*. Grainger and Associates Consulting Ltd. Salmon Arm, BC.

Grant, G. (1997). Critical flow constrains flow hydraulics in mobile-bed streams: a new hypothesis. *Water Resources Research, 33*(2), 349-358. 10.1029/96WR03134

Government of British Columbia. (2022). Forest Tenure Cutblock Polygons (FTA 4.0) [Dataset]. Forest Tenures Branch, Open Government License – British Columbia.

Guthrie, R. (2002). The effects of logging on frequency and distribution of landslides in three watersheds on Vancouver Island, British Columbia. *Geomorphology, 43,* 273-292. https://doi.org/10.1016/S0169-555X(01)00138-6

Guthrie, R.H., Friele, P., Allstadt, K., Roberts, N., Evans, S.G., Delaney, K.B., Roche, D., Clague, J.J., & Jakob, M. (2012). The 6 August 2010 Mount Meager rock slide-debris flow, Coast Mountains, British Columbia: characteristics, dynamics, and implications for hazard and risk assessment. *Natural Hazards and Earth System Sciences, 12*, 1277-1294. https://doi.org/10.5194/nhess-12-1277-2012

Griswold, J., & Iverson, R. (2008). *Mobility statistics and automated hazard mapping for debris flows and rock avalanches*. Scientific Investigations Report 2007-5276, Version 1.1. United States Geological Survey.

Hungr, O., & Evans, S. (2004) Entrainment of debris in rock avalanches: An analysis of a long run-out mechanism. *Geological Society of America Bulletin, 116(9-10),* 1240-1252. https://doi.org/10.1130/B25362.1

Hungr, O., Morgan, G.D., & Kellerhals, R. (1984) Quantitative analysis of debris torrent hazards for design of remedial measures. *Canadian Geotechnical Journal, 21*, 663-677. https://doi.org/10.1139/t84-073

Hungr, O., Leroueil, S., & Picarelli, L. (2014). Varnes classification of landslide types, an update. *Landslides*, *11*, 167-194. https://doi.org/10.1007/s10346-013-0436-y

Iverson, R.M. (2014). Debris flows: behaviour and hazard assessment. *Geology Today, 30(1)*, 15-20. https://doi.org/10.1111/gto.12037

Ivey Lake Planning Team. (May 16, 2001). Ivey Lake Local Resource Use Plan.

Jakob, M. (2000). The impacts of logging on landslide activity at Clayoquot Sound, British Columbia. *Catena, 38,* 279-300. https://doi.org/10.1016/S0341-8162(99)00078-8

Jakob, M. (2021). Landslides in a changing climate. In J. Shroder, T. Davies, & N. Rosser (Eds.), *Landslide hazards, risks, and disasters* (2nd ed., pp. 505-579). Amsterdam, Netherlands: Elsevier.

Jakob, M. & Jordan, P. (2001). Design flood estimates in mountain streams – the need for a geomorphic approach. *Canadian Journal of Civil Engineering, 28*, 425-239. https://doi.org/10.1139/l01-010.

Jakob, M. & Owen, T. (2021). Projected effects of climate change on shallow landslides, North Shore Mountains, Vancouver, Canada. *Geomorphology, 393.* https://doi.org/10.1016/j.geomorph.2021.107921

Jakob, M. & Nolde, N. (2022). Statistical techniques for debris-flow frequency-magnitude analysis. In: Jakob, M., McDougall, S., Santi, P. (2022). Advances in debris-flow science and practice. Springer – Heidelberg. In preparation.

Jakob, M., Bovis, M., & Oden, M. (2005). The significance of channel recharge rates for estimating debris-flow magnitude and frequency. *Earth Surface Processes and Landforms, 30*(6), 755-766. https://doi.org/10.1002/esp.1188

Jakob, M., Stein, D., & Ulmi, M. (2012). Vulnerability of buildings to debris-flow impact. *Natural Hazards, 60(2)*, 241-261. https://doi.org/10.1007/s11069-011-0007-2

Jakob, M., McDougall, S., Bale, S., & Friele, P. (2016). Regional Debris-flow Frequency-Magnitude Curves. GeoVancouver. Vancouver, BC.

Jakob, M., Mark, E., McDougall, S., Friele, P., Lau, C.A., & Bale, S. (2020). Regional debris-flow and debris-flood frequency-magnitude relationships. *Earth Surface Processes and Landforms.* 10.1002/esp.4942

Jakob, M., Davidson, S., Bullard, G., Busslinger, M., Collier-Pandya, B., Grover, P., & Lau, C-A. (2022). Debris-Flood Hazard Assessments in Steep Streams. *Water Resources Research, 58.* https://doi.org/10.1029/2021WR030907

Jarrett, R. (1984). Hydraulics of high-gradient streams. *Journal of Hydraulic Engineering, 110*(11). https://doi.org/10.1061/(ASCE)0733-9429(1984)110:11(1519)

Jordan, P. (2001). Regional incidence of landslides. In D.A.A. Toews and S. Chatwin (Eds.) *Watershed Assessment in the Southern Interior of British Columbia,* Proceedings of a Workshop, March 9-10, 2000, Penticton, B.C. British Columbia, Ministry of Forests. Victoria, B.C.

Jordan, P. (2002). Landslide frequencies and terrain attributes in Arrow and Kootenay Lake forest districts. *In* Terrain Stability and Forest Management in the Interior of British Columbia: Workshop Proc. P. Jordan and J. Orban (editors). Nelson, B.C., May 23–25, 2001. B.C. Min. For., For. Sci. Program, Victoria, B.C. Tech. Rep. 003. Jordan, P. and J. Orban (editors). 2002. Terrain stability and forest management in the Interior of British Columbia: workshop proceedings, May 23–25, 2001 Nelson, British Columbia, Canada. Res. Br., B.C. Min. For., Victoria, B.C. Tech. Rep. 003.

Khangura Engineering Ltd. (1997, September 29) Squamish- Lillooet Regional District Jason Creek Flood Mitigation Works Operation and Maintenance Manual [Manual]. Prepared for the Squamish Lillooet Regional District.

Klock, G.O., & Helvey, J.D. (1976). Debris flows following wildfire in North Central Washington. *In* Proceedings of the 3rd Federal Inter-Agency Sedimentation Conference, March 22-25, Denver, Colorado. Water Resources Council, Denver, CO. pp. 91-98.

Kristensen, L., Pless, G., Blikra, L.H. & Anda, E. (2020). Management and monitoring of large rockslides in Norway. In Proceedings ISRM International Symposium Eurock 2020 – Hard Rock Engineeirng, Trondheim, Norway, 14-19 June.

Kwan, J. (2012). Supplementary Technical Guidance on Design of Rigid Debris-resisting Barriers. Geotechnical Engineering Office, Civil Engineering and Development Department, The Government of the Hong Kong Special Administrative Region. GEO Report No. 270.

Lau, C.A., 2017. Channel Scour on Temperate Alluvial Fans in British Columbia. M.Sc. thesis, Department of Earth Sciences, SFU, Burnaby, BC.

Loukas, A. (1994). *Mountain precipitation analysis for the estimation of flood runoff in Coastal British Columbia* (Ph.D. Thesis). Department of Civil Engineering, University of British Columbia.

Mark, E. (2018). *Guidance for debris-flow and debris-flood mitigation design in Canada* (Master's thesis). Simon Fraser University, Burnaby, BC. Retrieved from https://summit.sfu.ca/item/17457

McDougall, S., Hungr, O. (2004). A model for the analysis of rapid landslide motion across three-dimensional terrain. Canadian Geotechnical Journal, 41, 1084-1097.

McDougall, S., Hungr, O. (2005). Dynamic modelling of entrainment in rapid landslides. Canadian Geotechnical Journal 42, 1437-1448.

Melton, M.A. (1957). An analysis of the relation among elements of climate, surface properties and geomorphology. Office of Nav Res Dept Geol Columbia Univ, NY. Tech Rep 11.

Millard, T. (1999). Debris flow initiation in coastal British Columbia gullies. B.C. Ministry of Forests, Vancouver Forest Region, Nanaimo, B.C. Forest Research Technical Report tr-002.

Ministry of Transportation and Infrastructure (MoTI). (2015, February). *Subdivision Preliminary Layout Review – Natural Hazard Risk.*

Mizuyama, T., Kobashi, S., & Ou, G. (1992). Prediction of debris flow peak discharge. Interpraevent, International Symposium, Bern, Switzerland, Tagespublikation, 4, 99±108.

Montgomery, D.R., and J.M. Buffington. 1997. Channel reach morphology in mountain drainage basins. Geological Society of America Bulletin 109:596-611.

Moody, J. & Martin, D. (2001). Initial hydrologic and geomorphic response following a wildfire in the Colorado Front Range. *Earth Surface Processes and Landforms, 26*, 1049-1070. https://doi.org/10.1002/esp.253.

Parise, M. & Cannon, S. H. (2012). Wildfire impacts on the processes that generate debris flows in burned watersheds. *Natural Hazards*, *61*, 217-227. https://doi.org/10.1007/s11069-011-9769-9

Pacific Climate Impacts Consortium (PCIC). (2012). Plan2Adapt. https://www.pacificclimate.org/analysis-tools/plan2adapt. [Accessed August 17, 2018]

Piteau Gadbby Macliod Limited (1975, May 8). *Groundwater and Sewage Disposal, Feasibility Study Templar Holdings Pemberton, British Columbia* [Report]. Provided to Rodgers & Associates.

Piton, G., & Recking, A. (2019). Steep bedload-laden flows: near critical?. *Journal of Geophysical Research: Earth Surface, 124*. https://doi.org/10.1029/2019JF005021

Pierson, T.C. (1986). Flow behaviour of channelized debris flows. Mount St. Helens. Washington. In A.D. Abrahams (Ed.), *Hillslope Processes* (pp. 269-296). Boston: Allen and Unwin.

Piteau & Associates (Piteau) (1981). *Evaluation of the potential rockfall/landslide hazard for the proposed subdivision of DL2679 in Pemberton, BC* [Report]. Prepared for Templar Holdings Ltd., Vancouver, BC.

PK Read Engineering Ltd. (September 7, 2009). *Geotechnical Hazards Pertinent to the Development* [Report]. Prepared for Patrickson Residence Renovation.

PK Read Engineering Ltd. (April 2, 2010). *Geotechnical Hazards Pertinent to the Development* [Report]. Prepared for Patrickson Residence Renovation.

PK Read Engineering Ltd. (2016, March 3). *Assessment of the rockfall hazard referenced within the covenant #T59223 for Lot 5 Reid Road, DL2679, Lillooet District* [Report]. Prepared for Jeff Drenka, Pemberton, BC.

Prein, A.F., Rasmussen, R.M., Ikeda, K., Liu, C., Clark, M.P, & Holland, G.J. (2017). The future intensification of hourly precipitation extremes. *Nature Climate Change, 7*, 48-52. https://doi.org/10.1038/nclimate3168

Prochaska, A. B., Santi, P. M., & Higgins, J. D. (2008). Debris basin and deflection berm design for fire-related debris-flow mitigation. *Environmental and Engineering Geoscience, 14*(4), 297-313. https://doi.org/10.2113/gseegeosci.14.4.297

Protz, R., Ross, G. J., Martini, I. P. Terasmae. J. (1984). *Rate of Podzolic soil formation near Hudson Bay, Ontario. Can. J. Soil Sci.*64: 31-49.

Rengers, F., McGuire, L.A., Oakley, N.S., Kean, J.W., Staley, D.M., & Tang, H. (2020). Landslides after wildfire: initiation, magnitude, and mobility. *Landslides, 17*, 2631-2641. https://doi.org/10.1007/s10346-020-01506-3

Rickenmann, D., & Koschni, A. (2010). Sediment loads due to fluvial transport and debris flows during the 2005 flood events in Switzerland. *Hydrological Processes, 24*(8), 993-1007. https://doi.org/10.1002/hyp.7536

Riddell, J.M. (1992). *Structure stratigraphy and contact relationships in Mesozoic volcanic and sedimentary rocks east of Pemberton southwestern British Columbia* (Master's thesis). The University of Montana. Retrieved from https://scholarworks.umt.edu/etd/7499.

Rodgers & Associates (1974, September 26). *New Pemberton and Templar Holdings Feasibility Study* [Report]. Provided to Templar Holdings Ltd.

Sanborn, P., Lamontagne, L. and Hendershot, W. 2011. Podzolic soils of Canada: Genesis, distribution, and classification. *Can. J. Soil Sci. 91*: 843 880.

Sättele, M., Krautblatter, M., Bründl & Straub, D. (2016). Forecasting rock slope failure: how reliable and effective are warning systems? *Landslides* 13: 737-750.

Schiarizza, P. and Church., N. (1996). The Geology of the Thompson - Okanagan Mineral Assessment Region. British Columbia Ministry of Energy, Mines and Petroleum Resources, British Columbia Geological Survey Open File 1996-20.

Shakesby, R. & Doerr, S. (2006). Wildfire as a hydrological and geomorphological agent. *Earth-Science Reviews, 74*(3-4), 269-307. https://doi.org/10.1016/j.earscirev.2005.10.006.

Sharon, R. & Eberhardt, E. (2020). Guidelines for Slope Performance Monitoring. CRC Press, Leiden, 331 p.

Sidle, R.C. (1991). A conceptual model of changes in root cohesion in response to vegetation management. *Journal of Environmental Quality, 20,* 43-52. https://doi.org/10.2134/jeq1991.00472425002000010009x

Sidle, R.C. (2005). Influence of forest harvesting activities on debris avalanches and flows. In M. Jakob & O. Hungr (Eds.), *Debris-flow hazards and related phenomena* (pp. 387-409). Springer, Berlin, Heidelberg. https://doi.org/10.1007/3-540-27129-5_15

Simonovic, S.P., A. Schardong, R. Srivastav, and D. Sandink. (2015), *IDF_CC Web-based Tool for Updating Intensity-Duration-Frequency Curves to Changing Climate (ver 6.0)*. [Web page]. Retrieved from the Western University Facility for Intelligent Decision Support and Institute for Catastrophic Loss Reduction website: https://www.idf-cc-uwo.ca

SNC Lavalin (1998, July 27). *Geotechical Assessment – 1781 Reid Road, Ivey Lake – Supplemental Report* [Report]. Prepared for Mr. Sean Tribe

SNC Lavalin (1998, July 16). *Geotechical Assessment – 1781 Reid Road, Ivey Lake* [Report]. Prepared for Mr. Sean Tribe.

Squamish-Lillooet Regional District. (2022, May 11). Request for Proposals: Detailed Quantitative Landslide Hazard and Risk Assessment – Reid Road Area, Electoral Area C.

Squamish-Lillooet Regional District. (2022, February 24). Evacuation ORDER and ALERT areas – Updated February 24, 2022.

Staley, D., Kean, J., & Rengers, F. (2020). The recurrence interval of post-fire debris-flow generating rainfall in the southwestern United States. *Geomorphology, 370*(1). https://doi.org/10.1016/j.geomorph.2020.107392.

Takahashi, T. (1991). *Debris flows*. Rotterdam, Balkema.

United States Geological Survey (2020). How Wildfires threaten U.S. Water Supplies [website]. Accessed at https://labs.waterdata.usgs.gov/visualizations/fire-hydro/index.html#/.

US Army Corps of Engineers. HEC-RAS (Version 6.2) [Computer software]. Retrieved from https://www.hec.usace.army.mil/confluence/rasdocs/rasrn

Valentine W. W. G., Sprout P. N., Baker T. E., and Lavkulich L. M. The soil landscapes of British Columbia. BC Ministry of Environment. Victoria, BC.

Westrek Geotechnical Services Ltd., October 12, 2016. Phase 3, Refinement of Assessment of Risk from Upslope Landslides to Transmission Line Structures - Area 1, Birken Sub-Basin, British Columbia (File No. 016-009). Prepared for BC Hydro Transmission Engineering, Burnaby, BC.

Wilford, D., Sakals, M., Innes, J., Sidle, R., & Bergerud, W.A. (2004). Recognition of debris flow, debris flood and flood hazard through watershed morphometrics. *Landslides, 1*(1), 61-66. https://doi.org/10.1007/s10346-003-0002-0

Zimmermann, A. (2010). Flow resistance in steep streams: An experimental study. *Water Resources Research, 46*. https://doi.org/10.1029/2009WR007913

Zubrycky, S., Mitchell, A., Aaron, J., McDougall, S. (2019). Preliminary calibration of a numerical runout model for debris flows in Southwestern British Columbia. 7th International Conference on Debris-Flow Hazards Mitigation, Golden, CO, June 10 – 13.

APPENDIX A
DATA COMPILATION AND SUMMARY OF PREVIOUS REPORTS

The following data sources, organized by date of publication, were reviewed by BGC for the Jason and Mungye Creek Hazard and Risk Assessment:

- Groundwater resources and sewage disposal for Templar Holdings Ltd. Subdivision near Pemberton (Blunden, 1981; Piteau Gadbby Macleod Limited, May 8, 1975).
- New Pemberton and Templar Holdings Feasibility Study (Rodgers & Associates, September 26, 1974)
- Request for topographic data regarding Proposed Subdivision D.L. 2679 and 4100 Lillooet District due to geohazards perceived on Jason Creek (BC Ministry of Transportation, Communications and Highways, June 26, 1979).
- Assorted communications pertaining to permitting and development of D.L. 2679 and 4100 Lillooet District between 1974 and 1981.
- A water quality and quantity inventory for the Ivey Lake Local Resource Use Plan, encompassing the Ivey Lake and Jason Creek watershed area (Gartner Lee Limited, June, 1998).
- Detailed Terrain Mapping, including stope stability, potential erosion, and sediment delivery interpretations (Baumann Engineering, October, 1977)
- Geotechnical hazard assessment of 1781 Reid Road, 1723 Reid Road, 1794 Reid Road (Baumann Engineering, September 16, 2003; PK Read Engineering Ltd., September 7, 2009; April 2, 2010; SNC Lavalin, July 27, 1998; July 16, 1998).
- Operation and Maintenance Manual for the Jason Creek Flood Mitigation Works (Khangura Engineering Ltd. September 29, 1977).
- Ivey Lake Local Resource Use Plan (Ivey Lake Planning Team, May 16, 2001)

A summary of review comments is provided in Table A-1. BGC's review was completed for the purposes of familiarizing ourselves with the site and assessments completed to date.

Table A-1. Summary of review comments on previous reports within the study area.

Author/Date	Client/Addressee	Purpose	Finding(s)	BGC Comments
Rodgers & Associates, September 26, 1974	Squamish-Lillooet Regional District (SLRD)	Feasibility Study		Jason Creek is mentioned but without any notes on geohazards.
Rodgers & Associates, October 1, 1974	District Highways Manager	Proposed subdivision of DLs 2679 and 4100	N/A	No mention of geohazards.
Piteau Gadsby Macleod Ltd., May 8, 1975	Rodgers & Associates	Groundwater and Sewage Disposal, Feasibility Study	High chance of successful well development. Sewage disposal possible and sites are suitable.	No mention of geohazards.
Department of Highways (DoH), September 8, 1975	Templar Holding Ltd.	Notification	Department of Highways (DoH) advises that preliminary layout approval for DL 2679 and 4100 had not been granted. DoH states that given severe planning problems due to the isolated nature of the proposal that the proposal is not in the public interest and is premature.	No mention of geohazards.
DoH. February 3, 1977	SLRD	Notification	Notes that the SLRD was not in favour of a proposed subdivision of DL 2679 (January 14, 1976 letter from SLRD to MoT). Solicitor approached DoH to reconsider the application for subdivision plan approval. Letter seeks clarification if the SLRD's original refusal of the subdivision approval was contingent of the lots being 5 acres in size.	N/A
Department of Highways, 4 March 1977	LaCroix, Stewart, Siddall & Saunders (solicitors)	Notification	Notes that SLRD is now prepared to reconsider granting tentative approval for a subdivision of DL 2679 as long as lots are 5 acres in size and each lot provided with water.	N/A
Ministry of Transportation, Communications and Highways (MoTCH), June 26., 1979	Capilano Highlands Limited	Notification	Subdivision proposal DL 2679 and 4100. Preliminary layout approval is not granted because significant portions of DL 2679are rock slide-prone. MoTCH requires contour map showing the maximum extent of the rock slide to delineate affected areas. Requirement of Jason Creek being identified on maps through the subject subdivision.	Rockslide hazard identified. No mention of debris-flow hazards.
Piteau, May 1981	Templar Holdings Ltd.	Rockfall, landslide assessment for District Lot 2679	"relatively old" landslide was identified in the vicinity and upslope of Lots 8, 9, 10 and 11. Bare scarp identified as the potential source of the rock slide. Significant rock fall hazard identified. Author notes difficulty in specifying if a block is a glacial erratic in some areas or a rock fall block and speculates that the rock fall must have occurred prior to the slope being tree-covered. No rock fall problem in Lot 8. Notes potential for snow avalanches. Major potential for future rock fall identified. Proposes development restrictions in northeast corner of Lot 9, 10 and 11 and southwest half of Lot 8 as well as a depression. Recommends against any timber harvesting upslope of the subdivision at DL 2679.	Did not discuss or recognize major debris-flow hazards on Mungye or Jason Creek fans. Did not consider the possibility that rock slides could trigger deep-seated landslides due to undrained loading and plastic deformation of clay-rich colluvium underlying bedrock. No subsurface investigations were conducted. Study was conducted before availability of 1/20,000 scale TRIM or high resolution lidar mapping.
Blunden, December 1981	Templar Holdings Ltd.	Groundwater and sewage disposal evaluation	Substantial disagreement with the earlier Piteau (1981) report. Evokes periglacial processes as being responsible for boulder transport and felsenmeer (boulder field) development. Pattern of faulting and shears associated with Owl Creek fault noted.	No evidence is presented to support the periglacial hypothesis. It is possible that some earthflow-type movement (plastic deformation of clay-rich soils) may have occurred in the immediate post-glacial time.

Author/Date	Client/Addressee	Purpose	Finding(s)	BGC Comments
Blunden, 1981			Rock slide led to “sinuous solifluction transporting glacial erratics and landslide blocks”.	Observation may be correct, but BGC does not agree with the interpretation (landslide-triggered boulder movement, not by solifluction). Does not mention debris flow or debris flood hazards on Mungye Creek.
Blunden, Nov. 5, 1981	Dr. R.S. Rodgers	Locate groundwater and sewage disposal area for subdivision	Substantial potential for use of groundwater in proposed subdivision.	Report has little relevance to the present study.
Khangura Engineering Ltd. and Bland Engineering Ltd., Sept 29, 1997	BC Ministry of Environment, Lands and Parks	Flood mitigation works O&M manual	Proposed dike 230 m long from fan apex to Reid Road, wire mesh gabions on creek side at pre-existing house (1781 Reid Road). Designed for 200-yr flood (assessed to be 42 m^3/s) plus 0.6 m freeboard.	Only considered clear water floods plus freeboard. The proposed dike alignment is not clear to BGC.
Baumann Engineering, Oct. 1997	Ministry of Forests	Detailed terrain mapping, slope stability, erosion, and sediment delivery in the Ivey Lake area. Initiated because of residents’ concerns about upslope proposed timber harvesting relating to water resources.	Potential for large timber-harvesting-related landslides considered low. Most hazard concentrated along middle reaches of Jason and Mungye creeks where small logging-related landslides could trigger large debris flows. Deep bedrock-instabilities were recognized. Recognition of large bedrock failures resulting in potentially catastrophic debris flows on Jason Creek fan. Recommendations are made for how to minimize logging- and logging-road related instabilities. Unstable and altered poor bedrock quality was recognized. Entire fan of Jason Creek considered active and subject to debris flows. At least 4 debris flows since 1900 noted. Large inactive bedrock slump identified west of Jason Creek fan.	Very thorough report supported with ample fieldwork. No radiocarbon dating from test trenches, but some dendrochronology. Clear recognition of debris-flow hazards on Jason Creek fan.
SNC Lavalin, July 27, 1998	Mr. Sean Tribe	Geotechnical Investigation 1781 Reid Road (Lot 7). Potential for debris floods, debris flow, and rock fall hazards.	Concludes, based on size and age of trees, that major flows have not occurred for at least 75 years. Log jams could hold up to 250 m^3 of debris. Largest identified instability could contribute approx. 450 m^3 of debris to the channel. 1900 debris flow noted by Baumann (1997) with cross-section area of 50 m^2, classified by author as “relatively small”. Bedrock failures are believed to be small in the order of 100s to 1000s of m^3. Maximum debris-flow volume of 500 m^3 in the last 100 years. 2000 m^3 estimated as 500-year event. Deflection berm proposed for 35 m length plus swaled driveway. Considers that 2000 m^3 of debris would stop upstream of Reid Road. Notes that Reid Road culvert on Jason Creek is undersized.	A cross-section of 50 m^2 with a typical debris flow velocity of 5 – 7 m/s would be a 250 to 350 m^3/s discharge, which would not be considered a “relatively small” flow. Severe underestimation of debris flow volumes. Flow cross-section and associated peak discharge would require much larger volumes that those estimated.
Ivey Lake Planning Team		Local Resource Use Plan	Local Resource Use Plan (LRUP) developed with input from planning team including area residents, Ministry of Forests, Ministry of Environment (Water Management, Fish and Wildlife), woodlot licensee, Walkerville developer, Pemberton, and Walkerville residents. Debris flow hazards on Jason and Mungye creeks identified based on Baumann report (October, 1997). Influence of forestry activities on hazards identified. Avulsion and flooding hazards are also acknowledged. Report acknowledges that recommendations for management of sensitive terrain in proximity to the creeks should be adopted and recommends property owners of most at-risk lots (7, 8, 28, and 29 on Jason Creek and 14 and 13 on Mungye Creek).	The recommendations in LRUP indicate that members of the planning team were aware of the hazards posed by Jason and Mungye Creeks.
Baumann Engineering, Sept 16, 2003	Peter and Nicole Jean, Lot 14, 1723 Reid Road	Geotechnical / water availability / septic field suitability assessment for proposed subdivision of 5-acre lot.	Existing house site on north side of Mungye Creek mapped as off the fan and underlain by till. The house site was deemed unaffected by alluvial fan hazards. The Mungye Creek fan was classified as active in the proximity of the creek, and relatively “inactive” in the lower (southern) portion of the property but subject to rare (<1/500 per annum) debris flow and avulsions. No recent debris-flow activity was noted. Debris flows judged to be relatively small (low < 5000 m^3), avulsion locations identified. The existing home and the land beyond the top of bank along the incised southern portion of Mungye Creek is “safe for the use intended” with no apparent hazard at the existing house site and a residual risk of < 1:475 years) on the southern portion of the lot..	No trenching or radiocarbon dating completed (and likely would not have been expected for the purpose of this report at the time of writing).

Author/Date	Client/Addressee	Purpose	Finding(s)	BGC Comments
P.K. Reid, Sept 7, 2009 and amended with lot area reference on April 2, 2010	Patrickson Residence, Lot 26, DL 2679	Geotechnical hazard assessment.	Large boulder identified on lot assessed as being an older rock fall, possibly glacier-assisted transport or moved during subdivision road construction. Area outside the 27.5 degree rock fall shadow zone as per the empirical analysis by Hungr and Evans (2004).	The site was assumed to be underlain by till, and the fan landform was not recognised. The possibility of large boulder transport by debris flows was not considered.
P.K. Reid Engineering Ltd.	Jay Drenka, Lot 5	Restrictive covenant modification, reassessment of geological hazards.	During the 1982 subdivision process a restrictive covenant was placed on Lot 5 due to concerns of rock fall hazards. Detailed study using empirical rock fall shadow angle and numerical rock fall runout modeling suggests a relaxation of rock fall-related covenants.	Outside the scope of BGC's current assignment. The report does not mention debris-flow hazards.

BGC also reviewed aerial imagery (air photos and satellite imagery) of the study area between 1932 and 2020 (Table A-2).

Table A-2. Air photo imagery used in hazard assessment.

Roll	Photo Numbers	Imagery Date	Source	Scale	Notes
A10363	144-145	1946	National Air Photo Library	1:20,000	
A13323	111-112	1951	National Air Photo Library	1:70,000	
Bc5341	33-34	1969	GeoBC	1:45,000	
A25827	10-11	1981	National Air Photo Library	1:25,000	
BC81113	102	1981	GeoBC	1:40,000	Reviewed in low-resolution
BC81117	0243-024			1:20,000	Reviewed in low-resolution
BC86066	088-089	1986	GeoBC	1:23,000	Reviewed in low-resolution
Bcc94119	158-159	1994	GeoBC	1:15,000	Reviewed in low-resolution
Bcc84160	004-005				
Bcc05086	209-210	2005	GeoBC	1:15,000	Reviewed in low-resolution
Bc09017	129-130	2009	GeoBC	1:30,000	
Bcd16403	273-276, 355-357	2016	GeoBC	1:6,250	Reviewed in low-resolution
ESRI World Imagery		4/9/2020		-	

APPENDIX B
STEEP CREEK PROCESSES

B.1. INTRODUCTION

Steep creeks (here-in defined as having channel gradients steeper than 5%, or 3°) may be subject to a spectrum of sediment transport processes ranging with increasing sediment concentration from clearwater floods to debris floods, hyperconcentrated flows (in fine-rich sediment), to debris flows. These events can be referred to collectively as hydrogeomorphic processes because water and sediment (in suspension and bedload) are being transported. Depending on process and severity, hydrogeomorphic processes can alter landscapes (Figure B-1).

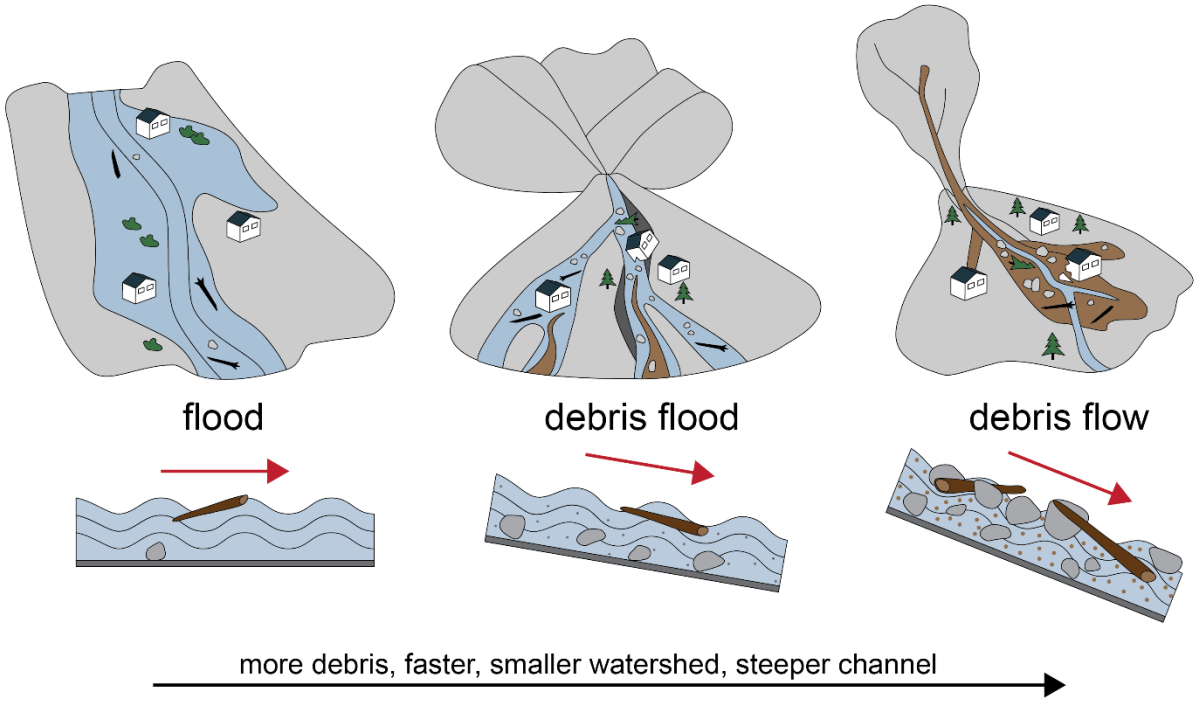

Figure B-1. Simplified illustration summarizing the hazards associated with each hydrogeomorphic process. BGC-created figure.

Clearwater floods do transport bedload and other sediments; they are not completely clear. The transition of a flood into a debris flood occurs when most of the channel bed is mobilized except possibly the largest clasts (Church and Jakob, 2020). As more and more fines (clays, silts and fine sands) are incorporated into the flow, hyperconcentrated flows may develop (not of relevance to Jason or Mungye creeks). Debris flows are typically triggered by side slope landslides or progressive bulking with erodible sediment in particularly steep (>15°) channels. Debris flows are more prevalent following wildfires of moderate to high burn severity when there is ample surface sediment exposed without the sheltering vegetative cover. Dilution of a debris flow through partial sediment deposition on lower gradients (approximately less than <15°) channels, and tributary injection of water can lead to a transition towards hyperconcentrated flows or debris floods and eventually floods. Most steep creeks can be classified as hybrids, implying variable hydrogeomorphic processes at different return periods.

Figure B-2 summarizes the different hydrogeomorphic processes by their appearance in plan form, velocity, and sediment concentration

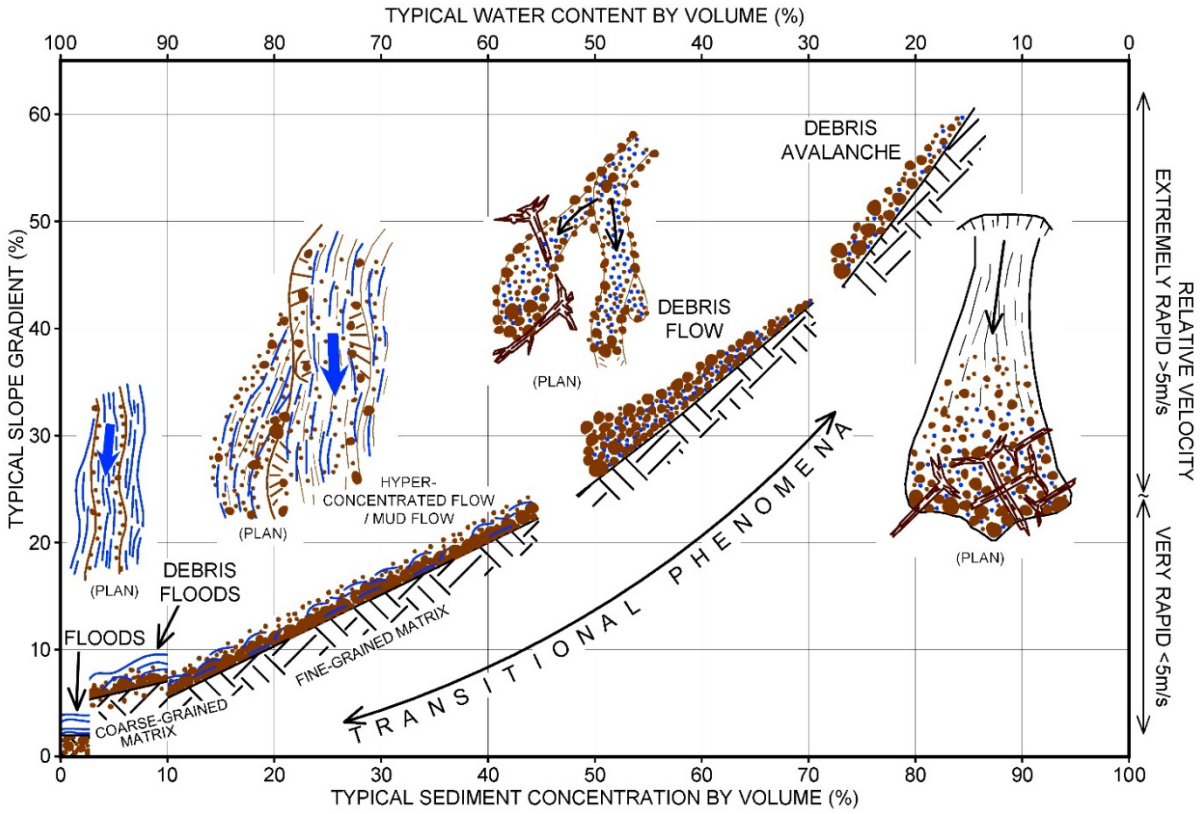

Figure B-2. Hydrogeomorphic process classification by sediment concentration, slope velocity and planform appearance. BGC-created figure.

B.1.1. Debris Floods

Debris floods typically occur on creeks with channel gradients between 5 and 30% (3-17°), but in contrast to common belief, can also occur on lower gradient gravel bed rivers. Debris floods occur when large volumes of water in a creek or river entrain the gravel, cobbles and boulders on the channel bed; this is known as “full bed mobilization”. The peak discharges are often very similar to those of clearwater floods, but the flow is more heavily charged with debris and sediment. Debris floods are known for their ability to cause extensive and rapid bank erosion (Church and Jakob, 2020; Jakob et al. 2022), scour, and aggrade channel beds increasing the risk of channel avulsion (Hungr et al., 2014). Cycles of scour and aggradation can occur in different phases throughout a debris flood.

Church and Jakob (2020) developed a three-fold typology for debris floods, which had previously not been defined well. This typology is summarized in Table B-1. Identifying the correct debris-flood type is important in understanding the sediment concentration the debris flood may carry and the changes to peak discharge, both which feed into the frequency-magnitude relationship discussed in Appendix G. Type 1 debris floods are initiated from rainfall or snowmelt generated streamflow that is sufficiently powerful to fully mobilize the channel bed. Type 2 debris floods are generated from diluted debris flows. Type 3 are generated by natural or man-made dam

breaches. Type 1 and Type 2 debris floods are of relevance to Mungye Creek while Type 2 debris floods are relevant for Jason Creek.

Table B-1. Debris-flood classification based on Church and Jakob (2020).

Term	Definition	Typical sediment concentration by volume (%)	Typical factor applied to clearwater peak discharge	Typical impacts
Type 1 (Meteorologically generated debris flood)	Rainfall/snowmelt generated through exceedance of critical shear stress threshold when most of the surface bed grains are being mobilized.	< 5	1.02 to 1.2 (depending on the proximity of major debris sources to the fan apex as well as organic debris loading)	Widespread bank erosion, avulsions, alternating reaches of bed aggradation and degradation, blocked culverts, scoured bridge abutments, damaged buried infrastructure particularly in channel reaches u/s of fans.
Type 2 (Debris flow to debris flood dilution)	Substantially higher sediment concentration compared to a Type 1 debris flood and can transport larger volumes of sediment. All grain sizes are mobilized, except those from lag deposits (big glacial or rock fall boulders)	< 50	Up to 1.5 depending on the distance of the debris-flow transition to the area of interest. If the debris flow tributary is immediately upstream of the fan apex, the bulking factor may be higher.	
Type 3 (Outbreak floods)	Outbreak flood in channels that are not steep enough for debris-flow generation. The critical shear stress for debris-flood initiation is exceeded abruptly due to sharp hydrograph associated with the outbreak flood. All grains are mobilized in the channel bed and non-cohesive banks.	< 10 (except immediately downstream of the outbreak)	Up to 100 depending on size of dam and distance to dam failure. Peak discharges should be calculated through dam breach analyses and flood routing	Vast bank erosion, avulsions, substantial bed degradation along channels and aggradation on fans, destroyed culverts, outflanked or overwhelmed bridges, damaged buried infrastructure on channels and fans.

B.1.2. Debris Flows

Debris flows originate from a single or distributed source area(s) of sediment mobilized by the influx of ground or surface water. Liquefaction occurs shortly after the onset of landsliding due to turbulent mixing of water and sediment, and the slurry begins to flow downstream, ‘bulking’ by entraining additional water and channel debris as the flow moves down a confined gully or channel. Post-wildfire debris flows are a special case where the lack of vegetation and root strength can lead to abundant rilling and gullying that deliver sediment to the main channel where

mixing leads to the formation of debris flows. In those cases, no single source or sudden liquefaction is required to initiate or maintain a debris flow.

Coarse granular debris flows require a channel gradient of at least 27% (15°) for transport over significant distances (Takahashi, 1991) and have volumetric sediment concentrations greater than 50% (i.e., there is more debris and sediment than there is water). Transport is possible at gradients as low as 20% (11°), although some momentum transfer from side-slope landslides is needed to sustain flow on those slopes. Debris flows may continue to run out onto lower gradients even as they lose momentum and drain.

Flow velocities typically range from 1 to 10 m/s leading to peak discharges during debris flows that are at least an order of magnitude larger than those of clearwater floods of comparable return period floods and can be 50 times larger or more (Jakob & Jordan, 2001; Jakob et al., 2016).

Debris flows are more than 50% sediment by volume and typically transport large boulders and woody debris meaning the flow is quite dense. The dense flow travels at high speeds meaning it can have very high impact forces and can cause extensive damage to structures, infrastructure, and cause life loss.

Channel banks can be severely eroded during debris flows, although lateral erosion is often associated with the trailing hyperconcentrated flow phase that is characterized by lower volumetric sediment concentrations. The most severe damage results from direct impact of large clasts or coarse woody debris against structures that are not designed for the impact forces. Even where the supporting walls of buildings may be able to withstand the loads associated with debris flows, building windows and doors can be crushed and debris may enter the building, leading to extensive damage to the interior of the structure (Jakob et al., 2012). Similarly, linear infrastructure such as roads and railways can be subject to complete destruction. On the medial and distal fan (the lower 1/3 to 2/3), debris flows tend to deposit their sediment rather than scour. Therefore, exposure or rupture of buried infrastructure such as telecommunication lines or pipelines is rare. However, if a linear infrastructure is buried in the proximal fan portions that undergo cycles of incision and infill, or in a recent debris deposit, it is likely that over time or during a significant runoff event, the tractive forces of water will erode through the debris until an equilibrium slope is achieved, and the infrastructure thereby becomes exposed or may rupture due to boulder impact or abrasion. This necessitates understanding the geomorphic state of the fans being traversed by a buried linear infrastructure.

Channel avulsions are likely in poorly confined channel sections (particularly on the outside of channel bends where debris flows tend to super-elevate). Sudden loss of confinement and decrease in channel slope cause debris flows to decelerate, drain their inter-granular water, and increase shearing resistance, which slow the advancing bouldery flow front and block the channel. The more fluid afterflow (hyperconcentrated flow) is then often deflected by the slowing front, leading to secondary avulsions and the creation of distributary channels on the fan. Because debris flows often display surging behaviour, in which bouldery fronts alternate with hyperconcentrated afterflows, the cycle of coarse bouldery lobe and levee formation and afterflow deflection can be repeated several times during a single event. These flow aberrations and

varying rheological characteristics pose a challenge to numerical modelers seeking to create an equivalent fluid (Iverson, 2014).

B.1.3. Peak Discharge Estimation

Clear-water flood, debris-flood, and debris-flow processes can differ widely in terms of peak discharge. The peak discharge of a debris flood is typically 1 to 1.2 times that of a clear-water flood in the same creek but could be much greater for Type 2 and 3 debris floods. If the creek is subject to debris flows, the peak flow may be much higher (as much as 50 times) than the flood peak discharge (Jakob & Jordan, 2001). Figure B-3 shows a hypothetical cross-section of a steep creeks, including:

- Peak flow for the 2-year return period (Q_2)
- Peak flow for the 200-year return period flood (Q_{200})
- Peak flow for Type 1 debris flood (Q_{max} full bed mobilization)
- Peak flow for Type 3 debris flood (Q_{max} outburst flood)
- Peak flow for debris flow (Q_{max} debris flow).

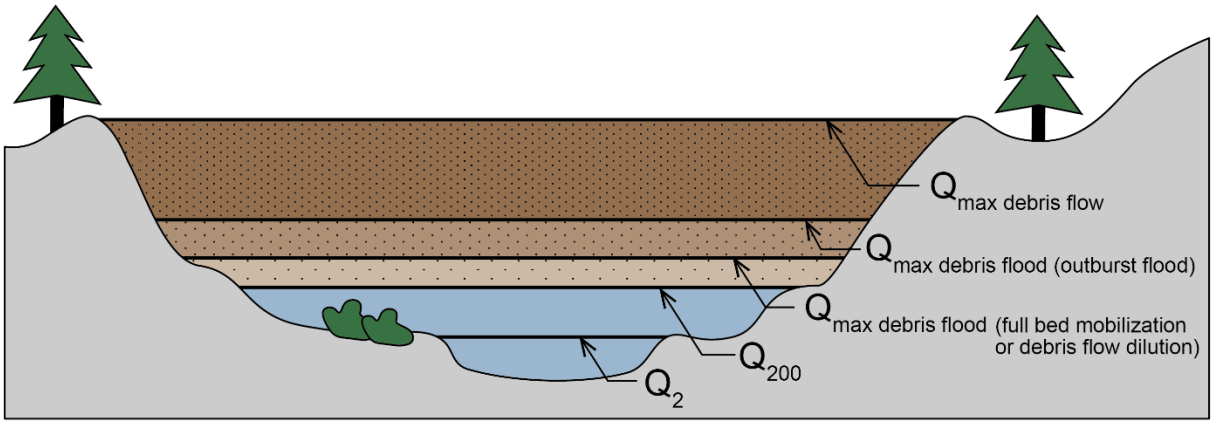

Figure B-3. Steep creek flood profile showing schematically peak flow levels for different events.

B.1.4. Avulsions

An avulsion occurs when a watercourse jumps out of its main channel into a new course across its fan or floodplain. This can happen because the main channel cannot convey the flood discharge and simply overflows, or because the momentum of a flow allows overtopping on the outside of a channel bend. Finally, an avulsion can occur because a log jam or blocked bridge redirects flow away from the present channel. The channel an avulsion flow travels down is referred to as an avulsion channel. An avulsion channel can be a new flow path that forms during a flooding event or a channel that was previously occupied.

In Figure B-4, a schematic of a steep creek and fan is shown where the creek avulses on either side of the main channel. The avulsion channels are shown as dashed blue lines as avulsions only occur during severe floods (i.e., rarely). On high resolution topographic maps generated from Lidar, avulsion channels are generally visible and are tell-tale signs of past and potential future avulsions.

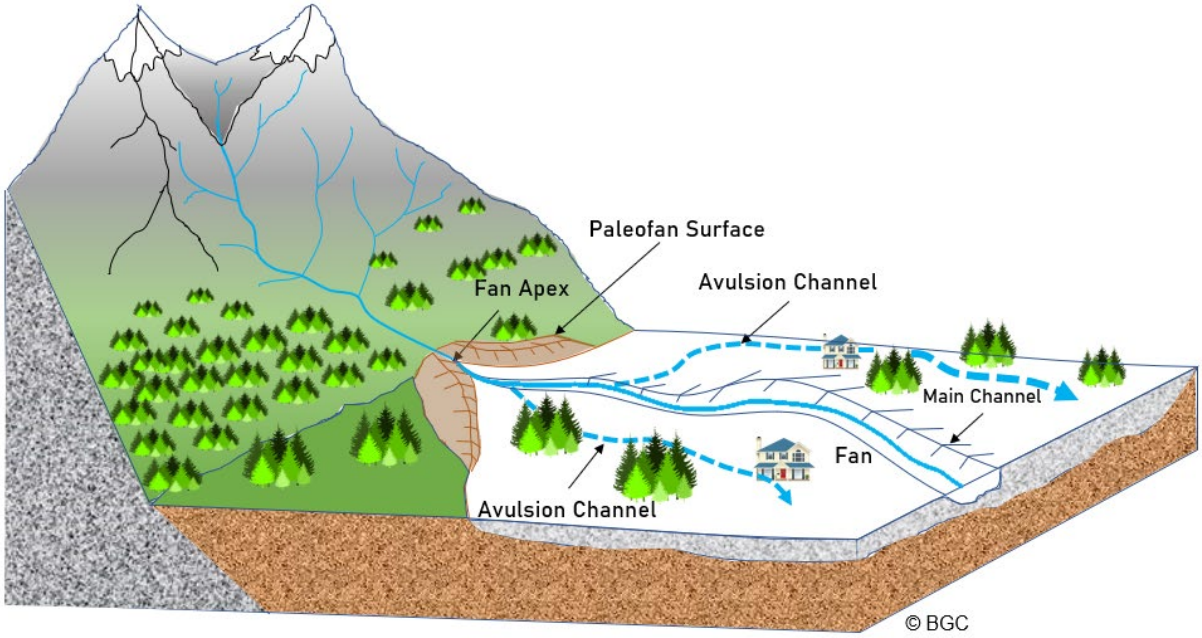

Figure B-4. Schematic of a steep creek channel with avulsions downstream of the fan apex. Artwork by BGC.

B.1.5. Bank Erosion

Floods and debris floods exert high shear stresses on channel banks which can lead to bank erosion. Alluvial fans may be particularly susceptible to bank erosion as channel bed armouring limits the erodibility of the bed relative to the channel banks, which are often composed of non-cohesive materials such as sands and gravels. In contrast, rivers that typically experience overbank flooding and deposition of fine sediment during clearwater floods are likely to have cohesive banks composed of silt and clay, which are relatively strong compared to the channel bed.

Bank erosion along steep creeks is not considered in standard hydraulic models, and therefore needs to be assessed separately. Bank erosion is a self-limiting process as channel widening lowers the flow depth and shear stress associated with a given flood magnitude (Figure B-5).

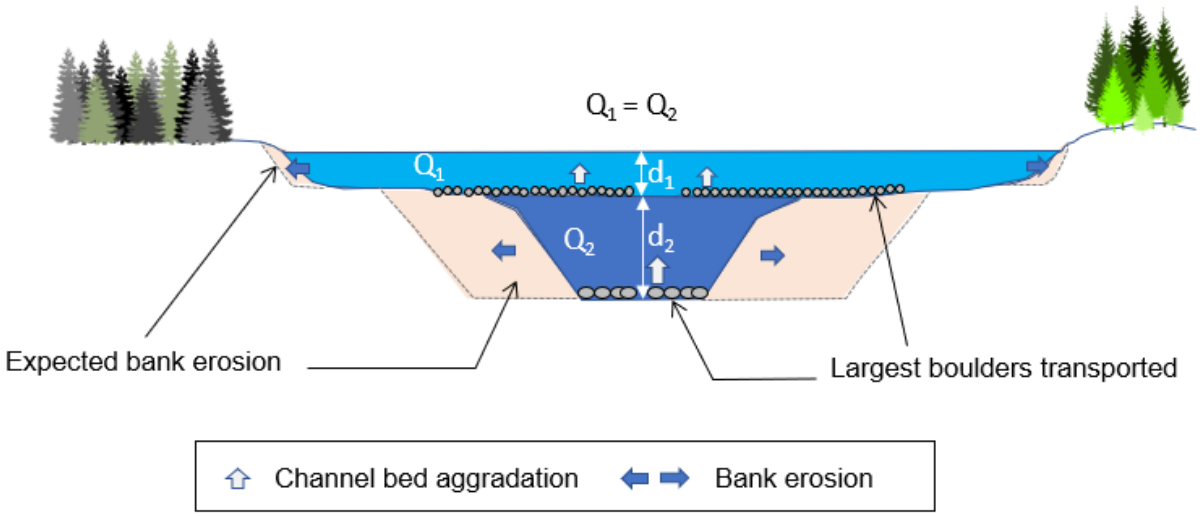

Channel configuration	Flow characteristics and bank erosion potential
Wide channel and floodplain (light blue)	• Low flow depth (d_1) and velocity lead to low shear stresses exerted on channel banks. • Lower bank erosion potential and smaller grain sizes transported. • Lesser erosion protection and channel maintenance requirements.
Narrow channel (dark blue)	• High flow depth (d_2) and velocity lead to high shear stresses exerted on channel banks. • Higher bank erosion potential and larger grain sizes transported. • Greater erosion protection and channel maintenance requirements.

Figure B-5. Schematic of channel configuration and associated bank erosion potential.

B.2. CLIMATE CHANGE

Climate change is expected to impact steep creek geohazards both directly and indirectly through complex feedback mechanisms. Given that hydrological and mass movement processes are higher order effects of air temperature increases, their prediction is highly complex and often site-specific.

Regional climate change projections indicate that there will be an increase in winter rainfall (PCIC, 2012), an increase in the hourly intensity of extreme rainfall and increase in frequency of events (Prein et al., 2017). Changes to short duration (one hour and less) rainfall intensities are particularly relevant for post-fire situations in debris-flow generating watersheds. Within the year to a few years after a wildfire affecting large portions of a given watershed, short duration and high intensity rainfall events are much more likely to trigger debris flows or debris floods, than prior to a wildfire event.

Steep creek basins can be generally categorized as being either:

- Supply-limited: meaning that debris available for transport is a limiting factor on the magnitude and frequency of steep creek events. In other words, once debris in the source

zone and transport zone has been depleted by a debris flow or debris flood, another event even with the same hydro-climatic trigger will be of lesser magnitude; or,

- Supply-unlimited: meaning that debris available for transport is not a limiting factor on the magnitude and frequency of steep creek events, and another factor (such as precipitation frequency/magnitude) is the limiting factor. In other words, there is always an abundance of debris along a channel and in source areas so that whenever a critical hydro-climatic threshold is exceeded, an event will occur. The more severe the hydro-climatic event, the higher the resulting magnitude of the debris flow or debris flood.

Further subdivisions into channel supply-limited and unlimited and basin supply-limited and unlimited are possible but not considered herein.

The sensitivity of the two basic types of basins to increases in rainfall (intensity and frequency increases) differ (Figure B-6):

- Supply-limited basins would likely see a decrease in individual geohazard event magnitude, but an increase in their frequency as smaller amounts of debris that remain in the channel are easily mobilized (i.e., more, but smaller events).
- Supply-unlimited basins would likely see an increase in hazard magnitude and a greater increase in frequency (i.e., significantly more, and larger events).

Supply-limited basins can transition into supply-unlimited due to landscape changes. For example, sediment supply could be increased by wildfires, landslide occurrence, or human activity (e.g., related to road building or resource extraction). In the case of wildfires, the impact on debris supply is greatest immediately after the wildfire, with its impact diminishing over time as vegetation regrows (see Section B.2.1). Wildfires are known to both increase the sediment supply and lower the precipitation threshold for steep creek events to occur.

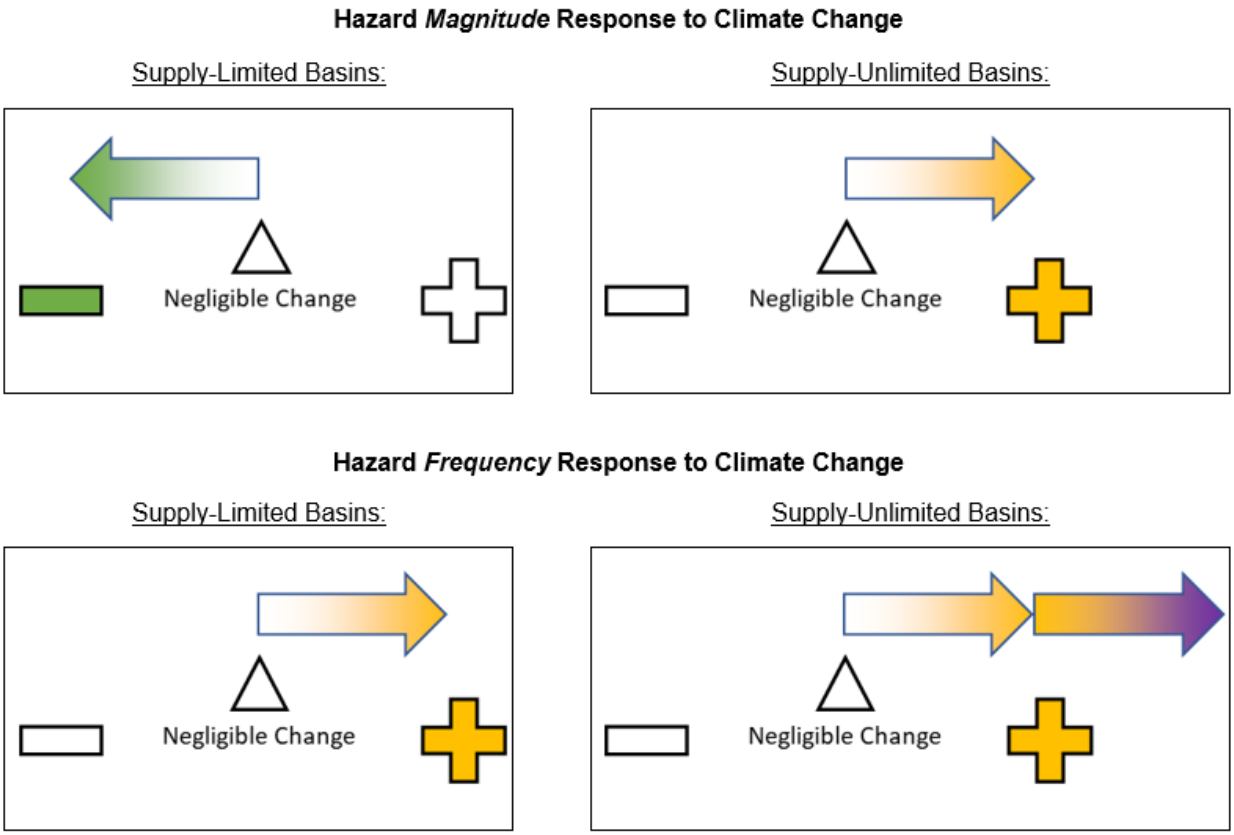

Figure B-6. Steep creek hazard sensitivity to climate change – supply-limited and supply unlimited basins.

B.2.1. Wildfires

Wildfires in steep mountainous terrain are often followed by a temporary period of increased geohazard activity. This period is most pronounced within the first three to five years after the fire (Cannon & Gartner, 2005; DeGraff et al., 2015). After about three to five years, vegetation can reestablish on hillslopes and loose, unconsolidated sediment mantling hillslopes and channels may have been eroded and deposited downstream. A second period of post-fire debris-flow activity is possible about ten years following a fire, when long duration storms with high rainfall totals or rain-on-snow events cause landslides that more easily mobilize due to a loss of cohesion caused by tree root decay (DeGraff et al., 2015; Klock & Helvey, 1976; Sidle, 1991; 2005). This second period of heightened debris-flow activity is rare.

B.2.2. Landslide Dam Outbreak Flood Potential

Some steep creek watersheds are prone to LDOFs, which could trigger flooding, debris floods, or debris flows with larger magnitudes than “typical” hazards. An example of this hazard in the Squamish Lillooet Regional District is landslides in the Mount Meager volcanic complex, which have generated several landslide dams along Meager Creek and Lillooet River (Figure B-7; Bovis & Jakob, 2000; Guthrie et al., 2012). LDOFs are not expected to occur on Jason or Mungye creeks and have not been included in the present assessment.

Figure B-7. Landslide dam on Meager Creek from the August 6, 2010 rockslide-debris flow from Capricorn Creek. The dam impounded Meager Creek for some time. Photo by D. Steers.

APPENDIX C
FIELD TRAVERSE AND OBSERVATIONS

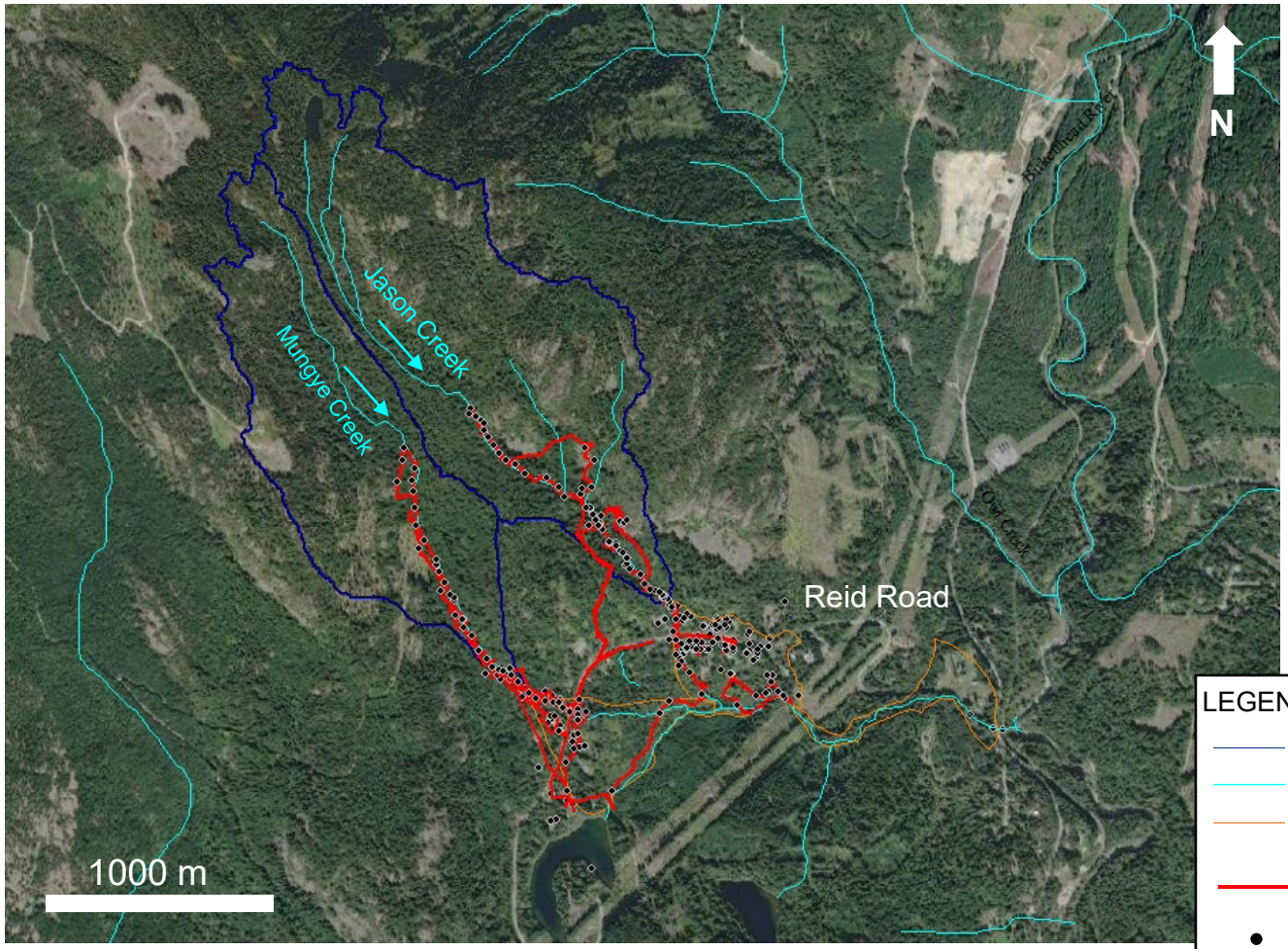

LEGEND

- WATERSHED
- STREAM
- APPROXIMATE FAN BOUNDARY
- FIELD TRAVERSE
- OBSERVATION POINT

NOTES

1. THIS FIGURE SHOULD BE READ IN CONJUNCTION WITH BGC'S REPORT TITLED 'QUANTITATIVE LANDSLIDE HAZARD AND RISK ASSESSMENT – REID ROAD AREA, ELECTORAL AREA C' AND DATED JANUARY 2023
2. BASE IMAGERY PROVIDED BY ESRI WORLD IMAGERY (2019).
3. APPROXIMATE FAN BOUNDARIES, WATERSHED BOUNDARIES AND CREEKS DIGITIZED BY BGC.
4. FIELD TRAVERSE AND OBSERVATIONS POINTS COLLECTED BY BGC AND CORDILLERAN ON JULY 20-22, 26-27, SEPTEMBER 10, 16, AND OCTOBER 19, 2022.

PREPARED BY:	FIGURE TITLE:		
HMS	FIELD TRAVERSES AND OBSERVATION POINTS FROM 2022 SITE INVESTIGATION		
CHECKED BY:	CLIENT:		
LCH	SQUAMISH – LILLOOET REGIONAL DISTRICT		
APPROVED BY:	SCALE:	PROJECT NO:	FIGURE NO:
LCH	3CM: 1000M	1358010	C-1

0 5 10 mm in ANSI A sized paper

BGC ENGINEERING INC.

APPENDIX E
INSAR ANALYSIS RESULTS

E.1. INTRODUCTION

BGC contracted TRE-Altamira (TRE) to complete Interferometric Synthetic Aperture Radar (InSAR) analysis of ground displacement over the study area. TRE analyzed Sentinel-1 satellite imagery from May 2017 to June 2022. Displacement in four directions (one-dimensional (1D) line of sight ascending and descending and two-dimensional (2D) vertical and east-west) was reported.

This appendix includes TRE's report along with timeseries plots for an unstable rock mass in the Jason Creek watershed.

InSAR Analysis of Ground Displacement over Reid Road Pemberton, BC

Summary Report

TRE ALTAMIRA
A CLS Group Company

August 08, 2022

Client:	**BGC Engineering Inc.**
Attention:	Dr. Jeanine Engelbrecht
Address:	#500 – 1045 Howe Street Vancouver, BC, V6Z 2A9

Reference:	
Title:	InSAR Analysis of Ground Displacement over Reid Road Pemberton, BC – Summary Report
Client Purchase Order (PO):	1358010
TRE ALTAMIRA Delivery Reference:	JO22-1892-CA REP 1.0

Prepared by:	**TRE ALTAMIRA Inc.**
Author(s):	Riccardo Tortini
Approved by:	Giacomo Falorni
Date:	08 August 2022
Version:	1.0

Project Team

Riccardo Tortini
Technical Responsible

riccardo.tortini@tre-altamira.com

Cyriac Sebastian
Account Manager

cyriac.sebastian@tre-altamira.com

Giacomo Falorni
Technical Director

giacomo.falorni@tre-altamira.com

Contents

TRE ALTAMIRA
A CLS Group Company

PROJECT OVERVIEW

Project overview

- **Objective**: InSAR monitoring of slope movement over the Reid Road area near Pemberton, BC

- **Scope of work**:
  - SqueeSAR analysis
    - 1D LOS (ascending & descending)
    - 2D (vertical & east-west)
  - InSAR baseline using low resolution Sentinel-1 imagery
    - 2017 – Jun 2022
  - Analysis overview through a brief map summary report/ppt

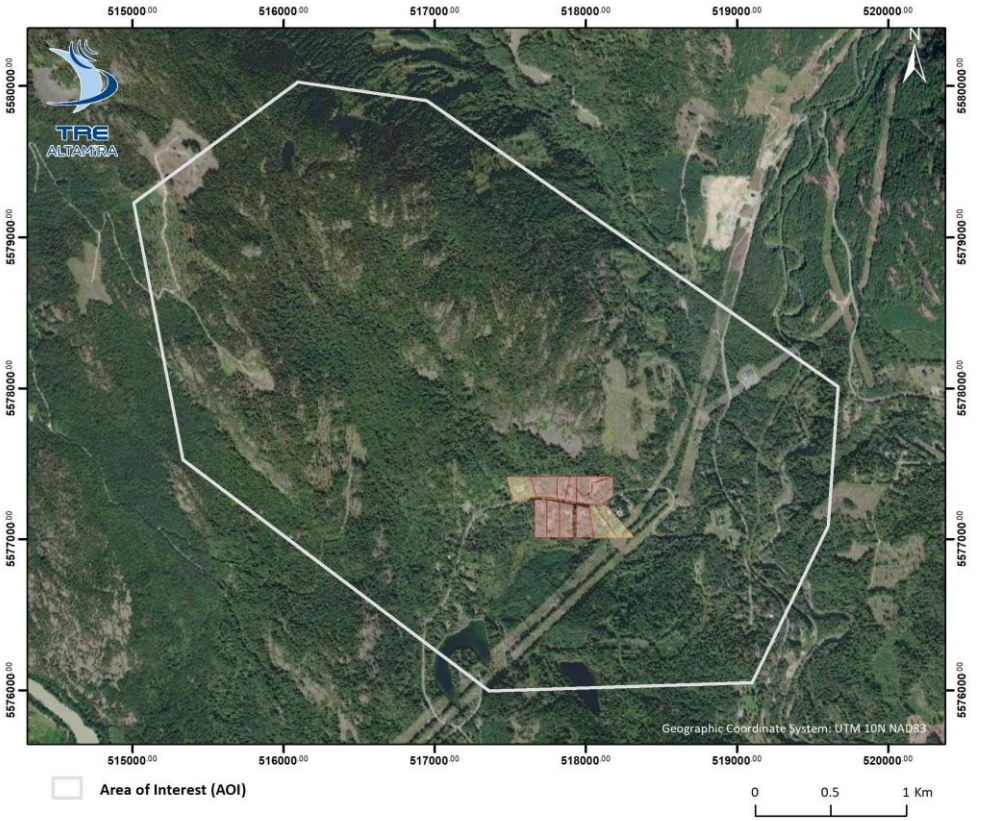

Satellite Characteristics & Radar Imagery

Satellite	Sentinel-1
Wavelength	C-band
Resolution	Low Resolution 20 x 5 m
Acquisition Frequency	12-day

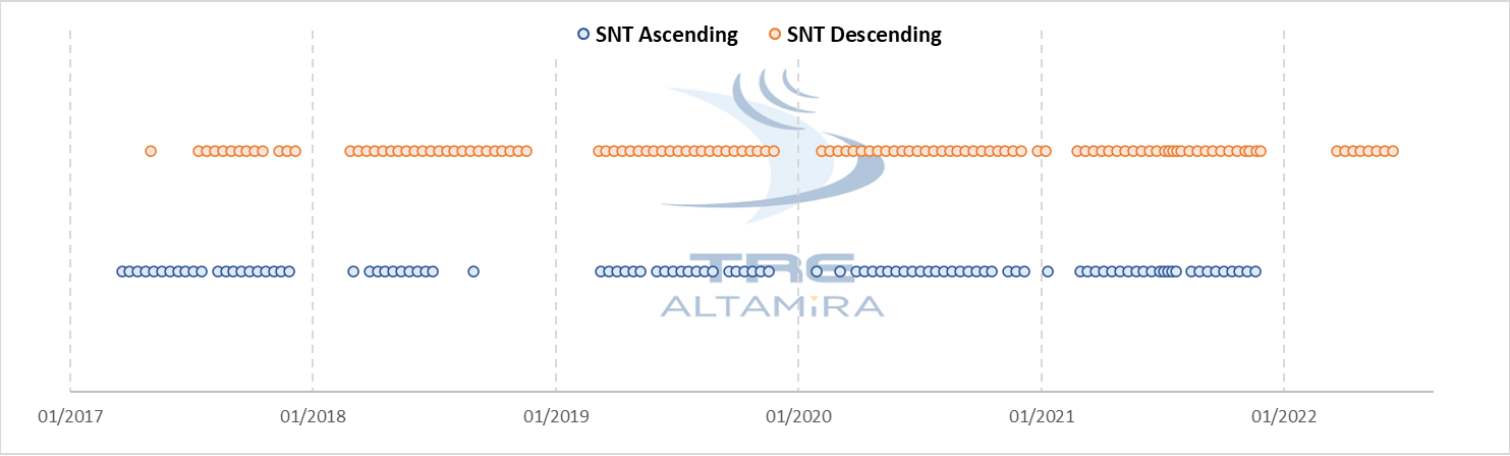

TRE ALTAMIRA
A CLS Group Company

RESULTS OVERVIEW

Line-Of-Sight (LOS) Results

	Ascending (T64, Θ = 32.7°)	Descending (T13, Θ = 41.6°)
LOS Date Range	03 Apr 2017 – 02 Dec 2021	17 May 2017 – 26 Jun 2022
N. of Images Processed	100	122
Reference Point Location (NAD83 UTM 10N, meters)	Lat = 5,577,447.647 Lon = 519,758.702	Lat = 5,577,386.793 Lon = 520,294.484
Number of MPs	13,590	10,330
Average Point Density	1,078 pts/km^2	820 pts/km^2
Average Displacement Rate Standard Deviation (V_STDEV)	± 0.4 mm/yr	± 0.4 mm/yr
Average Time Series Error Bar (STD_DEF)	± 4.2 mm	± 4.5 mm

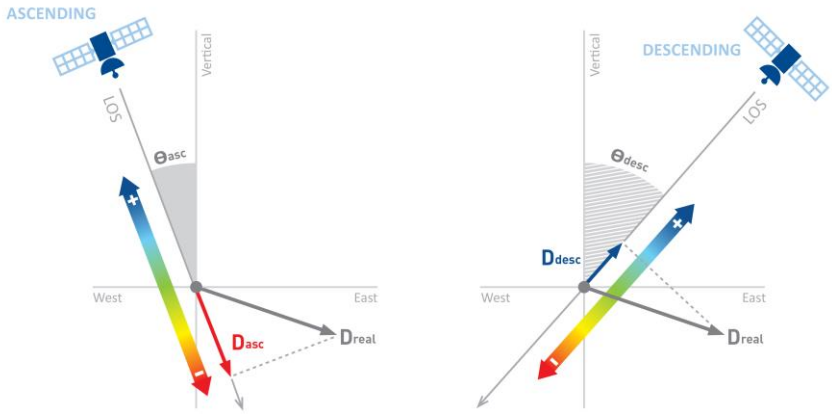

2D Results

	Vertical	East-West
Period Covered	17 May 2017 – 02 Dec 2021	
N. of Images	200	
Reference Point Location (NAD83 UTM 10N, meters)	Lat = 5,577,641.359 Lon = 517,925.084	
Number of Cells	1,347	
Cell Size	30 x 30 m	
Average Displacement Rate Standard Deviation (V_STDEV)	± 0.3 mm/yr	± 0.3 mm/yr

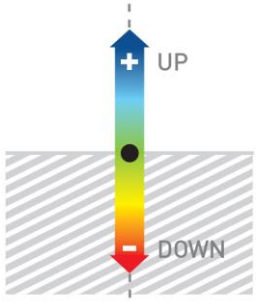

SqueeSAR – LOS Ascending

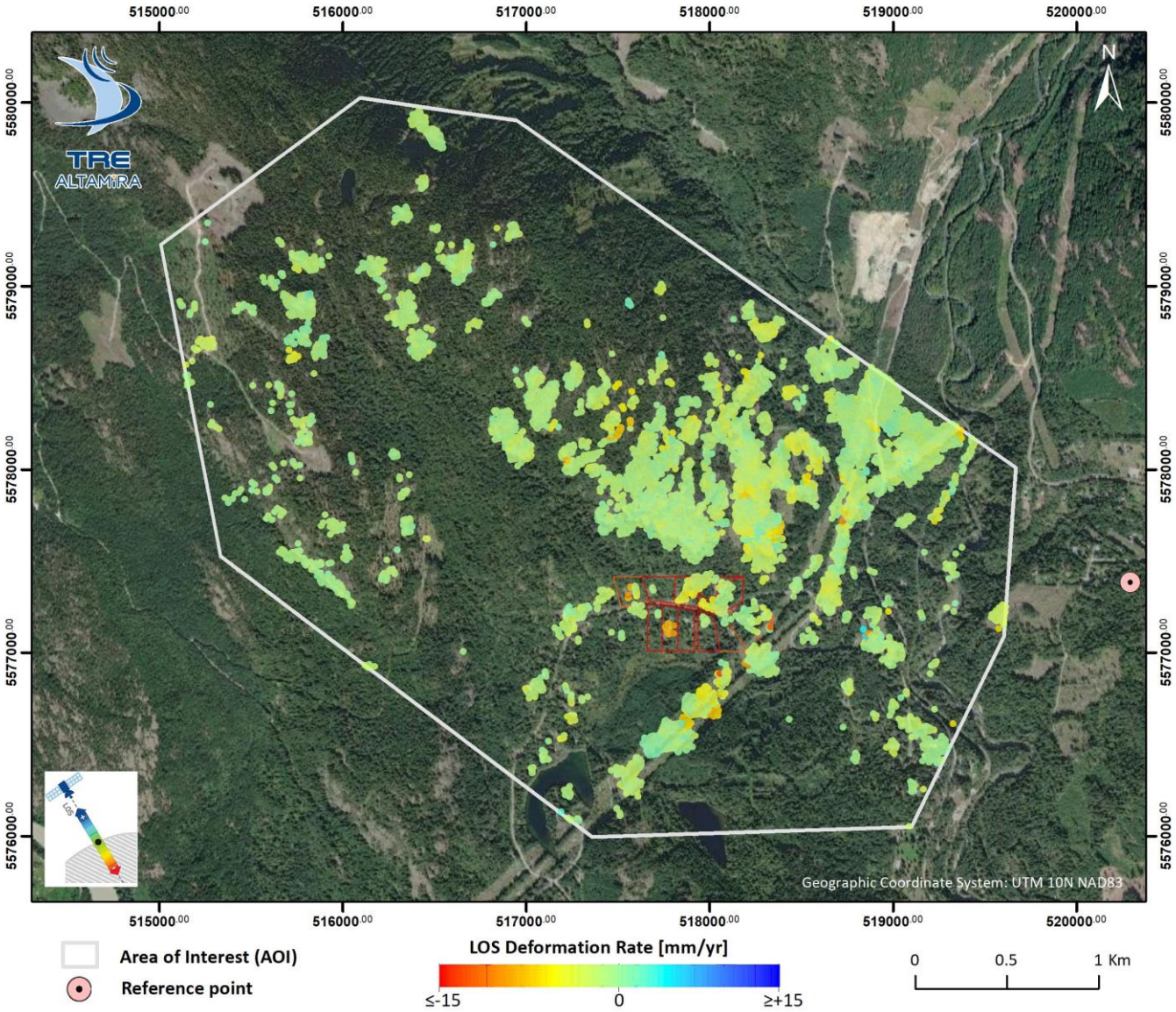

TCS – LOS Ascending

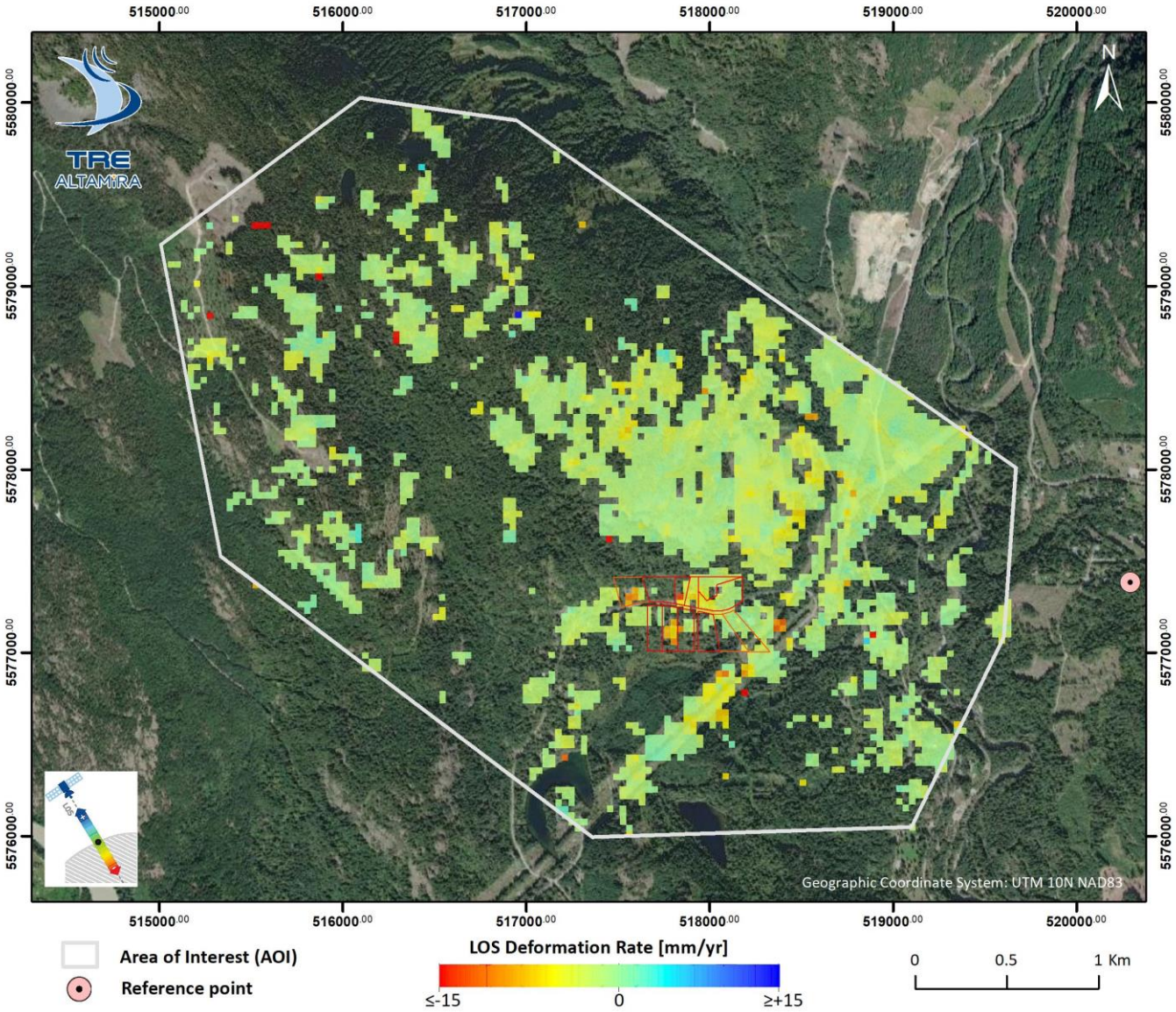

SqueeSAR – LOS Descending

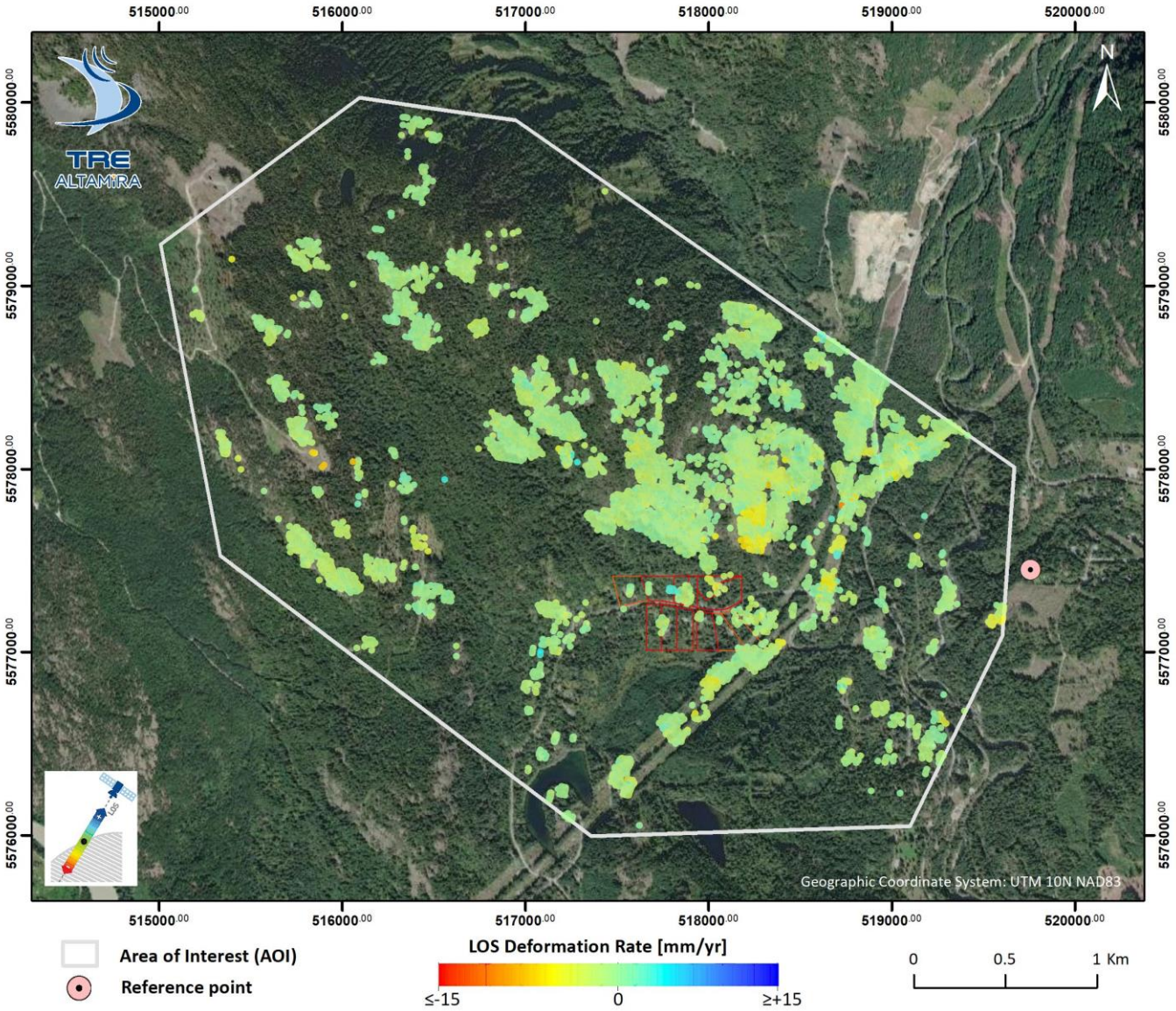

TCS – LOS Descending

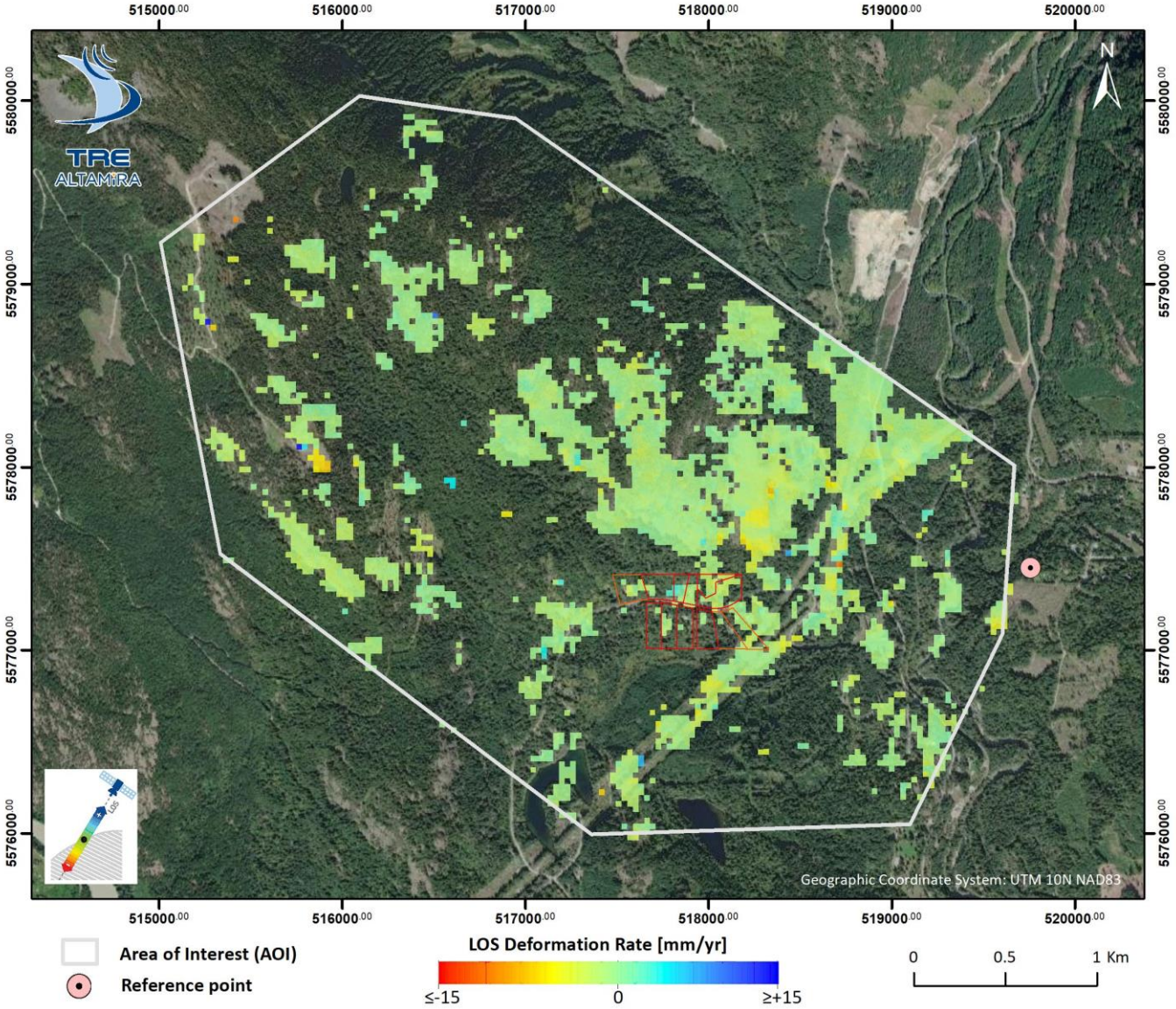

SqueeSAR – Vertical

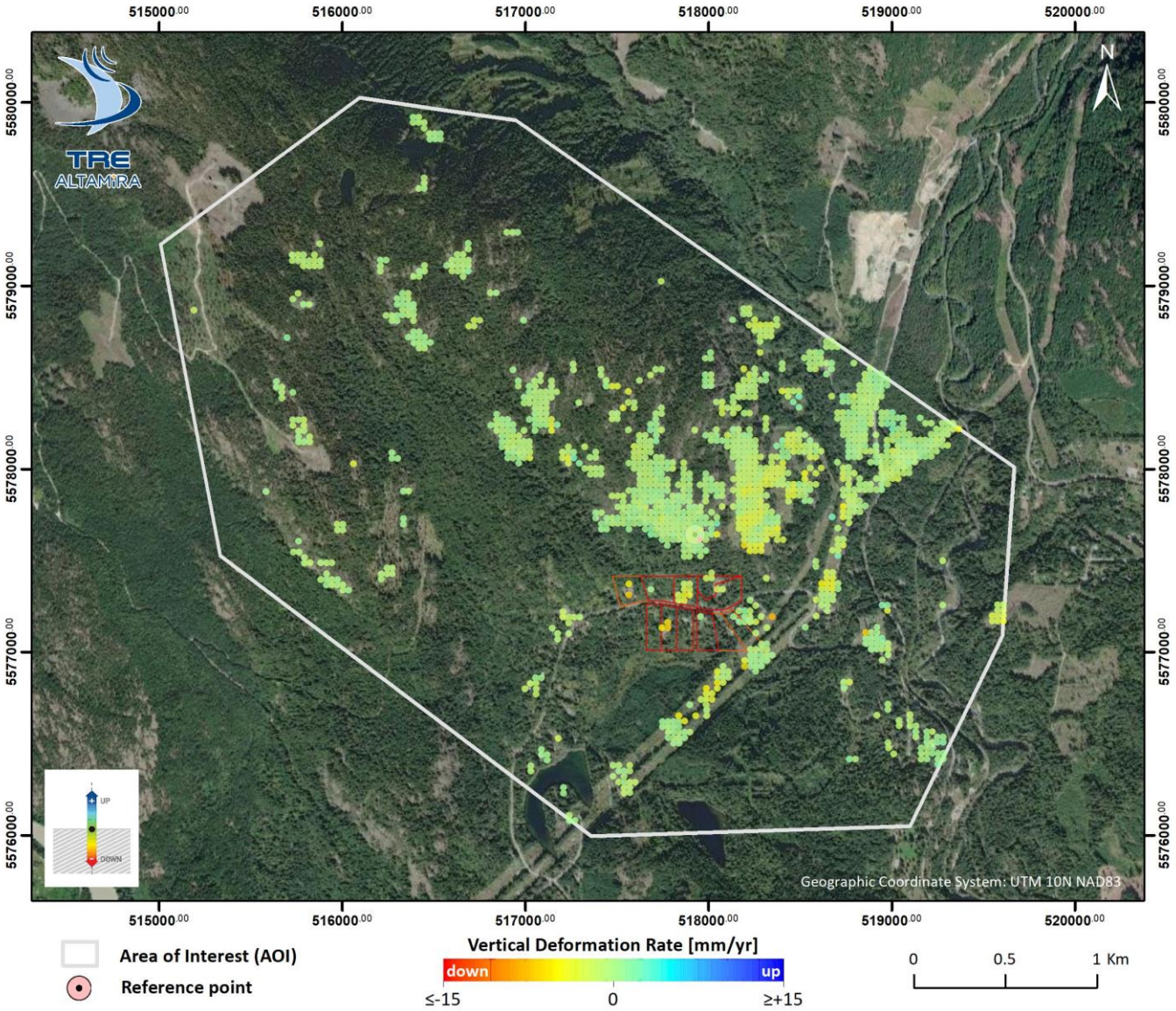

SqueeSAR – East-West

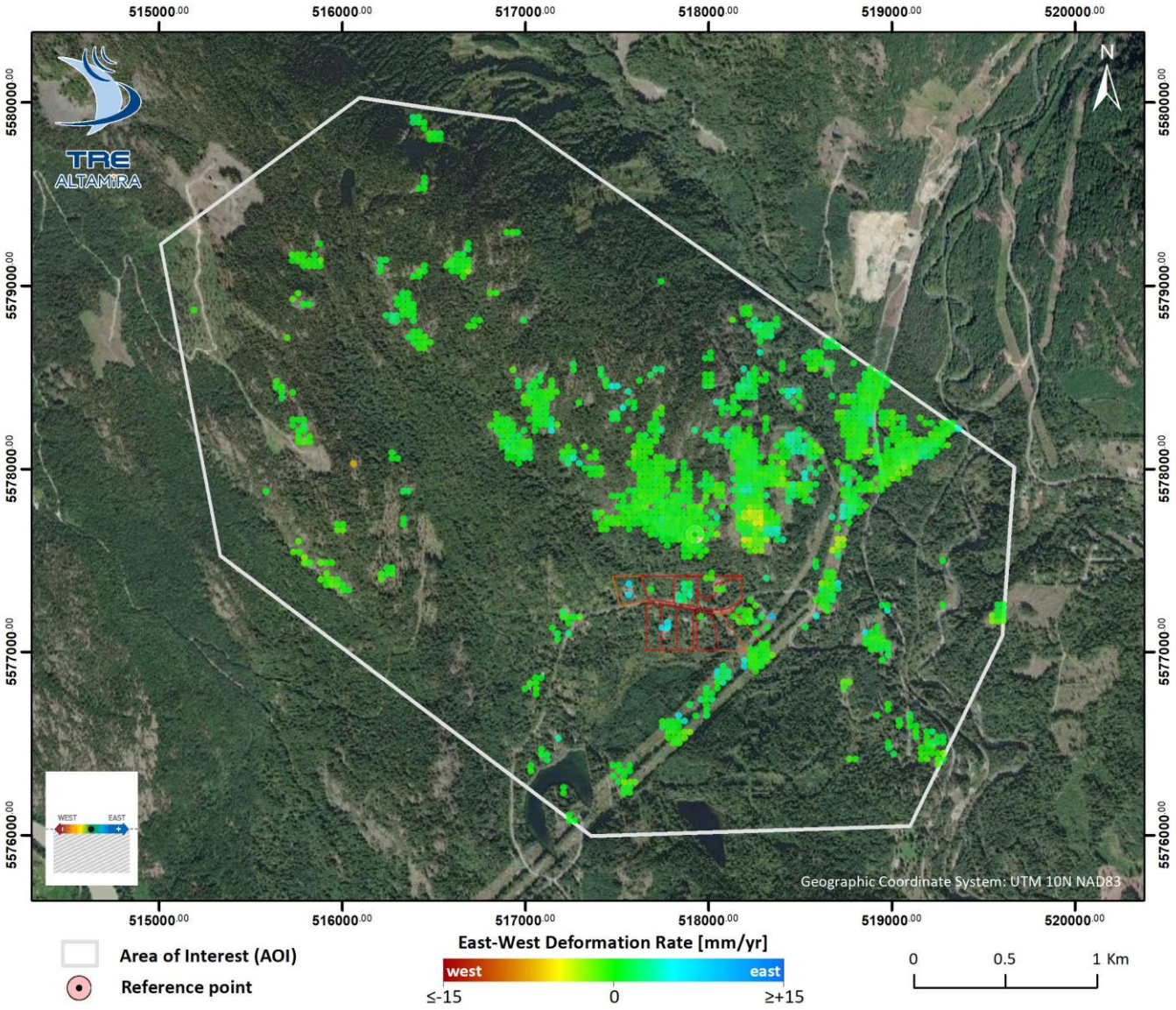

TRE ALTAMIRA
A CLS Group Company

DELIVERABLES

SqueeSAR Results

- **Delivery** via **TREmaps®**, our web platform to view, interrogate and download InSAR data.
  - Users: Jeanine Engelbrecht, Lauren Hutchinson, Matthias Jakob, Pierre Friele, Hilary Shirra, Sophia Zubrycky, Kris Holm, Alex Strouth
- **Data**
  - Format: shapefile (.shp)
  - Coordinate system: UTM 10N NAD83
  - Measurement Unit: metric
- **Summary Report**
  - Delivered in pdf format via email

List of Deliverables

Description	File name
SqueeSAR Data in shapefile (.shp) format	**Ascending (LOS): 03 Apr 2017 – 02 Dec 2021** REID_ROAD_SNT_T64_A_CA5992A005S **Descending (LOS): 17 May 2017 –26 Jun 2022** REID_ROAD_SNT_T13_D_CA5992A006S **2-D: 17 May 2017 – 02 Dec 2021** Vertical: REID_ROAD_SNT_VERT_CA5992A007V East-West: REID_ROAD_SNT_EAST_CA5992A008E
Change Detection in GeoTiff (.tif) format	**Ascending (LOS): 03 Apr 2017 – 02 Dec 2021** REID_ROAD_A_geoimage_site_change_map_data **Descending (LOS): 11 Jan 2021 – 12 Jun 2022** REID_ROAD_D_geoimage_site_change_map_data
Temporary Coherent Scatterers (TCS) in GeoTiff (.tif) format	**Ascending (LOS): 03 Apr 2017 – 02 Dec 2021** REID_ROAD_SNT_A_VEL_TCS_data **Descending (LOS): 11 Jan 2021 – 12 Jun 2022** REID_ROAD_SNT_D_VEL_TCS_data
Summary Report	TREA_InSAR_ReidRoad_SummaryReport.pdf

TREmaps

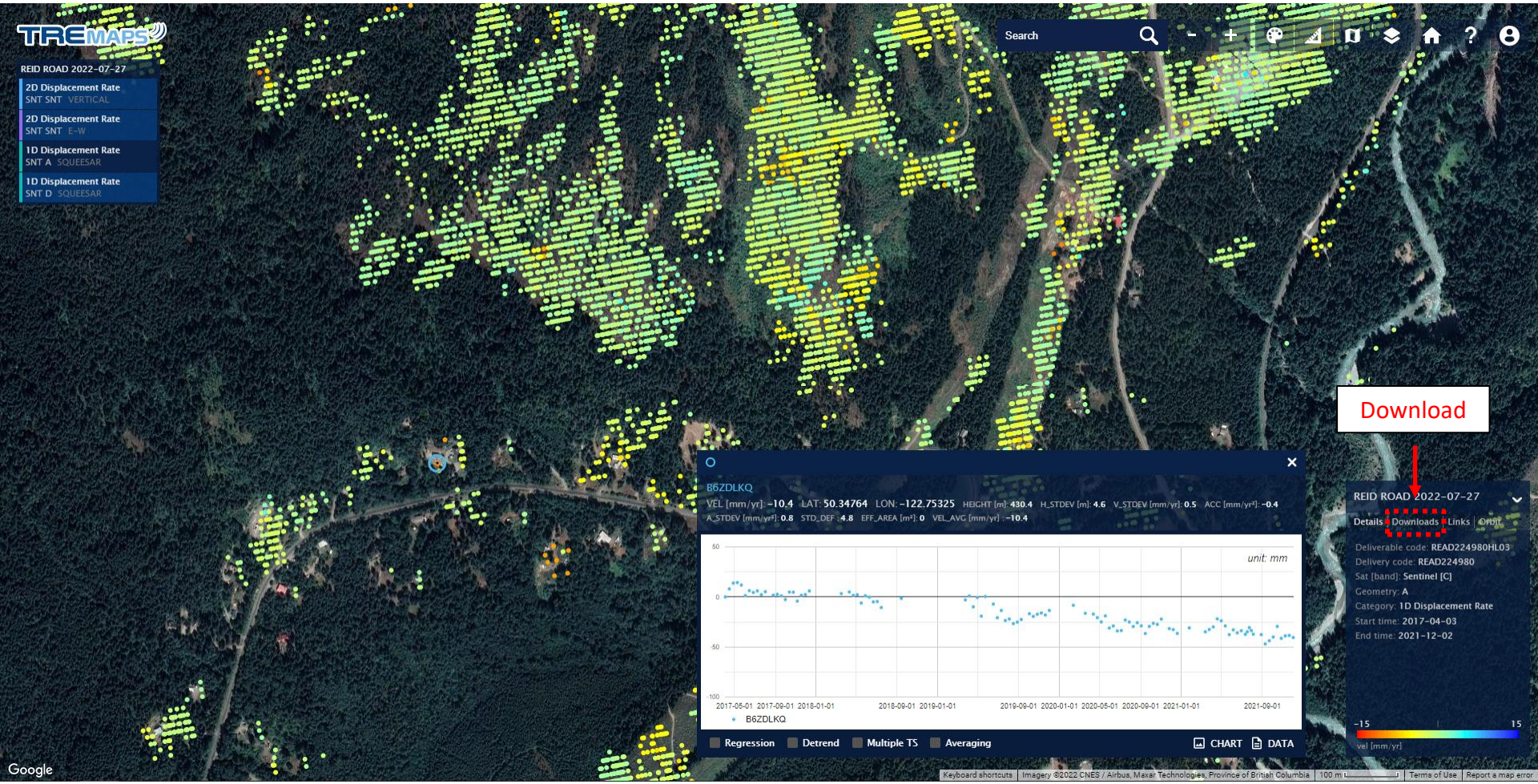

To log in, visit: https://tremaps.com/

For best performance, Google Chrome and Mozilla Firefox are recommended. For assistance, please click the "Help" icon on the viewer or go to: https://help.tremaps.com/

TRE ALTAMIRA
A CLS Group Company

TECHNIQUE OVERVIEW

SqueeSAR

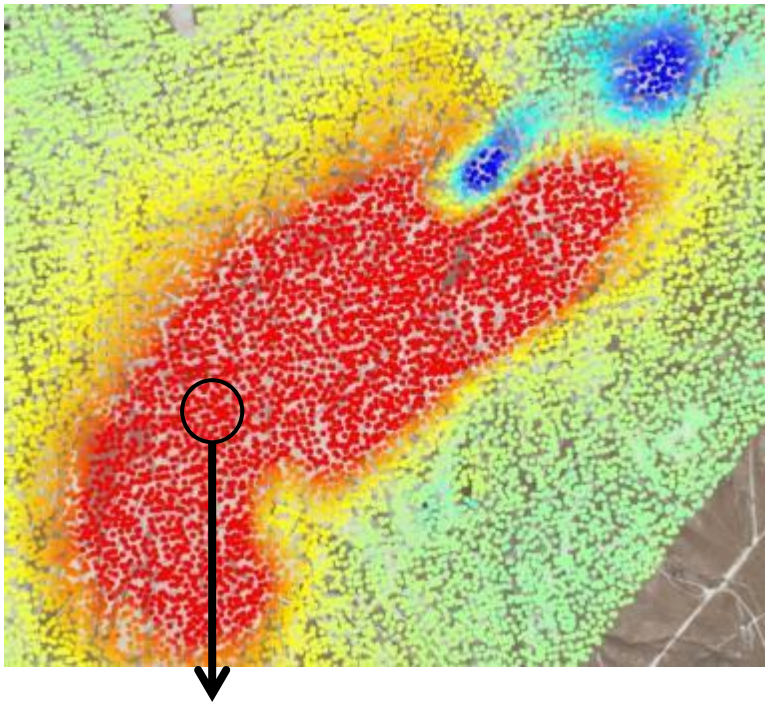

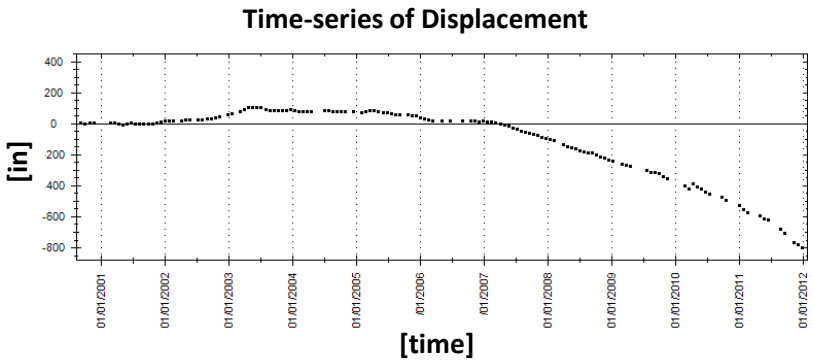

Identifies radar targets on the ground

- Precise measurements of ground movement (mm precision)
- Identify changes in displacement rates and non-linear movement
- Identify faults, movement boundaries & spatial variability

Output:

- Point Cloud
- Annual Displacement rate [mm/yr]
- Time-series of Deformation
- 1-D and 2-D (with two orbits)

Notes:

- Sensitive to surface changes
- Point density affected by presence of vegetation and/or snow
- Limited capability to monitor rapid movement

Orbits and 1-D measurements

- Satellites collect imagery from both ascending (south to north) and descending orbits (north to south).
- InSAR measures the projection of the true vector of displacement onto the LOS. 1D movement is observed as away or toward the satellite.
- Negative values (from green to red) indicate movement away from the satellite, while positive values (from green to blue) indicate movement towards the satellite.
- A same displacement produces different readings when viewed from different LOS angles.

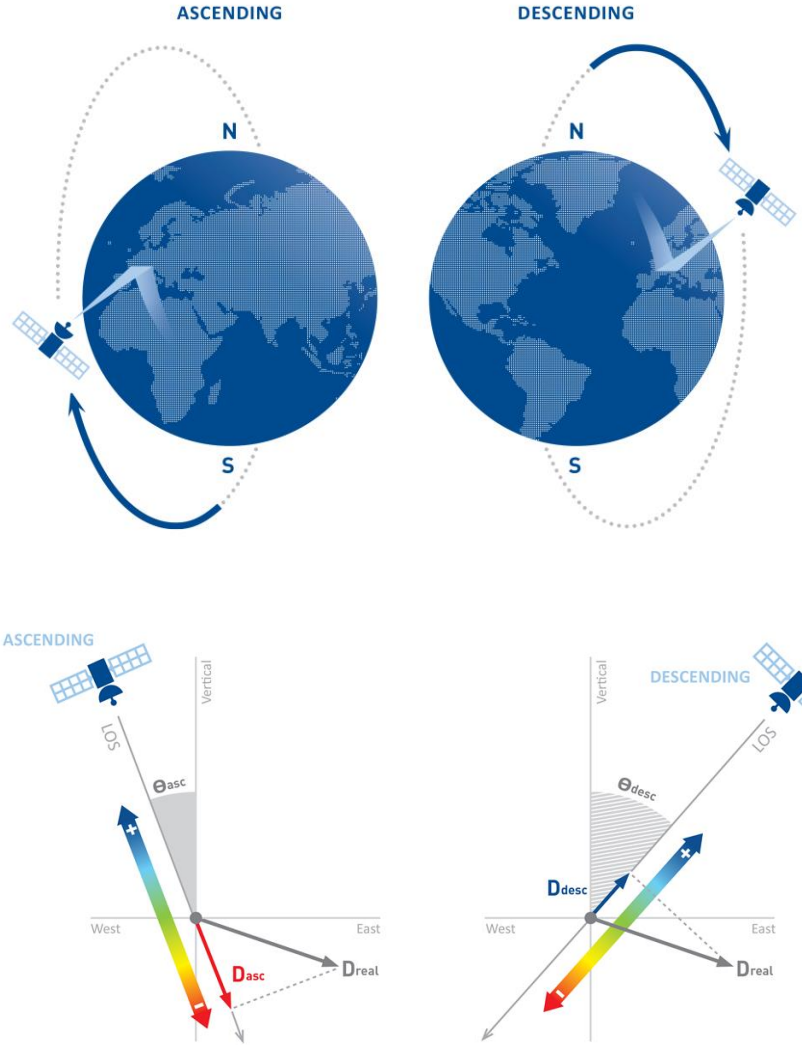

1-D LOS measurements

SAR satellites view the Earth at an angle, known as the Line-of-Sight (LOS)
InSAR measures the projection of a real displacement onto the LOS

1-D measurements

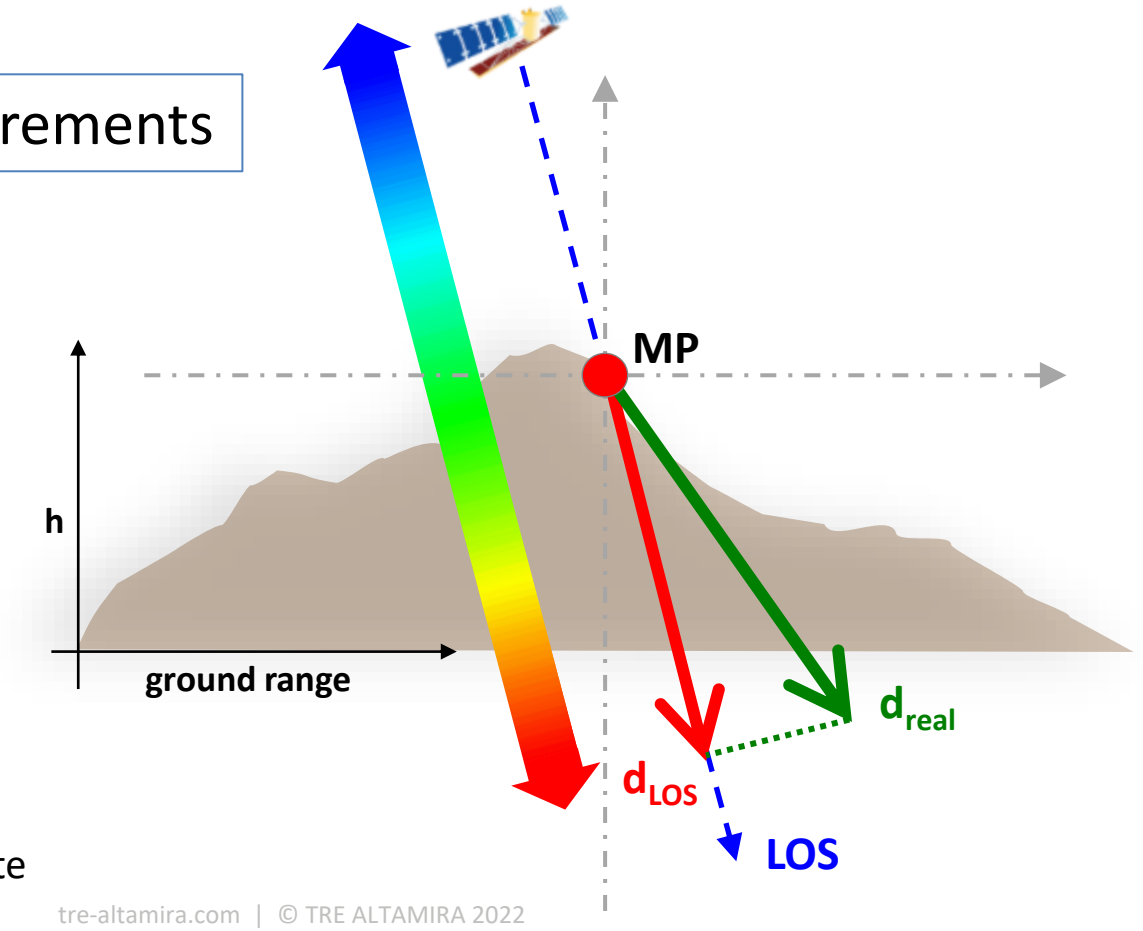

- Movement towards the satellite
- No movement
- Movement away from the satellite

2-D Measurements

- 2-D (vertical and East-West) components of movement are obtained by combining the LOS readings
- Ascending and descending LOS data are resampled to a common regular grid:
  - 2-D measurement points are cells of a grid (not individual radar targets)
  - 2-D points are only present where both ascending and descending data are available
- North-South movement cannot be measured

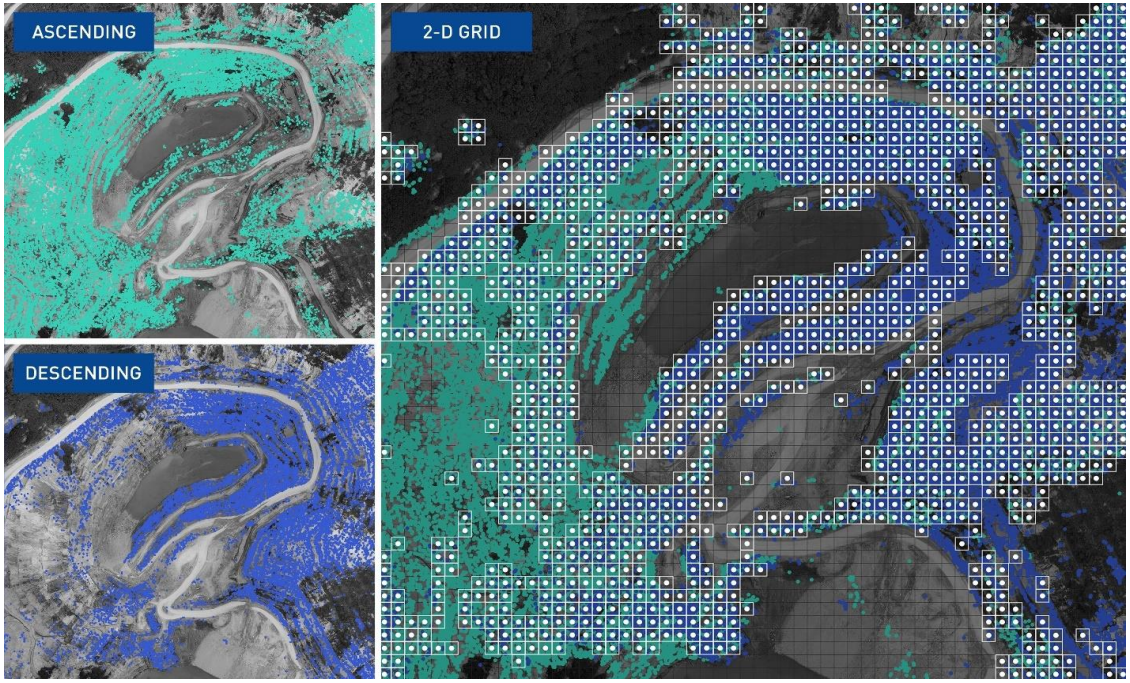

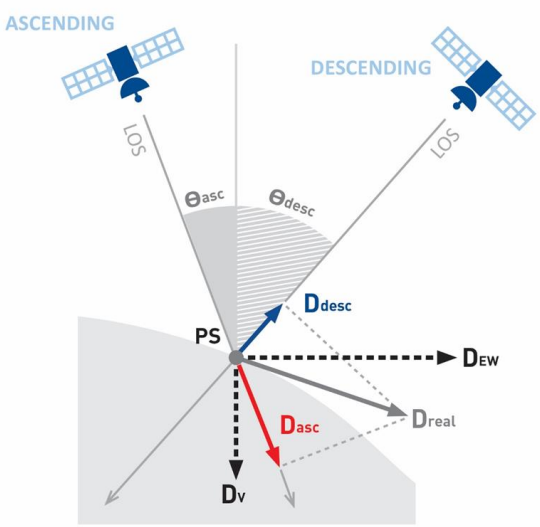

1-D (LOS) vs 2-D measurements

1-D LOS data
Max spatial resolution

2-D data
Regular grid of points

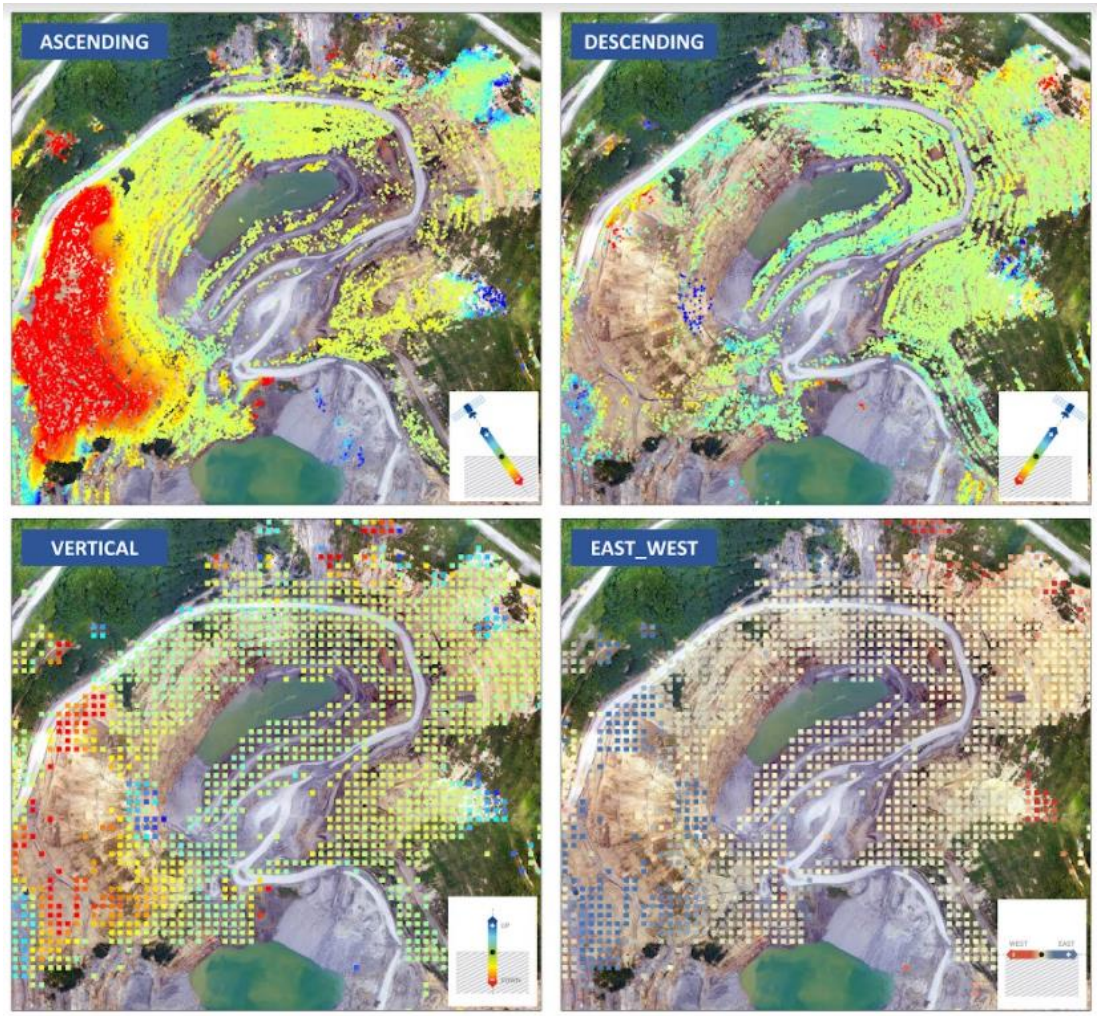

- 2-D measurements are easier to interpret than LOS data but have a lower density and spatial resolution
- In detailed analysis of localized features, it may be beneficial to use the full resolution LOS results

TRE ALTAMIRA
A CLS Group Company

MILANO

Ripa di Porta Ticinese, 79
20143 Milan - Italy
Tel: +39 02 4343 121

BARCELONA

Carrer de Còrsega, 381-387
08037 Barcelona - Spain
Tel: +34 93 183 57 50

VANCOUVER

Suite #410 475 W. Georgia Street
Vancouver, BC V6B 4M9 - Canada
Tel: +1 604 331 2512

sales@tre-altamira.com

Regional offices

FRANCE

Parc Technologique du Canal
11, Rue Hermès
F-31520 Ramonville St Agne
Tel.: +33 561 39 47 19

PERU

Av. Angamos Oeste 537
Miraflores, Lima
Tel: +51 1 4402717

AUSTRALIA

Suite 207 – 122 Toorak Road | South Yarra
Melbourne
Tel: +61 455 154552

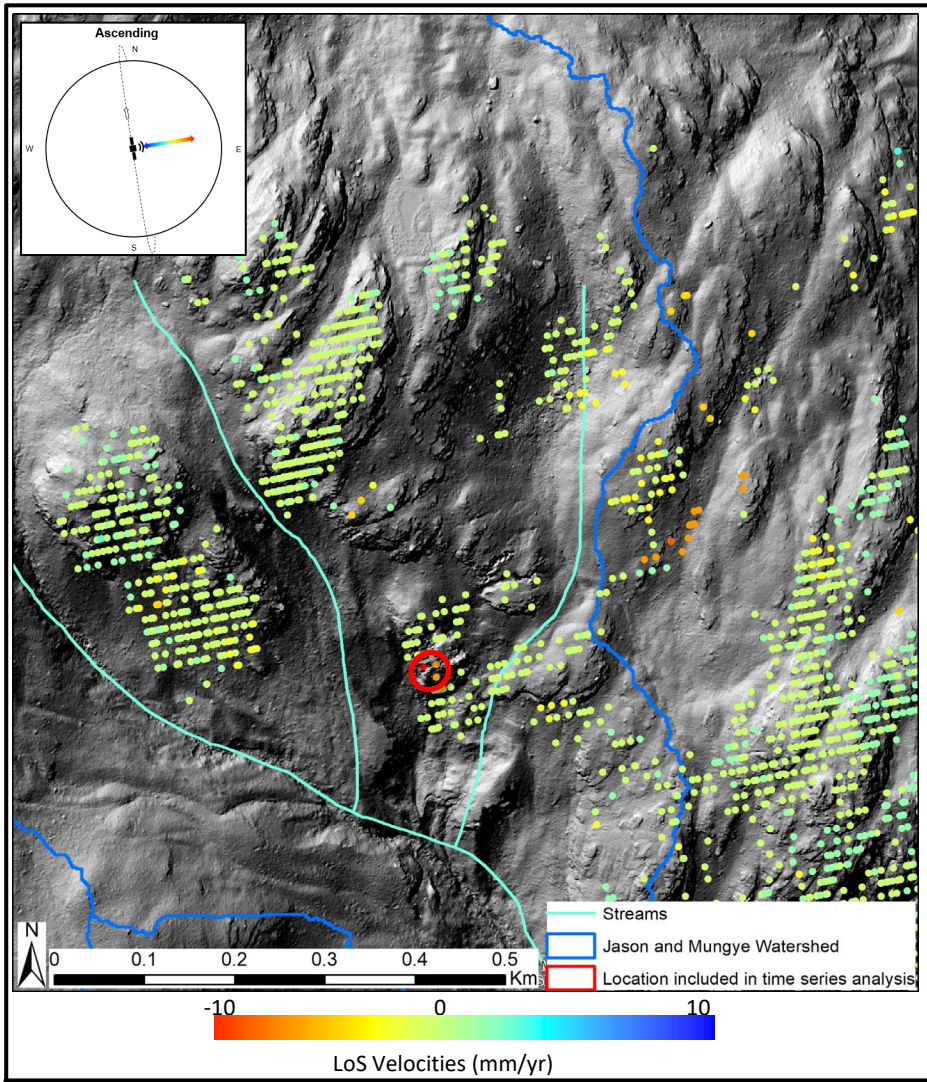

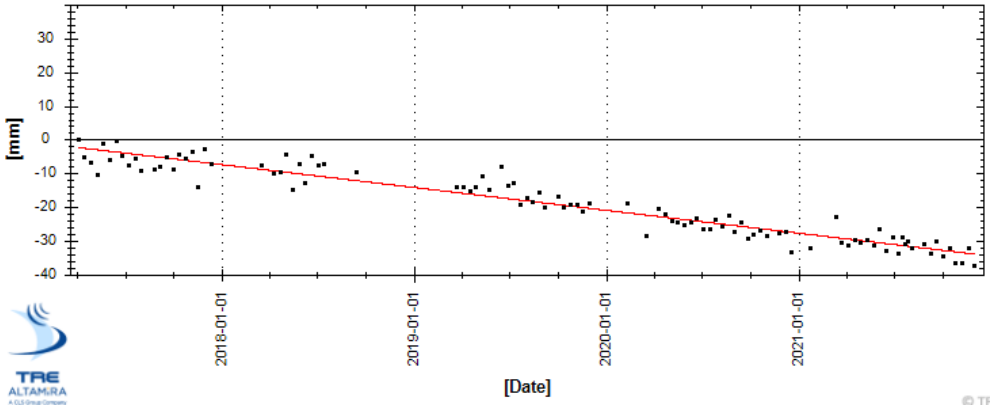

Observation Start Date	Observation End Date	Average Velocity (mm/yr)	Average Cumulative Displacement (mm)
2017-May-17	2021-Dec-02	-6.8	-37.4

NOTES

1. THIS FIGURE SHOULD BE READ IN CONJUNCTION WITH BGC'S REPORT TITLED "QUANTITATIVE LANDSLIDE HAZARD AND RISK ASSESSMENT – REID ROAD AREA, ELECTORAL AREA C", AND DATED JANUARY 2023.
2. THIS FIGURE DEPICTS THE SENTINEL-1 ASCENDING INSAR TIMESERIES EXTRACTED FOR THE SOUTHERN ROCK MASS. THE LOCATION INCLUDED IN THE TIMESERIES ANALYSIS IS SHOWN IN THE RED OUTLINE.
3. THE DATA PROCESSING WAS PERFORMED BY TRE-ALTAMIRA.
4. THIS FIGURE IS INTENDED AS A VISUAL REPRESENTATION AND IS NOT PROVIDED TO MATCH A STANDARD ENGINEERING SCALE.

PREPARED BY:	FIGURE TITLE:		
JE	ASCENDING INSAR TIMESERIES OF THE SOUTHERN ROCK MASS		
CHECKED BY:	CLIENT:		
CRF	SQUAMISH-LILLOOET REGIONAL DISTRICT		
APPROVED BY:	SCALE:	PROJECT NO:	FIGURE NO:
LCH	AS SHOWN	1358010	E-1

0 5 10 mm in ANSI A sized paper

BGC ENGINEERING INC.

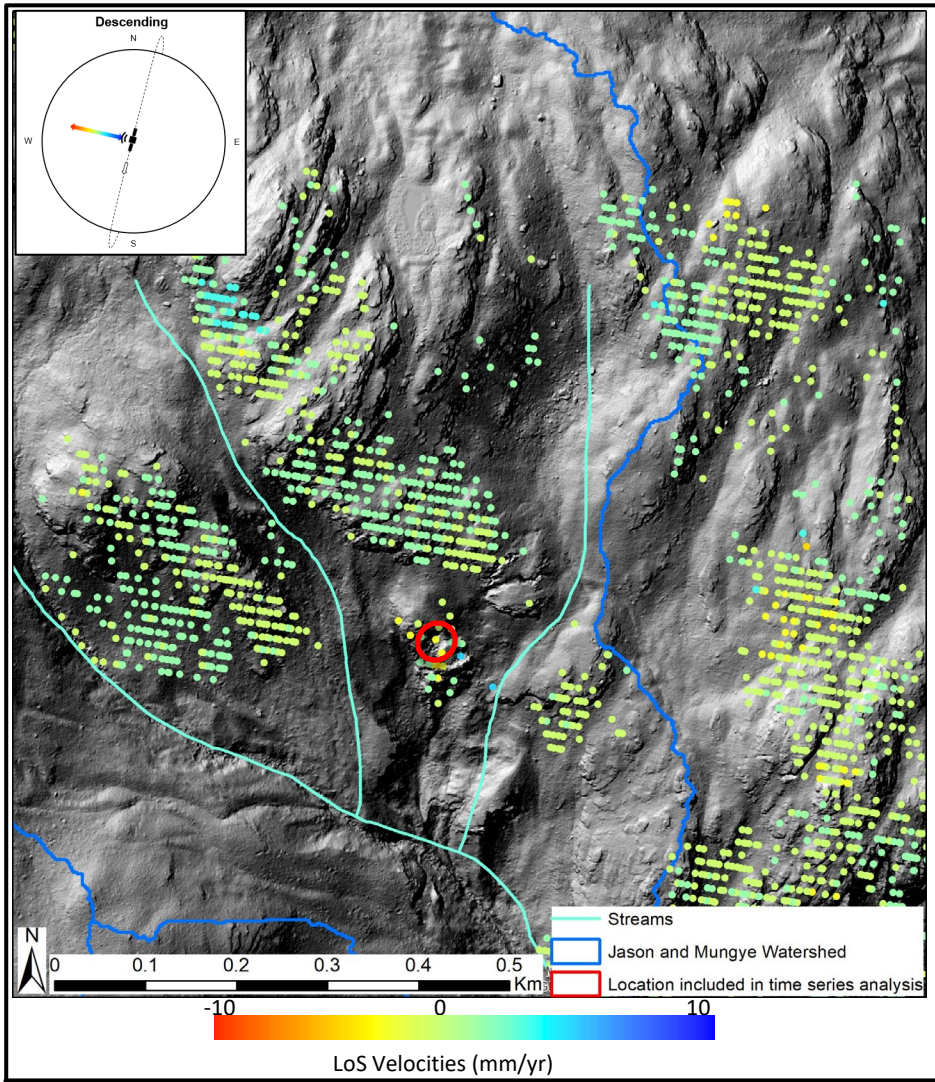

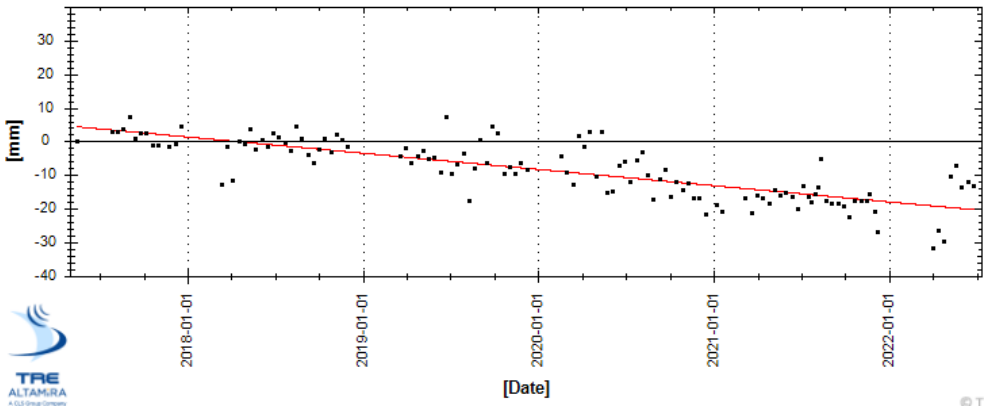

Observation Start Date	Observation End Date	Average Velocity (mm/yr)	Average Cumulative Displacement (mm)
2017-May-17	2022-Jun-26	-4.8	-20

NOTES

1. THIS FIGURE SHOULD BE READ IN CONJUNCTION WITH BGC'S REPORT TITLED "QUANTITATIVE LANDSLIDE HAZARD AND RISK ASSESSMENT – REID ROAD AREA, ELECTORAL AREA C", AND DATED JANUARY 2023.
2. THIS FIGURE DEPICTS THE SENTINEL-1 DESCENDING INSAR TIMESERIES EXTRACTED FOR THE SOUTHERN ROCK MASS THE LOCATION INCLUDED IN THE TIMESERIES ANALYSIS IS SHOWN IN THE RED OUTLINE.
3. THE DATA PROCESSING WAS PERFORMED BY TRE-ALTAMIRA.
4. THIS FIGURE IS INTENDED AS A VISUAL REPRESENTATION AND IS NOT PROVIDED TO MATCH A STANDARD ENGINEERING SCALE.

PREPARED BY:	FIGURE TITLE:		
JE	DESCENDING INSAR TIMESERIES OF THE SOUTHERN ROCK MASS		
CHECKED BY:	CLIENT:		
CRF	SQUAMISH-LILLOOET REGIONAL DISTRICT		
APPROVED BY:	SCALE:	PROJECT NO:	FIGURE NO:
LCH	AS SHOWN	1358010	E-2

0 5 10 mm in ANSI A sized paper

BGC ENGINEERING INC.

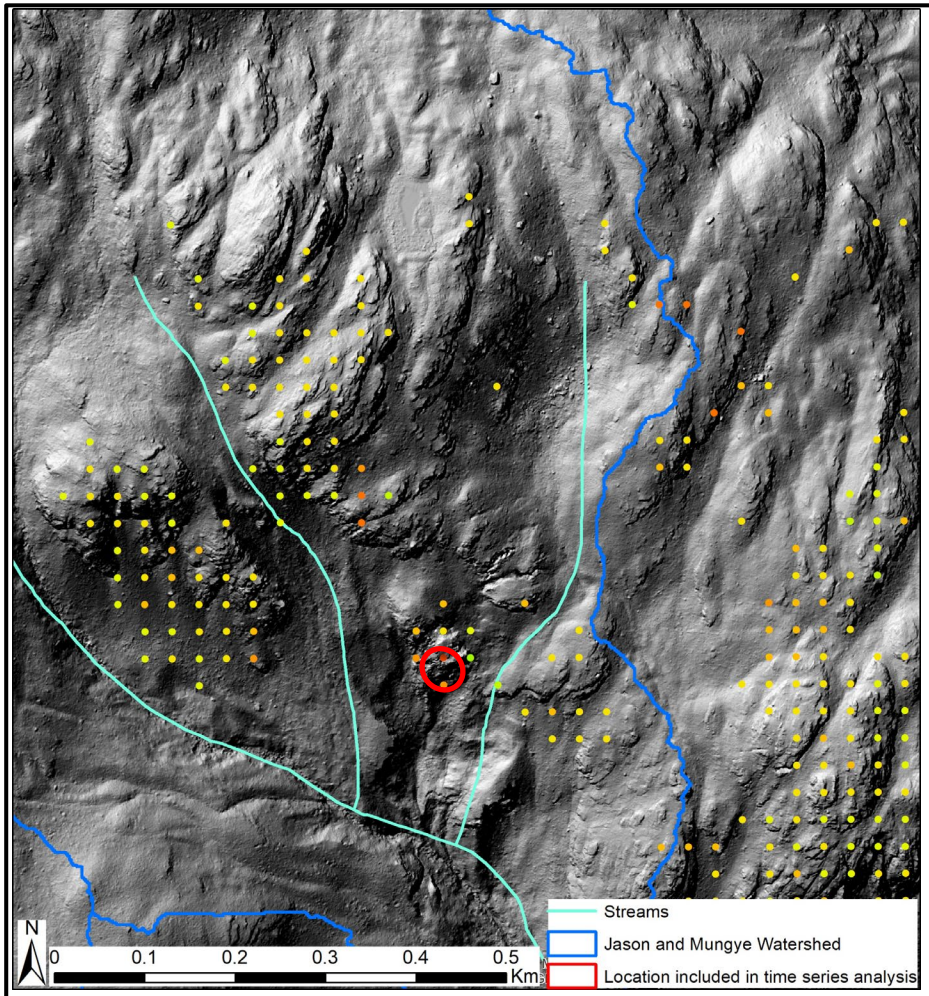

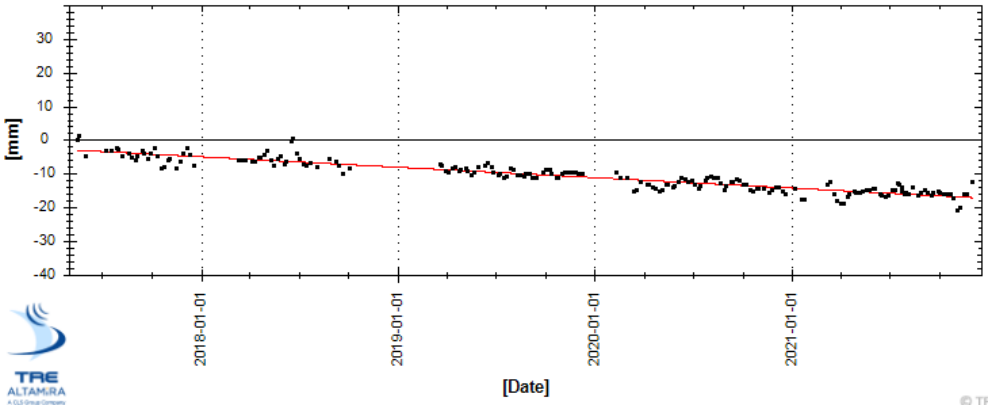

Observation Start Date	Observation End Date	Average Velocity (mm/yr)	Average Cumulative Displacement (mm)
2017-May-17	2021-Dec-02	-3.1	-17.1

NOTES

1. THIS FIGURE SHOULD BE READ IN CONJUNCTION WITH BGC'S REPORT TITLED "QUANTITATIVE LANDSLIDE HAZARD AND RISK ASSESSMENT – REID ROAD AREA, ELECTORAL AREA C", AND DATED JANUARY 2023.
2. THIS FIGURE DEPICTS THE SENTINEL-1 VERTICAL DECOMPOSITION OF THE INSAR TIMESERIES EXTRACTED FOR THE SOUTHERN ROCK MASS. THE LOCATION INCLUDED IN THE TIMESERIES ANALYSIS IS SHOWN IN THE RED OUTLINE.
3. THE DATA PROCESSING WAS PERFORMED BY TRE-ALTAMIRA.
4. THIS FIGURE IS INTENDED AS A VISUAL REPRESENTATION AND IS NOT PROVIDED TO MATCH A STANDARD ENGINEERING SCALE.

PREPARED BY:	FIGURE TITLE:		
JE	VERTICAL DECOMPOSITION OF THE INSAR TIMESERIES OF THE SOUTHERN ROCK MASS		
CHECKED BY:	CLIENT:		
CRF	SQUAMISH-LILLOOET REGIONAL DISTRICT		
APPROVED BY:	SCALE:	PROJECT NO:	FIGURE NO:
LCH	AS SHOWN	1358010	E-3

0 5 10 mm in ANSI A sized paper

BGC ENGINEERING INC.

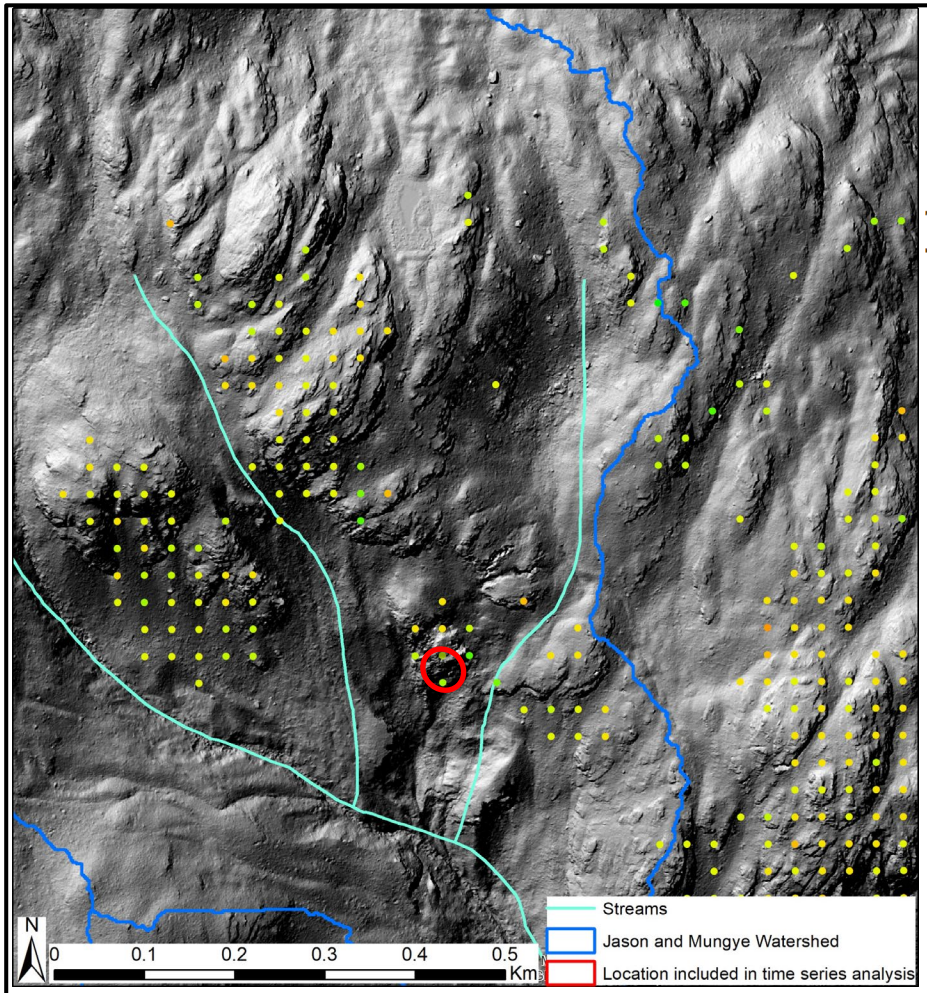

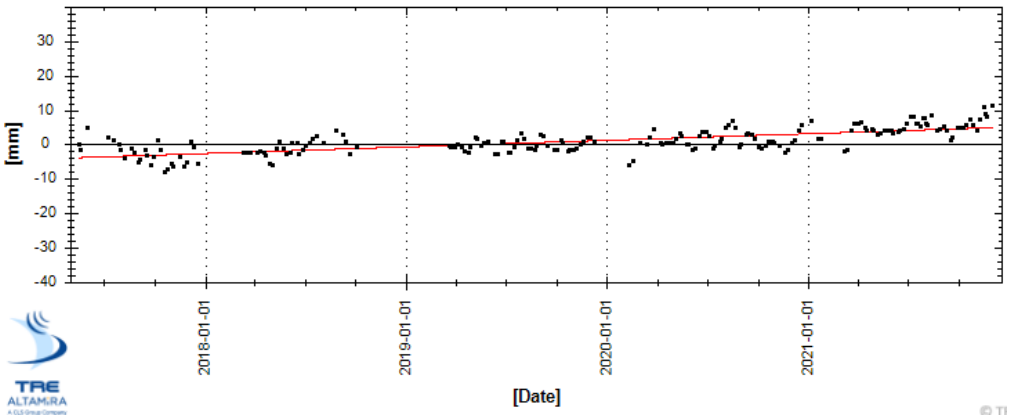

Observation Start Date	Observation End Date	Average Velocity (mm/yr)	Average Cumulative Displacement (mm)
2017-May-17	2021-Dec-02	1.9	4.8

NOTES

1. THIS FIGURE SHOULD BE READ IN CONJUNCTION WITH BGC'S REPORT TITLED "QUANTITATIVE LANDSLIDE HAZARD AND RISK ASSESSMENT – REID ROAD AREA, ELECTORAL AREA C", AND DATED JANUARY 2023.
2. THIS FIGURE DEPICTS THE SENTINEL-1 EAST-WEST DECOMPOSITION OF THE INSAR TIMESERIES EXTRACTED FOR THE SOUTHERN ROCK MASS. THE LOCATION INCLUDED IN THE TIMESERIES ANALYSIS IS SHOWN IN THE RED OUTLINE.
3. THE DATA PROCESSING WAS PERFORMED BY TRE-ALTAMIRA.
4. THIS FIGURE IS INTENDED AS A VISUAL REPRESENTATION AND IS NOT PROVIDED TO MATCH A STANDARD ENGINEERING SCALE.

PREPARED BY:	FIGURE TITLE:		
JE	EAST-WEST DECOMPOSITION OF THE INSAR TIMESERIES OF THE SOUTHERN ROCK MASS		
CHECKED BY:	CLIENT:		
CRF	SQUAMISH-LILLOOET REGIONAL DISTRICT		
APPROVED BY:	SCALE:	PROJECT NO:	FIGURE NO:
LCH	AS SHOWN	1358010	E-4

0 5 10 mm in ANSI A sized paper

APPENDIX F
SEDIMENTOLOGY, STRATIGRAPHY, AND RADIOCARBON DATING RESULTS

F.1. INTRODUCTION

Sedimentology, stratigraphy, and radiocarbon dating are techniques to develop a conceptual model of fan evolution. This appendix outlines the stratigraphy observed in test pits excavated and natural exposures mapped on Jason and Mungye creek fans along with radiocarbon dating results and presents the findings in the form of test pit logs. Raw radiocarbon dating results from Beta Analytics are included at the end.

F.1.1. Channel Condition

In steep gradient (10-20% slope), alluvial fan settings, sediments are typically coarse grained. Streams are typified by step-pool channel condition, whereby fines are eroded and flushed through, leaving a self-armoured, boulder-lag channel bed. Normal flood events, with low sediment supply, are erosive rather than depositional. See Montgomery and Buffington (1994) for geomorphic description of montane streams.

F.1.2. Sedimentary Architecture

The action of the stream under low sediment supply conditions will incise older deposits on the fan, and may dissect and disrupt the spatial continuity of different deposits. The alternation of periods of stability and erosion with debris floods and periodic debris flows gradually builds up the fan surface in an architecturally complex manner. Deciphering fan history requires detailed investigation, judgement and summary of observations into a conceptual model of fan evolution.

F.2. STRATIGRAPHY

F.2.1. Facies Descriptions

A facies is defined as a body of sediment or rock (typically a sequence of several strata, or beds) that is distinct from adjacent strata based on observable characteristics like grain colors and percent mineral composition, grain size, shape, and sorting, depositional/erosion features, geologic contacts of beds, and bedding pattern.

Cordilleran identified four basic facies in test pit logs, as described below:

F.2.1.1. Facies 1 – Debris Flood: Gravel, Massive Matrix To Clast Supported (Gm)

Extreme flood events may mobilize channel bed materials, causing bulking of the peak discharge, and forming debris floods (or flows) that may remain channel confined, or they may leave or avulse from the channel, spreading laterally depositing gravel ranging in texture from granular (2-4 mm dia) to boulder (0.25-4 m dia) size. The matrix of debris flood deposits is typically sandy; larger clasts (pebbles to boulders) may be in clast-to-clast contact, or as sediment bulking increases, some clasts may become “supported” by the finer grained matrix. Sediments may be subrounded to subangular in shape. When sediment supply is high, the stream may be laterally unstable, shifting its bed location and gradually aggrading the fan surface.

F.2.1.2. Facies 2 – Debris Flow: Very Poorly Sorted (Diamicton), Massive, Matrix-Supported (Dmm)

When bank failures or larger landslides enter the channel, the volume of sediment may overwhelm the volume of water and the material may evolve into a debris flow. These materials are typically very poorly sorted (i.e., diamicton), with material ranging from clay/silt to boulder size, and possibly larger (megablock, >4 m dia). The large clasts (cobble, boulder, megablock) are typically matrix-supported, meaning they float in the matrix of finer debris. Often debris flows display reverse grading (larger clasts at the top), but not always, especially in finer grained flows that may have massive structure.

Debris floods and flows are part of a continuum, and individual units defined by obvious contacts (paleosols; unconformities) may display gradations from flow to flood, or vice versa.

F.2.1.3. Facies 3 – Muddy Afterflow

A third type of sedimentary unit includes thin beds, typically about 3-5 cm thick (but sometimes thicker where accommodation space allows; i.e., filling topographic depressions), composed of mud (silt & clay), sometimes granular (2-4 mm dia grains), often with charcoal lamina or including charcoal fragments. These beds may be the final muddy phase (i.e., afterflow) of deposition of the bed immediately below, or they may record their own sediment pulse. The organics being derived from charcoal washed in during deposition, or from soil horizons developed on the surface, and buried by subsequent events.

F.2.1.4. Facies 4 - Paleosols

Buried pedogenic soil layers are termed paleosols. The former soil organic horizon (the Ah), upon burial may preserve carbon for radiocarbon dating. Selecting charcoal laminae from paleosols targets fossil carbon deposited insitu and contemporaneous with soil accumulation.

F.2.2. Radiocarbon Dating

Cordilleran submitted fifteen carbon samples collected from test pits to Beta Radiocarbon Laboratories in Florida for radiocarbon age determination (Table F-2).

The radiocarbon (^{14}C) method dates the death age of the organic sample. For example, the time when a twig broke from a tree (i.e., died) and fell onto the forest floor, or when a tree ring passed from being live cambium to an inner ring.

Thus, ^{14}C dating does not directly date what is of interest, the landslide. Rather, it provides maximum or minimum bracketing ages, depending on whether the sample was within or below (maximum age) or above (minimum age) the unit of interest. To avoid sampling modern roots that have penetrated deep into the soil, and may have been burnt by fires, charcoal in an old buried soil horizon, or a paleosol is dated. In this manner, carbon that was deposited during fan aggradation, by flood or debris flow, not something coming later, like the root is dated.

The bracketing may not provide a tight age constraint on the unit of interest: with further dating for instance, one may find that for a maximum age context (^{14}C sample within or below the unit of

interest) the age range of multiple samples may span centuries, and the youngest of the maximum ages will be the closest bracket; conversely, for a minimum age context (^{14}C sample above a unit of interest), the oldest of the ages will be the closest minimum age.

For example, if a charcoal sample in a paleosol returns an age of 1,000 years before present (yr BP), the wood fragment may have been from the inside ring of a 300 year old tree, and it may have been rotting on the soil surface for 200 years before being buried, therefore introducing a sampling error of 500 years, the true maximum would not be 1,000 but rather 500 yr BP. Therefore, the sample represents a poor maximum limiting age, and more samples might yield a better bracket. Since finding material to date is uncertain, and since dates are expensive, running multiple samples to get the closest bracketing age is not always feasible. Often the sampling errors are not known, and this introduces the need for judgement in the interpretation process.

When a tight bracketing age is desired, running more samples or being very specific with what is being dated is required; for example, one must find a buried tree with bark attached, convince yourself tree was killed by landslide (landslide age and tree death age are the same), then use a band saw to remove only the last ring and date that, then the lab error will be the only error.

The reported conventional age error (i.e., ±30 years) refers to lab error only. It is good to have it small, and ±20 to ±30 years is typical. Note though, as discussed above, the sample error is the uncertainty in the association between what is being dated and what we are interested in. The sample error (potentially centuries) is much greater than the lab error (typically decades), and is typically unknown.

There are two reported ages, conventional radiocarbon ages (Yr BP ^{14}C), and calibrated ages (Yr BP). Since the production of radioactive carbon in the atmosphere is not constant in time, raw conventional ages need to be calibrated to calendric time. The calibrated ages are reported as a group of ranges, each group explaining a percentage of the total, i.e., at site TP5, sample J-1794b-1, the conventional age is reported as 1230±30 yr BP ^{14}C, and the calibrated age as such,

- 67% certainty date lies between 1179-1066 Yr BP 1950
- 27.5% certainty date lies between 1268-1206 Yr BP 1950
- 0.8% certainty date lies between 1188-1184 Yr BP 1950.

Ignoring the last range, we estimate the mean age as (1179-1066)/2*(67/95*100)+ (1268-1206)/2*(28/95*100) = 1156 Yr BP 1950. The error is shown as the maximum minus the minimum of the ranges given divided by two (±101 years).

These calibrated ages are referenced to the year 1950 AD (Yr BP 1950). This marks a major radioactive carbon spike in the atmosphere due to the onset of nuclear bomb testing. We have corrected these calibrated ages to the reference year 2022 (Yr BP 2022) by adding 72 years.

F.2.3. Soil Development & Relative dating

In the region, the so-called zonal soil is referred to as a podzol (Valentine, 1978). Podzols are characteristic of wet temperate climates, and are the product of chemical weathering, leaching of minerals from the upper soil levels and translocation of oxidants to deeper soil depths. A well developed podzol may have an organic forest floor horizon (Duff, or Ah), a leached mineral zone

(Ae), and a B horizon enriched by humus (Bh) and by ferrous oxides (Bf). A well-developed podzol B-horizon typically has an orange to red colour. Based on local experience and on published literature (Protz 1984; Sanborn et al., 2011), it takes at least 1,000 years to begin to see an oxidized B-horizon. Deeply oxidized B-horizons will be several millenia in age. Thus, the presence and degree of podzolisation can aid interpretation of deposit age, at least in relative terms.

F.3. RESULTS

A total of 11 test pits and two natural exposures were described by Cordilleran on Jason Creek fan, and four test pits on Mungye Creek fan, above and below Reid Road (Table F-1). Test pit depths ranged from 2 – 4 m, typically about 3.5 m depth. Materials comprised interbedded debris flood gravel, debris flow diamicton deposits, and thin muddy afterflow beds. Unit thickness of both debris flood and debris flow beds range from decimetres to ~2 m. In one case (Test Pit 1) a debris flow diamicton unit was ~5 m in thickness.

Table F-1. Location of Test Pits on Jason and Mungye Creek fans.

Title	Northing (m)	Easting (m)	Fan (J, M)-Property ID
TP-1	5577362	517686	J-1781a
TP-2	5577297	517756	J-1781b
TP-3	5577170	517996	1802
TP-4	5577077	517884	J-1794a
TP-5	5577119	517837	J-1794b
TP-6	5577202	517888	J-1794c
TP-7	5577300	517862	J-1791
TP-8	5577208	517676	J-1782
TP-9	5577247	518031	J-1815
TP-10	5577148	517643	J-1770a
TP-11	5577196	517625	J-1770b
TP-12	5576973	517124	M-1723
TP-13	5576757	517207	M-1720
TP-14	5576850	517118	M-1719
TP-15	5576571	517170	M-1712
TP-16	5577215	517634	J-1770c-1; Natural exposure left bank Jason Creek
TP-17	5577070	517731	J-0000; Natural exposure left bank Jason Creek

A total of 15 radiocarbon samples were collected and sent to Beta Labs in Florida for radiometric analysis. Twelve samples were from Jason Creek fan, one from Jason Creek channel below the 2021 debris flow source area, and two were from Mungye Creek fan (Table F-2).

Table F-2. Radiocarbon sample meta data and results.

Pit	BGC ID	BETA ID	Material	Yr BP 14C	Yr BP 1950	Weighted mean ±range of error/2	
						Yr BP 2022	± yrs
1	J-1781a-1	635072	Root	108 +/- 40	-52	20	24
4	J-1794a-1	635073	Charcoal	9080 +/- 30	8276	8348	46
5	J-1794b-1	635074	Charcoal	1230 +/- 30	1156	1228	101
5	J-1794b-2	635075	Charcoal	1710 +/- 30	1606	1678	82
6	J-1794c-1	635076	Sediment	2020 +/- 30	1944	2016	88
7	J-1791-1	635077	Charcoal	3240 +/- 30	3442	3514	87
8	J-1782-2	635078	Charcoal	1860 +/- 30	1770	1842	79
8	J-1782-1	635079	Charcoal	3080 +/- 30	3292	3364	80
10	J-1770a-1	635080	Charcoal	260 +/- 30	312	384	79
12	M-1723-1	635081	Sediment	1330 +/- 30	1243	1315	63
13	M-1720-1	635082	Charcoal	1870 +/- 30	1775	1847	78
16	J-1770c-1	635083	Charcoal	190 +/- 30	173	245	82
17	J-0000-2	635084	Charcoal	440 +/- 30	491	563	95
17	J-0000-1	635085	Charcoal	3840 +/- 30	4266	4338	128
18	J-WP8	635086	Stick	2910 +/- 30	3061	3133	100

One date, collected from TP1, produced a modern result and was discounted. After we had conducted the excavation, the owner indicated the site at TP1 was likely disturbed by previous excavations. However, the excavated section reveals a 5 m thick deeply oxidized debris flow diamicton that does not look disturbed by prior excavation. In our opinion, exposed sediments are insitu, but the dated sample is inferred to be a modern root.

On Jason Creek fan, radiocarbon ages cluster into several broad groups:

- ~245-563 Yr BP 2022
- 1228-2016 Yr BP 2022
- 3133-4338 Yr BP 2022
- a single age at 8348 Yr BP 2022.

The younger cluster are from pits located along Jason Creek, on the west side of the fan, from near surface interbedded gravels in TPs 10, 16 & 17. These reflect debris flood/flow activity with apparent average return intervals ranging from 1/190 yr (TP10), 1/120 yr (TP16) to 140-190 yr (TP17).

In the central sector of Jason Creek fan, above and below the Reid Road, there is evidence of at least two and possibly 3 large (0.25-2 m thick) debris flows in the last 2-3 thousand years. The

surface unit, seen at TPs 2, 3, 5, 6, 7, 8, & 15 is <=1228 years old based on a best maximum age from TP5. At several other sites (TPs 6, 7) there is a 2nd unweathered debris flow unit, likely younger than 2-3 ka years in age.

These debris flow units may contain large clasts; in test pits, boulder size material ranging from 400-1000 mm was common, while clasts to 1500 mm were noted. However, most striking was the occurrence at the surface at many sites of angular blocks of 3-5 m in size.

Sediments older that 3.1 ka on Jason Creek fan are deeply oxidised. Oxidised gravels and diamicton at TPs 7, 8, 17 yielded ages ranging from 3368 – 4338 Yr BP 2022, and a muddy surface diamicton at TP4 was <=8348 Yr BP 2022.

Along the Jason Creek channel below the 2021 initiation zone (WP8) we discovered wood fragments buried on the bedrock contact by deeply oxidised diamicton. This sample yielded an age of 3133 Yr BP 2022, and suggests a debris flow <=3133 year ago may have affected the fan. On the Jason Creek fan, at TP7 a debris flow unit was capped by mud with charcoal yielding an age of 3514 Yr BP 2022; at TP8 an age of 3364 Yr BP 2022 in a muddy unit overlying over thick gravels may represent debris flood phase for this event; while at TP17 charcoal yielding an age of 4338 Yr BP 2022 came from massive mud unit at least 0.55 m thick, which may represent afterflow materials. This evidence supports the occurrence of a debris flow with a best maximum age of ~3100 Yr BP 2022.

The deeply oxidized sites at TP4 and TP 17 are farthest downslope of the test pits in the central sector of Jason Creek fan. These sites have not been covered by younger debris flow materials. This implies that debris flow has not runout below 380-400 m elevation in 4300-8300 years.

Test pitting on Mungye Creek revealed a relatively unweathered surface debris flow diamicton. This unit varies in thickness from 1.2 – 1.55 m thick. Charcoal from soil layers buried beneath the surface event yield ages of 1315 & 1847 Yr BP 2022. The best maximum age for the surface unit is then 1315 Yr BP 2022.

F.4. TEST PIT DESCRIPTIONS / INTERPRETATIONS (ACCOMPANIED BY PHOTO LOGS)

Pit 1. 6 m Depth (Jason)

This site consisted of a cutslope behind the house at 1781 Reid Road. The existing cut was ~4 m tall; the backhoe cut into and cleaned the face, and excavated an additional 2 m depth. Materials consisted of a 5 m thick oxidised muddy debris-flow diamicton containing clasts to 500-1000 mm diameter; overlying 1 m of washed gravels. Of note, a single large clast on surface of the was 4-5 m in dia. A carbon sample was collected from the contact between the two units at 5-m depth. It yielded a modern age of 20±24 Yr BP 2022, and is interpreted to be a modern root. Since the excavation made use of a cut, it is likely that vegetation growing on the cutslope face penetrated the slope and exploited the contact zone. Based on the degree of oxidation, and the ages of other deeply oxidized units in other pits, this debris flow unit may be older than 3.1 ka.

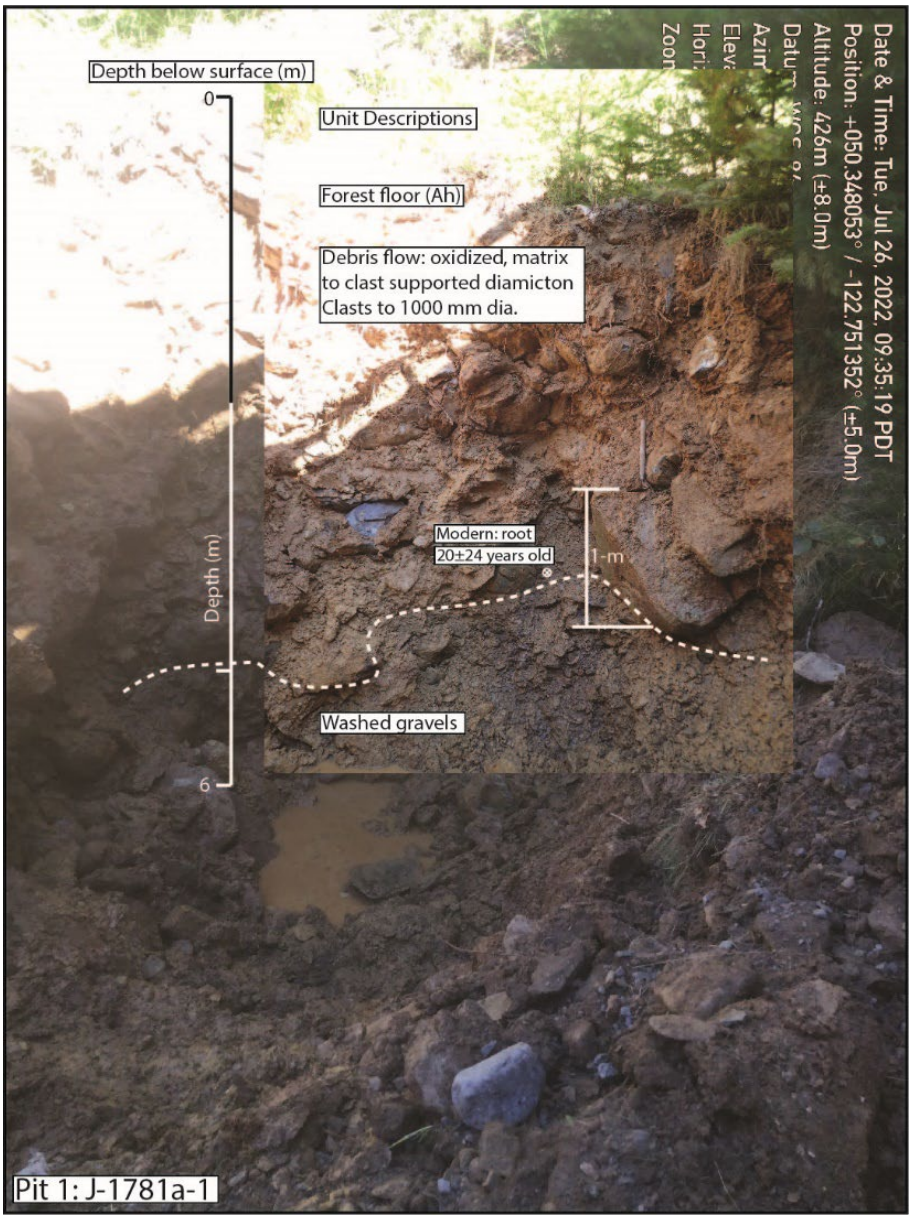

Pit 2 ~2.75 m Depth (Jason)

The surface 2 m consists of an unweathered debris-flow diamicton. Based on radiocarbon dates from (TPs 4, 5, 8), the surface debris flow is <=1.2 ka (best minimum 1230 Yr BP 2022 from TP4). This sharply overlies a deeply oxidized gravel that extends to the base of the pit. Based on dating of deeply oxidized materials at TPs 7, 8, 17, these materials are >3.1 ka in age.

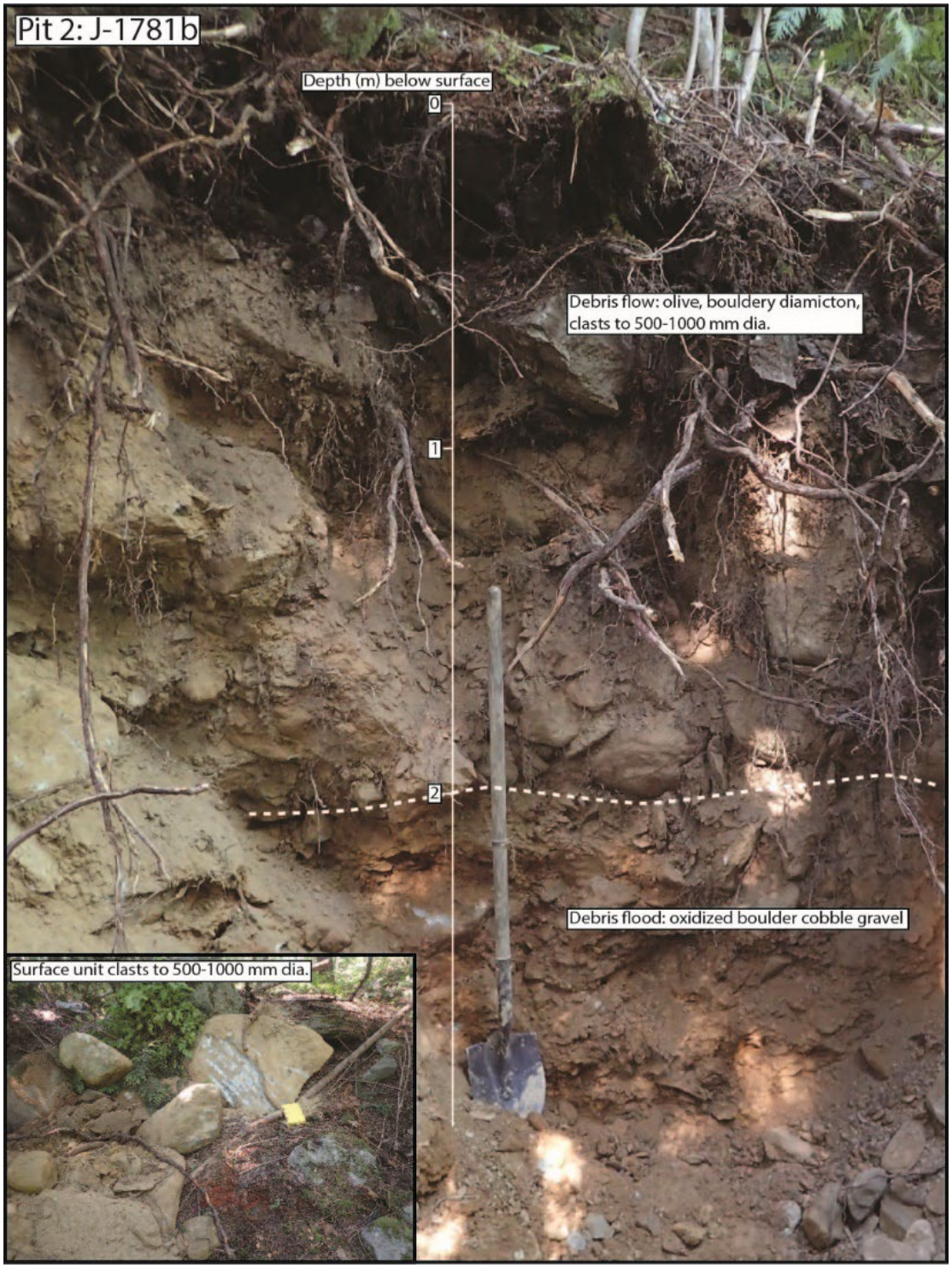

Pit 3. 4.2 m Depth (Jason)

The surface 1.8 m consist of an unweathered debris-flow diamicton. Based on radiocarbon dates from TPs 4, 5, 8, the surface debris flow is <1.2 ka. Below 1.2 m are bedded gravels with beds 0.1 – 2 m thick. The beds are not deeply oxidized, and based on the age of deeply oxidized materials at TPs 7, 8, 17, the unweathered sediments would be <3.1 ka in age.

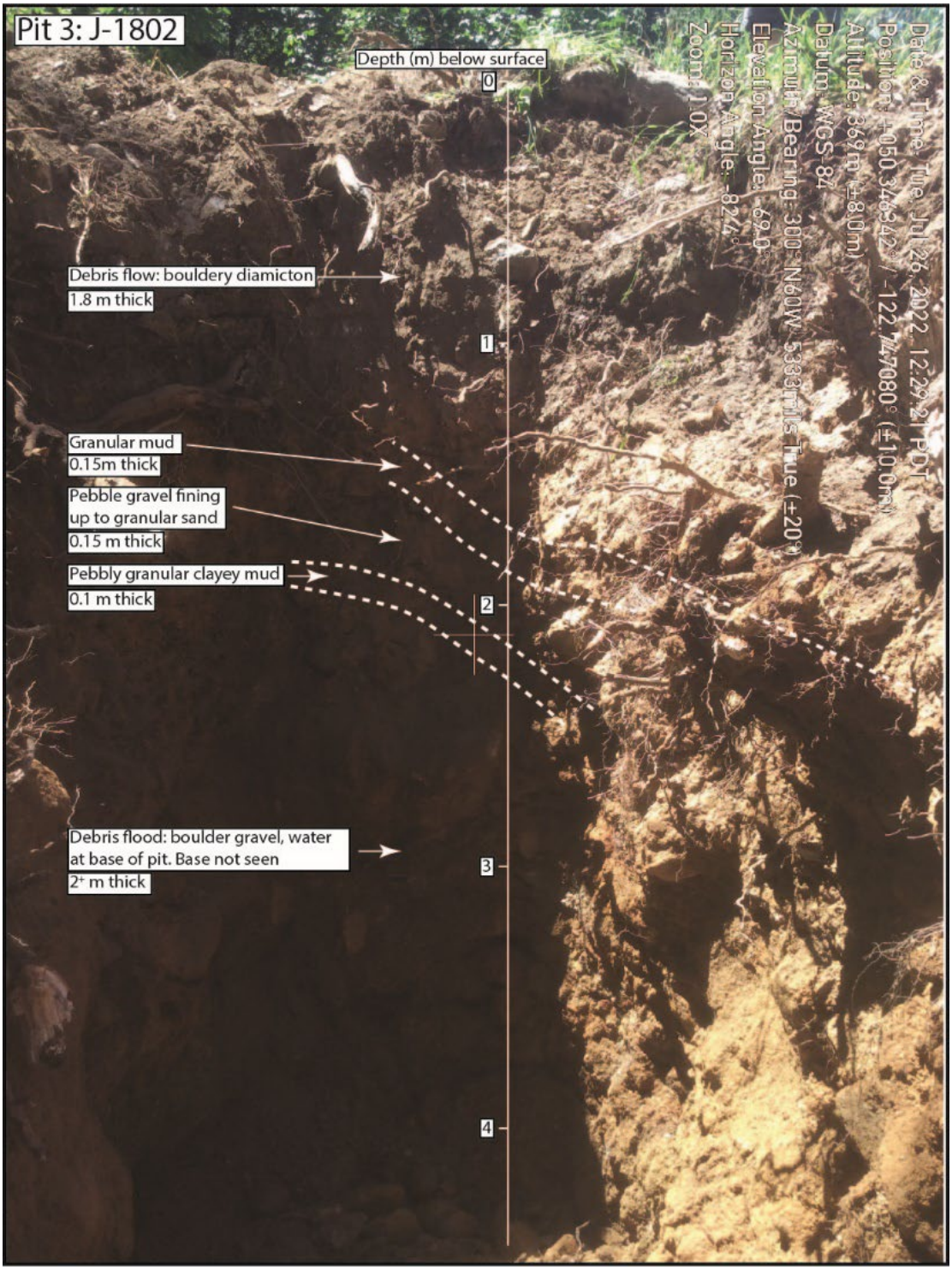

Pit 4. 2.7 m Depth (Jason)

The surface 2 m consists of deeply oxidized diamicton with two zones: a 1 m thick matrix-supported pebble cobble bed overlying a 1 m thick fault-gouge derived muddy bed. Charcoal from within the clay rich unit yielded an age of 8348 Yr BP 2022. Apparently, debris flow has not significantly affected this distal location on the fan in 8300 years. The presence of the fault-gouge bed is supportive of the “dynamic liquefaction" model at Jason Creek, whereby the brittle rock failure lands on thick fault gouge and mobilizes into debris flow.

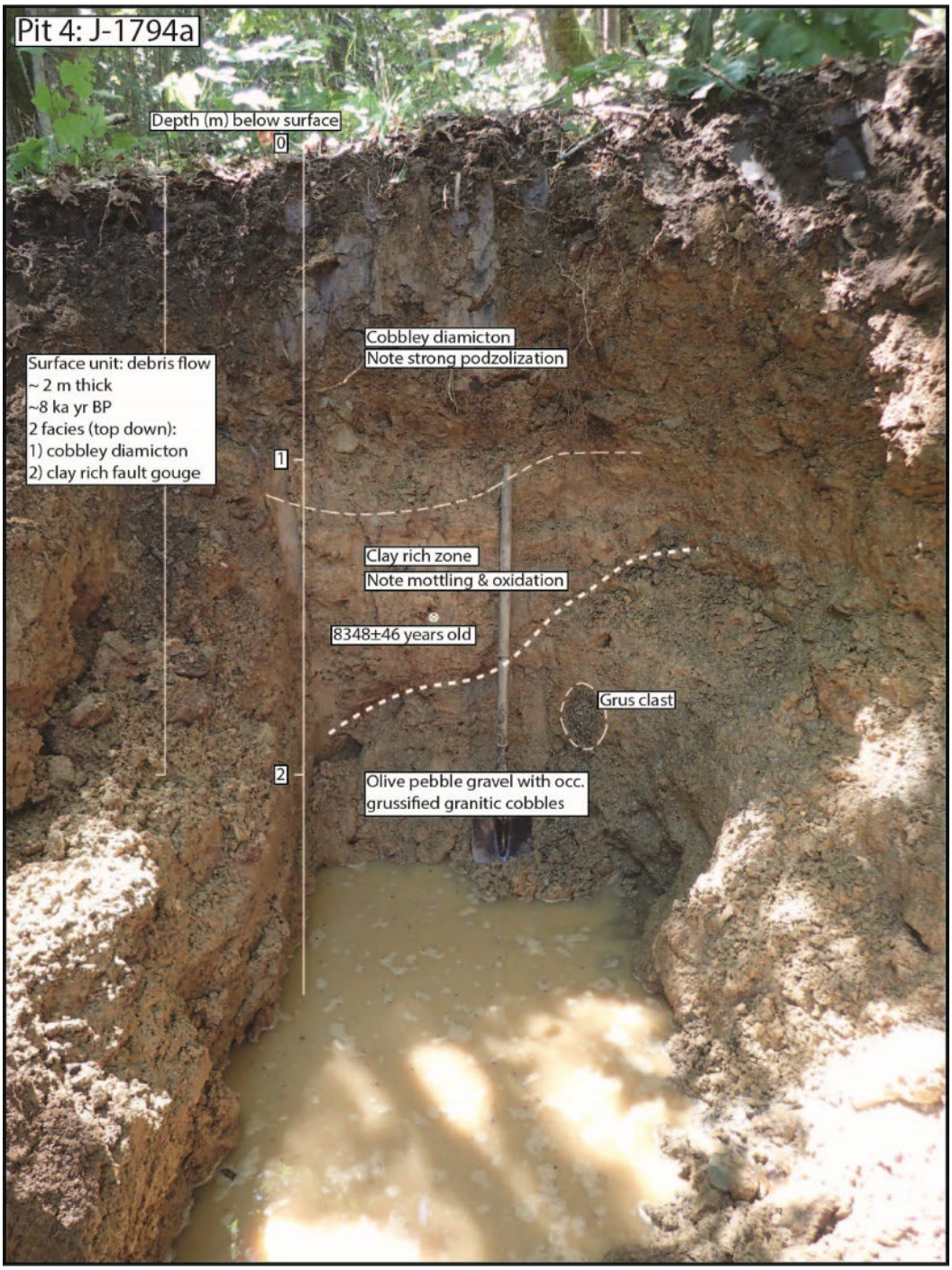

Pit 5. 3.8 m Deepth (Jason)

The surface 1.5 m consists of an unweathered bouldery debris-flow diamicton. This overlies bedded gravel and mud interbeds extending to the base of pit. The two mud interbeds contained charcoal, yielding 1228 Yr BP 2022 at 1.5 m depth, directly beneath the surface diamicton, and 1678 Yr BP 2022 at 1.76 m depth. This site provides a best maximum age of <=1228 Yr BP 2022 for the unweathered surface diamicton found at other sites (TPs 2, 3, 6, 7, 8, 15).

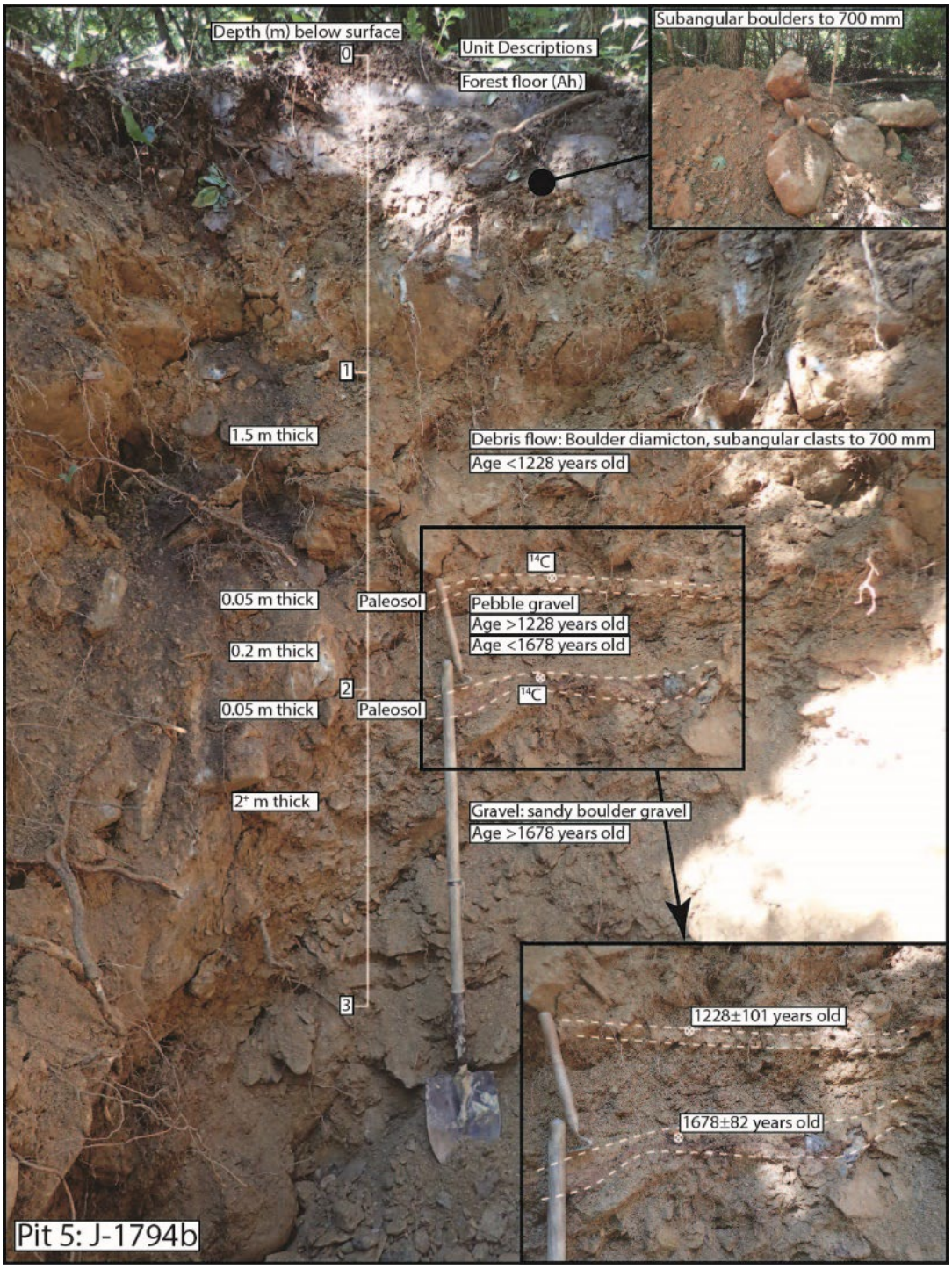

Pit 6. 3.8 m Depth (Jason)

The surface 3 m consists of three bedded debris flow diamictons, with beds ranging from 0.55-1.45 m thickness. Charcoal found within the 3rd bed down yielded an age of 2016 Yr BP 2022. This provides an apparent debris flow frequency of 1/670 yrs, but if beds 1 & 2 down are considered different phases of a single event, then the debris flow frequency would be 1/1000 yrs. From 3 m depth to the base are unweathered gravelly materials.

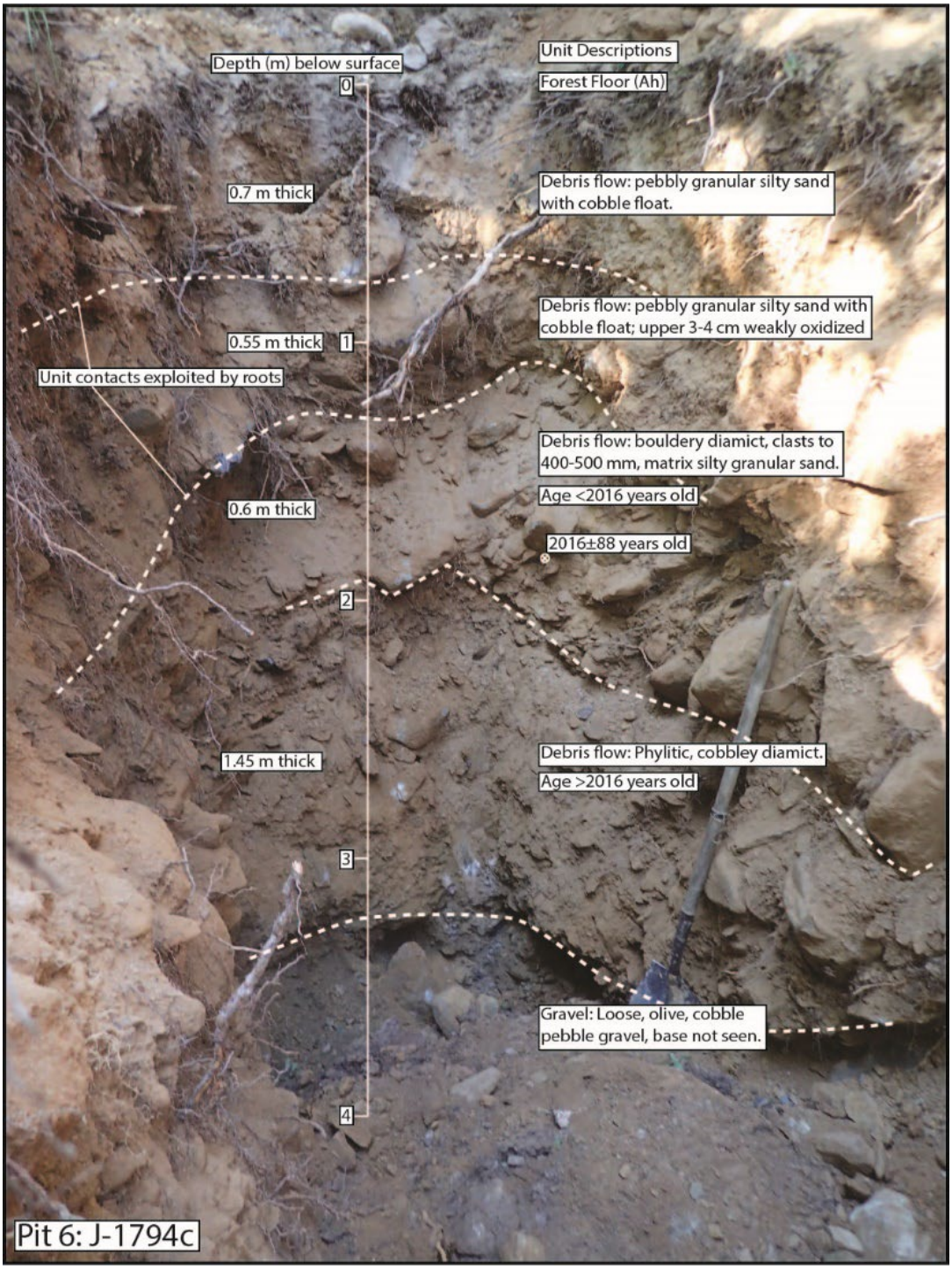

Pit 7. ~3.5 m Depth (Jason)

The surface 2.4 m is underlain by 2 debris flow units, each 1.2 m thick. The upper unit is unweathered; while the lower unit is deeply oxidized. A charcoal lens sampled at the top of the oxidized unit yielded an age of 3514 Yr BP 2022. The date provides a maximum age constraint of <3500 years on the overlying debris flow. Given the unweathered condition of the upper debris flow unit, and based on dates from other pits, the surface <1.2ka (TP5) and the basal one may be >3.1 ka (see Pit 6).

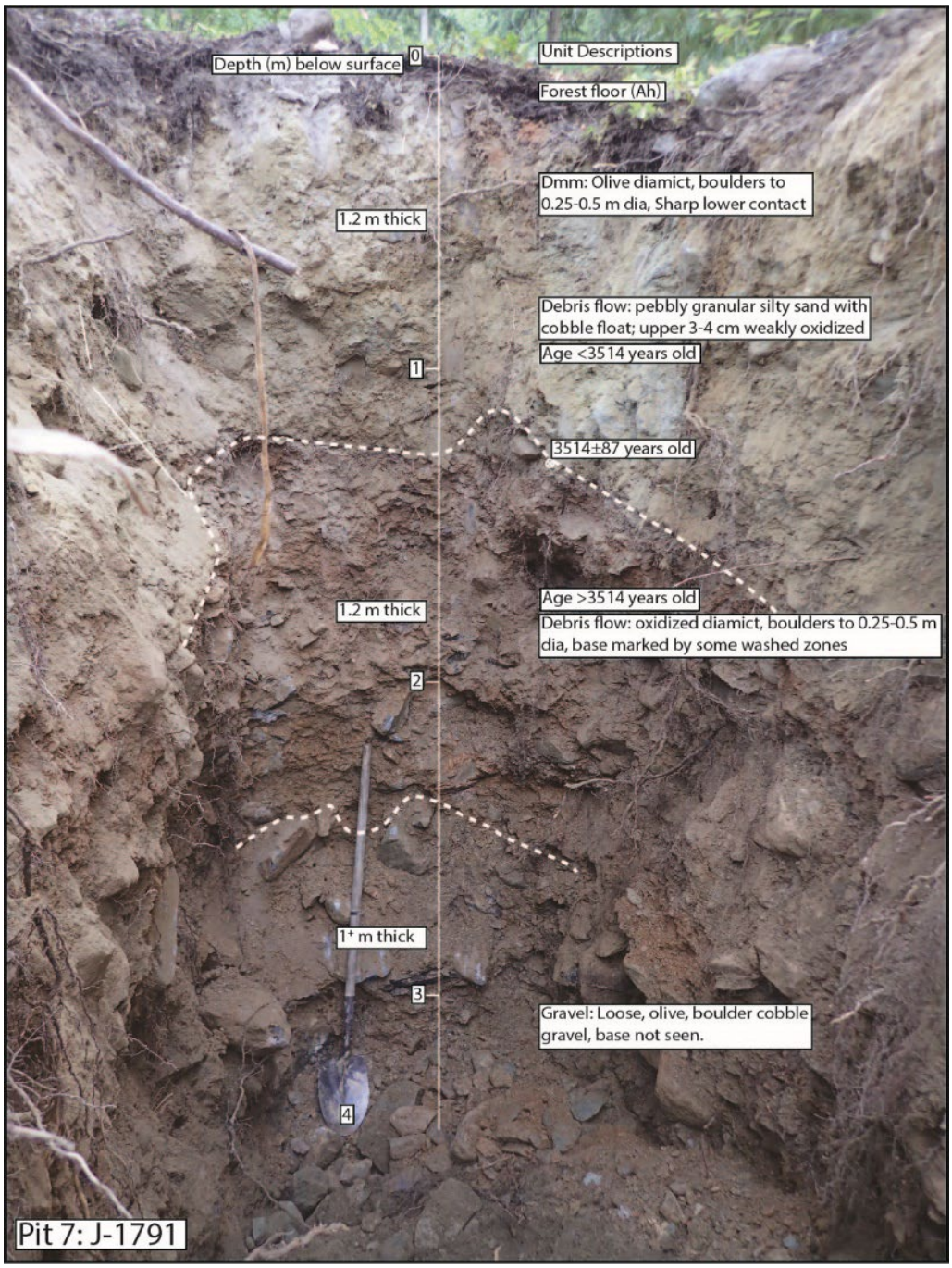

Pit 8. ~3.5 m Depth (Jason)

The upper 0.5 m consist of a diamicton overlying a gravel bed. Beneath these surface layers are 2, ~1.5 m thick beds. The upper is matrix-supported diamicton at the base grading up to gravelly at the top; it is capped by a 0.05 m thick mud with charcoal yielding an age of 1842 Yr BP 2022. The underlying bed is a deeply oxidized gravel, with a mud cap with charcoal lamina yielding an age of 3364 Yr BP 2022. The dates indicate that at least two shallow debris flood and debris flow events affected the site sometime after 1842 years, with apparent flood and flow frequencies of 1/900 years; and between 3364-1842 years there was a significant debris flood event, with a long-term average of 1/1120 years.

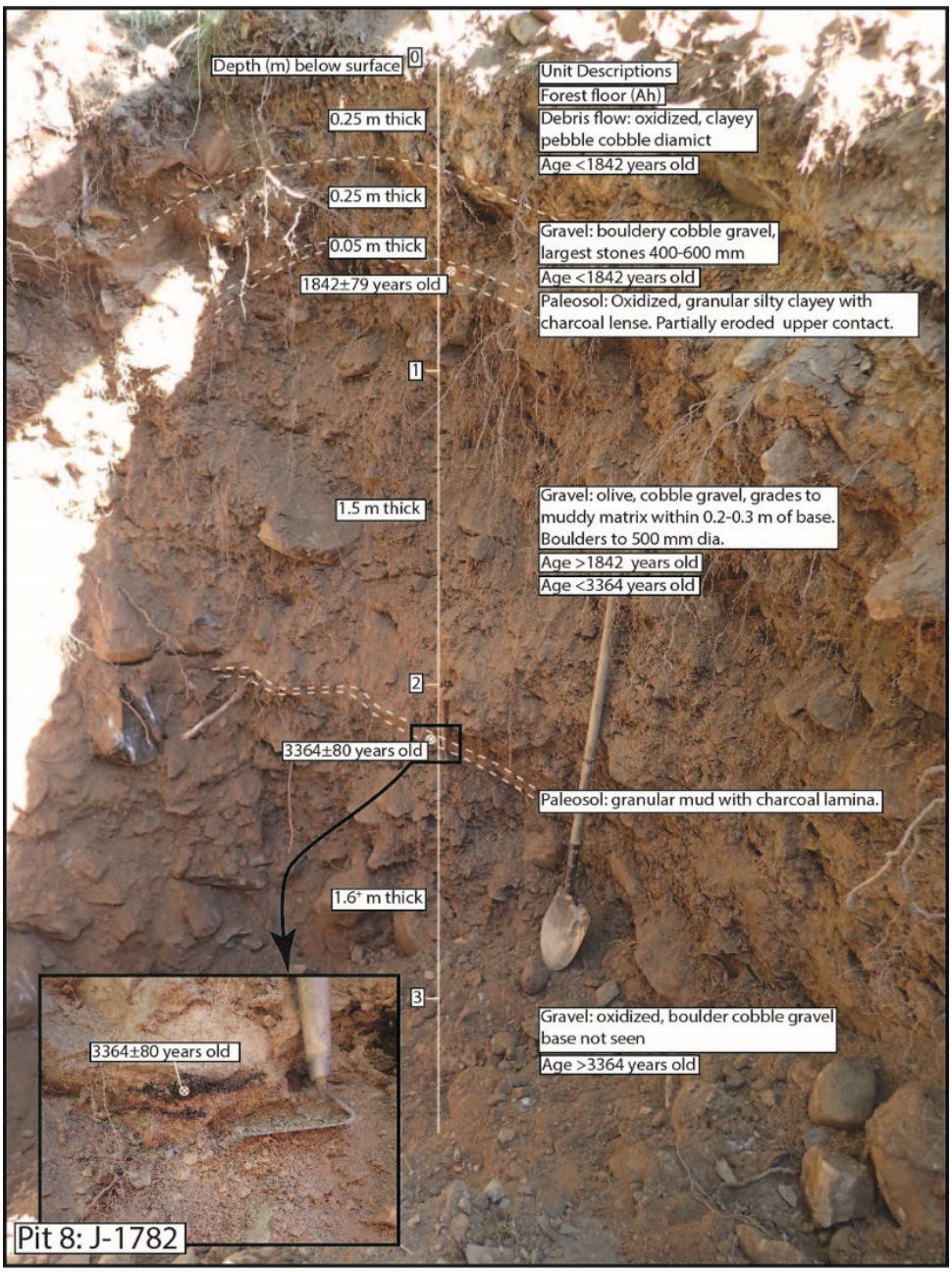

Pit 9. ~3.5 m Depth (Jason)

This pit consists of three massive matrix- to clast-supported, cobble pebble gravel beds ~80-100 cm thick, each separated by thin mud drapes or marked by sharp colour change. No charcoal was found for dating. This suggests primarily debris flood activity has affected this site, at least in the last few (~3 ka) thousand years.

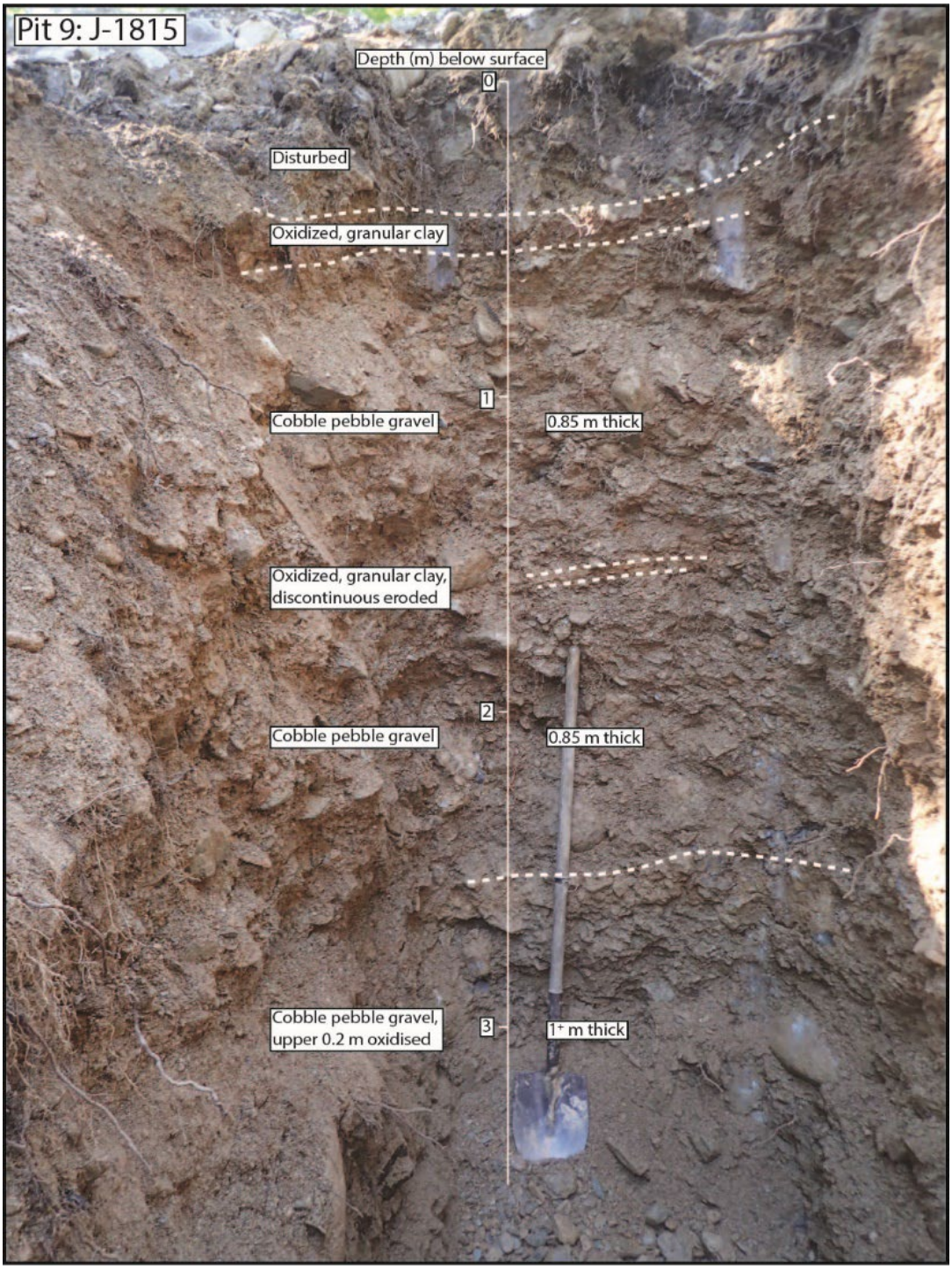

Pit 10. ~3.5 m Depth (Jason)

The surface 2.5 m consist of 3 gravel beds 0.5-1.3 m thick. There is a mud interbed between the 2nd and 3rd down, with charcoal yielding an age of 384 Yr BP 2022. Thus, the apparent debris flood frequency is 1/190 yrs. The gravels unconformably overly a deeply oxidized diamicton containing striated clasts, and on the basis of deep weathering and striated clasts was inferred to be till.

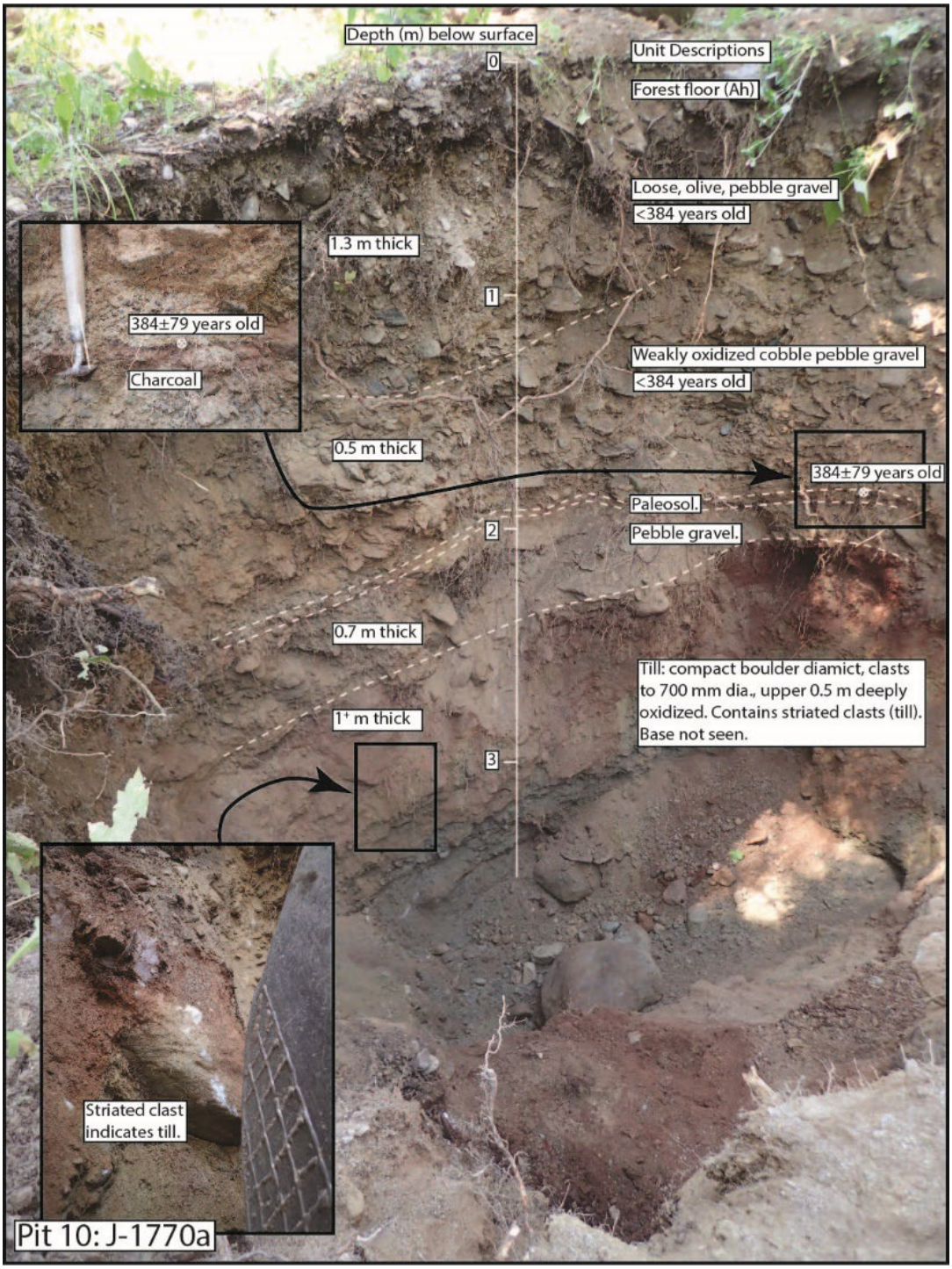

Pit 11. (Jason)

This pit consists of a diamicton similar to that at the base of Pit 10. The material was inferred to be till. TP10 & TP11 are located on the west margin of the alluvial fan.

Pit 12. ~3.5 m Depth (Mungye)

This pit consists of two matrix-supported boulder diamictons separated by a mud layer with charcoal dated to 1315 Yr BP 2022. Neither unit shows significant oxidation. The surface units is <1315 years old, and the underlying debris flow may be <2-3 ka.

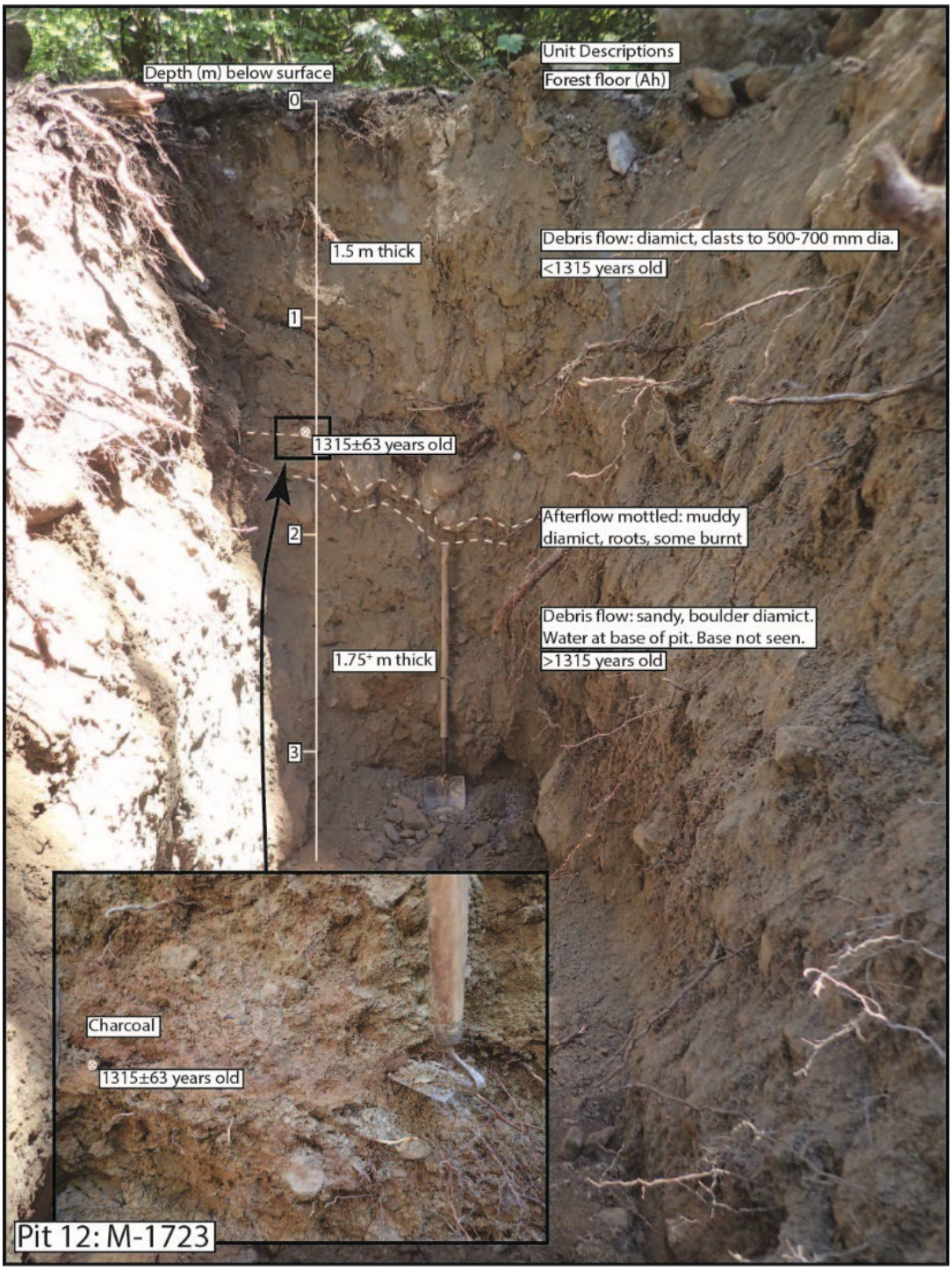

Pit 13. ~2 m Depth (Mungye)

This pit revealed very clayey diamicton, with soil development marked by oxidation processes driven by soil saturation (in the upper 120 cm, oxidation & mottling within the seasonal high water table; gleying below seasonal water table, where persistently saturated). A charcoal sample from 140 cm depth yielded an age of 1847 CYr BP 2022. This provides a maximum age for the last debris flow affecting the site.

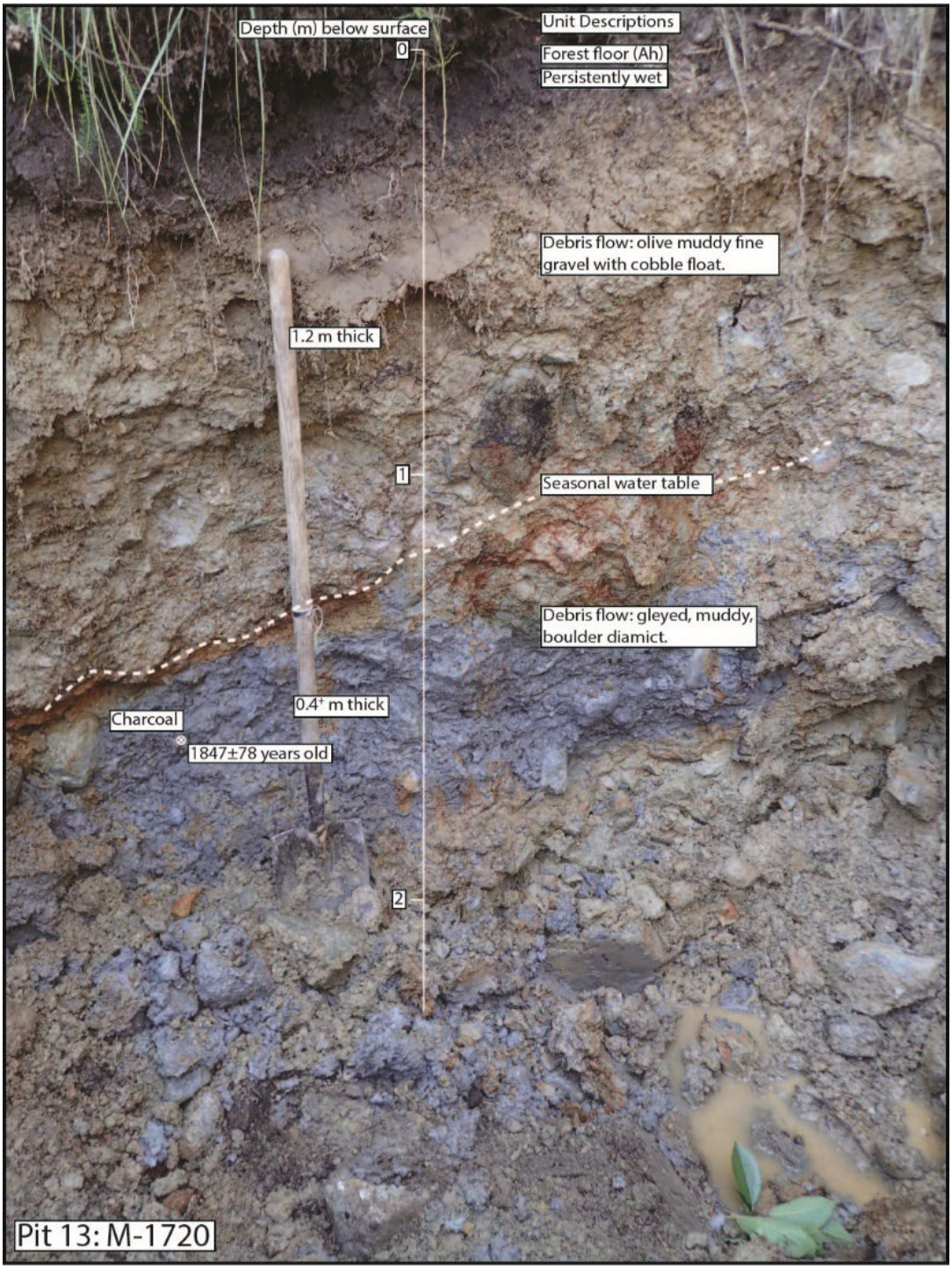

Pit 14. ~2.5 m Depth (Mungye)

This pit consists of 2 unweathered diamicton units, each 1.3-1.5 m thick. No carbon was found for dating control. Based on the unweathered condition they are likely <3 ka.

Pit 15 ~325 cm Depth (Mungye)

The surface 1.3 m depth consists of an unweathered boulder diamicton. It overlies gravelly material which extends to the base of the pit. The debris flow unit is unconstrained by radiocarbon, but based on its lack of oxidation it is judged to be <=1.2 ka. The best maximum age for the surface debris flow unit is 1230 Yr BP 2022 from TP5. This may be the same event at all sites, with a best maximum age of 1230 Yr BP 2022. The unweathered gravels beneath have been active in late Holocene, likely spanning 2-3 ka.

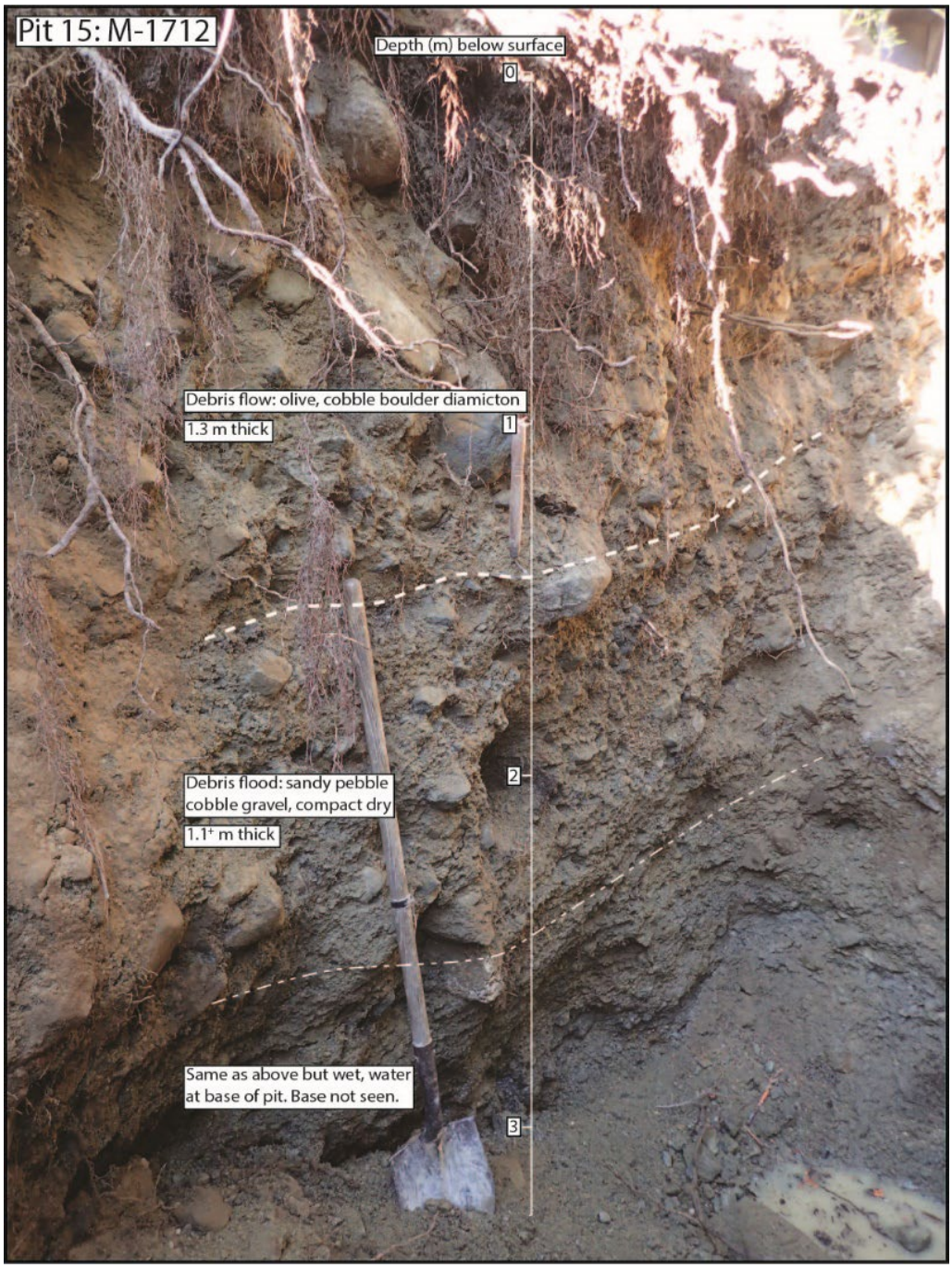

Pit 16 ~2.5 m Depth (Jason, Streambank exposure)

Surface to 1 m depth consists of bedded cobble pebble gravel and sand, with beds 0.15-0.35 m thick. At 65 cm bs date of 245 Yr BP 2022 was returned from charcoal. With two beds above the sample, the apparent debris flood frequency is 1/120 yr. Below 1 m depth there is a 75 cm thick debris flow diamicton. The event would be older than 245 Yr BP 2022, and since it is not oxidized, it appears younger than ~2-3 ka, likely correlative with the surface diamicton at other site (TPs 2, 3, 6, 7, 8, 15). This unit overlies more gravel which extends to the base of the pit.

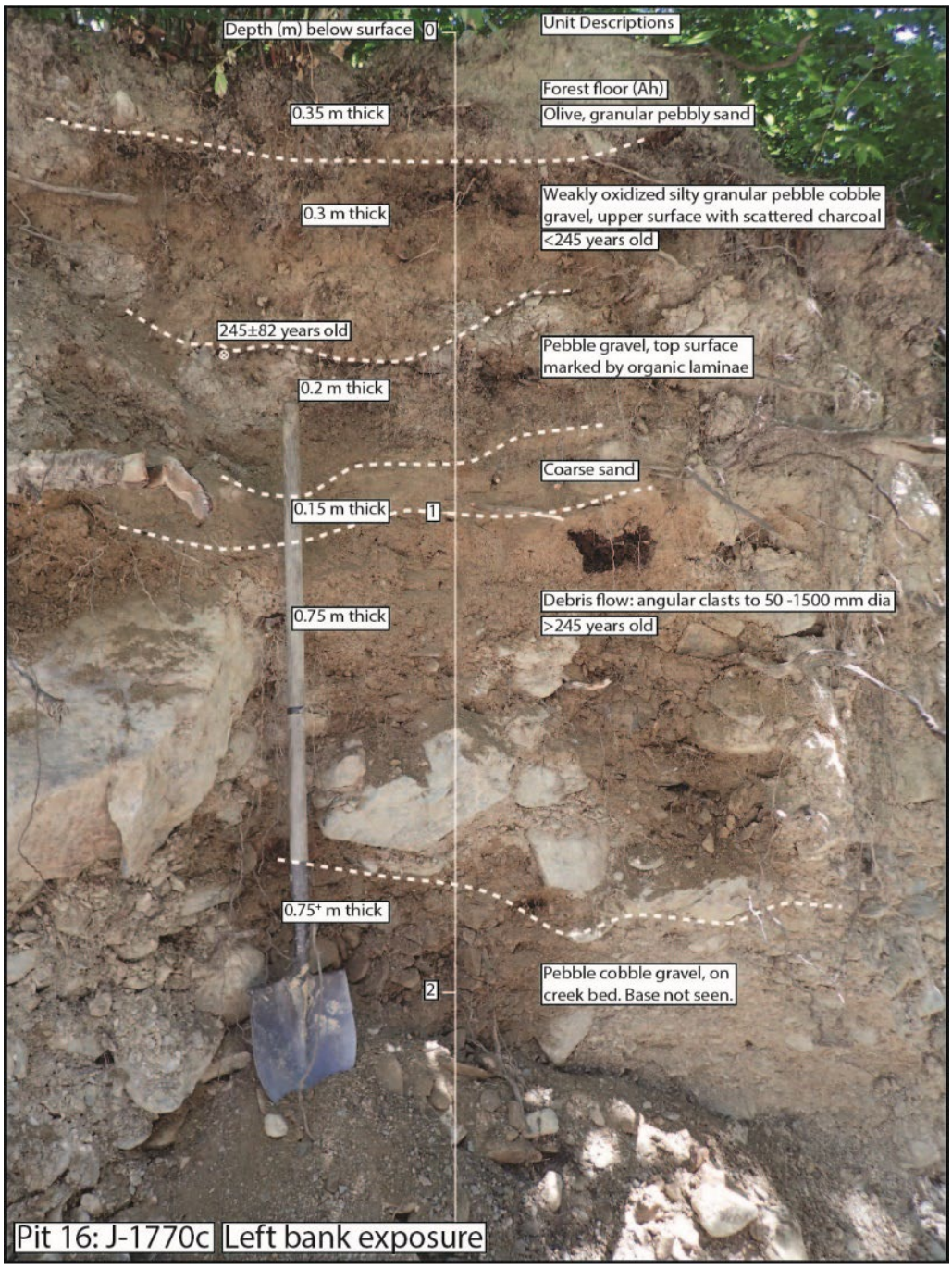

Pit 17 ~2.5 m Depth (Jason, Streambank exposure)

The surface 2 m is comprised of bedded pebble-cobble gravel, with beds 0.25-0.65 m thick. Two interbeds consist of ~0.05 m gritty mud. The lower mud unit at 130-135 cm depth contains charcoal dated to 563 Yr BP 2022. With 3 bed units above, the apparent debris flood frequency is 1/190 yr. The gravels erosionally overlie a deeply oxidized massive mud unit which extends to the base of the exposure. Charcoal from within the mud yielded an age of 4338 Yr BP 2022. Apparently, debris flow has not significantly affected this distal location on the fan in 4300 years.

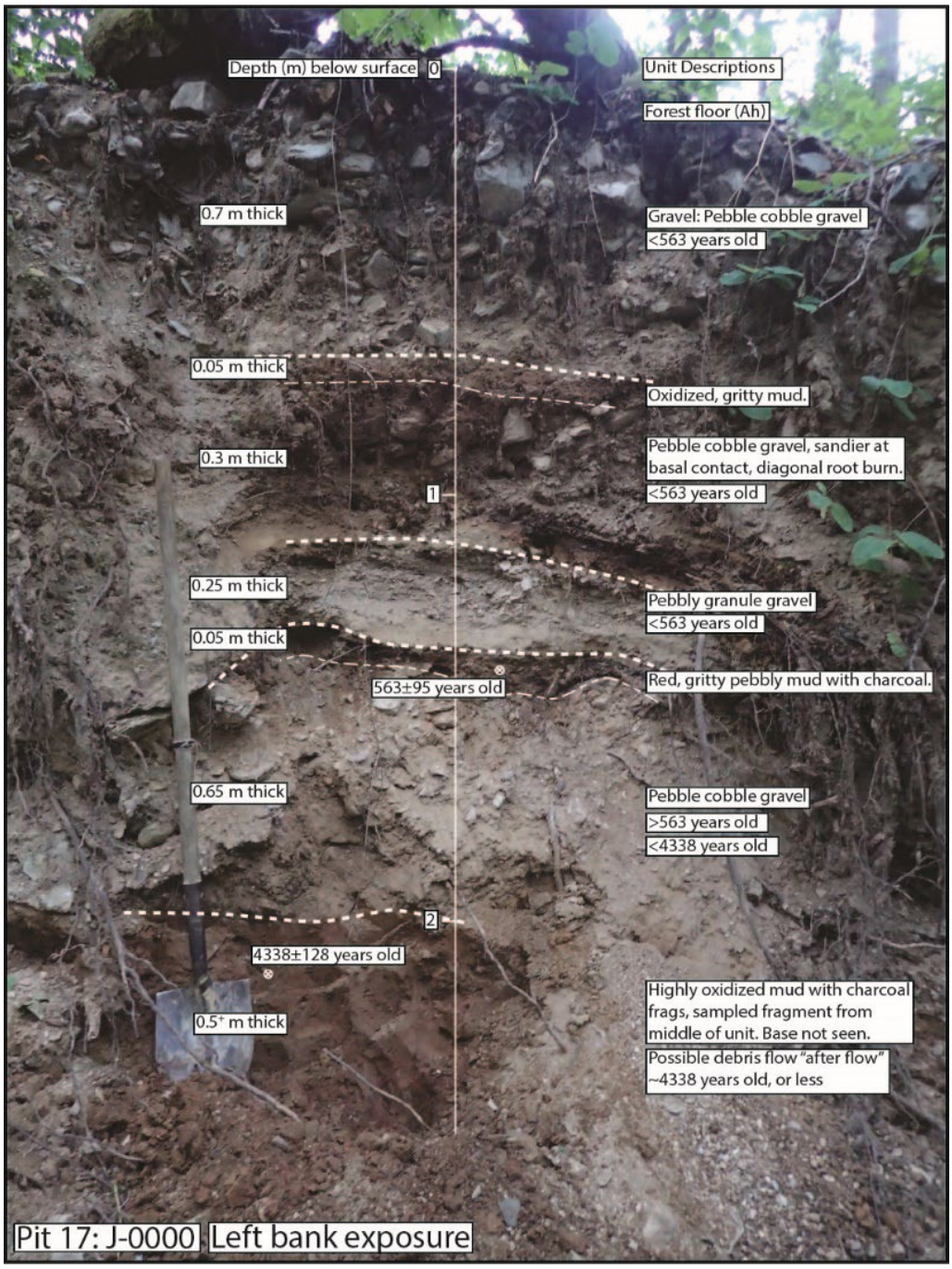

WP8

This site is located along the Jason Creek channel at 660 m elevation just below the 1990 & 2021 headscarp area. The 2021 debris flow has scoured the channel down to bedrock, leaving exposure of old debris flow diamicton on either creek sidewall. Wood (logs, fragments and sticks) were observed in the debris flow sediment, and a stick selected for radiocarbon dating yielded an ages of 3133 Yr BP 2022. This documents a significant debris flow event <= 3100 Yr BP 2022.

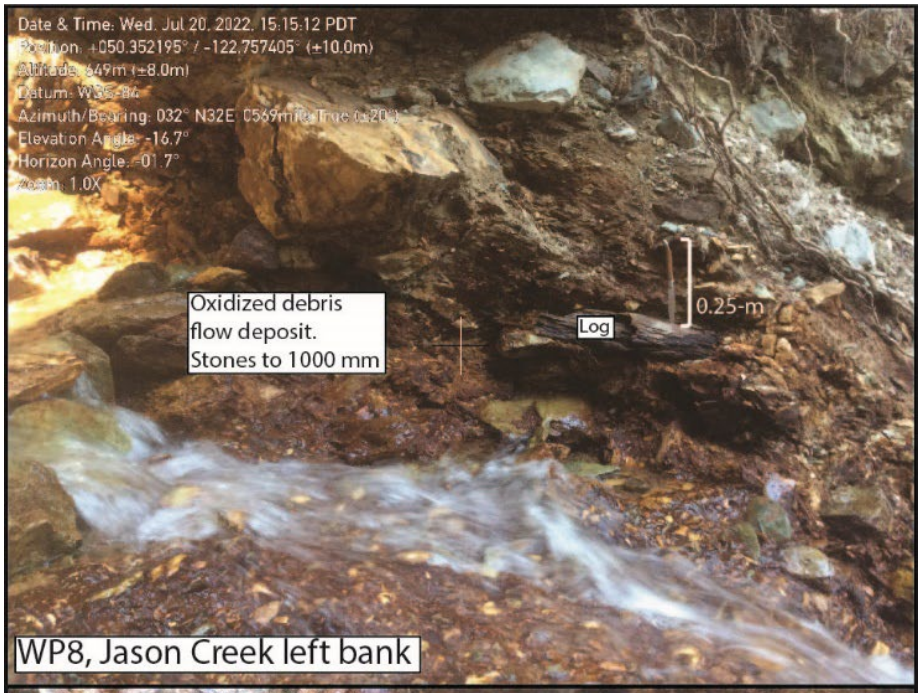

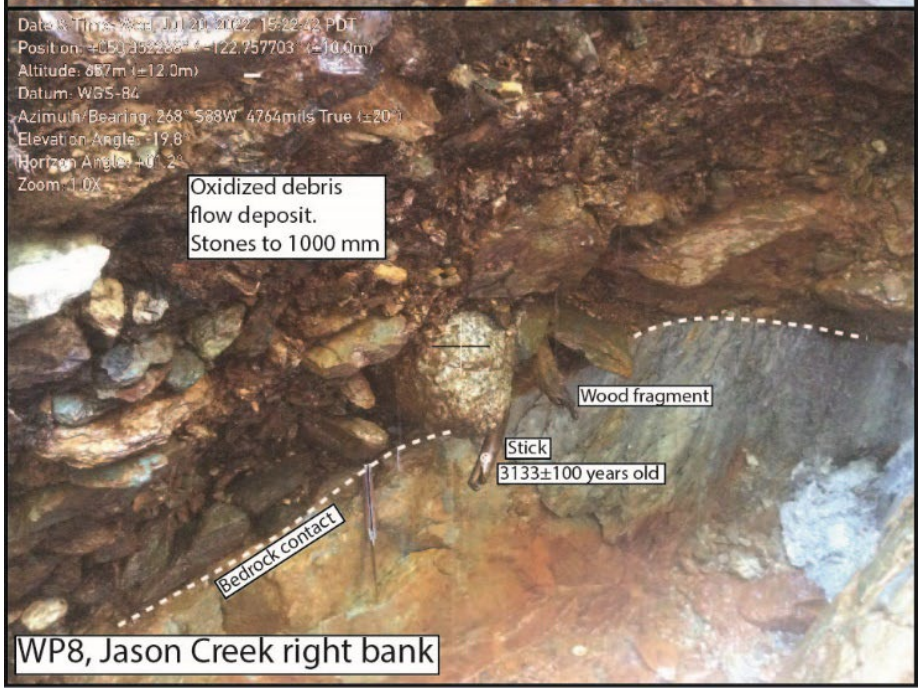

F.5. BETA ANALYTICS REPORT

Beta Analytic, Inc.
4985 SW 74th Court
Miami, FL 33155 USA
Tel: 305-667-5167
Fax: 305-663-0964
info@betalabservices.com

ISO/IEC 17025:2017-Accredited Testing Laboratory

August 22, 2022

Mr. Pierre Friele
Cordilleran Geoscience
1021 Raven Drive
P.O. Box 612
Squamish, British Columbia V8B 0A5
Canada

RE: Radiocarbon Dating Results

Dear Mr. Friele,

Enclosed are the radiocarbon dating results for 15 samples recently sent to us. As usual, the method of analysis is listed on the report with the results and calibration data is provided where applicable. The Conventional Radiocarbon Ages have all been corrected for total fractionation effects and where applicable, calibration was performed using 2020 calibration databases (cited on the graph pages).

The web directory containing the table of results and PDF download also contains pictures, a cvs spreadsheet download option and a quality assurance report containing expected vs. measured values for 3-5 working standards analyzed simultaneously with your samples.

Reported results are accredited to ISO/IEC 17025:2017 Testing Accreditation PJLA #59423 standards and all chemistry was performed here in our laboratory and counted in our own accelerators here. Since Beta is not a teaching laboratory, only graduates trained to strict protocols of the ISO/IEC 17025:2017 Testing Accreditation PJLA #59423 program participated in the analyses.

As always Conventional Radiocarbon Ages and sigmas are rounded to the nearest 10 years per the conventions of the 1977 International Radiocarbon Conference. When counting statistics produce sigmas lower than +/- 30 years, a conservative +/- 30 BP is cited for the result unless otherwise requested. The reported d13C values were measured separately in an IRMS (isotope ratio mass spectrometer). They are NOT the AMS d13C which would include fractionation effects from natural, chemistry and AMS induced sources.

When interpreting the results, please consider any communications you may have had with us regarding the samples.

Thank you for prepaying the analyses. As always, if you have any questions or would like to discuss the results, don't hesitate to contact us.

Sincerely,

Chris Patrick
Vice President of Laboratory Operations

Beta Analytic, Inc.
4985 SW 74th Court
Miami, FL 33155 USA
Tel: 305-667-5167
Fax: 305-663-0964
info@betalabservices.com

ISO/IEC 17025:2017-Accredited Testing Laboratory

REPORT OF RADIOCARBON DATING ANALYSES

Pierre Friele — Report Date: August 22, 2022

Cordilleran Geoscience — Material Received: August 03, 2022

Laboratory Number	Sample Code Number	Conventional Radiocarbon Age (BP) or Percent Modern Carbon (pMC) & Stable Isotopes	
Beta - 635072	**J-1781a-1**	**108.02 +/- 0.40 pMC**	IRMS δ13C: -25.8 o/oo

(93.2%)	**2000 - 2004 cal AD**	**(-51 - -55 cal BP)**
(2.2%)	**1956 cal AD**	**(-7 cal BP)**

Submitter Material: Woody Material
Pretreatment: (wood) acid/alkali/acid
Analyzed Material: Wood
Analysis Service: AMS-Standard delivery
Conventional Radiocarbon Age: -620 +/- 30 BP
Fraction Modern Carbon: 1.0802 +/- 0.0040
D14C: 80.24 +/- 4.03 o/oo
Δ14C: 70.87 +/- 4.03 o/oo (1950:2022)
Raw pMC: (without d13C correction): 107.85 +/- 0.40 pMC
Calibration: BetaCal4.20: HPD method: INTCAL13 + NHZ1

Results are ISO/IEC-17025:2017 accredited. No sub-contracting or student labor was used in the analyses. All work was done at Beta in 4 in-house NEC accelerator mass spectrometers and 4 Thermo IRMSs. The "Conventional Radiocarbon Age" was calculated using the Libby half-life (5568 years), is corrected for total isotopic fraction and was used for calendar calibration where applicable. The Age is rounded to the nearest 10 years and is reported as radiocarbon years before present (BP), "present" = AD 1950. Results greater than the modern reference are reported as percent modern carbon (pMC). The modern reference standard was 95% the 14C signature of NIST SRM-4990C (oxalic acid). Quoted errors are 1 sigma counting statistics. Calculated sigmas less than 30 BP on the Conventional Radiocarbon Age are conservatively rounded up to 30. d13C values are on the material itself (not the AMS d13C). d13C and d15N values are relative to VPDB. References for calendar calibrations are cited at the bottom of calibration graph pages.

Beta Analytic, Inc.
4985 SW 74th Court
Miami, FL 33155 USA
Tel: 305-667-5167
Fax: 305-663-0964
info@betalabservices.com

ISO/IEC 17025:2017-Accredited Testing Laboratory

REPORT OF RADIOCARBON DATING ANALYSES

Pierre Friele

Cordilleran Geoscience

Report Date: August 22, 2022

Material Received: August 03, 2022

Laboratory Number	Sample Code Number	Conventional Radiocarbon Age (BP) or Percent Modern Carbon (pMC) & Stable Isotopes	
Beta - 635073	**J-1794a-1**	**9080 +/- 30 BP**	IRMS δ13C: -23.6 o/oo

(93.7%) 8311 - 8240 cal BC (10260 - 10189 cal BP)
(1.7%) 8332 - 8319 cal BC (10281 - 10268 cal BP)

Submitter Material: Charcoal
Pretreatment: (charred material) acid/alkali/acid
Analyzed Material: Charred material
Analysis Service: AMS-Standard delivery
Percent Modern Carbon: 32.29 +/- 0.12 pMC
Fraction Modern Carbon: 0.3229 +/- 0.0012
D14C: -677.08 +/- 1.21 o/oo
Δ14C: -679.88 +/- 1.21 o/oo (1950:2022)
Measured Radiocarbon Age: (without d13C correction): 9060 +/- 30 BP
Calibration: BetaCal4.20: HPD method: INTCAL20

Results are ISO/IEC-17025:2017 accredited. No sub-contracting or student labor was used in the analyses. All work was done at Beta in 4 in-house NEC accelerator mass spectrometers and 4 Thermo IRMSs. The "Conventional Radiocarbon Age" was calculated using the Libby half-life (5568 years), is corrected for total isotopic fraction and was used for calendar calibration where applicable. The Age is rounded to the nearest 10 years and is reported as radiocarbon years before present (BP), "present" = AD 1950. Results greater than the modern reference are reported as percent modern carbon (pMC). The modern reference standard was 95% the 14C signature of NIST SRM-4990C (oxalic acid). Quoted errors are 1 sigma counting statistics. Calculated sigmas less than 30 BP on the Conventional Radiocarbon Age are conservatively rounded up to 30. d13C values are on the material itself (not the AMS d13C). d13C and d15N values are relative to VPDB. References for calendar calibrations are cited at the bottom of calibration graph pages.

Beta Analytic, Inc.
4985 SW 74th Court
Miami, FL 33155 USA
Tel: 305-667-5167
Fax: 305-663-0964
info@betalabservices.com

ISO/IEC 17025:2017-Accredited Testing Laboratory

REPORT OF RADIOCARBON DATING ANALYSES

Pierre Friele — Report Date: August 22, 2022

Cordilleran Geoscience — Material Received: August 03, 2022

Laboratory Number	Sample Code Number	Conventional Radiocarbon Age (BP) or Percent Modern Carbon (pMC) & Stable Isotopes	
Beta - 635074	**J-1794b-1**	**1230 +/- 30 BP**	IRMS δ13C: -24.5 o/oo
(67.1%)	**771 - 884 cal AD**	**(1179 - 1066 cal BP)**	
(27.5%)	**682 - 744 cal AD**	**(1268 - 1206 cal BP)**	
(0.8%)	**762 - 766 cal AD**	**(1188 - 1184 cal BP)**	

Submitter Material: Charcoal
Pretreatment: (charred material) acid/alkali/acid
Analyzed Material: Charred material
Analysis Service: AMS-Standard delivery
Percent Modern Carbon: 85.80 +/- 0.32 pMC
Fraction Modern Carbon: 0.8580 +/- 0.0032
D14C: -141.97 +/- 3.20 o/oo
Δ14C: -149.41 +/- 3.20 o/oo (1950:2022)
Measured Radiocarbon Age: (without d13C correction): 1220 +/- 30 BP
Calibration: BetaCal4.20: HPD method: INTCAL20

Results are ISO/IEC-17025:2017 accredited. No sub-contracting or student labor was used in the analyses. All work was done at Beta in 4 in-house NEC accelerator mass spectrometers and 4 Thermo IRMSs. The "Conventional Radiocarbon Age" was calculated using the Libby half-life (5568 years), is corrected for total isotopic fraction and was used for calendar calibration where applicable. The Age is rounded to the nearest 10 years and is reported as radiocarbon years before present (BP), "present" = AD 1950. Results greater than the modern reference are reported as percent modern carbon (pMC). The modern reference standard was 95% the 14C signature of NIST SRM-4990C (oxalic acid). Quoted errors are 1 sigma counting statistics. Calculated sigmas less than 30 BP on the Conventional Radiocarbon Age are conservatively rounded up to 30. d13C values are on the material itself (not the AMS d13C). d13C and d15N values are relative to VPDB. References for calendar calibrations are cited at the bottom of calibration graph pages.

Beta Analytic, Inc.
4985 SW 74th Court
Miami, FL 33155 USA
Tel: 305-667-5167
Fax: 305-663-0964
info@betalabservices.com

ISO/IEC 17025:2017-Accredited Testing Laboratory

REPORT OF RADIOCARBON DATING ANALYSES

Pierre Friele

Cordilleran Geoscience

Report Date: August 22, 2022

Material Received: August 03, 2022

Laboratory Number	Sample Code Number	Conventional Radiocarbon Age (BP) or Percent Modern Carbon (pMC) & Stable Isotopes	
Beta - 635075	**J-1794b-2**	**1710 +/- 30 BP**	IRMS δ13C: -22.9 o/oo

(71.6%)	**320 - 415 cal AD**	**(1630 - 1535 cal BP)**
(23.8%)	**252 - 291 cal AD**	**(1698 - 1659 cal BP)**

Submitter Material: Charcoal
Pretreatment: (charred material) acid/alkali/acid
Analyzed Material: Charred material
Analysis Service: AMS-Standard delivery
Percent Modern Carbon: 80.83 +/- 0.30 pMC
Fraction Modern Carbon: 0.8083 +/- 0.0030
D14C: -191.74 +/- 3.02 o/oo
Δ14C: -198.75 +/- 3.02 o/oo (1950:2022)
Measured Radiocarbon Age: (without d13C correction): 1670 +/- 30 BP
Calibration: BetaCal4.20: HPD method: INTCAL20

Results are ISO/IEC-17025:2017 accredited. No sub-contracting or student labor was used in the analyses. All work was done at Beta in 4 in-house NEC accelerator mass spectrometers and 4 Thermo IRMSs. The "Conventional Radiocarbon Age" was calculated using the Libby half-life (5568 years), is corrected for total isotopic fraction and was used for calendar calibration where applicable. The Age is rounded to the nearest 10 years and is reported as radiocarbon years before present (BP), "present" = AD 1950. Results greater than the modern reference are reported as percent modern carbon (pMC). The modern reference standard was 95% the 14C signature of NIST SRM-4990C (oxalic acid). Quoted errors are 1 sigma counting statistics. Calculated sigmas less than 30 BP on the Conventional Radiocarbon Age are conservatively rounded up to 30. d13C values are on the material itself (not the AMS d13C). d13C and d15N values are relative to VPDB. References for calendar calibrations are cited at the bottom of calibration graph pages.

Beta Analytic, Inc.
4985 SW 74th Court
Miami, FL 33155 USA
Tel: 305-667-5167
Fax: 305-663-0964
info@betalabservices.com

ISO/IEC 17025:2017-Accredited Testing Laboratory

REPORT OF RADIOCARBON DATING ANALYSES

Pierre Friele

Cordilleran Geoscience

Report Date: August 22, 2022

Material Received: August 03, 2022

Laboratory Number	Sample Code Number	Conventional Radiocarbon Age (BP) or Percent Modern Carbon (pMC) & Stable Isotopes	
Beta - 635076	**J-1794c-1**	**2020 +/- 30 BP**	IRMS δ13C: -24.9 o/oo

(89.5%)	**58 cal BC - 78 cal AD**	**(2007 - 1872 cal BP)**
(5.3%)	**98 - 71 cal BC**	**(2047 - 2020 cal BP)**
(0.5%)	**102 - 106 cal AD**	**(1848 - 1844 cal BP)**

Submitter Material: Charcoal
Pretreatment: (organic sediment) acid washes
Analyzed Material: Organic sediment
Analysis Service: AMS-Standard delivery
Percent Modern Carbon: 77.77 +/- 0.29 pMC
Fraction Modern Carbon: 0.7777 +/- 0.0029
D14C: -222.34 +/- 2.90 o/oo
Δ14C: -229.08 +/- 2.90 o/oo (1950:2022)
Measured Radiocarbon Age: (without d13C correction): 2020 +/- 30 BP
Calibration: BetaCal4.20: HPD method: INTCAL20

Results are ISO/IEC-17025:2017 accredited. No sub-contracting or student labor was used in the analyses. All work was done at Beta in 4 in-house NEC accelerator mass spectrometers and 4 Thermo IRMSs. The "Conventional Radiocarbon Age" was calculated using the Libby half-life (5568 years), is corrected for total isotopic fraction and was used for calendar calibration where applicable. The Age is rounded to the nearest 10 years and is reported as radiocarbon years before present (BP), "present" = AD 1950. Results greater than the modern reference are reported as percent modern carbon (pMC). The modern reference standard was 95% the 14C signature of NIST SRM-4990C (oxalic acid). Quoted errors are 1 sigma counting statistics. Calculated sigmas less than 30 BP on the Conventional Radiocarbon Age are conservatively rounded up to 30. d13C values are on the material itself (not the AMS d13C). d13C and d15N values are relative to VPDB. References for calendar calibrations are cited at the bottom of calibration graph pages.

Beta Analytic, Inc.
4985 SW 74th Court
Miami, FL 33155 USA
Tel: 305-667-5167
Fax: 305-663-0964
info@betalabservices.com

ISO/IEC 17025:2017-Accredited Testing Laboratory

REPORT OF RADIOCARBON DATING ANALYSES

Pierre Friele

Cordilleran Geoscience

Report Date: August 22, 2022

Material Received: August 03, 2022

Laboratory Number	Sample Code Number	Conventional Radiocarbon Age (BP) or Percent Modern Carbon (pMC) & Stable Isotopes	
Beta - 635077	**J-1791-1**	**3240 +/- 30 BP**	IRMS δ13C: -24.0 o/oo

(91.0%) 1545 - 1433 cal BC (3494 - 3382 cal BP)
(4.4%) 1607 - 1582 cal BC (3556 - 3531 cal BP)

Submitter Material: Charcoal
Pretreatment: (charred material) acid/alkali/acid
Analyzed Material: Charred material
Analysis Service: AMS-Standard delivery
Percent Modern Carbon: 66.81 +/- 0.25 pMC
Fraction Modern Carbon: 0.6681 +/- 0.0025
D14C: -331.92 +/- 2.50 o/oo
Δ14C: -337.71 +/- 2.50 o/oo (1950:2022)
Measured Radiocarbon Age: (without d13C correction): 3220 +/- 30 BP
Calibration: BetaCal4.20: HPD method: INTCAL20

Results are ISO/IEC-17025:2017 accredited. No sub-contracting or student labor was used in the analyses. All work was done at Beta in 4 in-house NEC accelerator mass spectrometers and 4 Thermo IRMSs. The "Conventional Radiocarbon Age" was calculated using the Libby half-life (5568 years), is corrected for total isotopic fraction and was used for calendar calibration where applicable. The Age is rounded to the nearest 10 years and is reported as radiocarbon years before present (BP), "present" = AD 1950. Results greater than the modern reference are reported as percent modern carbon (pMC). The modern reference standard was 95% the 14C signature of NIST SRM-4990C (oxalic acid). Quoted errors are 1 sigma counting statistics. Calculated sigmas less than 30 BP on the Conventional Radiocarbon Age are conservatively rounded up to 30. d13C values are on the material itself (not the AMS d13C). d13C and d15N values are relative to VPDB. References for calendar calibrations are cited at the bottom of calibration graph pages.

Beta Analytic, Inc.
4985 SW 74th Court
Miami, FL 33155 USA
Tel: 305-667-5167
Fax: 305-663-0964
info@betalabservices.com

ISO/IEC 17025:2017-Accredited Testing Laboratory

REPORT OF RADIOCARBON DATING ANALYSES

Pierre Friele

Cordilleran Geoscience

Report Date: August 22, 2022

Material Received: August 03, 2022

Laboratory Number	Sample Code Number	Conventional Radiocarbon Age (BP) or Percent Modern Carbon (pMC) & Stable Isotopes	
Beta - 635078	**J-1782-2**	**1860 +/- 30 BP**	IRMS δ13C: -25.4 o/oo

(94.4%)	**118 - 244 cal AD**	**(1832 - 1706 cal BP)**
(1.0%)	**86 - 93 cal AD**	**(1864 - 1857 cal BP)**

Submitter Material: Charcoal
Pretreatment: (charred material) acid/alkali/acid
Analyzed Material: Charred material
Analysis Service: AMS-Standard delivery
Percent Modern Carbon: 79.33 +/- 0.30 pMC
Fraction Modern Carbon: 0.7933 +/- 0.0030
D14C: -206.69 +/- 2.96 o/oo
Δ14C: -213.57 +/- 2.96 o/oo (1950:2022)
Measured Radiocarbon Age: (without d13C correction): 1870 +/- 30 BP
Calibration: BetaCal4.20: HPD method: INTCAL20

Results are ISO/IEC-17025:2017 accredited. No sub-contracting or student labor was used in the analyses. All work was done at Beta in 4 in-house NEC accelerator mass spectrometers and 4 Thermo IRMSs. The "Conventional Radiocarbon Age" was calculated using the Libby half-life (5568 years), is corrected for total isotopic fraction and was used for calendar calibration where applicable. The Age is rounded to the nearest 10 years and is reported as radiocarbon years before present (BP), "present" = AD 1950. Results greater than the modern reference are reported as percent modern carbon (pMC). The modern reference standard was 95% the 14C signature of NIST SRM-4990C (oxalic acid). Quoted errors are 1 sigma counting statistics. Calculated sigmas less than 30 BP on the Conventional Radiocarbon Age are conservatively rounded up to 30. d13C values are on the material itself (not the AMS d13C). d13C and d15N values are relative to VPDB. References for calendar calibrations are cited at the bottom of calibration graph pages.

Beta Analytic, Inc.
4985 SW 74th Court
Miami, FL 33155 USA
Tel: 305-667-5167
Fax: 305-663-0964
info@betalabservices.com

ISO/IEC 17025:2017-Accredited Testing Laboratory

REPORT OF RADIOCARBON DATING ANALYSES

Pierre Friele

Cordilleran Geoscience

Report Date: August 22, 2022

Material Received: August 03, 2022

Laboratory Number	Sample Code Number	Conventional Radiocarbon Age (BP) or Percent Modern Carbon (pMC) & Stable Isotopes	
Beta - 635079	**J-1782-1**	**3080 +/- 30 BP**	IRMS δ13C: -23.1 o/oo

(95.4%) 1422 - 1263 cal BC (3371 - 3212 cal BP)

Submitter Material: Charcoal
Pretreatment: (charred material) acid/alkali/acid
Analyzed Material: Charred material
Analysis Service: AMS-Standard delivery
Percent Modern Carbon: 68.15 +/- 0.25 pMC
Fraction Modern Carbon: 0.6815 +/- 0.0025
D14C: -318.47 +/- 2.55 o/oo
Δ14C: -324.38 +/- 2.55 o/oo (1950:2022)
Measured Radiocarbon Age: (without d13C correction): 3050 +/- 30 BP
Calibration: BetaCal4.20: HPD method: INTCAL20

Results are ISO/IEC-17025:2017 accredited. No sub-contracting or student labor was used in the analyses. All work was done at Beta in 4 in-house NEC accelerator mass spectrometers and 4 Thermo IRMSs. The "Conventional Radiocarbon Age" was calculated using the Libby half-life (5568 years), is corrected for total isotopic fraction and was used for calendar calibration where applicable. The Age is rounded to the nearest 10 years and is reported as radiocarbon years before present (BP), "present" = AD 1950. Results greater than the modern reference are reported as percent modern carbon (pMC). The modern reference standard was 95% the 14C signature of NIST SRM-4990C (oxalic acid). Quoted errors are 1 sigma counting statistics. Calculated sigmas less than 30 BP on the Conventional Radiocarbon Age are conservatively rounded up to 30. d13C values are on the material itself (not the AMS d13C). d13C and d15N values are relative to VPDB. References for calendar calibrations are cited at the bottom of calibration graph pages.

Beta Analytic, Inc.
4985 SW 74th Court
Miami, FL 33155 USA
Tel: 305-667-5167
Fax: 305-663-0964
info@betalabservices.com

ISO/IEC 17025:2017-Accredited Testing Laboratory

REPORT OF RADIOCARBON DATING ANALYSES

Pierre Friele — Report Date: August 22, 2022

Cordilleran Geoscience — Material Received: August 03, 2022

Laboratory Number	Sample Code Number	Conventional Radiocarbon Age (BP) or Percent Modern Carbon (pMC) & Stable Isotopes	
Beta - 635080	**J-1770a-1**	**260 +/- 30 BP**	IRMS δ13C: -23.6 o/oo
(51.5%)	**1620 - 1674 cal AD**	**(330 - 276 cal BP)**	
(28.7%)	**1516 - 1590 cal AD**	**(434 - 360 cal BP)**	
(13.6%)	**1766 - 1800 cal AD**	**(184 - 150 cal BP)**	
(1.6%)	**1942 - Post AD 1950**	**(8 - Post BP 0)**	

Submitter Material: Charcoal
Pretreatment: (charred material) acid/alkali/acid
Analyzed Material: Charred material
Analysis Service: AMS-Standard delivery
Percent Modern Carbon: 96.82 +/- 0.36 pMC
Fraction Modern Carbon: 0.9682 +/- 0.0036
D14C: -31.85 +/- 3.62 o/oo
Δ14C: -40.24 +/- 3.62 o/oo (1950:2022)
Measured Radiocarbon Age: (without d13C correction): 240 +/- 30 BP
Calibration: BetaCal4.20: HPD method: INTCAL20

Results are ISO/IEC-17025:2017 accredited. No sub-contracting or student labor was used in the analyses. All work was done at Beta in 4 in-house NEC accelerator mass spectrometers and 4 Thermo IRMSs. The "Conventional Radiocarbon Age" was calculated using the Libby half-life (5568 years), is corrected for total isotopic fraction and was used for calendar calibration where applicable. The Age is rounded to the nearest 10 years and is reported as radiocarbon years before present (BP), "present" = AD 1950. Results greater than the modern reference are reported as percent modern carbon (pMC). The modern reference standard was 95% the 14C signature of NIST SRM-4990C (oxalic acid). Quoted errors are 1 sigma counting statistics. Calculated sigmas less than 30 BP on the Conventional Radiocarbon Age are conservatively rounded up to 30. d13C values are on the material itself (not the AMS d13C). d13C and d15N values are relative to VPDB. References for calendar calibrations are cited at the bottom of calibration graph pages.

Beta Analytic, Inc.
4985 SW 74th Court
Miami, FL 33155 USA
Tel: 305-667-5167
Fax: 305-663-0964
info@betalabservices.com

ISO/IEC 17025:2017-Accredited Testing Laboratory

REPORT OF RADIOCARBON DATING ANALYSES

Pierre Friele

Cordilleran Geoscience

Report Date: August 22, 2022

Material Received: August 03, 2022

Laboratory Number	Sample Code Number	Conventional Radiocarbon Age (BP) or Percent Modern Carbon (pMC) & Stable Isotopes	
Beta - 635081	**M-1723-1**	**1330 +/- 30 BP**	IRMS δ13C: -22.5 o/oo

(57.1%)	**649 - 708 cal AD**	**(1301 - 1242 cal BP)**
(38.3%)	**728 - 774 cal AD**	**(1222 - 1176 cal BP)**

Submitter Material: Charcoal
Pretreatment: (organic sediment) acid washes
Analyzed Material: Organic sediment
Analysis Service: AMS-Standard delivery
Percent Modern Carbon: 84.74 +/- 0.32 pMC
Fraction Modern Carbon: 0.8474 +/- 0.0032
D14C: -152.59 +/- 3.16 o/oo
Δ14C: -159.94 +/- 3.16 o/oo (1950:2022)
Measured Radiocarbon Age: (without d13C correction): 1290 +/- 30 BP
Calibration: BetaCal4.20: HPD method: INTCAL20

Results are ISO/IEC-17025:2017 accredited. No sub-contracting or student labor was used in the analyses. All work was done at Beta in 4 in-house NEC accelerator mass spectrometers and 4 Thermo IRMSs. The "Conventional Radiocarbon Age" was calculated using the Libby half-life (5568 years), is corrected for total isotopic fraction and was used for calendar calibration where applicable. The Age is rounded to the nearest 10 years and is reported as radiocarbon years before present (BP), "present" = AD 1950. Results greater than the modern reference are reported as percent modern carbon (pMC). The modern reference standard was 95% the 14C signature of NIST SRM-4990C (oxalic acid). Quoted errors are 1 sigma counting statistics. Calculated sigmas less than 30 BP on the Conventional Radiocarbon Age are conservatively rounded up to 30. d13C values are on the material itself (not the AMS d13C). d13C and d15N values are relative to VPDB. References for calendar calibrations are cited at the bottom of calibration graph pages.

Beta Analytic, Inc.
4985 SW 74th Court
Miami, FL 33155 USA
Tel: 305-667-5167
Fax: 305-663-0964
info@betalabservices.com

ISO/IEC 17025:2017-Accredited Testing Laboratory

REPORT OF RADIOCARBON DATING ANALYSES

Pierre Friele

Cordilleran Geoscience

Report Date: August 22, 2022

Material Received: August 03, 2022

Laboratory Number	Sample Code Number	Conventional Radiocarbon Age (BP) or Percent Modern Carbon (pMC) & Stable Isotopes	
Beta - 635082	**M-1720-1**	**1870 +/- 30 BP**	IRMS δ13C: -25.2 o/oo
(92.8%)	**116 - 239 cal AD**	**(1834 - 1711 cal BP)**	
(2.6%)	**84 - 96 cal AD**	**(1866 - 1854 cal BP)**	

Submitter Material: Charcoal
Pretreatment: (charred material) acid/alkali/acid
Analyzed Material: Charred material
Analysis Service: AMS-Standard delivery
Percent Modern Carbon: 79.23 +/- 0.30 pMC
Fraction Modern Carbon: 0.7923 +/- 0.0030
D14C: -207.68 +/- 2.96 o/oo
Δ14C: -214.55 +/- 2.96 o/oo (1950:2022)
Measured Radiocarbon Age: (without d13C correction): 1870 +/- 30 BP
Calibration: BetaCal4.20: HPD method: INTCAL20

Results are ISO/IEC-17025:2017 accredited. No sub-contracting or student labor was used in the analyses. All work was done at Beta in 4 in-house NEC accelerator mass spectrometers and 4 Thermo IRMSs. The "Conventional Radiocarbon Age" was calculated using the Libby half-life (5568 years), is corrected for total isotopic fraction and was used for calendar calibration where applicable. The Age is rounded to the nearest 10 years and is reported as radiocarbon years before present (BP), "present" = AD 1950. Results greater than the modern reference are reported as percent modern carbon (pMC). The modern reference standard was 95% the 14C signature of NIST SRM-4990C (oxalic acid). Quoted errors are 1 sigma counting statistics. Calculated sigmas less than 30 BP on the Conventional Radiocarbon Age are conservatively rounded up to 30. d13C values are on the material itself (not the AMS d13C). d13C and d15N values are relative to VPDB. References for calendar calibrations are cited at the bottom of calibration graph pages.

Beta Analytic, Inc.
4985 SW 74th Court
Miami, FL 33155 USA
Tel: 305-667-5167
Fax: 305-663-0964
info@betalabservices.com

ISO/IEC 17025:2017-Accredited Testing Laboratory

REPORT OF RADIOCARBON DATING ANALYSES

Pierre Friele — Report Date: August 22, 2022

Cordilleran Geoscience — Material Received: August 03, 2022

Laboratory Number	Sample Code Number	Conventional Radiocarbon Age (BP) or Percent Modern Carbon (pMC) & Stable Isotopes	
Beta - 635083	**J-1770c-1**	**190 +/- 30 BP**	IRMS δ13C: -24.6 o/oo
(52.0%)	**1724 - 1812 cal AD**	**(226 - 138 cal BP)**	
(21.8%)	**1648 - 1695 cal AD**	**(302 - 255 cal BP)**	
(17.8%)	**1916 - Post AD 1950**	**(34 - Post BP 0)**	
(3.8%)	**1838 - 1878 cal AD**	**(112 - 72 cal BP)**	

Submitter Material: Charcoal
Pretreatment: (charred material) acid/alkali/acid
Analyzed Material: Charred material
Analysis Service: AMS-Standard delivery
Percent Modern Carbon: 97.66 +/- 0.36 pMC
Fraction Modern Carbon: 0.9766 +/- 0.0036
D14C: -23.38 +/- 3.65 o/oo
Δ14C: -31.84 +/- 3.65 o/oo (1950:2022)
Measured Radiocarbon Age: (without d13C correction): 180 +/- 30 BP
Calibration: BetaCal4.20: HPD method: INTCAL20

Results are ISO/IEC-17025:2017 accredited. No sub-contracting or student labor was used in the analyses. All work was done at Beta in 4 in-house NEC accelerator mass spectrometers and 4 Thermo IRMSs. The "Conventional Radiocarbon Age" was calculated using the Libby half-life (5568 years), is corrected for total isotopic fraction and was used for calendar calibration where applicable. The Age is rounded to the nearest 10 years and is reported as radiocarbon years before present (BP), "present" = AD 1950. Results greater than the modern reference are reported as percent modern carbon (pMC). The modern reference standard was 95% the 14C signature of NIST SRM-4990C (oxalic acid). Quoted errors are 1 sigma counting statistics. Calculated sigmas less than 30 BP on the Conventional Radiocarbon Age are conservatively rounded up to 30. d13C values are on the material itself (not the AMS d13C). d13C and d15N values are relative to VPDB. References for calendar calibrations are cited at the bottom of calibration graph pages.

Beta Analytic, Inc.
4985 SW 74th Court
Miami, FL 33155 USA
Tel: 305-667-5167
Fax: 305-663-0964
info@betalabservices.com

ISO/IEC 17025:2017-Accredited Testing Laboratory

REPORT OF RADIOCARBON DATING ANALYSES

Pierre Friele

Cordilleran Geoscience

Report Date: August 22, 2022

Material Received: August 03, 2022

Laboratory Number	Sample Code Number	Conventional Radiocarbon Age (BP) or Percent Modern Carbon (pMC) & Stable Isotopes	
Beta - 635084	**J-0000-2**	**440 +/- 30 BP**	IRMS δ13C: -24.5 o/oo

(94.0%) 1420 - 1495 cal AD (530 - 455 cal BP)
(1.4%) 1601 - 1610 cal AD (349 - 340 cal BP)

Submitter Material: Charcoal
Pretreatment: (charred material) acid/alkali/acid
Analyzed Material: Charred material
Analysis Service: AMS-Standard delivery
Percent Modern Carbon: 94.67 +/- 0.35 pMC
Fraction Modern Carbon: 0.9467 +/- 0.0035
D14C: -53.30 +/- 3.54 o/oo
Δ14C: -61.51 +/- 3.54 o/oo (1950:2022)
Measured Radiocarbon Age: (without d13C correction): 430 +/- 30 BP
Calibration: BetaCal4.20: HPD method: INTCAL20

Results are ISO/IEC-17025:2017 accredited. No sub-contracting or student labor was used in the analyses. All work was done at Beta in 4 in-house NEC accelerator mass spectrometers and 4 Thermo IRMSs. The "Conventional Radiocarbon Age" was calculated using the Libby half-life (5568 years), is corrected for total isotopic fraction and was used for calendar calibration where applicable. The Age is rounded to the nearest 10 years and is reported as radiocarbon years before present (BP), "present" = AD 1950. Results greater than the modern reference are reported as percent modern carbon (pMC). The modern reference standard was 95% the 14C signature of NIST SRM-4990C (oxalic acid). Quoted errors are 1 sigma counting statistics. Calculated sigmas less than 30 BP on the Conventional Radiocarbon Age are conservatively rounded up to 30. d13C values are on the material itself (not the AMS d13C). d13C and d15N values are relative to VPDB. References for calendar calibrations are cited at the bottom of calibration graph pages.

Beta Analytic, Inc.
4985 SW 74th Court
Miami, FL 33155 USA
Tel: 305-667-5167
Fax: 305-663-0964
info@betalabservices.com

ISO/IEC 17025:2017-Accredited Testing Laboratory

REPORT OF RADIOCARBON DATING ANALYSES

Pierre Friele

Cordilleran Geoscience

Report Date: August 22, 2022

Material Received: August 03, 2022

Laboratory Number	Sample Code Number	Conventional Radiocarbon Age (BP) or Percent Modern Carbon (pMC) & Stable Isotopes	
Beta - 635085	**J-0000-1**	**3840 +/- 30 BP**	IRMS δ13C: -23.3 o/oo

(87.4%) 2410 - 2201 cal BC (4359 - 4150 cal BP)
(8.0%) 2456 - 2417 cal BC (4405 - 4366 cal BP)

Submitter Material: Charcoal
Pretreatment: (charred material) acid/alkali/acid
Analyzed Material: Charred material
Analysis Service: AMS-Standard delivery
Percent Modern Carbon: 62.00 +/- 0.23 pMC
Fraction Modern Carbon: 0.6200 +/- 0.0023
D14C: -380.00 +/- 2.32 o/oo
Δ14C: -385.37 +/- 2.32 o/oo (1950:2022)
Measured Radiocarbon Age: (without d13C correction): 3810 +/- 30 BP
Calibration: BetaCal4.20: HPD method: INTCAL20

Results are ISO/IEC-17025:2017 accredited. No sub-contracting or student labor was used in the analyses. All work was done at Beta in 4 in-house NEC accelerator mass spectrometers and 4 Thermo IRMSs. The "Conventional Radiocarbon Age" was calculated using the Libby half-life (5568 years), is corrected for total isotopic fraction and was used for calendar calibration where applicable. The Age is rounded to the nearest 10 years and is reported as radiocarbon years before present (BP), "present" = AD 1950. Results greater than the modern reference are reported as percent modern carbon (pMC). The modern reference standard was 95% the 14C signature of NIST SRM-4990C (oxalic acid). Quoted errors are 1 sigma counting statistics. Calculated sigmas less than 30 BP on the Conventional Radiocarbon Age are conservatively rounded up to 30. d13C values are on the material itself (not the AMS d13C). d13C and d15N values are relative to VPDB. References for calendar calibrations are cited at the bottom of calibration graph pages.

Beta Analytic, Inc.
4985 SW 74th Court
Miami, FL 33155 USA
Tel: 305-667-5167
Fax: 305-663-0964
info@betalabservices.com

ISO/IEC 17025:2017-Accredited Testing Laboratory

REPORT OF RADIOCARBON DATING ANALYSES

Pierre Friele

Cordilleran Geoscience

Report Date: August 22, 2022

Material Received: August 03, 2022

Laboratory Number	Sample Code Number	Conventional Radiocarbon Age (BP) or Percent Modern Carbon (pMC) & Stable Isotopes	
Beta - 635086	**J-WP8a**	**2910 +/- 30 BP**	IRMS δ13C: -24.2 o/oo
(95.4%)	**1211 - 1012 cal BC**	**(3160 - 2961 cal BP)**	

Submitter Material: Woody Material
Pretreatment: (wood) acid/alkali/acid
Analyzed Material: Wood
Analysis Service: AMS-Standard delivery
Percent Modern Carbon: 69.61 +/- 0.26 pMC
Fraction Modern Carbon: 0.6961 +/- 0.0026
D14C: -303.90 +/- 2.60 o/oo
Δ14C: -309.93 +/- 2.60 o/oo (1950:2022)
Measured Radiocarbon Age: (without d13C correction): 2900 +/- 30 BP
Calibration: BetaCal4.20: HPD method: INTCAL20

Results are ISO/IEC-17025:2017 accredited. No sub-contracting or student labor was used in the analyses. All work was done at Beta in 4 in-house NEC accelerator mass spectrometers and 4 Thermo IRMSs. The "Conventional Radiocarbon Age" was calculated using the Libby half-life (5568 years), is corrected for total isotopic fraction and was used for calendar calibration where applicable. The Age is rounded to the nearest 10 years and is reported as radiocarbon years before present (BP), "present" = AD 1950. Results greater than the modern reference are reported as percent modern carbon (pMC). The modern reference standard was 95% the 14C signature of NIST SRM-4990C (oxalic acid). Quoted errors are 1 sigma counting statistics. Calculated sigmas less than 30 BP on the Conventional Radiocarbon Age are conservatively rounded up to 30. d13C values are on the material itself (not the AMS d13C). d13C and d15N values are relative to VPDB. References for calendar calibrations are cited at the bottom of calibration graph pages.

Calibration of Radiocarbon Age to Calendar Years

(High Probability Density Range Method (HPD): INTCAL13 + NHZ1)

(Variables: d13C = -25.8 o/oo)

Laboratory number **Beta-635072**

Percent modern carbon **108.02 +/- 0.40 pMC**

95.4% probability

(93.2%)	2000 - 2004 cal AD	(-51 - -55 cal BP)
(2.2%)	1956 cal AD	(-7 cal BP)

68.2% probability

(61.4%)	2001 - 2003 cal AD	(-52 - -54 cal BP)
(6.8%)	2000 cal AD	(-51 cal BP)

J-1781a-1

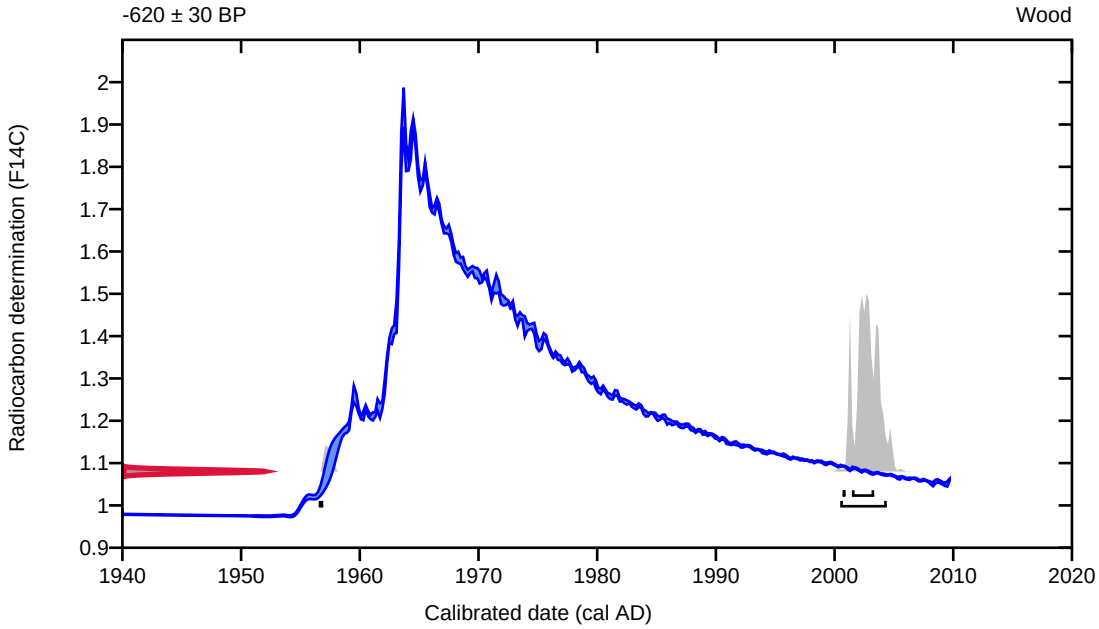

Database used

INTCAL13 + NHZ1

References

References to Probability Method

Bronk Ramsey, C. (2009). Bayesian analysis of radiocarbon dates. Radiocarbon, 51(1), 337-360.

References to Database INTCAL13 + NHZ1

Hua, et.al.,2013, Radiocarbon, 55(4). Reimer, et.al., 2013, Radiocarbon55(4).

Beta Analytic Radiocarbon Dating Laboratory

4985 S.W. 74th Court, Miami, Florida 33155 • Tel: (305)667-5167 • Fax: (305)663-0964 • Email: beta@radiocarbon.com

Calibration of Radiocarbon Age to Calendar Years

(High Probability Density Range Method (HPD): INTCAL20)

(Variables: d13C = -23.6 o/oo)

Laboratory number **Beta-635073**

Conventional radiocarbon age **9080 ± 30 BP**

95.4% probability

(93.7%)	8311 - 8240 cal BC	(10260 - 10189 cal BP)
(1.7%)	8332 - 8319 cal BC	(10281 - 10268 cal BP)

68.2% probability

(68.2%)	8298 - 8268 cal BC	(10247 - 10217 cal BP)

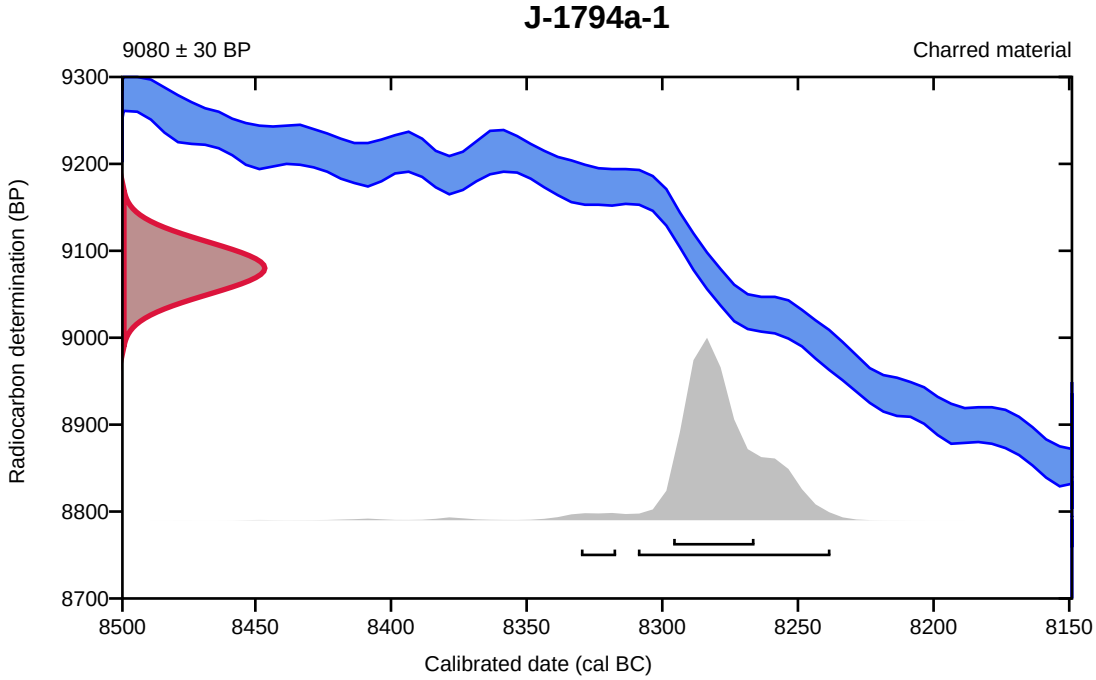

Database used

INTCAL20

References

References to Probability Method

Bronk Ramsey, C. (2009). Bayesian analysis of radiocarbon dates. Radiocarbon, 51(1), 337-360.

References to Database INTCAL20

Reimer, et al., 2020, Radiocarbon 62(4):725-757.

Beta Analytic Radiocarbon Dating Laboratory
4985 S.W. 74th Court, Miami, Florida 33155 • Tel: (305)667-5167 • Fax: (305)663-0964 • Email: beta@radiocarbon.com

Calibration of Radiocarbon Age to Calendar Years

(High Probability Density Range Method (HPD): INTCAL20)

(Variables: d13C = -24.5 o/oo)

Laboratory number **Beta-635074**

Conventional radiocarbon age **1230 ± 30 BP**

95.4% probability

(67.1%)	771 - 884 cal AD	(1179 - 1066 cal BP)
(27.5%)	682 - 744 cal AD	(1268 - 1206 cal BP)
(0.8%)	762 - 766 cal AD	(1188 - 1184 cal BP)

68.2% probability

(35.9%)	786 - 830 cal AD	(1164 - 1120 cal BP)
(17.8%)	706 - 736 cal AD	(1244 - 1214 cal BP)
(13.1%)	852 - 874 cal AD	(1098 - 1076 cal BP)
(1.4%)	774 - 776 cal AD	(1176 - 1174 cal BP)

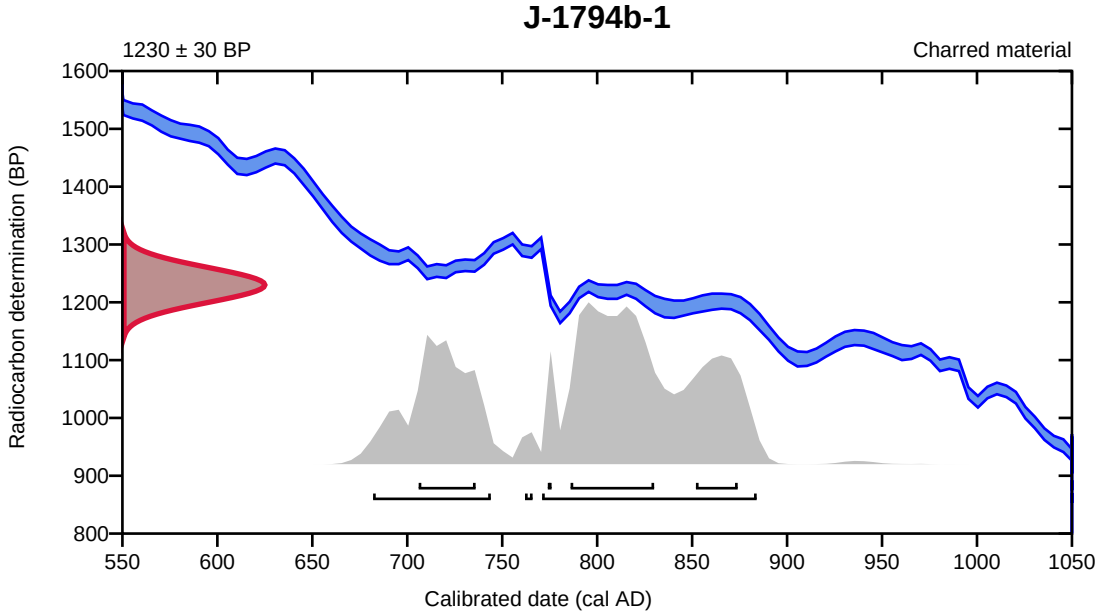

Database used

INTCAL20

References

References to Probability Method

Bronk Ramsey, C. (2009). Bayesian analysis of radiocarbon dates. Radiocarbon, 51(1), 337-360.

References to Database INTCAL20

Reimer, et al., 2020, Radiocarbon 62(4):725-757.

Calibration of Radiocarbon Age to Calendar Years

(High Probability Density Range Method (HPD): INTCAL20)

(Variables: d13C = -22.9 o/oo)

Laboratory number **Beta-635075**

Conventional radiocarbon age **1710 ± 30 BP**

95.4% probability

(71.6%)	320 - 415 cal AD	(1630 - 1535 cal BP)
(23.8%)	252 - 291 cal AD	(1698 - 1659 cal BP)

68.2% probability

(55.4%)	340 - 402 cal AD	(1610 - 1548 cal BP)
(12.8%)	262 - 276 cal AD	(1688 - 1674 cal BP)

J-1794b-2

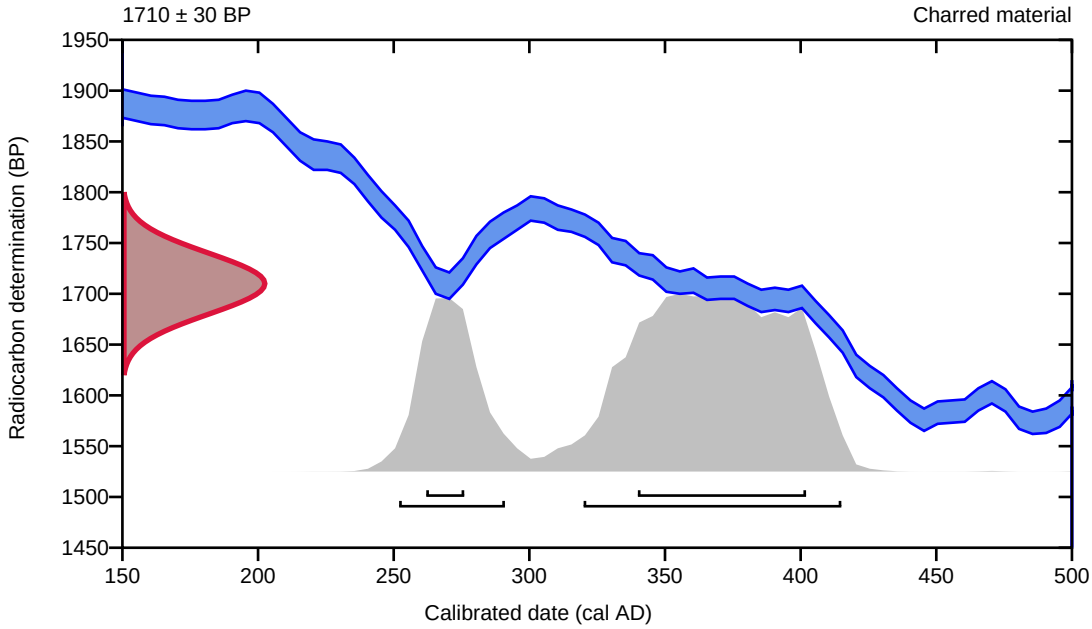

Database used

INTCAL20

References

References to Probability Method

Bronk Ramsey, C. (2009). Bayesian analysis of radiocarbon dates. Radiocarbon, 51(1), 337-360.

References to Database INTCAL20

Reimer, et al., 2020, Radiocarbon 62(4):725-757.

Calibration of Radiocarbon Age to Calendar Years

(High Probability Density Range Method (HPD): INTCAL20)

(Variables: d13C = -24.9 o/oo)

Laboratory number **Beta-635076**

Conventional radiocarbon age **2020 ± 30 BP**

95.4% probability

(89.5%)	58 cal BC - 78 cal AD	(2007 - 1872 cal BP)
(5.3%)	98 - 71 cal BC	(2047 - 2020 cal BP)
(0.5%)	102 - 106 cal AD	(1848 - 1844 cal BP)

68.2% probability

(68.2%)	48 cal BC - 25 cal AD	(1997 - 1925 cal BP)

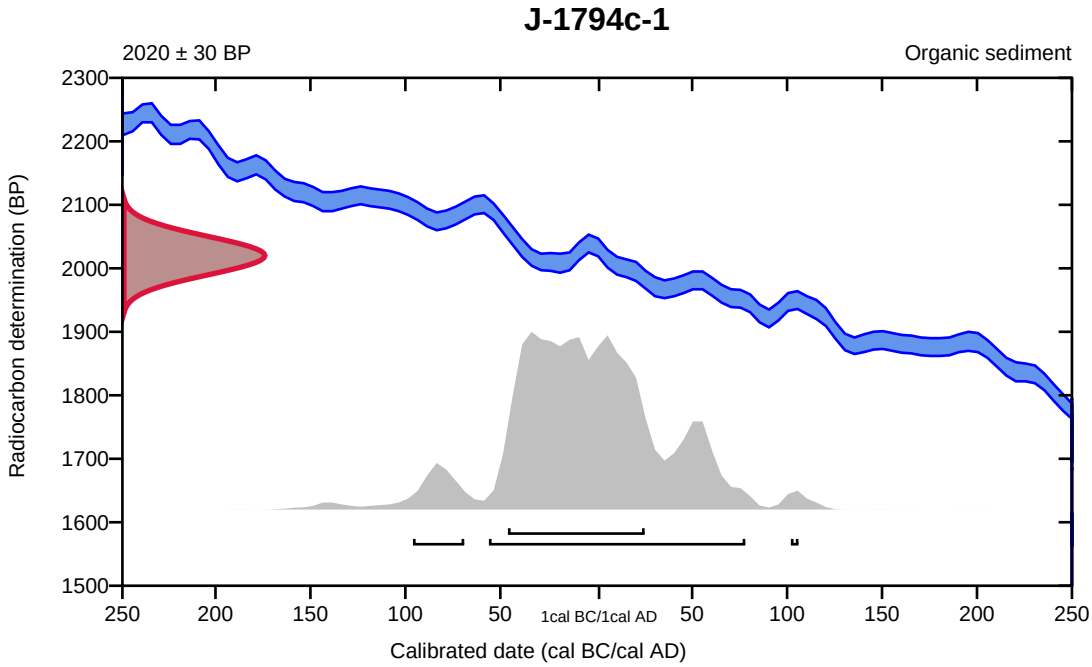

Database used

INTCAL20

References

References to Probability Method

Bronk Ramsey, C. (2009). Bayesian analysis of radiocarbon dates. Radiocarbon, 51(1), 337-360.

References to Database INTCAL20

Reimer, et al., 2020, Radiocarbon 62(4):725-757.

Calibration of Radiocarbon Age to Calendar Years

(High Probability Density Range Method (HPD): INTCAL20)

(Variables: d13C = -24.0 o/oo)

Laboratory number **Beta-635077**

Conventional radiocarbon age **3240 ± 30 BP**

95.4% probability

(91%)	1545 - 1433 cal BC	(3494 - 3382 cal BP)
(4.4%)	1607 - 1582 cal BC	(3556 - 3531 cal BP)

68.2% probability

(42.4%)	1533 - 1494 cal BC	(3482 - 3443 cal BP)
(25.8%)	1480 - 1453 cal BC	(3429 - 3402 cal BP)

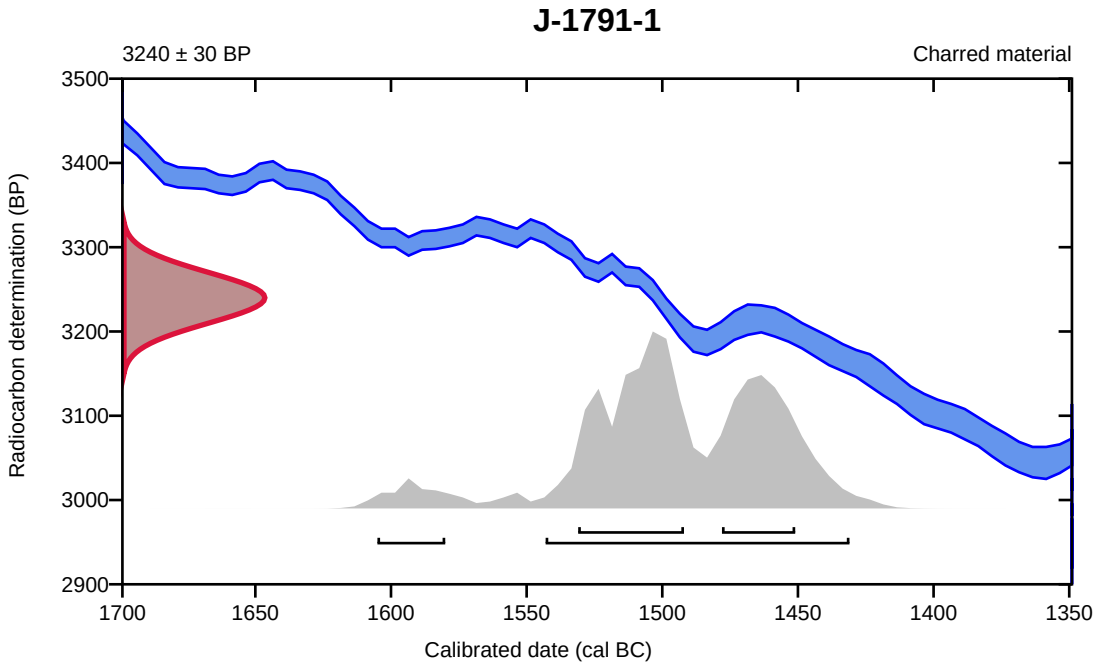

Database used

INTCAL20

References

References to Probability Method

Bronk Ramsey, C. (2009). Bayesian analysis of radiocarbon dates. Radiocarbon, 51(1), 337-360.

References to Database INTCAL20

Reimer, et al., 2020, Radiocarbon 62(4):725-757.

Beta Analytic Radiocarbon Dating Laboratory
4985 S.W. 74th Court, Miami, Florida 33155 • Tel: (305)667-5167 • Fax: (305)663-0964 • Email: beta@radiocarbon.com

Calibration of Radiocarbon Age to Calendar Years

(High Probability Density Range Method (HPD): INTCAL20)

(Variables: d13C = -25.4 o/oo)

Laboratory number **Beta-635078**

Conventional radiocarbon age **1860 ± 30 BP**

95.4% probability

(94.4%)	118 - 244 cal AD	(1832 - 1706 cal BP)
(1%)	86 - 93 cal AD	(1864 - 1857 cal BP)

68.2% probability

(33.5%)	155 - 193 cal AD	(1795 - 1757 cal BP)
(24%)	198 - 225 cal AD	(1752 - 1725 cal BP)
(10.7%)	130 - 142 cal AD	(1820 - 1808 cal BP)

J-1782-2

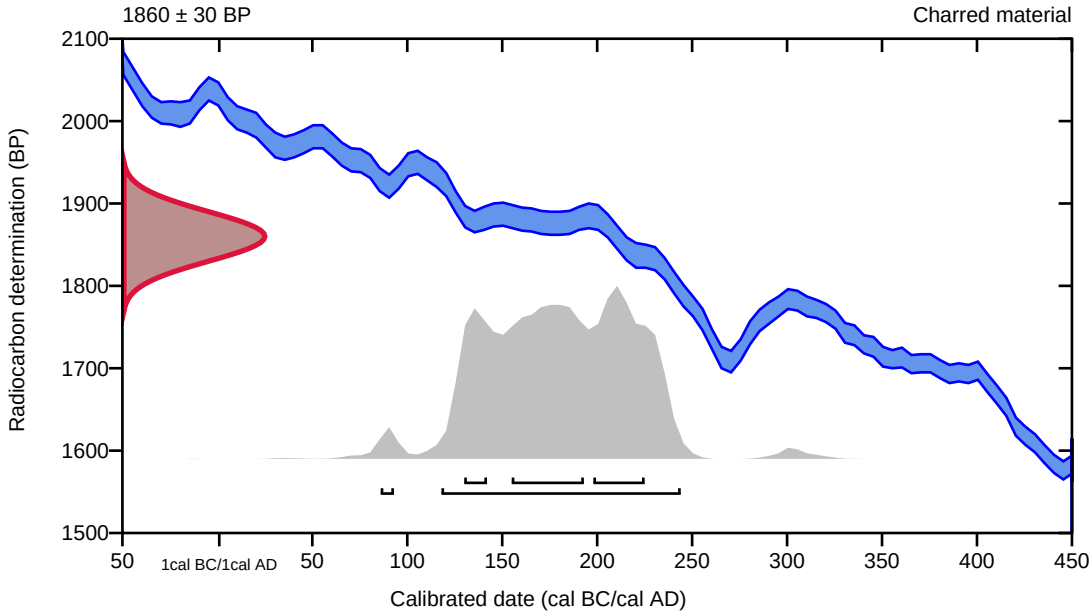

Database used

INTCAL20

References

References to Probability Method

Bronk Ramsey, C. (2009). Bayesian analysis of radiocarbon dates. Radiocarbon, 51(1), 337-360.

References to Database INTCAL20

Reimer, et al., 2020, Radiocarbon 62(4):725-757.

BetaCal 4.20

Calibration of Radiocarbon Age to Calendar Years

(High Probability Density Range Method (HPD): INTCAL20)

(Variables: d13C = -23.1 o/oo)

Laboratory number **Beta-635079**

Conventional radiocarbon age **3080 ± 30 BP**

95.4% probability

(95.4%)	1422 - 1263 cal BC	(3371 - 3212 cal BP)

68.2% probability

(43.3%)	1355 - 1297 cal BC	(3304 - 3246 cal BP)
(24.9%)	1407 - 1371 cal BC	(3356 - 3320 cal BP)

J-1782-1

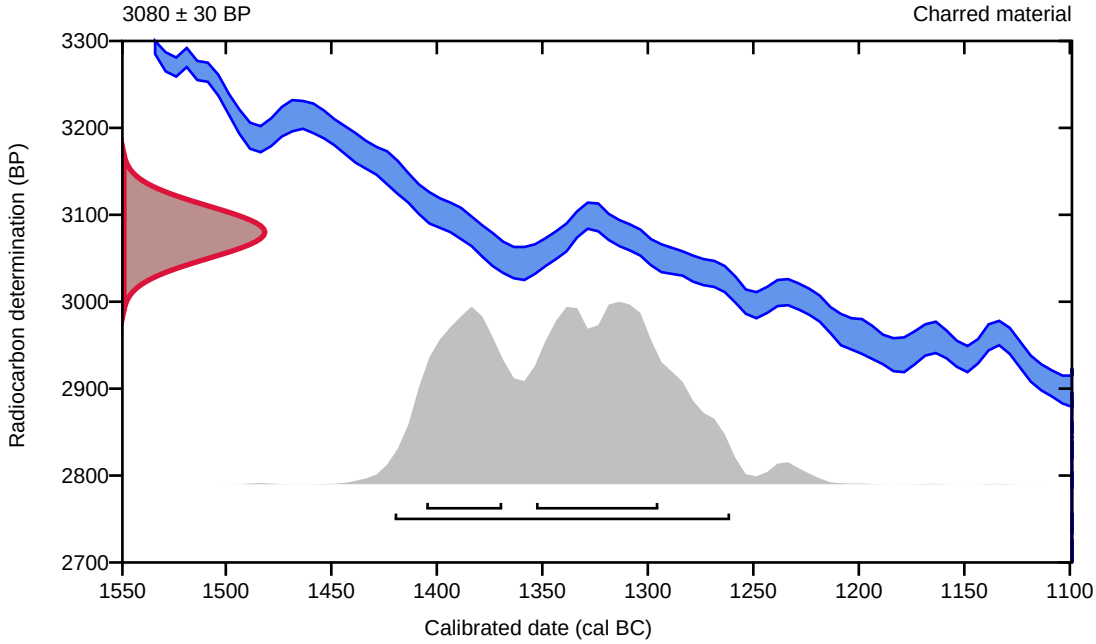

Database used

INTCAL20

References

References to Probability Method

Bronk Ramsey, C. (2009). Bayesian analysis of radiocarbon dates. Radiocarbon, 51(1), 337-360.

References to Database INTCAL20

Reimer, et al., 2020, Radiocarbon 62(4):725-757.

Calibration of Radiocarbon Age to Calendar Years

(High Probability Density Range Method (HPD): INTCAL20)

(Variables: d13C = -23.6 o/oo)

Laboratory number **Beta-635080**

Conventional radiocarbon age **260 ± 30 BP**

95.4% probability

(51.5%)	1620 - 1674 cal AD	(330 - 276 cal BP)
(28.7%)	1516 - 1590 cal AD	(434 - 360 cal BP)
(13.6%)	1766 - 1800 cal AD	(184 - 150 cal BP)
(1.6%)	1942 - Post cal AD 1950	(8 - Post cal BP 0)

68.2% probability

(44.1%)	1634 - 1665 cal AD	(316 - 285 cal BP)
(15.3%)	1528 - 1550 cal AD	(422 - 400 cal BP)
(8.8%)	1784 - 1794 cal AD	(166 - 156 cal BP)

J-1770a-1

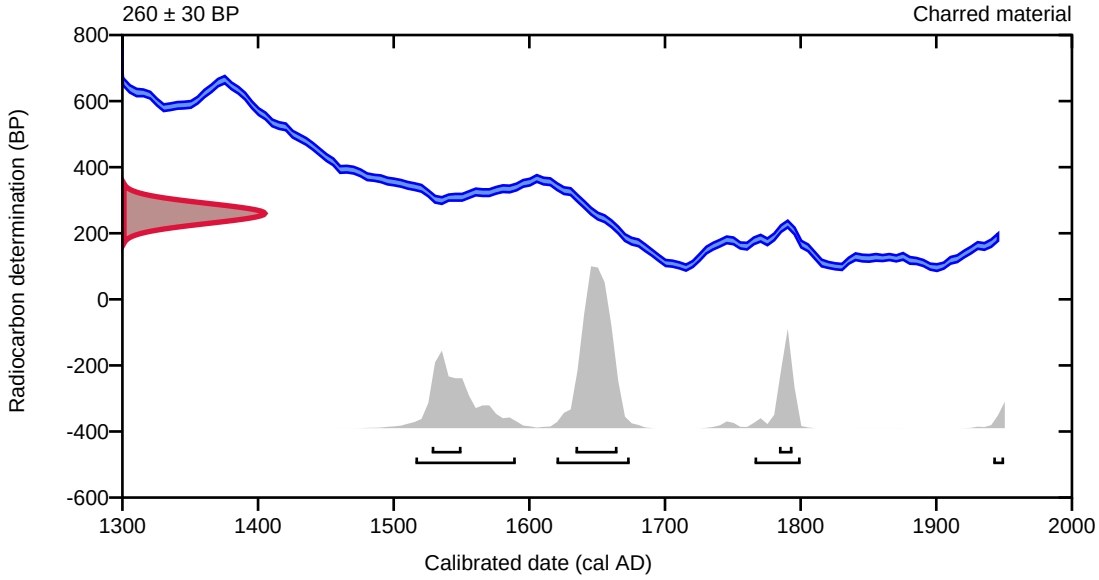

Database used

INTCAL20

References

References to Probability Method

Bronk Ramsey, C. (2009). Bayesian analysis of radiocarbon dates. Radiocarbon, 51(1), 337-360.

References to Database INTCAL20

Reimer, et al., 2020, Radiocarbon 62(4):725-757.

Calibration of Radiocarbon Age to Calendar Years

(High Probability Density Range Method (HPD): INTCAL20)

(Variables: d13C = -22.5 o/oo)

Laboratory number **Beta-635081**

Conventional radiocarbon age **1330 ± 30 BP**

95.4% probability

(57.1%)	649 - 708 cal AD	(1301 - 1242 cal BP)
(38.3%)	728 - 774 cal AD	(1222 - 1176 cal BP)

68.2% probability

(39.2%)	656 - 684 cal AD	(1294 - 1266 cal BP)
(29%)	744 - 772 cal AD	(1206 - 1178 cal BP)

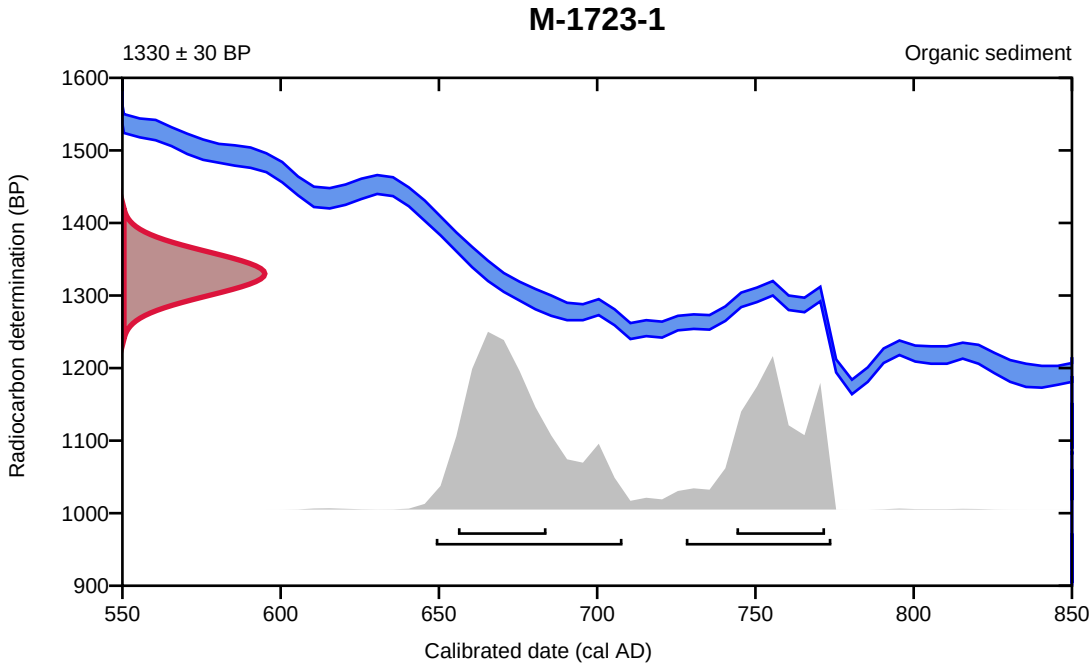

Database used

INTCAL20

References

References to Probability Method

Bronk Ramsey, C. (2009). Bayesian analysis of radiocarbon dates. Radiocarbon, 51(1), 337-360.

References to Database INTCAL20

Reimer, et al., 2020, Radiocarbon 62(4):725-757.

Calibration of Radiocarbon Age to Calendar Years

(High Probability Density Range Method (HPD): INTCAL20)

(Variables: d13C = -25.2 o/oo)

Laboratory number **Beta-635082**

Conventional radiocarbon age **1870 ± 30 BP**

95.4% probability

(92.8%)	116 - 239 cal AD	(1834 - 1711 cal BP)
(2.6%)	84 - 96 cal AD	(1866 - 1854 cal BP)

68.2% probability

(54.3%)	152 - 212 cal AD	(1798 - 1738 cal BP)
(13.9%)	130 - 145 cal AD	(1820 - 1805 cal BP)

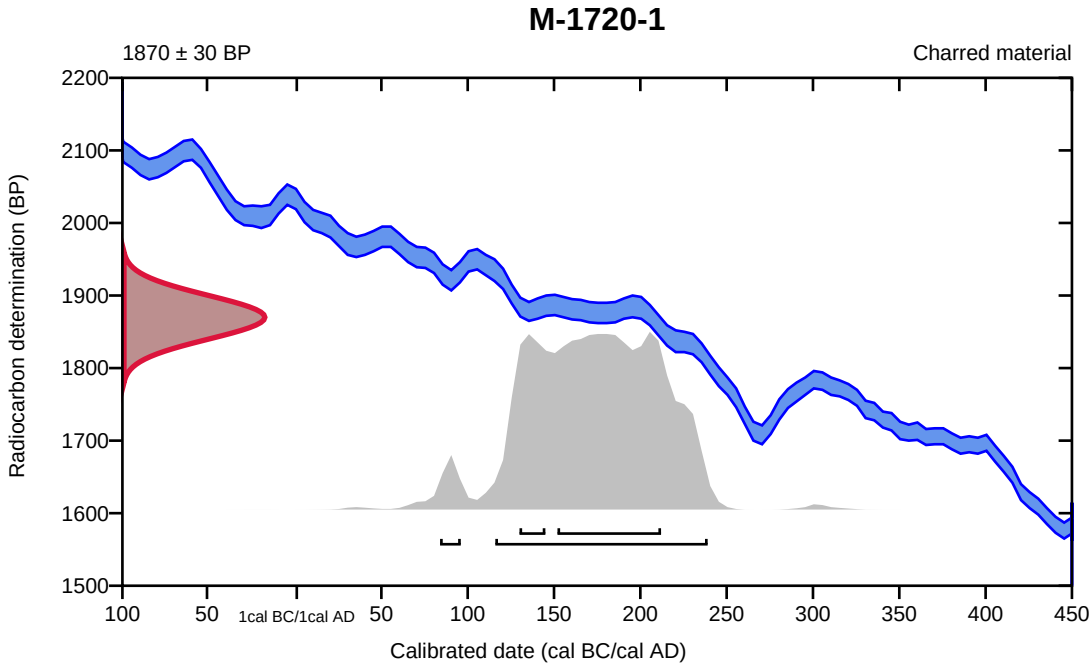

Database used

INTCAL20

References

References to Probability Method

Bronk Ramsey, C. (2009). Bayesian analysis of radiocarbon dates. Radiocarbon, 51(1), 337-360.

References to Database INTCAL20

Reimer, et al., 2020, Radiocarbon 62(4):725-757.

Beta Analytic Radiocarbon Dating Laboratory

4985 S.W. 74th Court, Miami, Florida 33155 • Tel: (305)667-5167 • Fax: (305)663-0964 • Email: beta@radiocarbon.com

Calibration of Radiocarbon Age to Calendar Years

(High Probability Density Range Method (HPD): INTCAL20)

(Variables: d13C = -24.6 o/oo)

Laboratory number **Beta-635083**

Conventional radiocarbon age **190 ± 30 BP**

95.4% probability

(52%)	1724 - 1812 cal AD	(226 - 138 cal BP)
(21.8%)	1648 - 1695 cal AD	(302 - 255 cal BP)
(17.8%)	1916 - Post cal AD 1950	(34 - Post cal BP 0)
(3.8%)	1838 - 1878 cal AD	(112 - 72 cal BP)

68.2% probability

(35.2%)	1735 - 1787 cal AD	(215 - 163 cal BP)
(14.4%)	1662 - 1684 cal AD	(288 - 266 cal BP)
(12.3%)	1930 - Post cal AD 1950	(20 - Post cal BP 0)
(6.2%)	1792 - 1802 cal AD	(158 - 148 cal BP)

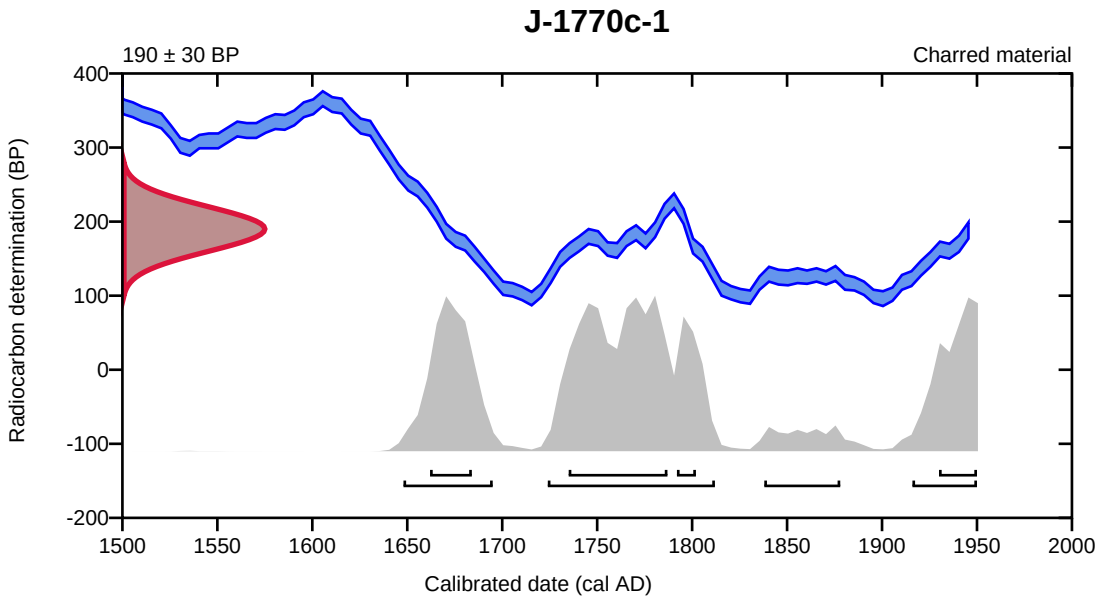

Database used

INTCAL20

References

References to Probability Method

Bronk Ramsey, C. (2009). Bayesian analysis of radiocarbon dates. Radiocarbon, 51(1), 337-360.

References to Database INTCAL20

Reimer, et al., 2020, Radiocarbon 62(4):725-757.

Beta Analytic Radiocarbon Dating Laboratory

4985 S.W. 74th Court, Miami, Florida 33155 • Tel: (305)667-5167 • Fax: (305)663-0964 • Email: beta@radiocarbon.com

Calibration of Radiocarbon Age to Calendar Years

(High Probability Density Range Method (HPD): INTCAL20)

(Variables: d13C = -24.5 o/oo)

Laboratory number **Beta-635084**

Conventional radiocarbon age **440 ± 30 BP**

95.4% probability

(94%)	1420 - 1495 cal AD	(530 - 455 cal BP)
(1.4%)	1601 - 1610 cal AD	(349 - 340 cal BP)

68.2% probability

(68.2%)	1431 - 1466 cal AD	(519 - 484 cal BP)

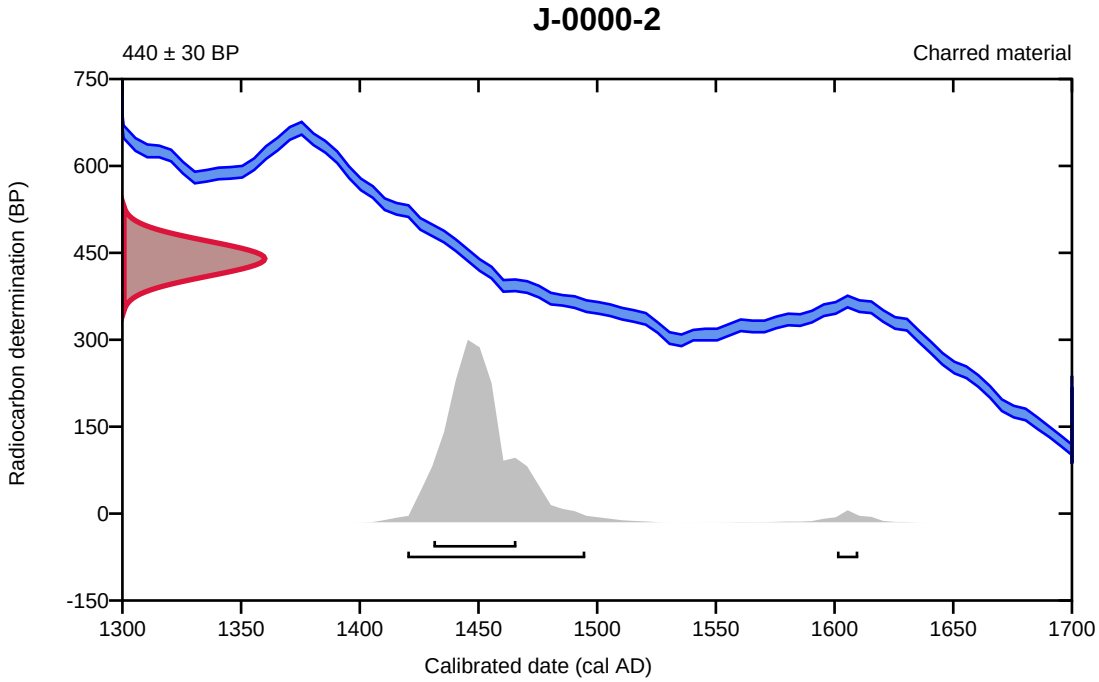

Database used

INTCAL20

References

References to Probability Method

Bronk Ramsey, C. (2009). Bayesian analysis of radiocarbon dates. Radiocarbon, 51(1), 337-360.

References to Database INTCAL20

Reimer, et al., 2020, Radiocarbon 62(4):725-757.

Calibration of Radiocarbon Age to Calendar Years

(High Probability Density Range Method (HPD): INTCAL20)

(Variables: d13C = -23.3 o/oo)

Laboratory number **Beta-635085**

Conventional radiocarbon age **3840 ± 30 BP**

95.4% probability

(87.4%)	2410 - 2201 cal BC	(4359 - 4150 cal BP)
(8%)	2456 - 2417 cal BC	(4405 - 4366 cal BP)

68.2% probability

(37%)	2344 - 2275 cal BC	(4293 - 4224 cal BP)
(27.9%)	2256 - 2206 cal BC	(4205 - 4155 cal BP)
(3.3%)	2396 - 2388 cal BC	(4345 - 4337 cal BP)

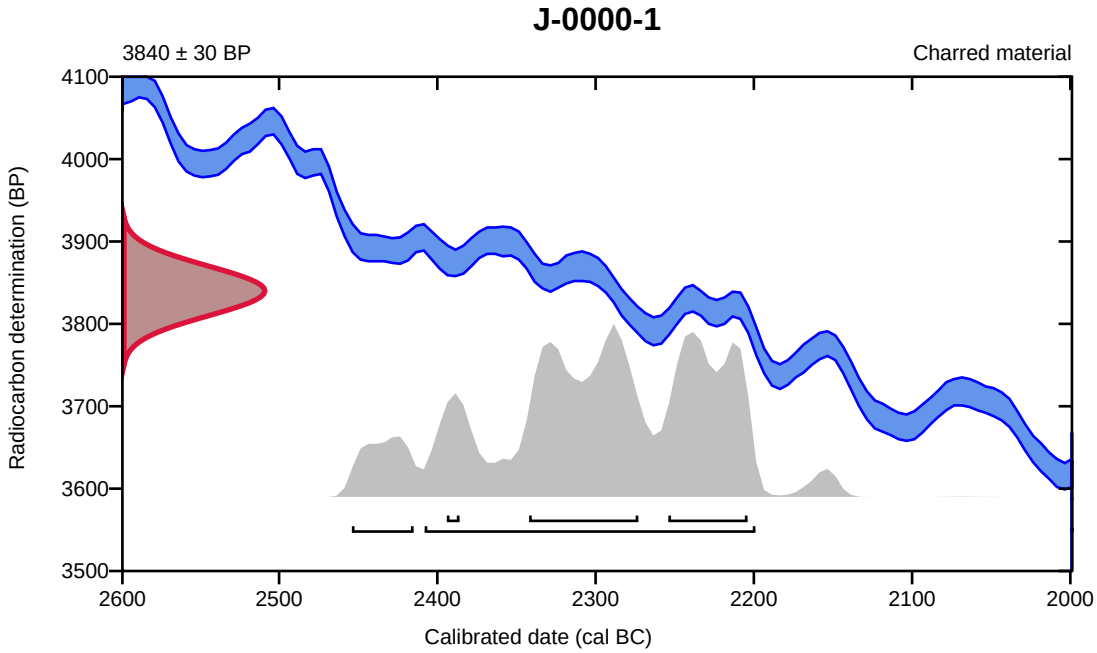

Database used

INTCAL20

References

References to Probability Method

Bronk Ramsey, C. (2009). Bayesian analysis of radiocarbon dates. Radiocarbon, 51(1), 337-360.

References to Database INTCAL20

Reimer, et al., 2020, Radiocarbon 62(4):725-757.

Calibration of Radiocarbon Age to Calendar Years

(High Probability Density Range Method (HPD): INTCAL20)

(Variables: d13C = -24.2 o/oo)

Laboratory number **Beta-635086**

Conventional radiocarbon age **2910 ± 30 BP**

95.4% probability

(95.4%)	1211 - 1012 cal BC	(3160 - 2961 cal BP)

68.2% probability

(54.1%)	1127 - 1047 cal BC	(3076 - 2996 cal BP)
(5.9%)	1158 - 1146 cal BC	(3107 - 3095 cal BP)
(4.9%)	1189 - 1179 cal BC	(3138 - 3128 cal BP)
(3.3%)	1028 - 1021 cal BC	(2977 - 2970 cal BP)

J-WP8a

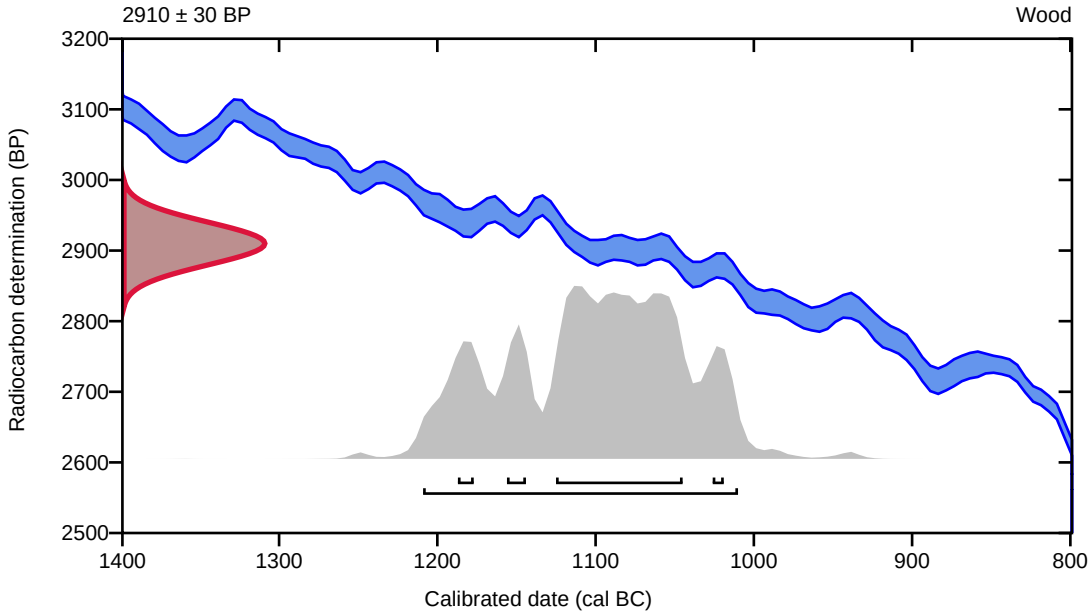

Database used

INTCAL20

References

References to Probability Method

Bronk Ramsey, C. (2009). Bayesian analysis of radiocarbon dates. Radiocarbon, 51(1), 337-360.

References to Database INTCAL20

Reimer, et al., 2020, Radiocarbon 62(4):725-757.

Beta Analytic Radiocarbon Dating Laboratory
4985 S.W. 74th Court, Miami, Florida 33155 • Tel: (305)667-5167 • Fax: (305)663-0964 • Email: beta@radiocarbon.com

APPENDIX G
FREQUENCY-MAGNITUDE ANALYSIS METHODS

G.1. INTRODUCTION

A frequency-magnitude (F-M) relationship answers the question "how often (frequency) and how big (magnitude) can steep creek hazards events become?" The objective of an F-M analysis is to develop a relationship between the frequency of the hazard and its magnitude. For this assessment, frequency is expressed using return periods[1]. Both peak discharge (for clearwater flows, debris floods and debris flows) and volume (for debris floods and debris flows) are used as measures of magnitude. This appendix describes the methods employed by BGC to develop F - M relationships for debris floods and debris flows on Jason and Mungye creeks and includes:

1. Review of historical events
2. Application of suite of techniques appropriate to the dominant process type(s) for the creek
3. Development of range and best estimate F-M relationship.

F-M relationships are dependent on the dominant steep creek process type(s) for each creek, in recognition that creeks may be subject to a continuum of processes over different return periods (Appendix B). The return periods to consider in an assessment are informed by Engineers and Geoscientist of British Columbia (EGBC) Professional Practice Guidelines. In this assessment, BGC considered return periods up to the 1,000 to 3,000-year range consistent with Class 2 (medium to large subdivisions of 6 to 50 single-family lots) (EGBC, September 29, 2018). Table G-1 outlines the dominant steep creek process for each return period considered on the study creeks.

Table G-1. Range of return periods for the hazard assessment on Jason and Mungye creeks.

Return Period Range (years)	Representative Return Period (years)	Jason Creek	Mungye Creek
10 to 30	20	Debris flow	Flood
30 to 100	50	Debris flow	Debris flood (Type 1)[2]
100 to 300	200	Debris flow	Debris flood (Type 2)[2]
300 to 1,000	500	Debris flow	Debris flow
1,000 to 3,000	2,000	Debris flow	Debris flow

Notes:

1. The 50-, 500-, 2,000-, and 5,000-year events do not precisely fall at the geomean of the return period ranges but were chosen as round figures due to uncertainties and because these return periods have a long tradition of use in BC.
2. BGC adopted the debris flood categories presented in Church & Jakob (2020) as described in Appendix B.

In the following sections BGC describes the review of historical events which is common to both creeks, and then for clarity outlines the techniques applied to develop the range and best estimate F-M relationships for each study creek individually.

[1] Except for periods of T<10, the return period (T) is the inverse number of frequency F (i.e., T=1/F). A return period of 100 years is equivalent to a frequency of 0.01 events/year, or a 1% probability that an event may occur in any given year. In a changing climate or because of adverse human interference with watershed processes, the return period of a given magnitude event may decrease over time. For example, a 100-year return period debris flood based on historical data, may become a 20-year return period debris flood by the end of the century.

G.2. HISTORICAL EVENTS

Historical evidence of geohazard events can be observed via historical records, field assessments and aerial imagery interpretations.

G.2.1. Historical Records

On Jason Creek, Baumann (October 1997) cited four historical events dating to about 1900 AD. The dating on these events is approximate and occurred in the 1920s, 1950s, 1970, and 1990. The debris flows in November-December 2021 add to this list of events. No historical records of debris floods or debris flows on Mungye Creek were identified by BGC.

G.2.2. Aerial Imagery Interpretation

BGC reviewed air photos from 1946 to 2016, satellite imagery from 2019, and a high-resolution orthophoto acquired in July 2022. Table G-2 provides observations from BGC's detailed review of aerial imagery and relevant observations are marked on Drawing 06. A high-level review of GeoBC imagery from 1981, 1986, 1994, 2005 and 2016 was also undertaken. As no evidence of historic debris floods or debris flows were present in the GeoBC images, they were not examined further.

Table G-2. Summary of observations from aerial imagery review.

Air Photo / Imagery Date	Source	Key Observations
1946	National Air Photo Library	Debris deposition is suspected in the Jason Creek, Mungye Creek, and Lower fans. A suspected landslide scar can be seen in the Jason Creek watershed. This coincides with an event identified from dendro observation (~1952±5 yrs) by Baumann (October, 1997). Several bare patches (suspected bedrock) are visible in the Jason Creek fan and watershed. These patches are visible in subsequent years. A road is present adjacent to the Lower fan. The Lower fan has been clear cut for a suspected Right of Way (RoW).
1951	National Air Photo Library	Clearcutting more distinct than in 1946.
1969	GeoBC	Clearcutting visible across Jason Creek and Lower fans. Since 1951 a new road was constructed across the Lower fan. Clearcutting visible in the Mungye Creek watershed. Since 1951, trails were constructed in the Jason Creek watershed, likely due to mining activity [note old adit near 1990, 2021 landslide headscarps (Cordilleran, 2021). The bare patch previously noted in the Jason Creek watershed is less visible than in previous photos.
1981	National Air Photo Library	Clearcutting is visible adjacent to the Jason and Mungye Creek watersheds, as well as on the Jason Creek fan.
2009	Geo	Anthropomorphic modifications associated with residential development to the Jason Creek and Mungye Creek fans are visible. Reid Road was developed, along with the surrounding community.
2019	ESRI World Imagery	Additional anthropomorphic modifications made to the fan since 2009. Additional clearcutting since 2009 is visible adjacent to the Jason and Mungye Creek watersheds.

G.2.3. Fieldwork

BGC completed field traverses and collected observations on the study creeks in July, September, and October 2022. The locations of the field traverses and observation points are shown in Appendix C. As part of field work, BGC:

- Completed channel hikes to assess channel condition, yield rate, bedrock instability, condition of 2021 source area, and potential source areas for future debris floods/debris flows.
- Collected relevant observations from infrastructure (buildings and culverts) on the study creek fans, including delineation of high water mark and splash height from the 2021 debris flows on Jason Creek (Appendix D).
- Mapped boulders on the Jason Creek fan to delineate the approximate location and density distribution of past debris-flow runout of sufficient intensity to transport large boulders (1 to >3 m diameter)
- Excavated 11 test pits and examined two natural exposures on Jason Creek fan and excavated four test pits on Mungye Creek fan (Appendix F, Drawing 07).
- Collected tree core and tree slice samples from trees interpreted to be scarred by debris-flow impact to date the debris flows (Drawing 07).

G.2.3.1. Dendrogeomorphology (Tree-Dating)

BGC collected 20 tree core samples and six tree slice samples during field visits in July and September 2022 (Drawing 07). BGC estimated the age of historical debris flows using evidence of impacts to the tree and tree ring dating. Evidence to impact includes:

- Scars
- Traumatic resin duct (TRD)
- Growth reduction.

Based on the samples collected, BGC estimated that debris flows have occurred approximately every 12 to 17 years on Jason Creek. There was not sufficient evidence to develop an estimate of frequency on Mungye Creek. The dendrogeomorphology results are summarized in Table G-3.

Table G-3. Summary of dendrogeomorphology results.

Date	Confidence[1]	Storm Date[2]	Annual Maximum Rainfall (mm/day)	Environment and Climate Change Canada Station	Evidence
1849	low	-	Unavailable	-	Strong line of TRD's noted in one sample.
1895	moderate	-	Unavailable	-	J-C-004 and J-WP-017 established. Growth reduction noted on one sample, also mentioned in 1997 Baumann report.
1934	moderate	Jan 24, 1935	50.8	Pemberton Meadows (1086090)	Scar visible on J-C-006 causing a warped ring, growth reduction noted on two samples in the following couple of years lasting until 1941 and 1957, J-C-010 established four years later.
1949	moderate	Nov 30, 1949	61.2	Pemberton Meadows	Scar noted on J-DF-011, two samples with moderate TRD's in the following year, rings warped on one sample in the following year
1963	low	Nov 1, 1963	66.8	Pemberton Meadows	Growth acceleration noted on two samples, moderate TRD's visible on one sample, J-C-015 established three years later.
1968	moderate	-	Unavailable	-	Tree scar on disk (J-C-010).
1972	moderate	Dec 26, 1972	87.6	Pemberton BCFS (1086083)	Growth acceleration noted on three samples in the following years, sample M-C-001 established.
1979	moderate	Dec17, 1979	88.8	Pemberton Meadows	Two samples with strong TRD's present, scar noted on J-DF-013B, J-DF-013 established, growth reduction noted on one sample.
1981	high	Dec 26, 1980	76.2	Pemberton Meadows	Scar on J-C-010, Scar J-C-05
1983	high	Oct 7,1984	68.4	Pemberton BCFS	Scar on J-DF-7, Scar J-DF-10
1990	high	Nov 12, 1990	55.0	Pemberton Airport CS (1086082)	1997 Baumann report, p. 6
2001	low	Jan 7, 2002	72.0	Pemberton Airport CS	One strong and one moderate line of TRD's noted on samples
2008	low	Mar 11, 2007	43.2	Pemberton Airport CS	Two samples with strong TRD's present, growth reduction noted on two samples.
2021	high	Dec 1, 2021	51.7	Pemberton Airport CS	Observed debris flow

Notes:

1. The confidence intervals are defined as follows: low confidence – few TRD's visible in samples, little to no other corroborative evidence in dendrogeomorphology samples, and no corroborative evidence found in air photos or other reports. No debris flows observed. Moderate confidence – few TRD's visible in samples, corroborative evidence found in dendrogeomorphology samples, or other reports. No corroborative evidence found in air photos. No debris flows observed. High confidence – Debris flow event observed, visible in air photo, recorded in historical report, or scar visible on dendrogeomorphology samples.
2. As tree growth does not always adhere to calendar time, maximum measured rainfall was taken from the event year and the two surrounding years.

G.2.4. JASON CREEK

Jason Creek is susceptible to debris flows at all return periods considered (Table G-1). The following sections describe the methods BGC applied to estimate debris-flow sediment volume and peak discharge.

G.2.4.1. Sediment Volume

BGC applied five individual techniques to estimate debris-flow magnitude (sediment volume) at Jason Creek (Table G-4).

Table G-4. Summary of F-M techniques applied at Jason Creek

Technique	Description
Regional (Jakob et al, 2020)	Jakob et al (2020) developed regional relationships based on detailed site-specific F-M relationships for debris flows in southern British Columbia and debris flows and debris floods in the Bow River valley near Canmore, Alberta. Site-specific F-M relationships were developed from detailed absolute dating methods, stratigraphic analysis, and analytical tools. The regional relationships provide a means to estimate sediment volumes at different return periods normalized by fan or watershed area. At Jason, BGC derived a F-M relationship normalized by watershed area using creeks of similar process type, morphology (watershed area ≤ 6.5 km^2, fan area ≤ 1.5 km^2), and geologic setting.
Yield Rate (Hungr et al., 1984) and Point Source Estimation	Hungr et al. (1984) developed a method to estimate total debris-flow volume based on the volume of material eroded per meter of channel length. BGC collected channel yield rate estimates along Jason Creek up to the slope break at approximately mid-watershed (field traverse shown in Appendix C). The yield rate estimates provide an indication of how big the next debris flow could be based on material availability. To develop an F-M relationship from this technique, BGC supplemented the yield rate estimates with delineation of point source failures and engineering/geoscience judgement to assess the likely number of point sources that could fail in the return periods considered.
Charles Creek Analogue (Bovis & Jakob, 1999; Hungr & Wilson, unpublished; Jakob and Nolde, 2022)	BGC employed a channel recharge rate relationship (Bovis & Jakob, 1999) to Jason Creek and a heavily studied watershed analogue (Charles Creek, BC) to develop a scaling factor to estimate sediment volumes for different return periods. For each creek, the average debris-flow magnitude (V) is calculated using a weathering-limited or transport-limited equation: Weathering-limited: $V = 0.48 + 2 * Z_T + 0.1 * A_{\%}$ where Z_T = Total watershed relief (km) $A_{\%}$ = Percentage of watershed area actively contributing debris Transport-limited: $V = 420 * A_I^{0.82} * N_S^{2.55}$ where A_I = Active area index (area actively contributing debris * N_s) N_s = Weighted stability number

Technique	Description
	BGC compared the two equations for Jason Creek which yielded similar results. BGC relied on the weathering-limited estimate. The factor difference between V for Charles Creek and Jason Creek was then used to downscale the Charles Creek F-M relationship and develop a new curve fit equation for Jason Creek. BGC estimated the sediment volumes for the return periods considered at Jason using the curve fit equation developed through this method.
Radiocarbon dating and area-volume relationship (Griswold & Iverson, 2008)	BGC delineated approximate runout extents of historic debris flows using a combination of the stratigraphic analysis and radiocarbon dating (Appendix F) and field evidence from the November 2021 debris flows. The interpreted areal extent of debris flows was coupled with the deposit depths observed in the test pits to estimate a sediment volume range and best estimate for the approximately corresponding return period ranges based on radiocarbon dating results. BGC compared the ranges estimated from the test pit deposition depth to a published relationship between debris flow planimetric area and volume (Griswold & Iverson, 2008): $B = \alpha_2 * V^{\frac{2}{3}}$ where: B = planimetric area of debris flow α_2 = calibration coefficient for debris flows V = volume Griswold & Iverson (2008) recommend α_2 of 20, whereas, BGC's experience has demonstrated that in BC, 50 is more representative. Calibration using α_2 of 50 correlated well with observed deposition depths.
Post-fire (Gartner et al., 2014)	Gartner et al (2014) developed a relationship to estimate post-wildfire debris-flow volumes using: • Projected 15-min rainfall intensity rates (Intensity-Duration-Frequency (IDF)) • Area of watershed burned at moderate to high severity • Watershed relief BGC assessed post-wildfire debris-flow volumes at 20%, 40%, and 60% of total watershed area burned. Projected wildfire burn probabilities for the end of the century (2050-2100) based on BC Wildfire Service Annual Burn Probability for the study area were coupled with the IDF annual exceedance probabilities (AEPs) to estimate the conditional probability of rainfall events of those intensities occurring in the first two years post-fire. Gartner et al's relationship was developed in southern California. BGC's experience in British Columbia suggests a factor of two to four decrease in the predicted volume better approximates debris-flow volumes in this environment. BGC compared scaling factors of 0.25 and 0.5 before plotting the resultant data and using a power law curve-fit to estimate sediment volumes at each return period.

BGC applied a confidence weighting based on the quality and quantity of input date for each technique, applicability to Jason Creek, and professional judgement. BGC used the confidence weighting to develop a weighted average best estimate F-M relationship (Table G-5). BGC compared the estimated volumes from the model ensemble to post-fire volumes for the return

periods shown in Table G-5. For those return periods, post-fire volumes are estimated to be near to or less than the best estimates and were not modelled separately. This does not imply that a wildfire would have no effect on F-M in the watershed should it occur. BGC recommends that if a fire occurs in one of the study creek watersheds, a site-specific post-wildfire debris-flow assessment be undertaken.

Table G-5. F-M relationship for Jason Creek based on model ensemble.

Representative Return Period (years)	Model Ensemble for Sediment Volume (m^3)				Best Estimate
	Regional	Yield Rate/ Judgement	Basin Analogue	Radiocarbon Dating	
Confidence	Medium	Low-Medium	Low	Medium	Weighted Average
Rationale	Log. fit may overestimate volumes at low return periods.	Judgement-based	Confidence in Charles Ck. as analog, sensitive to contributing area delineation	Uncertainty associated with historic event area delineation	
Weighting Factor	2	1.5	1	2	
20	1,300	4,600	4,400	5,000	4,000
50	6,600	7,800	6,400	10,000	8,000
200	14,700	12,800	9,500	14,000	13,000
500	20,000	26,700	11,600	18,000	19,000
2,000	(rock slide triggered debris flow)			55,000	55,000

Note:
1. Regional, yield-rate, and basin analogue techniques were not applied for the 2,000-year return period when rock slide-triggered debris flows are expected to dominate. The best estimate for that return period was partially informed by DAN3D modelling results (Appendix H).
2. Sediment volumes rounded to nearest 100 m^3.

G.2.4.2. Peak Discharge

BGC estimated debris-flow peak discharge on Jason Creek using empirical relationships that relate the estimated debris-flow volumes to peak discharges for the same event (Bovis & Jakob, 1999; Mizuyama et al., 1992).

Bovis and Jakob (1999) provide empirical correlations between peak discharge and debris-flow volume based on observations of 33 debris flow basins in southwestern British Columbia. Mizuyama et al. (1992) similarly provide empirical correlations based on observations on creeks in Japan and Alberta. These relationships were constructed for “muddy” debris flows and “granular” debris flows. Muddy debris flows are those with a relatively fine-grained matrix as found from volcanic source areas or fine-grained sedimentary rocks, while granular debris flows are those typical for granitic source areas with large clasts embedded in the flow which slow the flow through friction thus creating large surge fronts.

Debris flows on Jason Creek are derived from marine sedimentary and volcanic rocks of the Lower Cretaceous Gambier Group (Riddel, 1992; Schiarizza and Church, 1996). BGC selected to use the relationships for granular flows (Equations G-1, G-2):

$$Q_{granular\ (Bovis\ \&\ Jakob)} = 0.105 \cdot (V)^{0.83} \quad \text{[Eq. G-1]}$$

$$Q_{granular\ (Mizuyama\ et\ al.)} = 0.135 \cdot (V)^{0.78} \quad \text{[Eq. G-2]}$$

BGC averaged the peak discharge derived from Eqs G-1, G-2 for the best estimate of peak discharge on Jason Creek (Table G-6). Peak discharge and total debris-flow volume were then input to the numerical modelling together with rheological parameters as outlined in Appendix H.

Table G-6. Best estimate of debris-flow peak discharge on Jason Creek.

Representative Return Period (years)	Sediment Volume (m^3)	Peak Discharge (m^3/s)
20	4,000	100
50	8,000	170
200	13,000	250
500	19,000	340
2,000	55,000	790

Notes:
1. Sediment volumes are rounded to nearest 1,000 m^3.
2. Peak discharges are rounded to nearest 10 m^3/s.

G.2.5. MUNGYE CREEK

Mungye Creek is susceptible to floods, debris floods, and debris flows (Table G-1). The following sections describe the methods BGC applied to estimate peak discharge and sediment volume.

G.2.5.1. Peak Discharge

BGC estimated peak discharge for floods and debris floods using rainfall-runoff modelling and flow bulking, and by using empirical relationships that relate sediment volume to peak discharge for debris flows as described in Section G.2.4.2.

G.2.5.1.1 Rainfall-Runoff Modelling

Rainfall-runoff modelling is a process of develop hydrographs and determine the peak discharge for clearwater flows in response to rainfall. BGC used the Watershed Management Method (BC MOTI, April, 2019) with the HEC-HMS (Version 4.9) program developed by the United States Army Corps of Engineers (USACE). This method is widely used to derive synthetic unit hydrographs and applies a design storm event and physical watershed characteristics to predict peak flows. On Mungye Creek, BGC completed rainfall-runoff modelling for flood and debris-flood dominated return periods (20-, 50-, 200-year).

BGC used 24 hour rainfall depths from the BC Met Portal (MetPortal v2.2.3 (shinyapps.io)) and adjusted them for climate change using data from the Pacific Climate Change Impacts Consortium

(PCIC) Bias Corrected CMIP5 model, accessed through the IDF CC tool (Simonovic et al., 2015) (Table G-7).

Table G-7. Summary of 24-hour rainfall estimates for Reid Road.

Representative Return Period (years)	Existing Conditions (mm)	Climate Change-Adjusted (2100) (mm)	Climate-Change Adjustment (%)
20	88	79	16
50	102	92	20
200	125	111	23

Notes:
1. Existing conditions are based on BC Met Portal (MetPortal v2.2.3 (shinyapps.io)).
2. Climate change conditions are based on adjustments applied to BC Met Portal data using CMIP5 model.

BGC used an SCS Type 1A storm event hyetograph. This storm type has been shown to accurately generate flood runoff from watersheds within the region (Loukas, 1994). Required parameters for hydrological analysis applied by BGC at Mungye Creek are summarized in Table G-8.

Table G-8. Hydrological parameters of the Mungye Creek Watershed.

Parameters	Mungye Creek
Watershed Area (km^2)	1.2
SCS Curve Number (CN II)[1]	75
Lag time (min)[2]	40

Notes:
1. Based on Soil Type C, for poor to fair quality woods.
2. Watershed Management Method Formula.

The resultant peak instantaneous discharges are summarized in Table G-9.

Table G-9. Estimated peak instantaneous discharge for Mungye Creek, including climate change impacts to end of century.

Return Period	Peak Instantaneous Discharge (m^3/s)
20	2.1
50	3.0
200	4.6

G.2.5.1.2 Debris-Flood Flow Bulking

Clearwater floods and debris floods as defined by Church and Jakob (2020) are related processes. However, debris floods have been characterized by their higher sediment concentrations and propensity to erode banks, scour and avulse (Hungr et al., 2014). BGC estimated debris-flood peak discharge by bulking clearwater flows (Table G-9) after the method

shown graphically in Figure G-1. The bulking factors selected are not precise as they are based on geomorphological indicators instead of direct observations of sediment concentration.

The bulking factors and bulked peak discharges for Mungye Creek are summarized in Table G-10.

Table G-10. Mungye Creek bulked peak discharge for representative return periods.

Return Period	Peak Instantaneous Discharge (m^3/s)	Debris Flood Type	Bulking Factor	Bulked Peak Instantaneous Discharge (m^3/s)
20	2.1	-	1.0	2.1
50	3.0	Type 1	1.1	3.3
200	4.6	Type 2	2.0	9.2

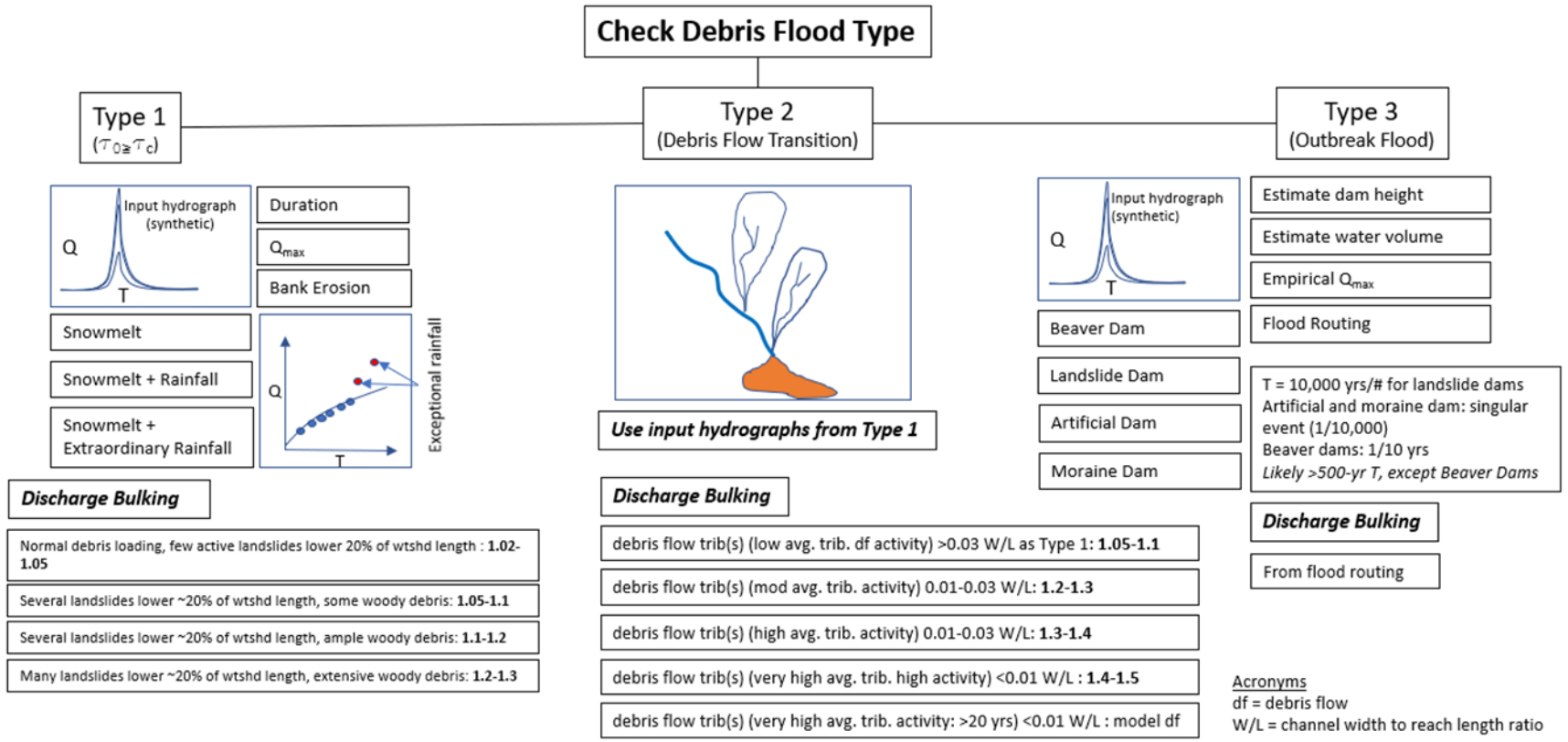

Figure G-1. Debris flood bulking method logic chart for Mungye Creek. Type 1 and Type 2 debris floods were considered.

G.2.5.2. Sediment Volume

BGC applied six individual techniques to estimate debris-flood and debris-flow magnitude (sediment volume) at Mungye Creek (Table G-11).

Table G-11. Summary of F-M techniques applied at Mungye Creek.

Technique	Description
Regional (Jakob et al., 2020)	As described in Table G-4.
Yield Rate (Hungr et al., 1984) and Point Source Estimation	As described in Table G-4.
Charles Creek Analogue (Bovis & Jakob, 1999; Hungr & Wilson, unpublished; Jakob and Nolde, 2022)	As described in Table G-4. At Mungye Creek, BGC only considered weathering-limited equation.
Rainfall-Sediment (Rickenmann & Koschni, 2010)	Following a 2005 storm in the Swiss Alps, Rickenmann & Koschni (2010) developed a database 33 debris flows and 39 fluvial sediment transport events. BGC analyzed the Swiss dataset and added an additional 14 creeks in the Bow Valley, AB that experienced debris floods during a June 2013 storm. Using both datasets, BGC developed an equation to estimate sediment volume from total rainfall volume: $logV_S = 0.740 logV_R - 0.4624,\ R^2 = 0.78$ where: V_S = total sediment volume displaced V_R = rainfall volume To determine the total rainfall volume, BGC used 24 rainfall totals (BC Met Portal) averaged over four locations in the watershed to account for orographic effects, added a climate change-adjustment based on CMIP5 (Table G-7), and added snowmelt contribution (10%).
Radiocarbon dating and area-volume relationship (Griswold & Iverson, 2008)	As described in Table G-4.
Post-fire (Gartner et al., 2014)	As described in Table G-4.

As at Jason Creek, BGC applied a confidence weighting based on the quality and quantity of input date for each technique, applicability to Mungye Creek, and professional judgement. BGC used the confidence weighting to develop a weighted average best estimate F-M relationship (Table G-12). BGC compared the estimated volumes from the model ensemble to post-fire volumes which showed that post-fire volumes are estimated to be near to or less than the best estimate and were not relied upon in the remainder of the hazard assessment.

Table G-12. F-M relationship for Mungye Creek based on model ensemble.

Representative Return Period (years)	Model Ensemble for Sediment Volume (m^3)					Best Estimate
	Regional	Yield Rate/ Judgement	Basin Analogue	Rainfall-Sediment	Radiocarbon Dating	
Confidence	Medium	Low-Medium	Low	Medium	Low	Weighted Average
Rationale	Log. fit may overestimate volumes at low return periods.	Judgement-based	Charles Ck, active contributing area	Small number of storms	Limited test pits and samples as basis	
Weighting Factor	2	1.5	1	2	2	
20	Flood					-
50	-	-	-	2,500	-	2,500
200	16,500	3,400	3,500	3,000	-	7,500
500	22,500	8,200	3,800	-	-	13,600
2,000	33,000	17,100	4,900	-	41,000	24,000

Notes:

1. Clearwater floods are capable of transporting sediment; however the concentrations are low enough that BGC did not calculate them for the purposes of this assessment.
2. Regional, yield rate/judgement, and basin analogue are only applied for Type 2 debris floods and debris flows.
3. Rainfall-sediment is only applied for debris floods.
4. Radiocarbon dating only possible for 2,000-year return period due to date of samples.
5. Sediment volumes rounded to nearest 500 m^3.

APPENDIX H
NUMERICAL MODELLING METHODS AND RESULTS

H.1. INTRODUCTION

Numerical modelling is a fundamental step in steep creek hazard and risk assessments. It uses computer models to simulate a fluid that approximates potential real debris-floods and debris-flows. This allows designation of hazard zones (Appendix I) and will guide eventual mitigation efforts.

BGC completed numerical modelling using a combination of DAN3D, used for the analysis of rapid landslide motion across complex 3D terrain, developed at the University of British Columbia, and HEC-RAS 2D (version 6.2), a public domain hydraulic modelling program developed and supported by the United States Army Corps of Engineers.

H.2. SOFTWARE DESCRIPTION AND METHODOLOGY

BGC used two modelling softwares to simulate geohazard events on Jason and Mungye Creeks: HEC-RAS and DAN3D. HEC-RAS was used to model floods, debris floods, and precipitation-triggered debris flows (Section E.4). DAN3D was used to model rock slide-triggered debris flows on Jason Creek (Section H.3).

H.2.1. HEC-RAS

HEC-RAS two-dimensional (2D) modelling uses an irregular mesh to simulate the flow of water over terrain. Irregular meshes are useful for development of numerically efficient 2D models to allow refinement of the model in locations where the flow is changing rapidly and/or where additional resolution is desired. With 2D models, the objective is to define a model with sufficient accuracy and resolution, but at the same time minimize model runtime.

H.2.1.1. Topography

HEC-RAS uses lidar-generated topography as an input. Additional processing is sometimes needed to digitally remove bridge decks and ensure the existing channel profile is maintained under bridges. Similarly, HEC-RAS allows integration of culverts to the model domain. Digital elevation models (DEM) derived from the lidar only capture the water surface. In shallow debris-flood prone creeks, the need for bathymetry not accounted by the lidar dataset is likely negligible. In lakes and larger mainstem rivers, the terrain should be modified to include estimated bathymetry at the downstream boundary (lake, river, ocean, reservoir). In these cases, the model domain can be extended approximately 500 m past the shoreline to ensure that the boundary condition does not affect the discharge on the fan.

H.2.1.2. Geometry

The default cell geometries created by HEC-RAS are rectangular but other geometries can be developed to transition between different refinement areas (varying cell size or breaklines). Within HEC-RAS, a 2D mesh is generated based on the following inputs:

H.2.1.3. The model perimeter (the model domain or extent of the model).

- Refinement areas to define sub-domains where the mesh properties (e.g., mesh resolution) are adjusted.
- Breaklines to align the mesh with terrain features which influence the flow such as dikes, stream channel banks, roadways, terraces, and embankments. HEC-RAS provides options to adjust the mesh resolution along breaklines, if the modeler chooses.

From these inputs, HEC-RAS generates a mesh consisting of computational points at the cell centroid and the faces of the cells. The mesh then needs to be cleaned and checked for errors such as a cell having more than 8 faces and large cells in the mesh that may be created when the breaklines are enforced. The general mesh for each site is developed with a site-specific grid size and additional breaklines refine spatial discretization to capture important topographic features, such as the stream channel banks, roadways, and other infrastructure. Refinement areas are used with a higher resolution grid along the stream channels, avulsion paths, and in areas of overland flooding to provide adequate model resolution and detail.

H.2.1.4. Newtonian Properties

HEC-RAS includes modelling capabilities for Newtonian (clearwater floods, debris floods) and non-Newtonian (debris flows) fluids. Non-Newtonian fluids are those whose viscosity changes when force is exerted on the fluid making it more liquid or more solid. Ketchup or mayonnaise are examples of non-Newtonian fluids. The capability to model all steep creek process types in the study area was a main driver to select HEC-RAS as a modelling package for this assessment.

H.2.2. DAN3D

Debris flow scenarios for Jason Creeks were modeled using the three-dimensional numerical model *DAN3D* (McDougall and Hungr 2004). *DAN3D* was developed specifically for the analysis of rapid landslide motion across complex 3D terrain and is well-suited to the simulation of coarse debris flows that deposit on relatively steep slopes, like the Jason Creek fan. BGC has used *DAN3D* for the same purposes on other projects.

The model simulates landslide motion from initiation to deposition and requires the following inputs, as described in detail below:

- A digital elevation model (DEM) of the topography in the study area, which defines the sliding surface across which the simulated landslide travels
- A corresponding DEM that delineates the extent and thickness of the initial landslide
- A corresponding DEM that delineates the extent and thickness of erodible material along the path that could be entrained by the landslide as it passes
- A user-specified entrainment rate that determines how much of the available erodible material is picked up by the landslide
- User-specified flow resistance parameters that control how fast and how far the simulated landslide travels.

H.2.2.1. Sliding Surface

BGC used a sliding surface based on the bare earth lidar DEM. BGC modified the lidar data to a 3 x 3 m grid spacing and smoothed to reduce surface roughness and improve numerical model stability. This generalization results in some loss of topographic details (e.g., large boulders or channel constrictions that could locally affect the flow path and flow depth) but does not substantively affect the debris-flow modelling results, especially for larger events with longer runout.

H.2.2.2. Source volumes and locations

BGC modelled three debris-flow volume scenarios. In all cases, constant entrainment rates were specified between the source area and the fan apex to achieve the final 'best estimate' volumes. BGC estimated the initial volumes from field observations of locations of potentially deforming rock slopes, lidar interpretation, and engineering judgement. BGC estimated entrainment based on field estimates of the depths of entrainable material along the potential runout path.

BGC modelled all debris flows as single events (as opposed to events involving multiple source failures and/or surges that result in the same total event volume). BGC used a constant unit weight of 18 kN/m^3 for all cases.

H.2.2.3. Resistance parameters

The Voellmy model is governed by two parameters: 1) a friction coefficient, f, which determines the slope angle on which material begins to deposit (i.e., if the friction coefficient is higher than the local slope gradient, material will decelerate and begin to deposit); and 2) a turbulence parameter, ξ, which produces a velocity-dependent resistance that tends to limit flow velocities (similar to air drag acting on a falling object).

BGC completed a parametric analysis to help narrow the range of plausible parameters to be used in later analysis. BGC selected the initial range of Voellmy parameters based on a regional study where six debris flow events from a variety of fans in southwestern BC were calibrated in DAN3D (Zubrycky et al., 2019), using the maximum volume scenario for Jason Creek. BGC evaluated the appropriateness of the parameter sets by comparing the impact area of the simulated event on the fan, with the assumption that the maximum volume event should approximately inundate to the fan toe, but not significantly beyond that, and by comparing the calculated peak discharge at the fan apex to empirical relationships for volume versus peak discharge, with the expectation that the two methods would produce similar peak discharges.

H.3. MODEL SCENARIOS

Different model scenarios were selected for the HEC-RAS models and the DAN3D models. These scenarios are discussed within this section.

H.3.1. HEC-RAS

BGC defined hazard scenarios for the representative return periods considered in the assessment. As the results of the numerical modelling were subsequently integrated into a risk

assessment, BGC assigned a conditional probability to each hazard scenario based on professional judgement in consideration of estimated culvert capacity and performance. When there is only one hazard scenario at a given return period, it has a conditional probability of 100%. When there are multiple hazard scenarios for a given return period, the total of the conditional probabilities of all the scenarios must sum to 100%. Slight changes in conditional probabilities are unlikely to affect the principal risk assessment results.

H.3.1.1. Mungye Creek

BGC used a single-phase model to simulate floods and debris floods, and a two-phase model to simulate the coarse front and muddy afterflow characteristic of debris flows (Appendix B) as described in Section H.4.2 and H.4.2. BGC used modelled floods, debris floods and debris flows to gain an understanding of potential depths, velocities, and areas inundated by Mungye Creek.

BGC modelled six scenarios on Mungye Creek (Table H-1).

Table H-1. Mungye Creek scenarios modelled in HEC-RAS.

Representative Return Period (years)	Process	Scenario Description	Conditional Probability[1.] (%)
20	Flood	Culvert blocked	50
		Culvert unblocked	50
50	Debris Flood (Type 1)	Culvert blocked	100
200	Debris Flood (Type 2)	Culvert blocked	100
500	Debris Flow	Culvert blocked	100
2,000	Debris Flow	Culvert blocked	100

Note:

1. Conditional probability is used in the risk assessment when multiple scenarios are included for a single return period. In these instances, the conditional probability is used to combine the result from the sub-scenarios and expresses the assessed likelihood of the sub-scenario. For every return period, the cumulative conditional probability of all sub-scenarios must total 100.

H.3.1.2. Jason Creek

BGC used a two-phase model to simulate the coarse front and muddy afterflow characteristic of debris flows (Appendix B) as described in Section H.4.2. BGC used modelled debris flows to gain an understanding of potential depths, velocities, and areas inundated by Jason Creek.

BGC modelled five scenarios on Jason Creek (Table H-2).

Table H-2. Jason Creek scenarios modelled in HEC-RAS.

Return Period (years)	Process	Scenario Description	Conditional Probability[1] (%)
20	Debris flow	Culverts blocked	100
50	Debris flow	Culverts blocked	100
200	Debris flow	Culverts blocked	100
500	Debris flow	Culverts blocked	100
2,000	Debris flow	Culverts blocked	100

Note:

1. Conditional probability is used in the risk assessment when multiple scenarios are included for a single return period. In these instances, the conditional probability is used to combine the result from the sub-scenarios and expresses the assessed likelihood of the sub-scenario. For every return period, the cumulative conditional probability of all sub-scenarios must total 100.

H.3.2. DAN3D

BGC chose DAN3D scenarios to estimate the effects of large debris flows triggered by distinct bedrock failures within the catchment area for Jason Creek. As opposed to selecting a volume from a return period as was completed for the HEC-RAS modelling, the volumes were estimated from analysis of the source area and estimated channel erosion yields. BGC used the F-M curve to infer the return period associated with the volume estimates. BGC modelled three scenarios with DAN3D, the best estimate for the 2,000-year return period is summarised in Table H-3.

Table H-3. DAN3D model scenarios.

Initial volume (m^3)	Final volume (m^3)	Approximate return period	Description
28,500	53,000	2,000-years	Rock slide-triggered debris flow with channel entrainment

BGC did not assign a conditional probability to the DAN3D model results as they informed the F - M relationship, hazard zonation, and risk assessment, but were not directly included.

One source location was considered in the modelling. Bedrock failures at other locations in the watershed could trigger debris flows. Regardless, experience with similar modelling on other projects indicates the impacts on the developed area of the fan are much more sensitive to the total volume of material arriving at the fan apex and the flow-resistance parameters used than they are to the location of the initial failure.

H.4. HEC-RAS MODEL INPUTS AND ASSUMPTIONS

H.4.1. Floods and Debris Floods

BGC modelled floods and debris floods with the hydrographs developed using HEC HMS modelling software (Appendix G) and assuming Newtonian conditions over the full duration of the hydrograph.

H.4.2. Debris Flows

Debris flows were modelled in HEC-RAS using the Bingham rheological model, which is parameterized by the dynamic viscosity[1] of the flow and the yield strength[2]. A material's rheology defines how it behaves under stress. Clearwater has a linear stress-strain relationship and deforms under any stress that is applied. A "Bingham" fluid also has a linear stress-strain relationship but requires that a certain threshold of stress is applied before the fluid deforms, in other words, it behaves more like warm ketchup than water when flowing downhill.

BGC split the model to simulate a quasi-two-phase flow. Debris flows are often characterized by a rigid viscous portion, and a more liquid afterflow. The more rigid plug (hereafter referred to as the 'coarse front') consists of large boulders and often trees that slow the flow through frictional resistance. Once that load has been deposited where the channel loses confinement, the more liquid, and often faster afterflow (hereafter referred to as the 'muddy afterflow') overshoots or bypasses the freshly deposited coarse front. This phenomenon is not easily simulated in a single rheology model. Multi-rheological models exist but are not yet readily available in a format easily applicable to consulting projects. To model debris flows as realistically as possible, BGC split the model into a more viscous and less viscous flow phase.

BGC modelled the coarse front (the more viscous phase) based on the frequency – magnitude relationship and associated peak flows discussed in Appendix G. BGC ended the simulation when the hydrograph was complete, and added the deposit of the coarse front to the base topography to allow a realistic representation of the obstruction caused by this phase of flow. BGC then ran the muddy afterflow phase over this altered topography until steady state was reached.

H.4.3. Model Geometry

BGC selected the domain (the area included in the model run) for each model to include the entire fan extent and the area beyond, so that debris floods and debris flows can outflow beyond the fan-delta boundaries, and any boundary conditions do not impact the model results. In this manner any overland flooding including avulsions are captured within the domain. Detailed topographic data of the channels and floodplain were available from the 2022 high resolution lidar. BGC used this lidar to generate a high-resolution digital elevation model (DEM) for the model terrain. BGC assumed that water depths in the channels were low, or the channel was dry at the

[1] Dynamic viscosity is the resistance to movement of one layer of a fluid over another.

[2] A fluid yield strength is a characteristic whereby the material does not flow unless the applied stress exceeds a certain value greater than zero. The yield strength is therefore defined as the stress that must be applied to the sample before it starts to flow.

time the lidar was flown and the channel topography was reasonably well-represented without requiring additional survey.

BGC developed the general mesh for each site with a 2 m grid, and used additional break lines to refine spatial discretization to capture important topographic features, such as the stream channel, and roadways.

H.4.4. Model Roughness

The values used for hydraulic roughness in the HEC-RAS 2D models are represented by Manning's roughness coefficients (Manning's *n*). The roughness coefficient defines the frictional resistance of the terrain to flow. Channels, fan surfaces, and roads should be assigned unique Manning's *n* values. These can be estimated using the empirical equations of Jarrett (1984) and Zimmerman (2010), which were developed for steep creeks of varying slopes. Additionally, several authors have proposed that, in mobile-bed rivers, channel adjustment limits Froude numbers from exceeding 1, except for short distances or short periods of time (e.g., Piton, 2019; Jarrett, 1984; Grant, 1997). Creek morphology varies between steep creeks, so unique values for each creek need to be selected to provide defensible results for each location. BGC selected appropriate in-channel Manning's *n* values using cross-sections measured along creeks and bed material grain size sampling along with channel slope estimates from lidar. The calculated values can vary along the length of a channel, but a typical Manning's *n* value can be selected for each stream within the range calculated and that maintains a Froude number below 1 (i.e., subcritical flow) along the channel except in particularly steep or constricted sections (e.g., bridges) under 1 in 20-year flood conditions. Floodplain values can be estimated through associating different land cover types with different values of Manning's *n*.

BGC estimated the Manning's n values by associating different land cover types with different values of Manning's n as summarized in Table H-4.

Table H-4. Assumed Manning's n-values for the Mungye and Jason Creek flood, debris flood, and debris-flow modeling.

Land Cover Layer	Manning's n
Channel	0.08
Road	0.01
Fan (other)	0.06

H.4.5. Boundary Conditions

The Mungye Creek downstream boundary conditions consisted of a normal depth of 0.01 m/m applied at Reid Road, a steady stage hydrograph of 412 m applied at Ivey Lake, and a normal depth of 0.09 m/m applied along Mungye Creek downstream of the fan boundary. The normal depth gradients and stage hydrograph were measured from the lidar.

The Jason Creek downstream boundary conditions consisted of a normal depth boundary of 0.02 m/m applied along Reid Road downstream of the lower fan, a normal depth boundary of 0.06 m/m along Jason Creek downstream of the lower fan.

All downstream boundary conditions were sufficiently distal to the areas of interest, that they did not impact modelling results. BGC applied an upstream boundary condition of inflow hydrographs to each creek.

H.4.5.1. Inflow Hydrographs

H.4.5.1.1 Floods and Debris Floods

BGC developed inflow hydrographs for flood and debris-flood modelling on Mungye Creek through rainfall-runoff modelling using the software HEC HMS, as described in Appendix G.

H.4.5.1.2 Debris Flows

The upstream boundary condition to each debris flow model is a flow hydrograph shaped roughly like a triangle with the rising limb of the hydrograph being 1/6 of the total flow hydrograph duration as informed by doctoral thesis research on debris-flow behaviour. The simplified flow hydrographs are bulked and thus include sediment in the flow assuming a constant sediment volumetric concentration (Cv) of approximately 50%, which is typical for debris flows. The triangular flow hydrograph shape and duration is set to transport the estimated volume of sediment/debris associated with each return period peak flow being modelled.

H.4.6. Rheology Calibration

BGC calibrated the rheological parameters of the debris-flow model to the observed November 2021 events on Jason Creek. The approximate deposition extents of this event were mapped, and the rheological parameters were varied to match the modelled event to the observed extents.

BGC calibrated the rheological parameters of the coarse front phase by varying first the yield strength and then the dynamic viscosity of the modelled November 2021 event, which had an estimated volume of 7,000 m^3. BGC varied the yield strength between 100 and 5,000 Pa, and the dynamic viscosity between 1 and 1,000 Pa*s.

BGC calibrated the rheological parameters of the muddy afterflow phase to allow flow across the entire fan, reaching the lower fan, which would be expected for this flow phase. The calibrated rheological input parameters used for modelled debris flows are listed in Table H-5.

Table H-5. Final model rheological parameters following model calibration.

Model Phase	Rheological Parameter	Value
Coarse Front	Yield strength, τ_y (Pa)	2,500
	Dynamic Viscosity, μ_m (Pa*s)	500
Muddy Afterflow	Yield strength, τ_y (Pa)	100
	Dynamic Viscosity, μ_m (Pa*s)	1

H.4.7. Model Sensitivity and Parametrization

Sensitivity modeling consists of identifying the model input parameters that are uncertain (i.e., cannot be directly measured or calculated) to examine the extent to which the parameters affect model outcome. The uncertain parameters of the model include, but are not limited to:

- The roughness coefficient, Manning's n.
- The volumetric concentration of sediment in the flow over the duration of the hydrograph.
- The rheological parameters: dynamic viscosity and yield strength of the fluid flow.

BGC completed a sensitivity analysis by varying the parameters listed above, and comparing depositional area, depths, and velocities between model variations. BGC used morphological clues and geoscientific reasoning to select the most realistic model parameters. The sensitivity parameters and results are presented in Table H-6.

Table H-6. Model sensitivity.

Parameter	Variance	Model Sensitivity	Notes
Manning's roughness coefficient	+/- 20%	Medium	The modelled flow area was largely unaffected by this change, but the depth and velocity were somewhat sensitive to the Manning's roughness coefficient.
Volumetric concentration of sediment in flow	+/-25%	Medium	The model was somewhat sensitive to the volumetric concentration of sediment in the flow. Varying the volumetric concentration of sediment from 25% to 75% impacted the velocity, depth, and flow area.
Rheology (dynamic viscosity and yield strength)	Credible minimum to credible maximum (reference Section H.4.6)	Medium	The model was sensitive to the dynamic viscosity and yield strength of the fluid flow (Section H.4.6).

H.5. DAN3D MODEL SELECTION AND MODIFICATION

BGC completed a parametric analysis of the flow resistance parameters by systematically testing combinations of f = 0.1, 0.12, 0.15, and 0.2, and ξ = 50, 100, 200, and 500 m/s^2. All simulations used the following inputs, selected based on experience with other debris-flow models:

- 4,000 particles and a smoothing length constant of 6
- Stiffness coefficient of 200
- Velocity smoothing coefficient of 0.01
- Internal friction angle of 35°
- Erosion rate of 0.00245.

Additional details on these model parameters can be found in McDougall & Hungr (2004; 2005).

BGC compared the total impact area to the fan boundary, and discharge calculated at the fan apex to assess which parameter combinations were reasonable for this site (Figures H-1 through H-4). Based on the results presented, BGC selected the following flow-resistance parameters:

- f = 0.12, ξ = 100 m/s^2;
- f = 0.15, ξ = 100 m/s^2; and,
- f = 0.15, ξ = 200 m/s^2.

BGC used the gridded model depth and velocity results output at 1-second increments to calculate the maximum impact intensity at any time in the model for the selected flow-resistance parameters.

BGC assessed one avulsion scenario involving a culvert blockage at Reid Road to assess the sensitivity of the runout model results to this scenario. BGC modelled the avulsion scenario by manually modifying the topography at Reid Road to block the channel in the vicinity of the culvert. The avulsion scenario did not have a substantial influence on the area inundated or the impact intensities at the elements at risk.

H.6. MODEL RESULTS

H.6.1. HEC-RAS Model Results

HEC-RAS model results are presented in Figures H-1 to H-11. The results informed the composite hazard map (Appendix I). The results are presented as intensity (flow depth x velocity^2) which is a measure of the destructive potential of flows and informs the risk assessment. The intensity shown is the maximum combined intensity of the coarse front and muddy afterflow. The model results are discussed more thoroughly in the main body of this report.

H.7. UNCERTAINTIES AND LIMITATIONS OF NUMERICAL MODELLING

BGC numerical modelled of floods, debris floods, and debris flows on the study creeks. This section summarizes the uncertainties and limitations associated with the modelling approach applied by BGC to assess potential impacts of these hazards. The uncertainties and limitations can be categorized according to the random nature of natural processes, model inputs, and model limitations as follows:

- Natural Processes
    - Steep creek hazards are natural processes with complex behavioural feedback mechanisms associated with meteorological, orographic, and topographic factors. Such interactions are complicated by future change associated with a changing climate and natural or man-made modifications to the landscape. Given this, there is a stochastic or unpredictable nature to these process types that lead to inherent uncertainty and limitations to the accuracy of numerical models.
- Model Inputs
    - The lidar-derived topography from 2022 is a ‘snapshot in time’. Future modification of the landscape will influence the flow behaviour.
    - The topography is ‘bare-earth’ meaning it does not include three-dimensional natural (e.g., trees) and man-made (e.g., buildings) structures that influence flow behaviour through flow restriction, concentration, and redirection.

  - Actual debris-flow rheology and surge sequencing (single vs. multiple surges) cannot be predicted with certainty, as rheology may vary depending on debris-flow triggering (in-channel vs. triggered by a debris avalanche) or grain sizes (high proportion of ash in post-fire debris flows vs. “normal” debris flows).

- Model limitations
  - HEC-RAS does not compute channel aggradation, bank erosion, or super-elevation of flow around channel bends. As such there is uncertainty in the precise flow behavior of each modelled scenario, as each of these factors can influence the flow path(s) and associated impact forces.
  - DAN3D utilizes a coarser topography model than HEC-RAS (3 m grid versus 1 m) and will not include topographic features that are smaller scale than the grid resolution used. Experience with the model on similar projects shows that the influence of small scale topography on events of the magnitude modelled with DAN3D is minor.
  - Neither model explicitly represents boulders and large woody debris that can cause channel or culvert blockages, so these behaviours need to be addressed by manual topographic model modifications informed by expert judgement.

The influence of future modifications in the study creek watersheds and fan areas (e.g., associated with mitigation) should be reviewed to determine if there is a resultant change in the hazard and risk.

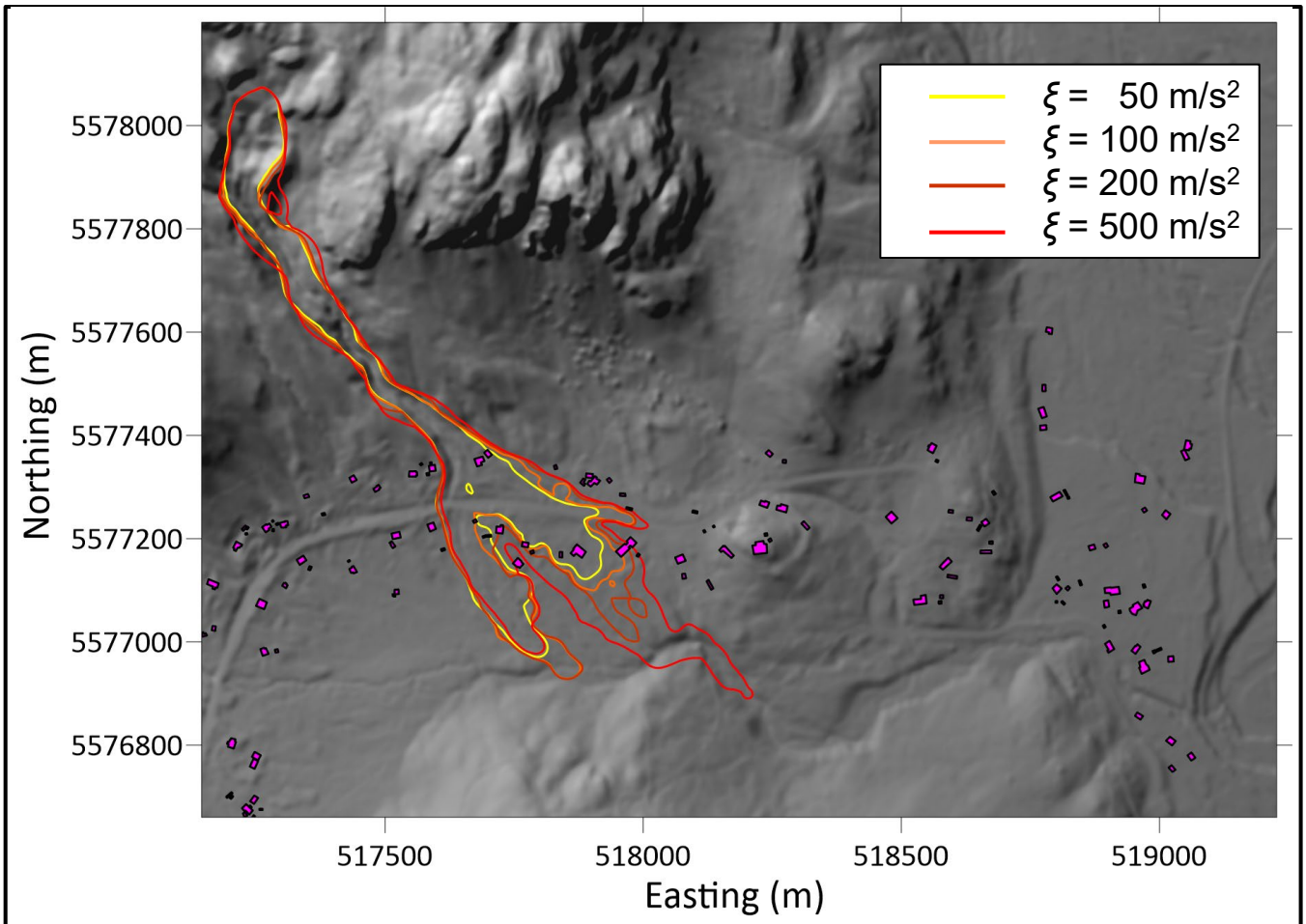

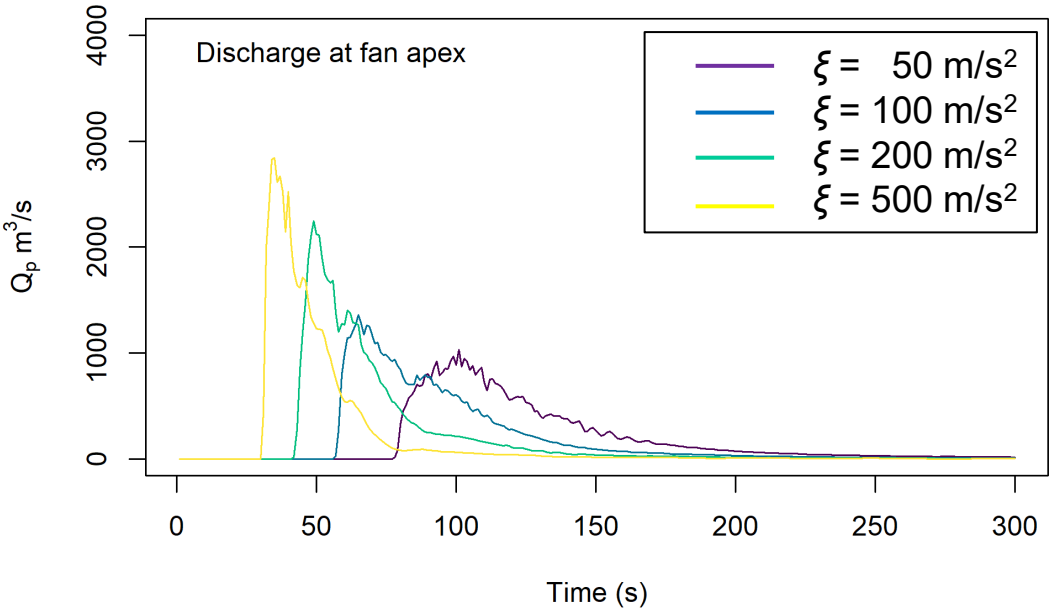

NOTES:

1. THIS FIGURE SHOULD BE READ IN CONJUNCTION WITH BGC'S REPORT TITLED 'QUANTITATIVE LANDSLIDE HAZARD AND RISK ASSESSMENT – REID ROAD AREA, ELECTORAL AREA C' AND DATED JANUARY 2023.
2. BASE TOPOGRAPHIC DATA BASED ON LIDAR PROVIDED BY McELHANNEY AND DATED JULY 22, 2022.
3. BUILDINGS DIGITIZED BY BGC.
4. MODEL IMPACT AREA RESULTS ARE FOR ALL AREAS WHERE SIMULATED FLOW DEPTHS ARE GREATER THAN OR EQUAL TO 0.3 m.
5. MODEL RESULTS ARE A SNAPSHOT IN TIME. CHANGES TO THE TOPOGRAPHY AND/OR ADDITION OF MITIGATION STRUCTURES MAY INFLUENCE THE FLOW PATTERNS AND BEHAVIOUR. MODEL RESULTS SHOULD BE REVIEWED AND REVISITED AFTER ANY SIGNIFICANT CHANGE.

PREPARED BY: AM	FIGURE TITLE: JASON CREEK – DAN3D PARAMETRIC ANALYSIS RESULTS, f = 0.1		
CHECKED BY: LCH	CLIENT: SQUAMISH – LILLOOET REGIONAL DISTRICT		
APPROVED BY: LCH	SCALE: 5CM: 200M	PROJECT NO: 1358010	FIGURE NO: H-1

0 5 10 mm in ANSI A sized paper

BGC ENGINEERING INC.

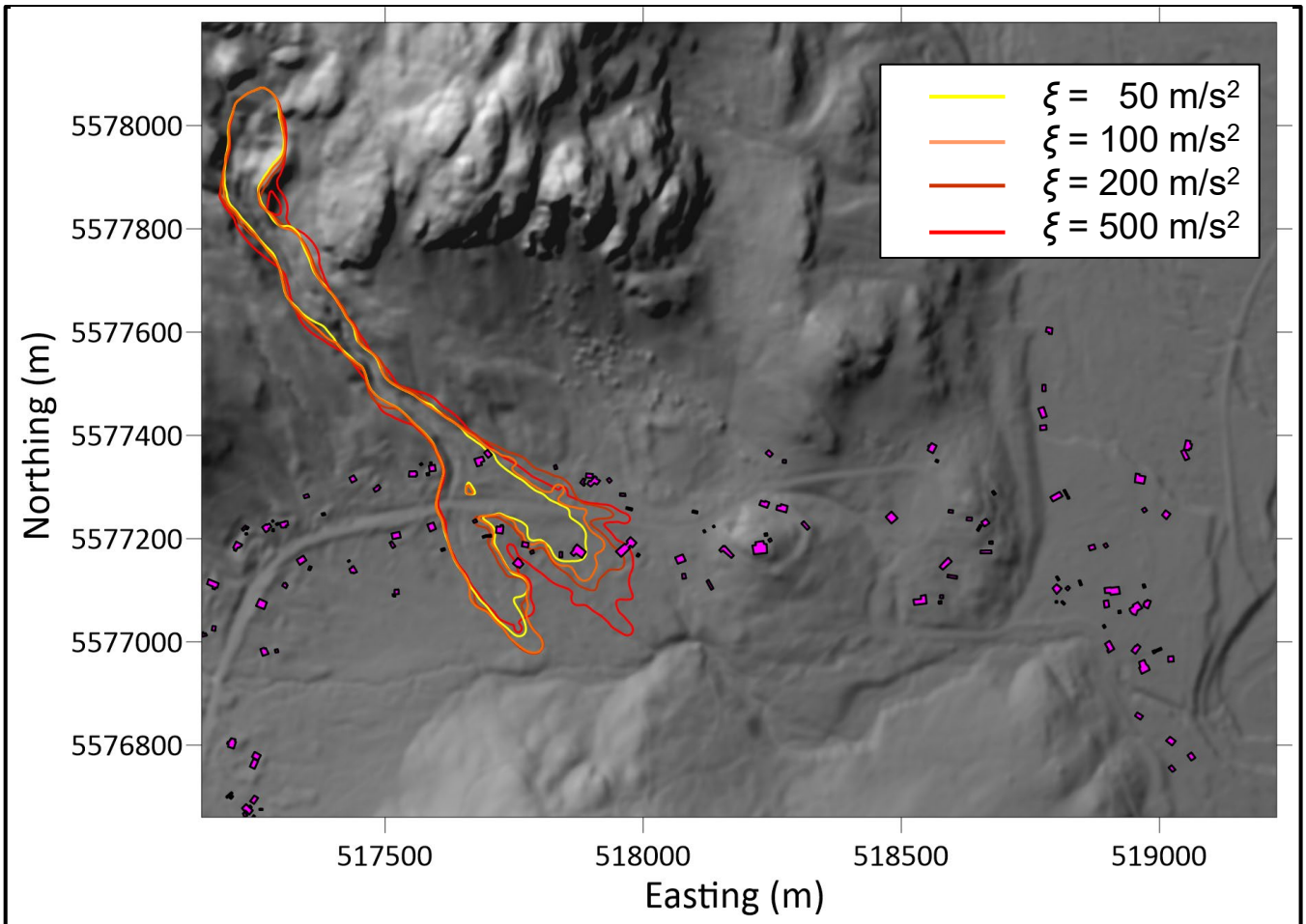

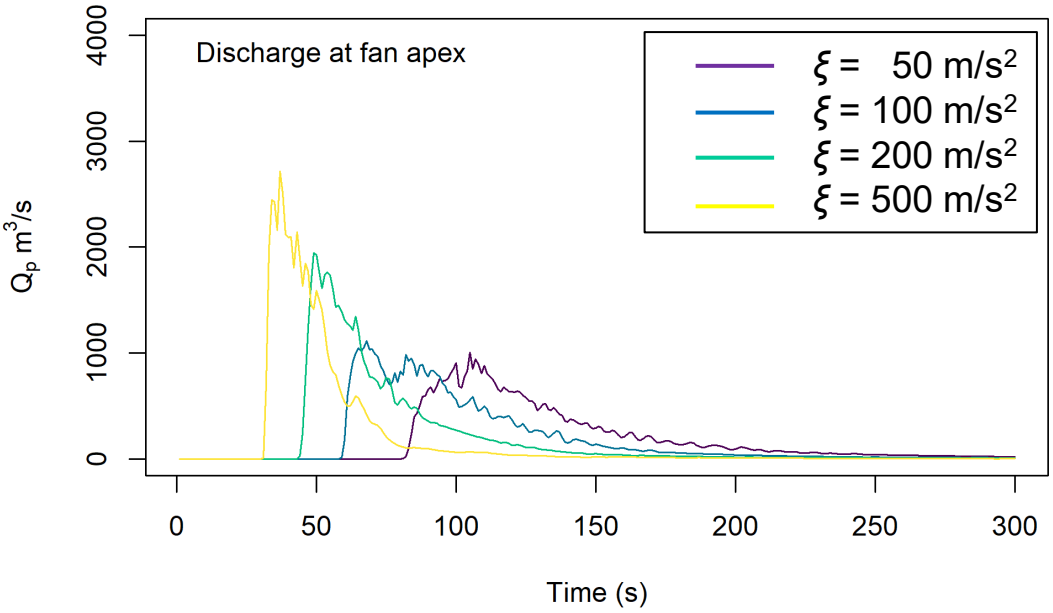

NOTES:

1. THIS FIGURE SHOULD BE READ IN CONJUNCTION WITH BGC'S REPORT TITLED 'QUANTITATIVE LANDSLIDE HAZARD AND RISK ASSESSMENT – REID ROAD AREA, ELECTORAL AREA C' AND DATED JANUARY 2023.
2. BASE TOPOGRAPHIC DATA BASED ON LIDAR PROVIDED BY McELHANNEY AND DATED JULY 22, 2022.
3. BUILDINGS DIGITIZED BY BGC.
4. MODEL IMPACT AREA RESULTS ARE FOR ALL AREAS WHERE SIMULATED FLOW DEPTHS ARE GREATER THAN OR EQUAL TO 0.3 m.
5. MODEL RESULTS ARE A SNAPSHOT IN TIME. CHANGES TO THE TOPOGRAPHY AND/OR ADDITION OF MITIGATION STRUCTURES MAY INFLUENCE THE FLOW PATTERNS AND BEHAVIOUR. MODEL RESULTS SHOULD BE REVIEWED AND REVISITED AFTER ANY SIGNIFICANT CHANGE.

PREPARED BY: AM	FIGURE TITLE: JASON CREEK – DAN3D PARAMETRIC ANALYSIS RESULTS, f = 0.12		
CHECKED BY: LCH	CLIENT: SQUAMISH – LILLOOET REGIONAL DISTRICT		
APPROVED BY: LCH	SCALE: 5CM: 200M	PROJECT NO: 1358010	FIGURE NO: H-2

0 5 10 mm in ANSI A sized paper

BGC ENGINEERING INC.

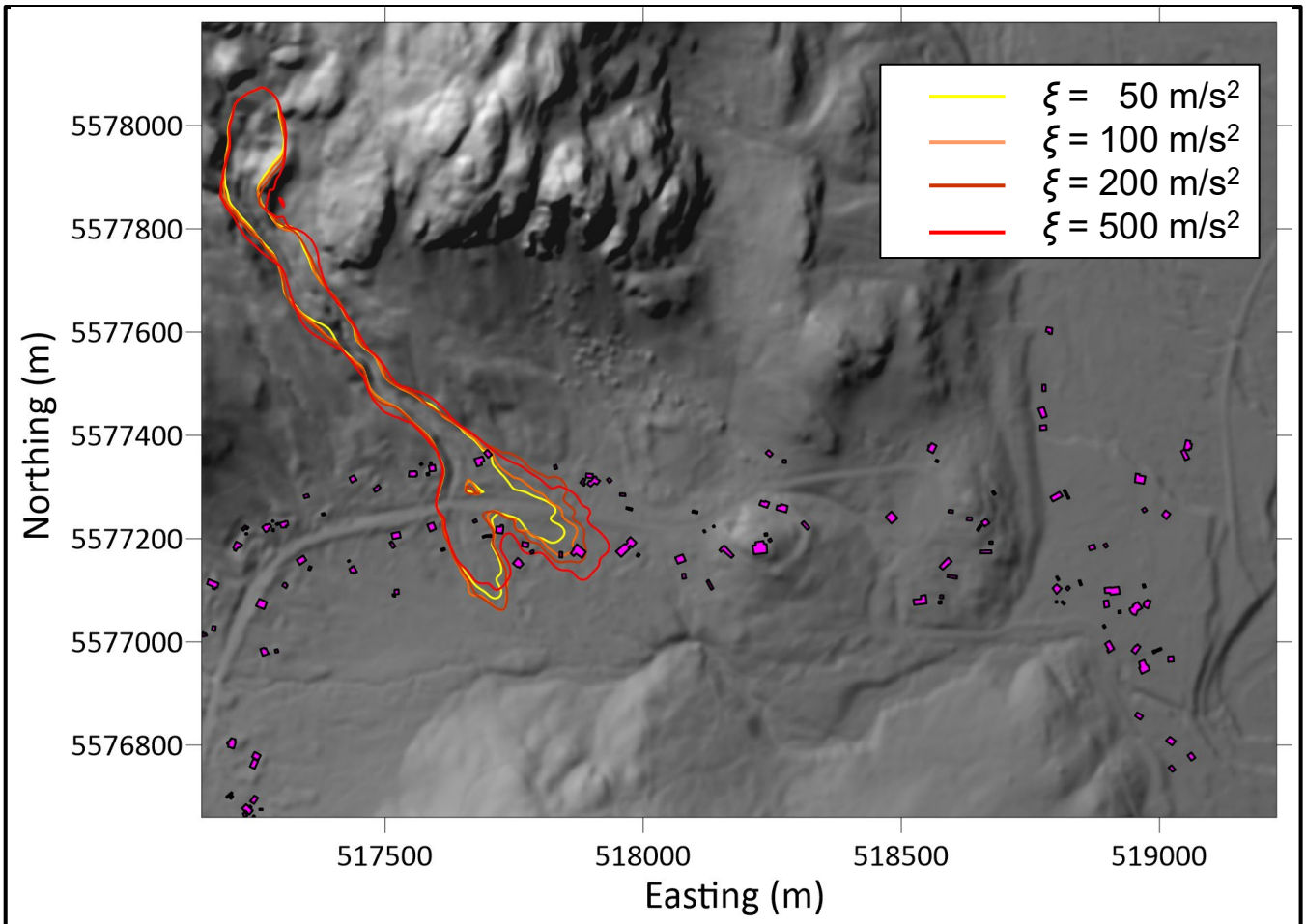

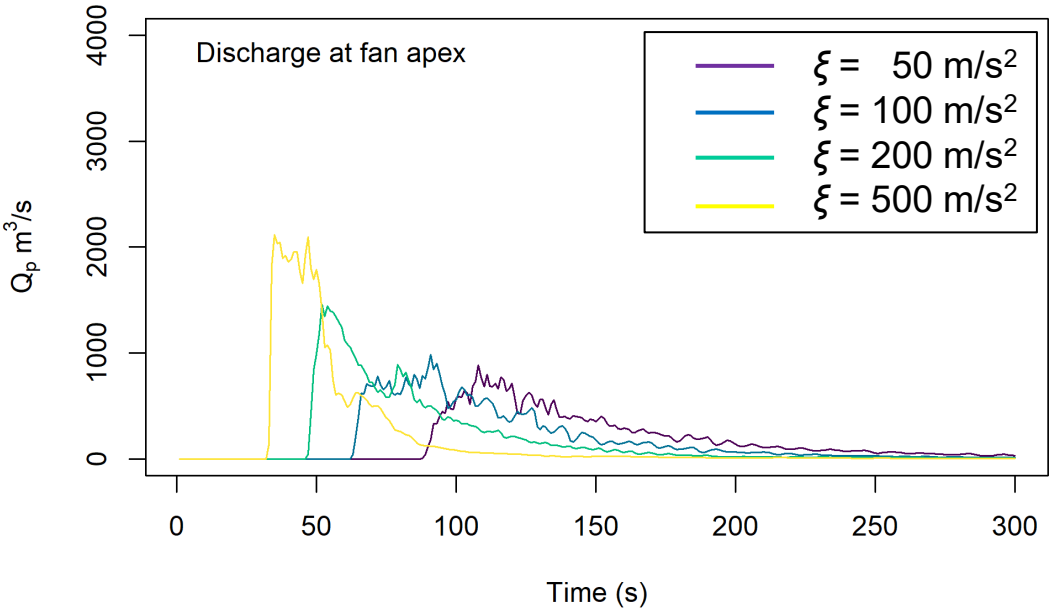

NOTES:

1. THIS FIGURE SHOULD BE READ IN CONJUNCTION WITH BGC'S REPORT TITLED 'QUANTITATIVE LANDSLIDE HAZARD AND RISK ASSESSMENT – REID ROAD AREA, ELECTORAL AREA C' AND DATED JANUARY 2023.
2. BASE TOPOGRAPHIC DATA BASED ON LIDAR PROVIDED BY McELHANNEY AND DATED JULY 22, 2022.
3. BUILDINGS DIGITIZED BY BGC.
4. MODEL IMPACT AREA RESULTS ARE FOR ALL AREAS WHERE SIMULATED FLOW DEPTHS ARE GREATER THAN OR EQUAL TO 0.3 m.
5. MODEL RESULTS ARE A SNAPSHOT IN TIME. CHANGES TO THE TOPOGRAPHY AND/OR ADDITION OF MITIGATION STRUCTURES MAY INFLUENCE THE FLOW PATTERNS AND BEHAVIOUR. MODEL RESULTS SHOULD BE REVIEWED AND REVISITED AFTER ANY SIGNIFICANT CHANGE.

PREPARED BY: AM	FIGURE TITLE: JASON CREEK – DAN3D PARAMETRIC ANALYSIS RESULTS, f = 0.15		
CHECKED BY: LCH	CLIENT: SQUAMISH – LILLOOET REGIONAL DISTRICT		
APPROVED BY: LCH	SCALE: 5CM: 200M	PROJECT NO: 1358010	FIGURE NO: H-3

0 5 10 mm in ANSI A sized paper

BGC ENGINEERING INC.

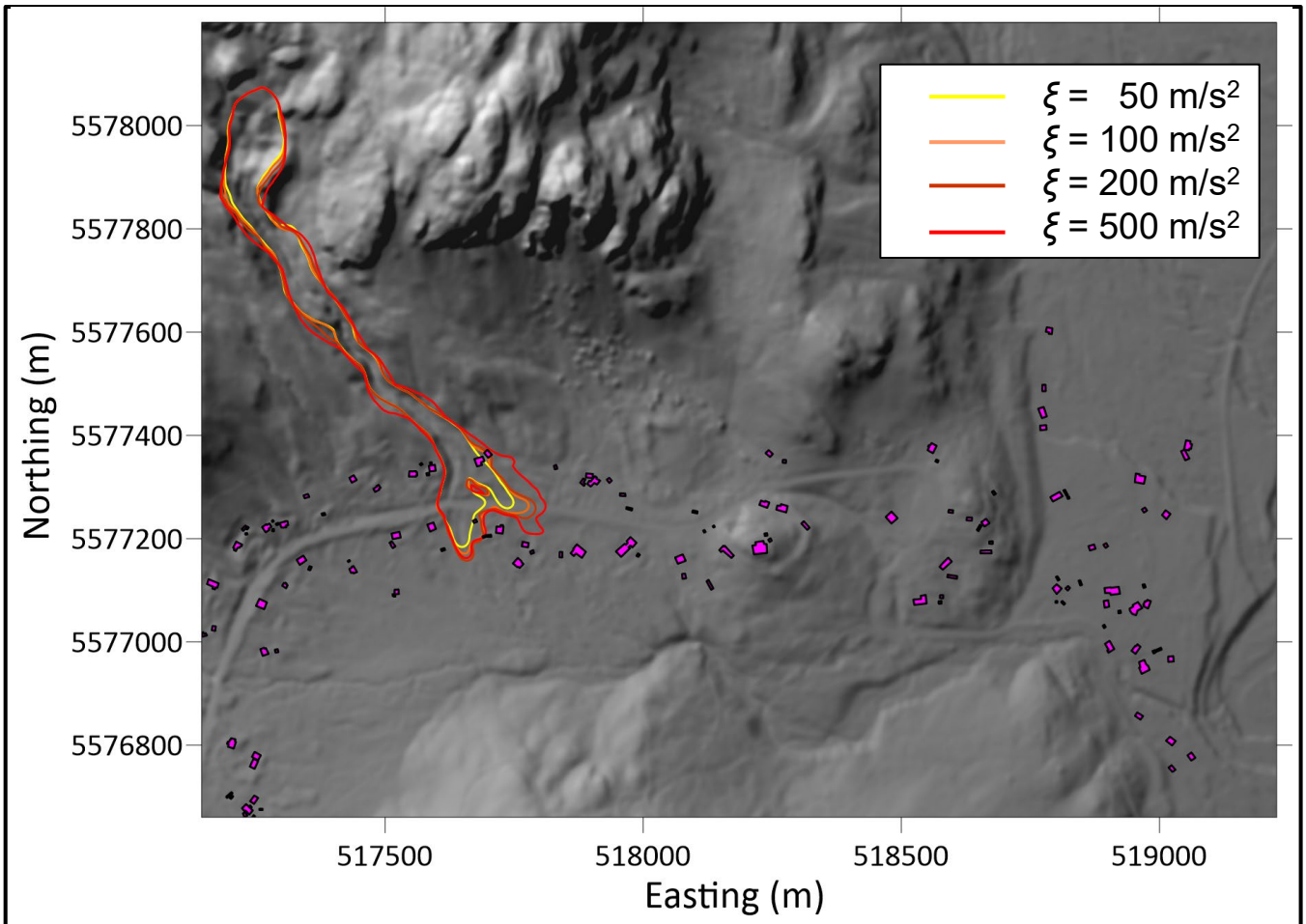

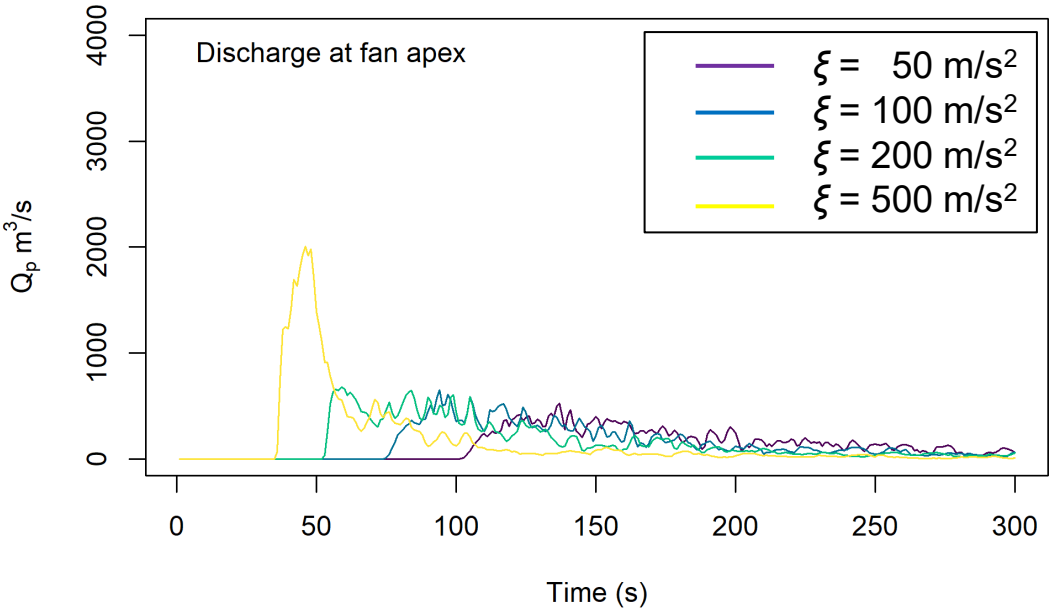

NOTES:

1. THIS FIGURE SHOULD BE READ IN CONJUNCTION WITH BGC'S REPORT TITLED 'QUANTITATIVE LANDSLIDE HAZARD AND RISK ASSESSMENT – REID ROAD AREA, ELECTORAL AREA C' AND DATED JANUARY 2023.
2. BASE TOPOGRAPHIC DATA BASED ON LIDAR PROVIDED BY McELHANNEY AND DATED JULY 22, 2022.
3. BUILDINGS DIGITIZED BY BGC.
4. MODEL IMPACT AREA RESULTS ARE FOR ALL AREAS WHERE SIMULATED FLOW DEPTHS ARE GREATER THAN OR EQUAL TO 0.3 m.
5. MODEL RESULTS ARE A SNAPSHOT IN TIME. CHANGES TO THE TOPOGRAPHY AND/OR ADDITION OF MITIGATION STRUCTURES MAY INFLUENCE THE FLOW PATTERNS AND BEHAVIOUR. MODEL RESULTS SHOULD BE REVIEWED AND REVISITED AFTER ANY SIGNIFICANT CHANGE.

PREPARED BY: AM	FIGURE TITLE: JASON CREEK – DAN3D PARAMETRIC ANALYSIS RESULTS, f = 0.2		
CHECKED BY: LCH	CLIENT: SQUAMISH – LILLOOET REGIONAL DISTRICT		
APPROVED BY: LCH	SCALE: 5CM: 200M	PROJECT NO: 1358010	FIGURE NO: H-4

0 5 10 mm in ANSI A sized paper

BGC ENGINEERING INC.

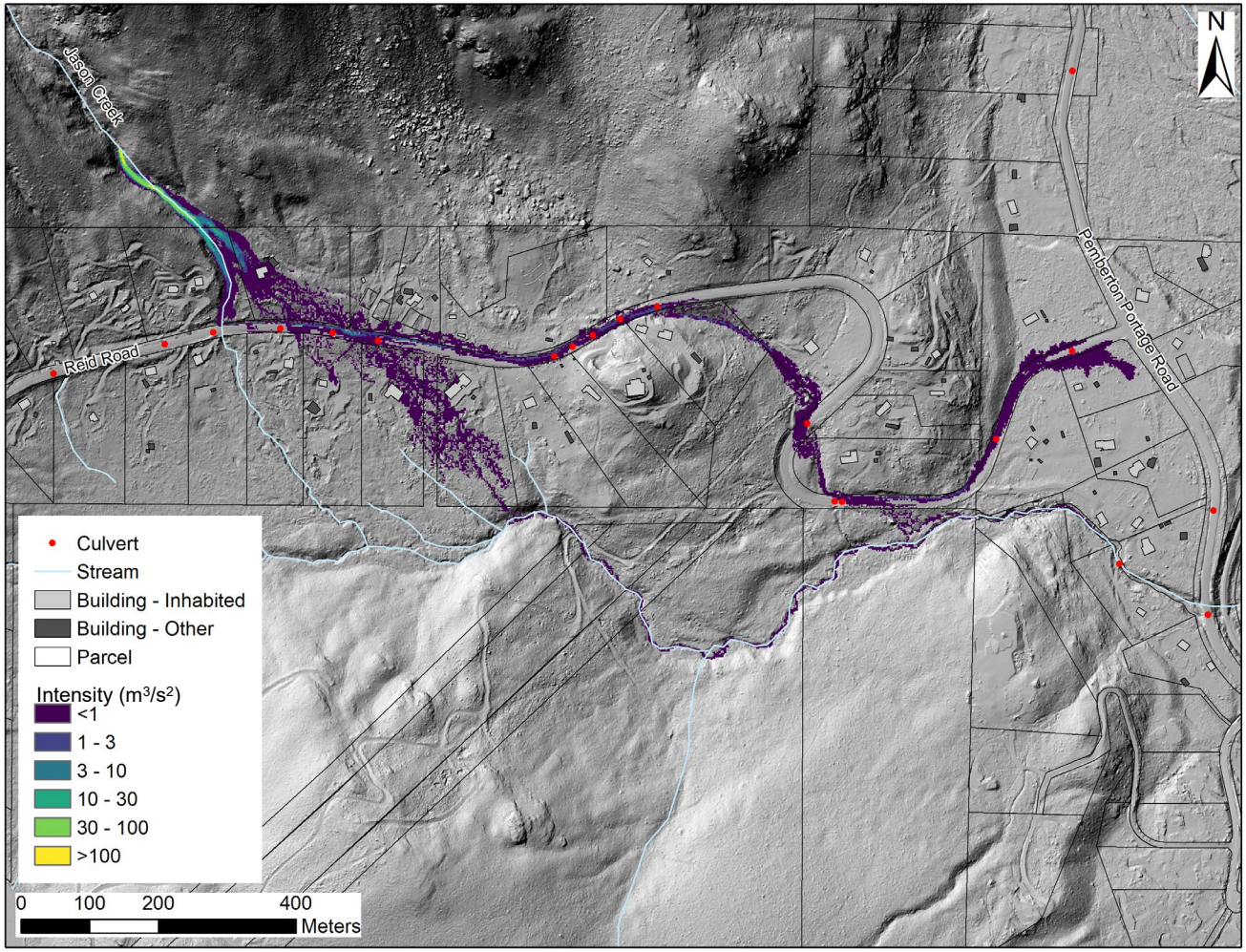

NOTES

1. THIS FIGURE SHOULD BE READ IN CONJUNCTION WITH BGC'S REPORT TITLED 'QUANTITATIVE LANDSLIDE HAZARD AND RISK ASSESSMENT – REID ROAD AREA, ELECTORAL AREA C' AND DATED JANUARY 2023
2. BASE TOPOGRAPHIC DATA BASED ON LIDAR PROVIDED BY MCELHANNEY AND DATED JULY 22, 2022.
3. BUILDINGS DIGITIZED BY BGC. BGC ASSESSED WHICH BUILDINGS WERE INHABITED BASED ON FIELD OBSERVATIONS, WHERE LANDOWNER PERMISSION TO ACCESS THE PROPERTY WAS PROVIDED. FOR OTHER BUILDINGS, BGC ASSESSED BASED ON SITE LAYOUT AND INTERPRETATION.
4. MODEL RESULTS ARE BASED ON THE MAXIMUM INTENSITY OF THE COARSE FRONT AND MUDDY AFTERFLOWS AS MODELLED BY BGC IN HEC-RAS. MODEL RESULTS.
5. MODEL RESULTS ARE A SNAPSHOT IN TIME. CHANGES TO THE TOPOGRAPHY AND/OR ADDITION OF MITIGATION STRUCTURES MAY INFLUENCE THE FLOW PATTERNS AND BEHAVIOUR. MODEL RESULTS SHOULD BE REVIEWED AND REVISITED AFTER ANY SIGNIFICANT CHANGE.

PREPARED BY:	FIGURE TITLE:		
HMS	JASON CREEK – 10 TO 30 YEAR RETURN PERIOD, CULVERTS BLOCKED		
CHECKED BY:	CLIENT:		
LCH	SQUAMISH – LILLOOET REGIONAL DISTRICT		
APPROVED BY:	SCALE:	PROJECT NO:	FIGURE NO:
LCH	1CM: 100M	1358010	H-5

0 5 10 mm in ANSI A sized paper

BGC ENGINEERING INC.

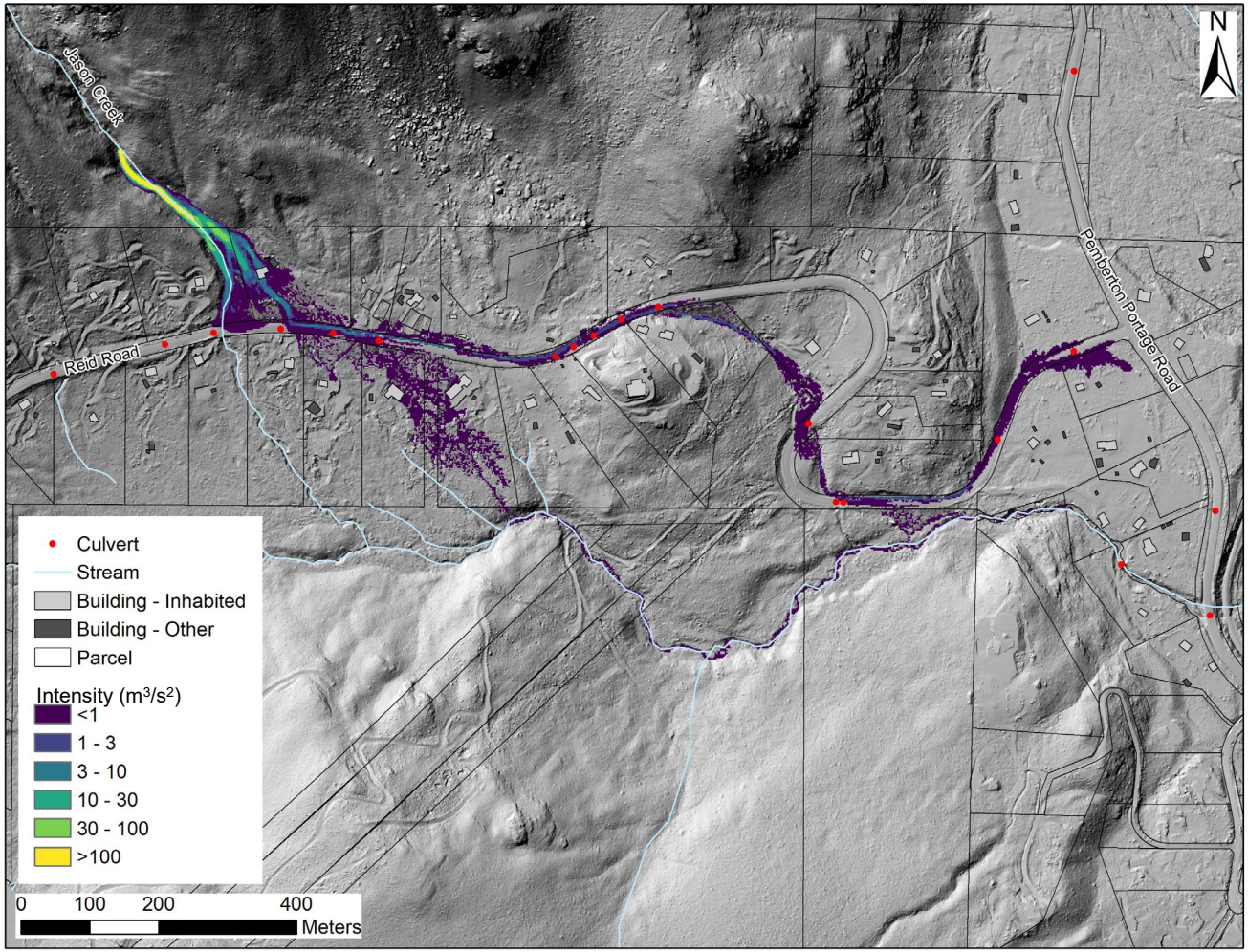

NOTES

1. THIS FIGURE SHOULD BE READ IN CONJUNCTION WITH BGC'S REPORT TITLED 'QUANTITATIVE LANDSLIDE HAZARD AND RISK ASSESSMENT – REID ROAD AREA, ELECTORAL AREA C' AND DATED JANUARY 2023.
2. BASE TOPOGRAPHIC DATA BASED ON LIDAR PROVIDED BY MCELHANNEY AND DATED JULY 22, 2022
3. BUILDINGS DIGITIZED BY BGC. BGC ASSESSED WHICH BUILDINGS WERE INHABITED BASED ON FIELD OBSERVATIONS, WHERE LANDOWNER PERMISSION TO ACCESS THE PROPERTY WAS PROVIDED. FOR OTHER BUILDINGS, BGC ASSESSED BASED ON SITE LAYOUT AND INTERPRETATION.
4. MODEL RESULTS ARE BASED ON THE MAXIMUM INTENSITY OF THE COARSE FRONT AND MUDDY AFTERFLOWS AS MODELLED BY BGC IN HEC-RAS. MODEL MODEL RESULTS ARE A SNAPSHOT IN TIME. CHANGES TO THE TOPOGRAPHY AND/OR ADDITION OF MITIGATION STRUCTURES MAY INFLUENCE THE FLOW PATTERNS AND BEHAVIOUR. MODEL RESULTS SHOULD BE REVIEWED AND REVISITED AFTER ANY SIGNIFICANT CHANGE.

PREPARED BY: HMS	FIGURE TITLE: JASON CREEK – 30 TO 100 YEAR RETURN PERIOD, CULVERTS BLOCKED		
CHECKED BY: LCH	CLIENT: SQUAMISH – LILLOOET REGIONAL DISTRICT		
APPROVED BY: LCH	SCALE: 1CM: 100M	PROJECT NO: 1358010	FIGURE NO: H-6

0 5 10 mm in ANSI A sized paper

BGC ENGINEERING INC.

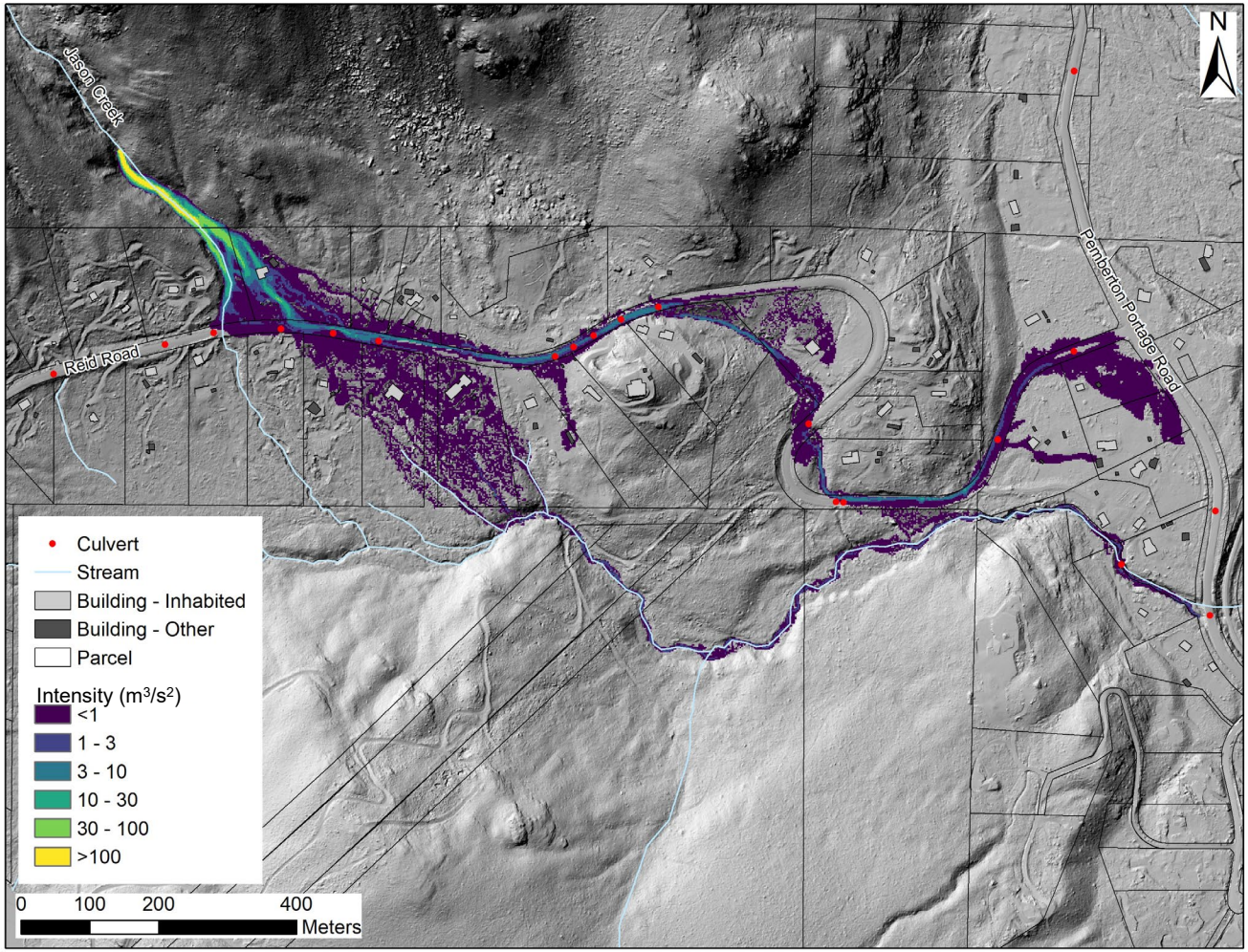

NOTES

1. THIS FIGURE SHOULD BE READ IN CONJUNCTION WITH BGC'S REPORT TITLED 'QUANTITATIVE LANDSLIDE HAZARD AND RISK ASSESSMENT – REID ROAD AREA, ELECTORAL AREA C' AND DATED JANUARY 2023.
2. BASE TOPOGRAPHIC DATA BASED ON LIDAR PROVIDED BY MCELHANNEY AND DATED JULY 22, 2022.
3. BUILDINGS DIGITIZED BY BGC. BGC ASSESSED WHICH BUILDINGS WERE INHABITED BASED ON FIELD OBSERVATIONS, WHERE LANDOWNER PERMISSION TO ACCESS THE PROPERTY WAS PROVIDED. FOR OTHER BUILDINGS, BGC ASSESSED BASED ON SITE LAYOUT AND INTERPRETATION.
4. MODEL RESULTS ARE BASED ON THE MAXIMUM INTENSITY OF THE COARSE FRONT AND MUDDY AFTERFLOWS AS MODELLED BY BGC IN HEC-RAS. MODEL
5. MODEL RESULTS ARE A SNAPSHOT IN TIME. CHANGES TO THE TOPOGRAPHY AND/OR ADDITION OF MITIGATION STRUCTURES MAY INFLUENCE THE FLOW PATTERNS AND BEHAVIOUR. MODEL RESULTS SHOULD BE REVIEWED AND REVISITED AFTER ANY SIGNIFICANT CHANGE.

PREPARED BY:	FIGURE TITLE:		
HMS	JASON CREEK – 100 TO 300 YEAR RETURN PERIOD, CULVERTS BLOCKED		
CHECKED BY:	CLIENT:		
LCH	SQUAMISH – LILLOOET REGIONAL DISTRICT		
APPROVED BY:	SCALE:	PROJECT NO:	FIGURE NO:
LCH	1CM: 100M	1358010	H-7

0 5 10 mm in ANSI A sized paper

BGC ENGINEERING INC.

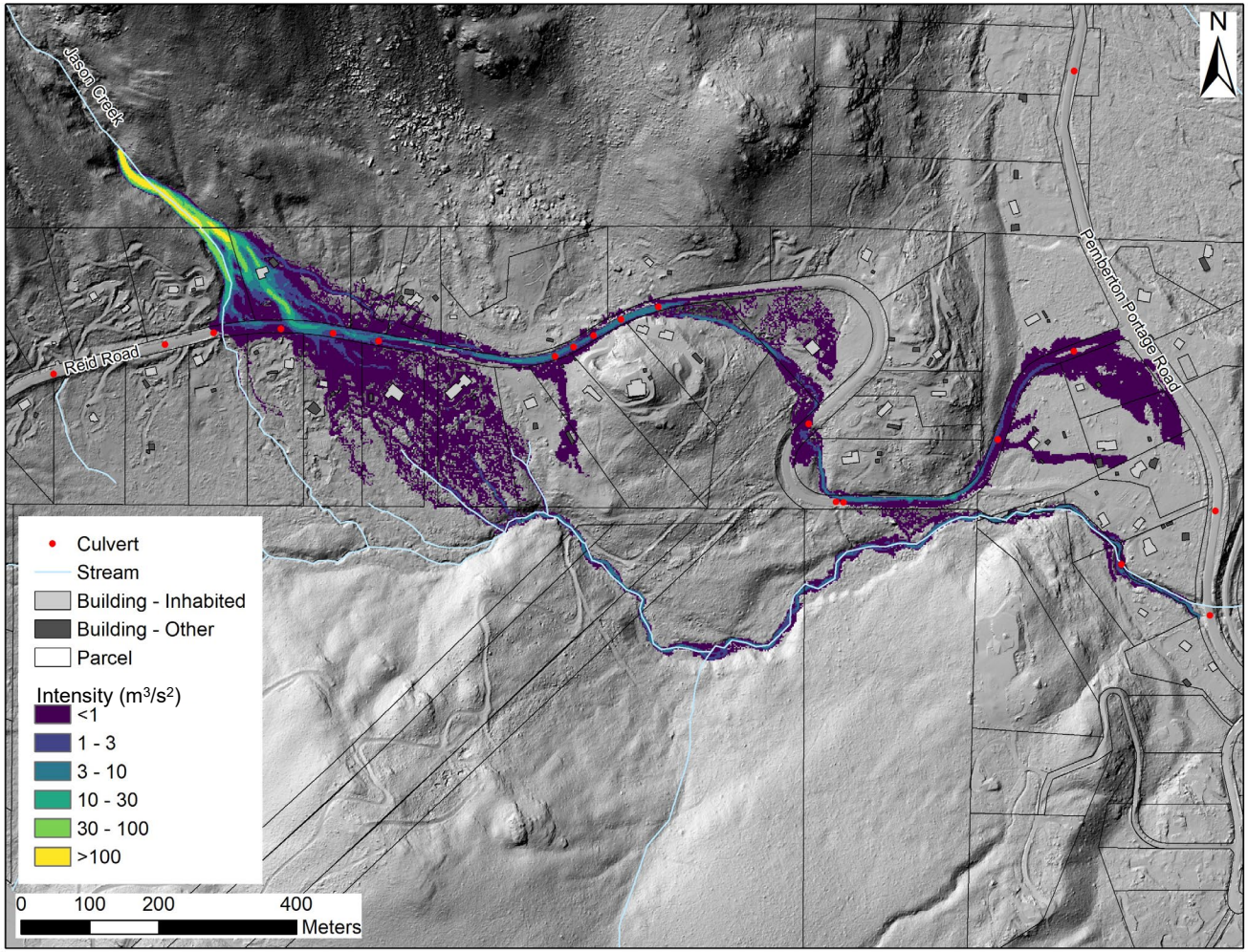

NOTES

1. THIS FIGURE SHOULD BE READ IN CONJUNCTION WITH BGC'S REPORT TITLED 'QUANTITATIVE LANDSLIDE HAZARD AND RISK ASSESSMENT – REID ROAD AREA, ELECTORAL AREA C' AND DATED JANUARY 2023.
2. BASE TOPOGRAPHIC DATA BASED ON LIDAR PROVIDED BY MCELHANNEY AND DATED JULY 22, 2022.
3. BUILDINGS DIGITIZED BY BGC. BGC ASSESSED WHICH BUILDINGS WERE INHABITED BASED ON FIELD OBSERVATIONS, WHERE LANDOWNER PERMISSION TO ACCESS THE PROPERTY WAS PROVIDED. FOR OTHER BUILDINGS, BGC ASSESSED BASED ON SITE LAYOUT AND INTERPRETATION.
4. MODEL RESULTS ARE BASED ON THE MAXIMUM INTENSITY OF THE COARSE FRONT AND MUDDY AFTERFLOWS AS MODELLED BY BGC IN HEC-RAS. MODEL
5. MODEL RESULTS ARE A SNAPSHOT IN TIME. CHANGES TO THE TOPOGRAPHY AND/OR ADDITION OF MITIGATION STRUCTURES MAY INFLUENCE THE FLOW PATTERNS AND BEHAVIOUR. MODEL RESULTS SHOULD BE REVIEWED AND REVISITED AFTER ANY SIGNIFICANT CHANGE.

PREPARED BY:	FIGURE TITLE:		
HMS	JASON CREEK – 300 TO 1,000 YEAR RETURN PERIOD, CULVERTS BLOCKED		
CHECKED BY:	CLIENT:		
LCH	SQUAMISH – LILLOOET REGIONAL DISTRICT		
APPROVED BY:	SCALE:	PROJECT NO:	FIGURE NO:
LCH	1CM: 100M	1358010	H-8

0 5 10 mm in ANSI A sized paper

BGC ENGINEERING INC.

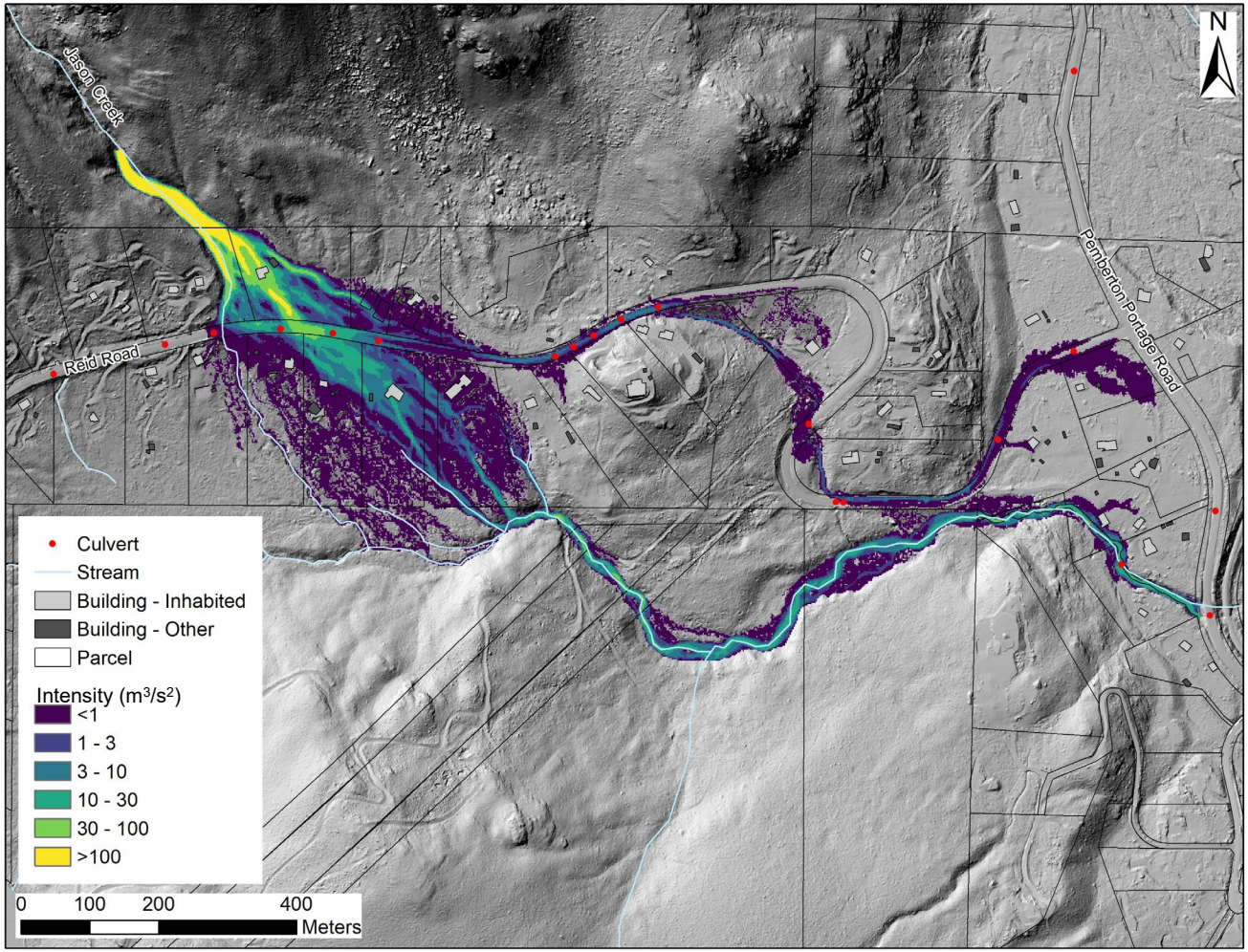

NOTES

1. THIS FIGURE SHOULD BE READ IN CONJUNCTION WITH BGC'S REPORT TITLED 'QUANTITATIVE LANDSLIDE HAZARD AND RISK ASSESSMENT – REID ROAD AREA, ELECTORAL AREA C' AND DATED JANUARY 2023.
2. BASE TOPOGRAPHIC DATA BASED ON LIDAR PROVIDED BY MCELHANNEY AND DATED JULY 22, 2022.
3. BUILDINGS DIGITIZED BY BGC. BGC ASSESSED WHICH BUILDINGS WERE INHABITED BASED ON FIELD OBSERVATIONS, WHERE LANDOWNER PERMISSION TO ACCESS THE PROPERTY WAS PROVIDED. FOR OTHER BUILDINGS, BGC ASSESSED BASED ON SITE LAYOUT AND INTERPRETATION.
4. MODEL RESULTS ARE BASED ON THE MAXIMUM INTENSITY OF THE COARSE FRONT AND MUDDY AFTERFLOWS AS MODELLED BY BGC IN HEC-RAS.
5. MODEL RESULTS ARE A SNAPSHOT IN TIME. CHANGES TO THE TOPOGRAPHY AND/OR ADDITION OF MITIGATION STRUCTURES MAY INFLUENCE THE FLOW PATTERNS AND BEHAVIOUR. MODEL RESULTS SHOULD BE REVIEWED AND REVISITED AFTER ANY SIGNIFICANT CHANGE.

PREPARED BY:	FIGURE TITLE:		
HMS	JASON CREEK – 1,000 TO 3,000 YEAR RETURN PERIOD, CULVERTS BLOCKED		
CHECKED BY:	CLIENT:		
LCH	SQUAMISH – LILLOOET REGIONAL DISTRICT		
APPROVED BY:	SCALE:	PROJECT NO:	FIGURE NO:
LCH	1CM: 100M	1358010	H-9

0 5 10 mm in ANSI A sized paper

BGC ENGINEERING INC.

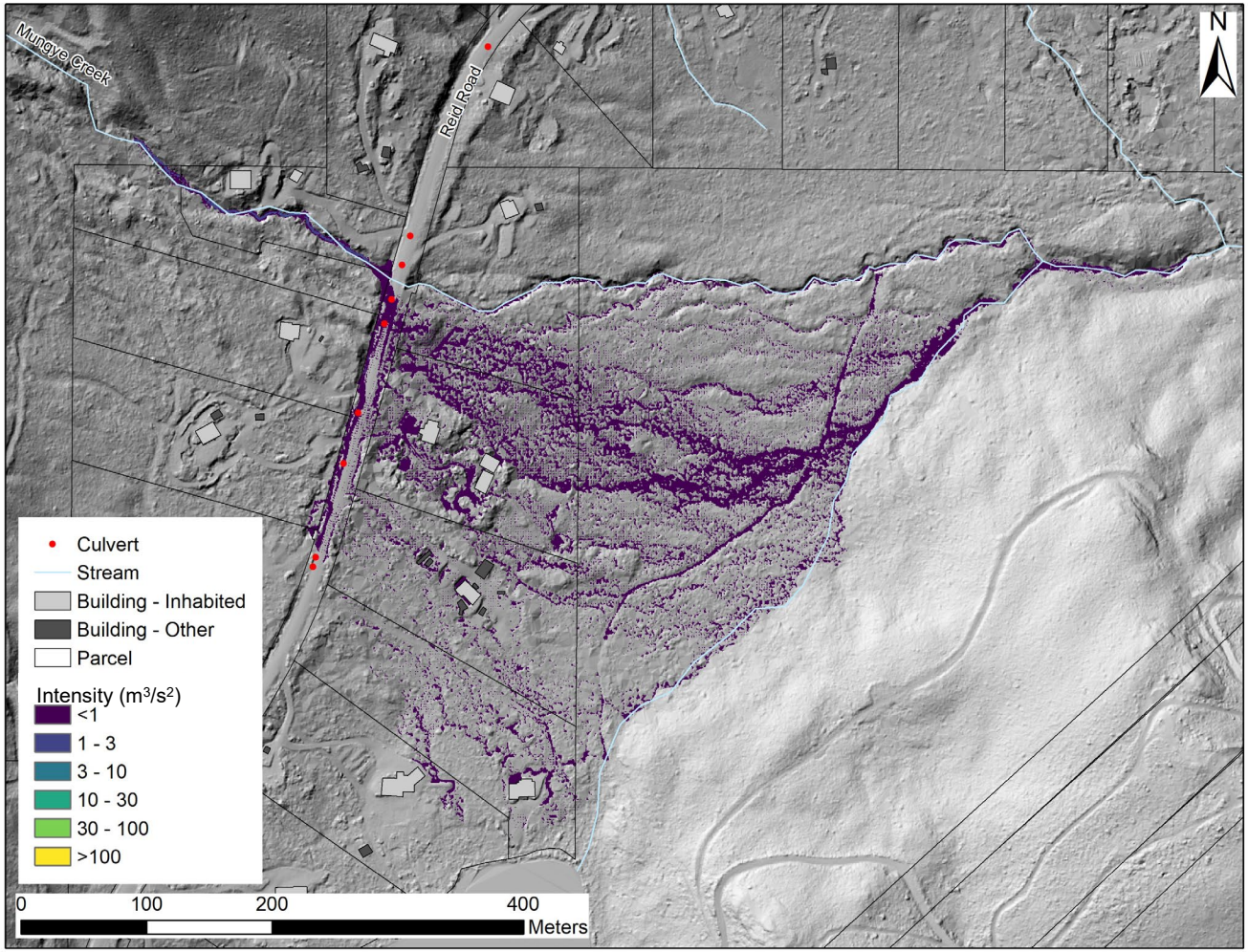

NOTES

1. THIS FIGURE SHOULD BE READ IN CONJUNCTION WITH BGC'S REPORT TITLED 'QUANTITATIVE LANDSLIDE HAZARD AND RISK ASSESSMENT – REID ROAD AREA, ELECTORAL AREA C' AND DATED JANUARY 2023.
2. BASE TOPOGRAPHIC DATA BASED ON LIDAR PROVIDED BY MCELHANNEY AND DATED JULY 22, 2022.
3. BUILDINGS DIGITIZED BY BGC. BGC ASSESSED WHICH BUILDINGS WERE INHABITED BASED ON FIELD OBSERVATIONS, WHERE LANDOWNER PERMISSION TO ACCESS THE PROPERTY WAS PROVIDED. FOR OTHER BUILDINGS, BGC ASSESSED BASED ON SITE LAYOUT AND INTERPRETATION.
4. MODEL RESULTS ARE BASED ON THE MAXIMUM INTENSITY OF THE COARSE FRONT AND MUDDY AFTERFLOWS AS MODELLED BY BGC IN HEC-RAS.
5. MODEL RESULTS ARE A SNAPSHOT IN TIME. CHANGES TO THE TOPOGRAPHY AND/OR ADDITION OF MITIGATION STRUCTURES MAY INFLUENCE THE FLOW PATTERNS AND BEHAVIOUR. MODEL RESULTS SHOULD BE REVIEWED AND REVISITED AFTER ANY SIGNIFICANT CHANGE.

PREPARED BY:	FIGURE TITLE:		
HMS	MUNGYE CREEK – 10 TO 30 YEAR RETURN PERIOD, CULVERTS BLOCKED		
CHECKED BY:	CLIENT:		
LCH	SQUAMISH – LILLOOET REGIONAL DISTRICT		
APPROVED BY:	SCALE:	PROJECT NO:	FIGURE NO:
LCH	7CM: 400M	1358010	H-10

0 5 10 mm in ANSI A sized paper

BGC ENGINEERING INC.

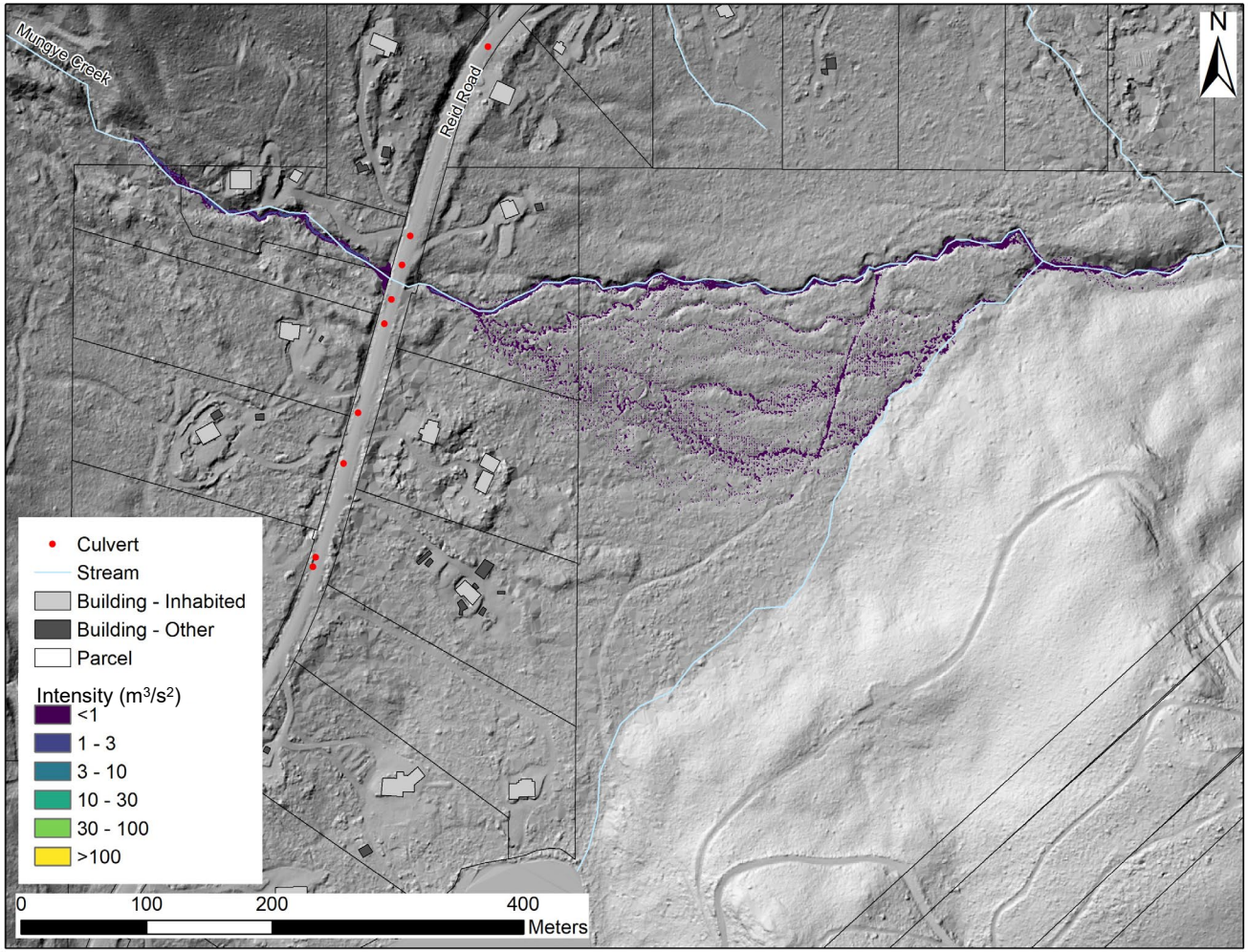

NOTES

1. THIS FIGURE SHOULD BE READ IN CONJUNCTION WITH BGC'S REPORT TITLED 'QUANTITATIVE LANDSLIDE HAZARD AND RISK ASSESSMENT – REID ROAD AREA, ELECTORAL AREA C' AND DATED JANUARY 2023.
2. BASE TOPOGRAPHIC DATA BASED ON LIDAR PROVIDED BY MCELHANNEY AND DATED JULY 22, 2022.
3. BUILDINGS DIGITIZED BY BGC. BGC ASSESSED WHICH BUILDINGS WERE INHABITED BASED ON FIELD OBSERVATIONS, WHERE LANDOWNER PERMISSION TO ACCESS THE PROPERTY WAS PROVIDED. FOR OTHER BUILDINGS, BGC ASSESSED BASED ON SITE LAYOUT AND INTERPRETATION.
4. MODEL RESULTS ARE BASED ON THE MAXIMUM INTENSITY OF THE COARSE FRONT AND MUDDY AFTERFLOWS AS MODELLED BY BGC IN HEC-RAS..
5. MODEL RESULTS ARE A SNAPSHOT IN TIME. CHANGES TO THE TOPOGRAPHY AND/OR ADDITION OF MITIGATION STRUCTURES MAY INFLUENCE THE FLOW PATTERNS AND BEHAVIOUR. MODEL RESULTS SHOULD BE REVIEWED AND REVISITED AFTER ANY SIGNIFICANT CHANGE.

PREPARED BY:	FIGURE TITLE:		
HMS	MUNGYE CREEK – 10 TO 30 YEAR RETURN PERIOD, CULVERTS UNBLOCKED		
CHECKED BY:	CLIENT:		
LCH	SQUAMISH – LILLOOET REGIONAL DISTRICT		
APPROVED BY:	SCALE:	PROJECT NO:	FIGURE NO:
LCH	7CM: 400M	1358010	H-11

0 5 10 mm in ANSI A sized paper

BGC ENGINEERING INC.

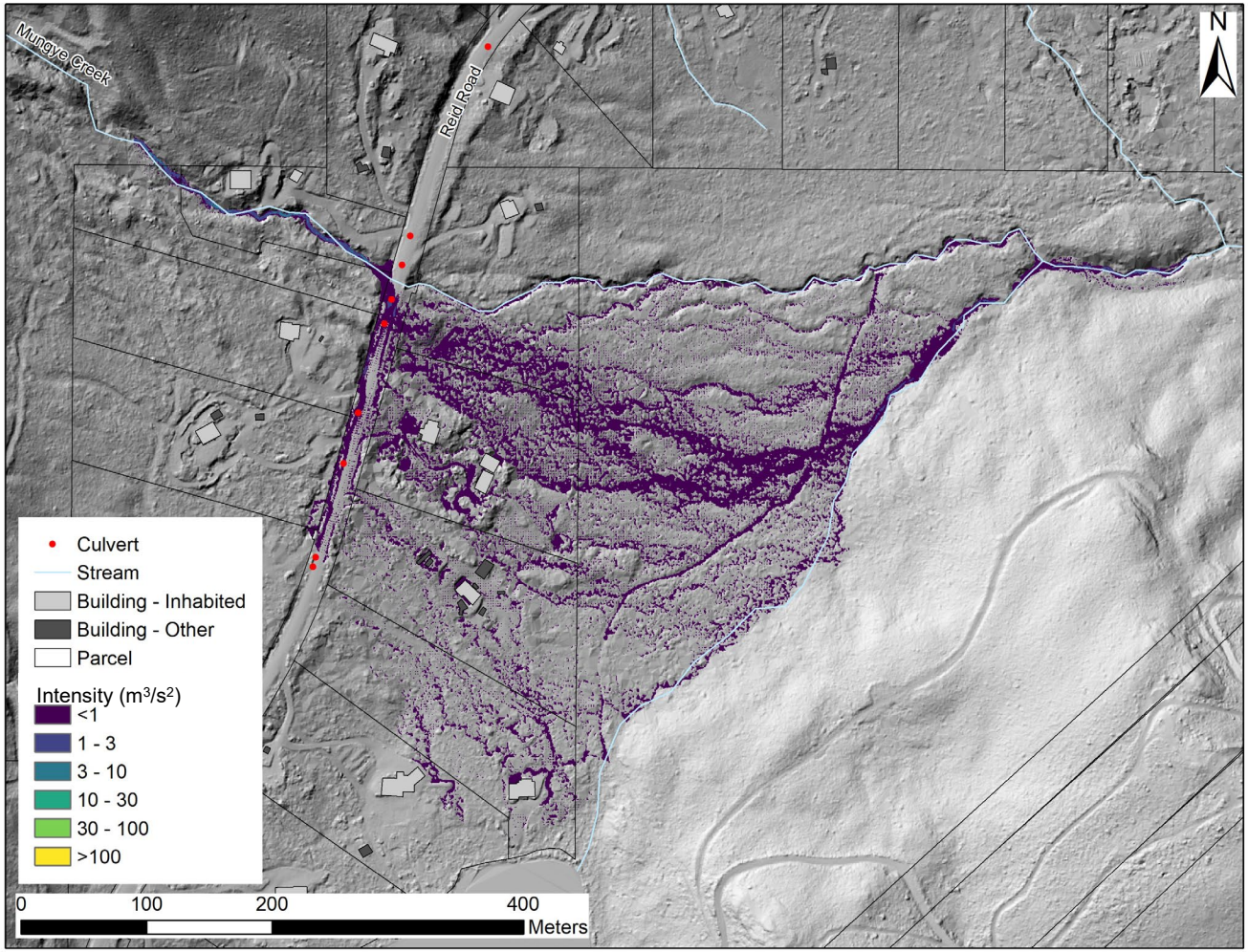

NOTES

1. THIS FIGURE SHOULD BE READ IN CONJUNCTION WITH BGC'S REPORT TITLED 'QUANTITATIVE LANDSLIDE HAZARD AND RISK ASSESSMENT – REID ROAD AREA, ELECTORAL AREA C' AND DATED JANUARY 2023.
2. BASE TOPOGRAPHIC DATA BASED ON LIDAR PROVIDED BY MCELHANNEY AND DATED JULY 22, 2022.
3. BUILDINGS DIGITIZED BY BGC. BGC ASSESSED WHICH BUILDINGS WERE INHABITED BASED ON FIELD OBSERVATIONS, WHERE LANDOWNER PERMISSION TO ACCESS THE PROPERTY WAS PROVIDED. FOR OTHER BUILDINGS, BGC ASSESSED BASED ON SITE LAYOUT AND INTERPRETATION.
4. MODEL RESULTS ARE BASED ON THE MAXIMUM INTENSITY OF THE COARSE FRONT AND MUDDY AFTERFLOWS AS MODELLED BY BGC IN HEC-RAS. MODEL RESULTS ARE CLIPPED TO THE JASON CREEK FAN BOUNDARY.
5. MODEL RESULTS ARE A SNAPSHOT IN TIME. CHANGES TO THE TOPOGRAPHY AND/OR ADDITION OF MITIGATION STRUCTURES MAY INFLUENCE THE FLOW PATTERNS AND BEHAVIOUR. MODEL RESULTS SHOULD BE REVIEWED AND REVISITED AFTER ANY SIGNIFICANT CHANGE.

PREPARED BY:	FIGURE TITLE:		
HMS	MUNGYE CREEK – 30 TO 100 YEAR RETURN PERIOD, CULVERTS BLOCKED		
CHECKED BY:	CLIENT:		
LCH	SQUAMISH – LILLOOET REGIONAL DISTRICT		
APPROVED BY:	SCALE:	PROJECT NO:	FIGURE NO:
LCH	7CM: 400M	1358010	H-12

0 5 10 mm in ANSI A sized paper

BGC ENGINEERING INC.

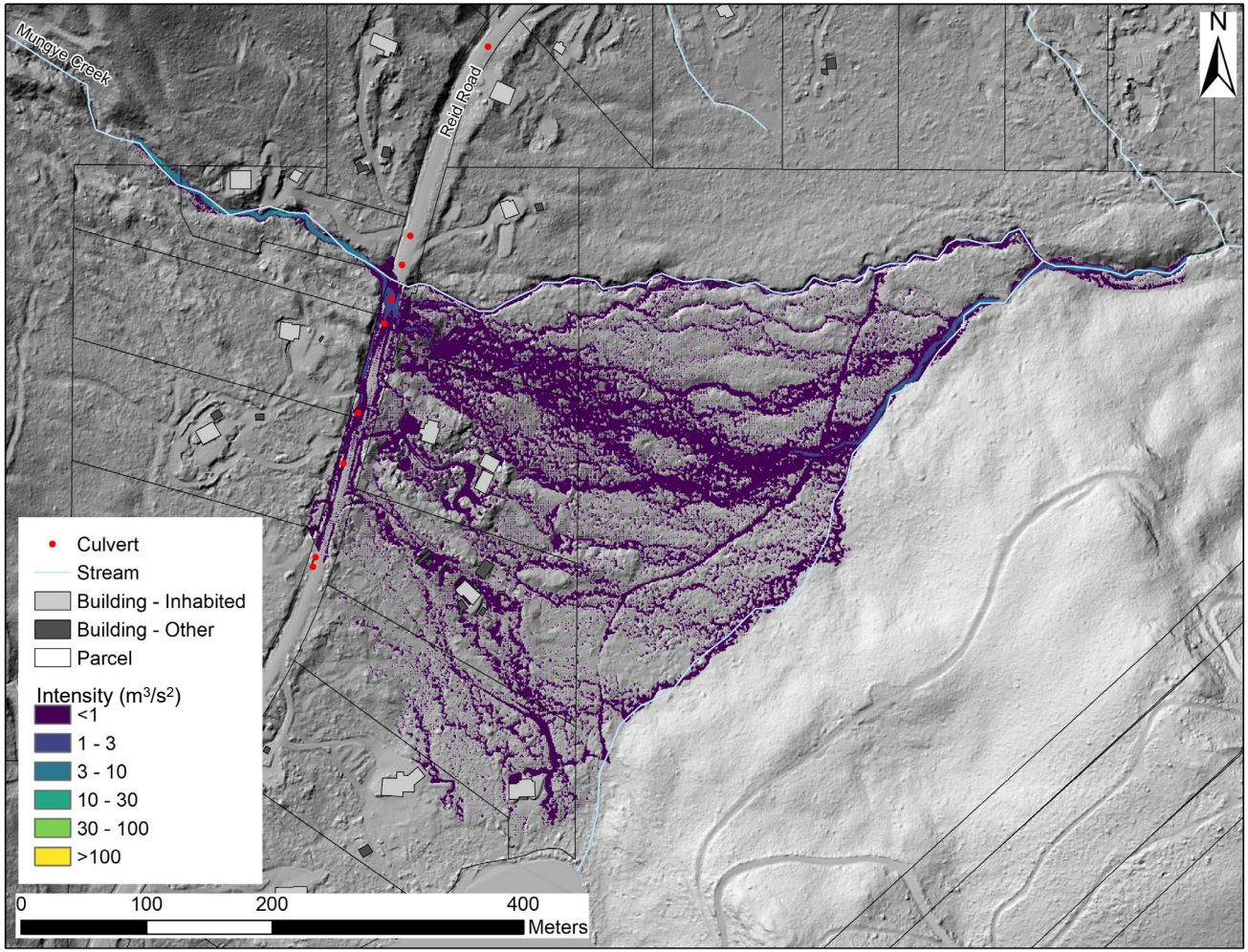

NOTES

1. THIS FIGURE SHOULD BE READ IN CONJUNCTION WITH BGC'S REPORT TITLED 'QUANTITATIVE LANDSLIDE HAZARD AND RISK ASSESSMENT – REID ROAD AREA, ELECTORAL AREA C' AND DATED JANUARY 2023.
2. BASE TOPOGRAPHIC DATA BASED ON LIDAR PROVIDED BY MCELHANNEY AND DATED JULY 22, 2022.
3. BUILDINGS DIGITIZED BY BGC. BGC ASSESSED WHICH BUILDINGS WERE INHABITED BASED ON FIELD OBSERVATIONS, WHERE LANDOWNER PERMISSION TO ACCESS THE PROPERTY WAS PROVIDED. FOR OTHER BUILDINGS, BGC ASSESSED BASED ON SITE LAYOUT AND INTERPRETATION.
4. MODEL RESULTS ARE BASED ON THE MAXIMUM INTENSITY OF THE COARSE FRONT AND MUDDY AFTERFLOWS AS MODELLED BY BGC IN HEC-RAS.
5. MODEL RESULTS ARE A SNAPSHOT IN TIME. CHANGES TO THE TOPOGRAPHY AND/OR ADDITION OF MITIGATION STRUCTURES MAY INFLUENCE THE FLOW PATTERNS AND BEHAVIOUR. MODEL RESULTS SHOULD BE REVIEWED AND REVISITED AFTER ANY SIGNIFICANT CHANGE.

PREPARED BY:	FIGURE TITLE:		
HMS	MUNGYE CREEK – 100 TO 300 YEAR RETURN PERIOD, CULVERTS BLOCKED		
CHECKED BY:	CLIENT:		
LCH	SQUAMISH – LILLOOET REGIONAL DISTRICT		
APPROVED BY:	SCALE:	PROJECT NO:	FIGURE NO:
LCH	7CM: 400M	1358010	H-13

0 5 10 mm in ANSI A sized paper

BGC ENGINEERING INC.

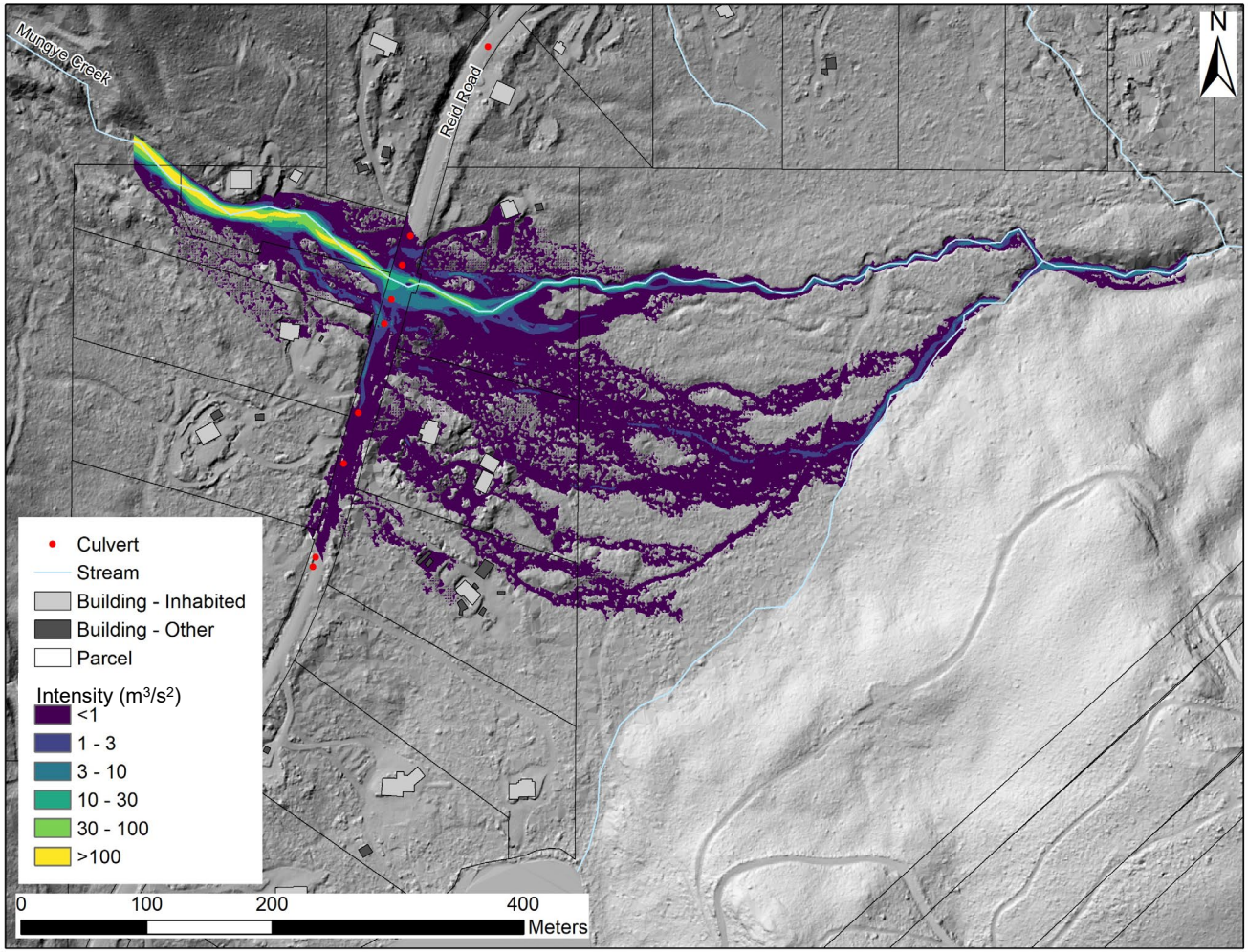

NOTES

1. THIS FIGURE SHOULD BE READ IN CONJUNCTION WITH BGC'S REPORT TITLED 'QUANTITATIVE LANDSLIDE HAZARD AND RISK ASSESSMENT – REID ROAD AREA, ELECTORAL AREA C' AND DATED JANUARY 2023.
2. BASE TOPOGRAPHIC DATA BASED ON LIDAR PROVIDED BY MCELHANNEY AND DATED JULY 22, 2022.
3. BUILDINGS DIGITIZED BY BGC. BGC ASSESSED WHICH BUILDINGS WERE INHABITED BASED ON FIELD OBSERVATIONS, WHERE LANDOWNER PERMISSION TO ACCESS THE PROPERTY WAS PROVIDED. FOR OTHER BUILDINGS, BGC ASSESSED BASED ON SITE LAYOUT AND INTERPRETATION.
4. MODEL RESULTS ARE BASED ON THE MAXIMUM INTENSITY OF THE COARSE FRONT AND MUDDY AFTERFLOWS AS MODELLED BY BGC IN HEC-RAS.
5. MODEL RESULTS ARE A SNAPSHOT IN TIME. CHANGES TO THE TOPOGRAPHY AND/OR ADDITION OF MITIGATION STRUCTURES MAY INFLUENCE THE FLOW PATTERNS AND BEHAVIOUR. MODEL RESULTS SHOULD BE REVIEWED AND REVISITED AFTER ANY SIGNIFICANT CHANGE.

PREPARED BY:	FIGURE TITLE:		
HMS	MUNGYE CREEK – 300 TO 1,000 YEAR RETURN PERIOD, CULVERTS BLOCKED		
CHECKED BY:	CLIENT:		
LCH	SQUAMISH – LILLOOET REGIONAL DISTRICT		
APPROVED BY:	SCALE:	PROJECT NO:	FIGURE NO:
LCH	7CM: 400M	1358010	H-14

0 5 10 mm in ANSI A sized paper

BGC ENGINEERING INC.

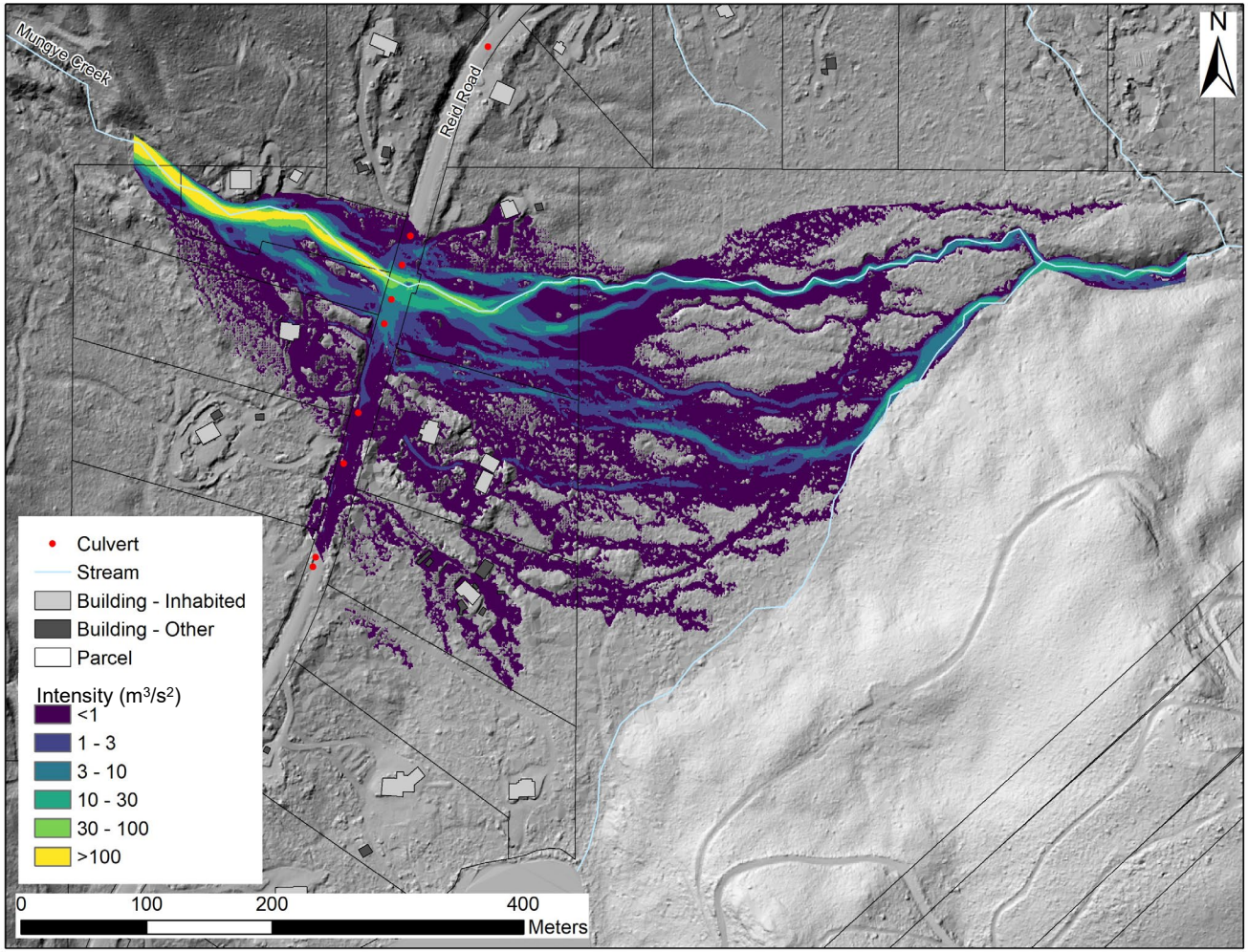

NOTES

1. THIS FIGURE SHOULD BE READ IN CONJUNCTION WITH BGC'S REPORT TITLED 'QUANTITATIVE LANDSLIDE HAZARD AND RISK ASSESSMENT – REID ROAD AREA, ELECTORAL AREA C' AND DATED JANUARY 2023.
2. BASE TOPOGRAPHIC DATA BASED ON LIDAR PROVIDED BY MCELHANNEY AND DATED JULY 22, 2022.
3. BUILDINGS DIGITIZED BY BGC. BGC ASSESSED WHICH BUILDINGS WERE INHABITED BASED ON FIELD OBSERVATIONS, WHERE LANDOWNER PERMISSION TO ACCESS THE PROPERTY WAS PROVIDED. FOR OTHER BUILDINGS, BGC ASSESSED BASED ON SITE LAYOUT AND INTERPRETATION.
4. MODEL RESULTS ARE BASED ON THE MAXIMUM INTENSITY OF THE COARSE FRONT AND MUDDY AFTERFLOWS AS MODELLED BY BGC IN HEC-RAS.
5. MODEL RESULTS ARE A SNAPSHOT IN TIME. CHANGES TO THE TOPOGRAPHY AND/OR ADDITION OF MITIGATION STRUCTURES MAY INFLUENCE THE FLOW PATTERNS AND BEHAVIOUR. MODEL RESULTS SHOULD BE REVIEWED AND REVISITED AFTER ANY SIGNIFICANT CHANGE.

PREPARED BY:	FIGURE TITLE:		
HMS	MUNGYE CREEK – 1,000 TO 3,000 YEAR RETURN PERIOD, CULVERTS BLOCKED		
CHECKED BY:	CLIENT:		
LCH	SQUAMISH – LILLOOET REGIONAL DISTRICT		
APPROVED BY:	SCALE:	PROJECT NO:	FIGURE NO:
LCH	7CM: 400M	1358010	H-15

0 5 10 mm in ANSI A sized paper

BGC ENGINEERING INC.

APPENDIX I
COMPOSITE HAZARD MAPPING METHODS

I.1. INTRODUCTION

A composite hazard map aggregates all hazard scenarios in a single map. It distinguishes areas of higher hazard (frequent and/or high intensity flows) from areas of lower hazard (rare and/or low intensity flows) for land-use planning and decision making. BGC derived the composite hazard map by combining the numerical modelling results and interpreting boundaries between higher and lower hazard areas using the methods described in this Appendix (Figure I-1).

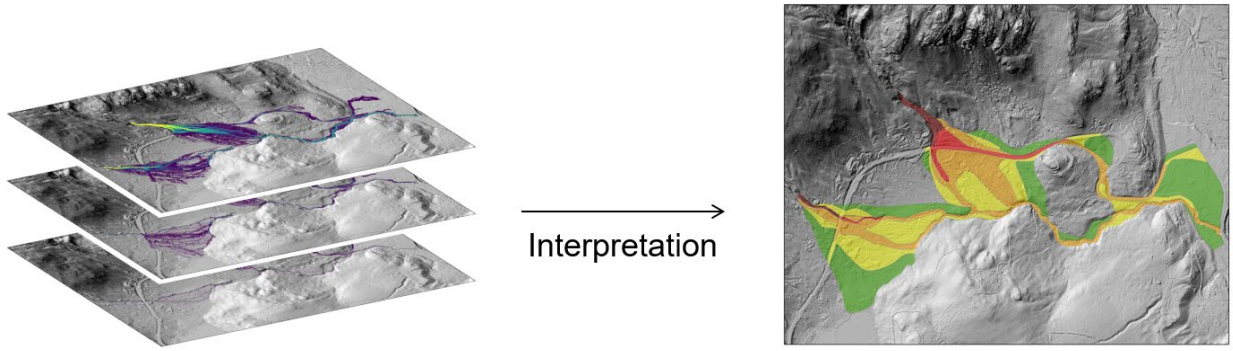

Figure I-1. Composite hazard mapping process.

I.2. IMPACT FORCE PROBABILITY

BGC combined numerical modelling results for all hazard scenarios using the impact force probability (IFP) index. The IFP is the annual probability of geohazard impact forces at a given location. It describes how often and how intense a rapid flow-type landslide (e.g., debris flow or debris flood) could be across a model domain. BGC calculated IFP as the product of the impact force per meter flow width and the respective probability of occurrence, summed for all geohazard hazard scenarios (Equation I-1) (Jakob et al., 2022):

$$IFP_j = \sum_{i=1}^{n} h_i \, \rho_i \, {v_{i,j}}^2 d_{i,j} \qquad \text{Equation I-1}$$

Where:

- IFP_j is the impact force probability at location (j) ($Nm^{-1}yr^{-1}$)
- h_i the annual probability of geohazard scenario (i) ($years^{-1}$)
- ρ_i is the fluid density of geohazard scenario (i) (kg/m^3)
- $v_{i,j}$ is the maximum flow velocity of geohazard scenario (i) at location (j) (m/s)
- $d_{i,j}$ is the maximum flow depth of geohazard scenario (i) at location (j) (m)
- n is the total number of geohazard scenarios considered.

The annual probability of a scenario is the probability of each assessed return period multiplied by a conditional probability. The return period probability is the difference between the probability of the lower-bound and upper-bound return periods (e.g., for the 20-year return period which represents a range from 10 to 30-year return periods, the probability is 1/10 – 1/30 = 0.067). The conditional probability is the relative likelihood of a sub-scenario occurring given a geohazard of a certain return period occurs. Conditional probabilities must sum to 1 for each return period. BGC determined geohazard scenario probabilities in the frequency-magnitude assessment (Appendix G).

BGC determined flow velocities and depths with numerical models for each scenario (Appendix H). Jakob et al. (2012) used the term d x v^2 in Equation I-1 as a proxy for impact force, correlated to building damage.

BGC assumed a spatially constant fluid density of 2,200 kg/m^3 for debris flows (Kwan, 2012), and 1,300 kg/m^3 and 1,500 kg/m^3 for Type 1 and 2 debris floods, respectively (Jakob & Church, 2020).

I.3. METHODS

Using the gridded IFP map (Section I.2), BGC delineated hazard areas with the same approximate IFP ranges listed in Table I-1. BGC smoothed the polygons such that small nuances from numerical modelling or topography are not included in the composite hazard map. BGC adjusted hazard boundaries using field observations, information about past events, numerical modelling (HEC-RAS, *DAN3D*), and professional judgement.

Table I-1. Composite hazard rating categories, modified from EGBC Landslide Guidelines (2022).

Composite Hazard Rating	Approximate Range of IFP ($Nm^{-1}yr^{-1}$)	Hazard and Consequence Description Given Impact to Standard Wood Frame Building	Approximate Range of Corresponding Annual Probability of Death of an Individual (PDI)
Very Low	< 1	Hazard is very rare or of minor intensity and does not constitute a credible life-loss risk but can cause nuisance building damage.	Less than 1:100,000
Low	1 to 10	Hazard is rare or of moderate intensity and is unlikely to lead to life loss, but will cause building damage.	1:100,000 to 1:10,000
Moderate	10 to 100	Hazard likely occurs within a person's lifetime or of substantial intensity and may lead to life loss and considerable building damage.	1:10,000 to 1:1,000
High	100 to 1,000	Hazard occurs frequently and/or with very high intensity and is likely to lead to life loss and requires building reconstruction.	Greater than 1:1,000
Very High	>1,000	Hazard occurs frequently and/or with extreme intensity and is very likely to lead to life loss and total building destruction.	

I.4. LIMITATIONS

The composite hazard map is based on BGC's current understanding of steep creek hazards and topography at the site. BGC interpreted hazard polygons from numerical modelling and other described resources. The hazard zones are not and cannot be precise and should not be interpreted as such. Debris flows and debris floods are to some extent chaotic processes and their exact behavior cannot be predicted. The composite hazard map fails to account for any major fan surface alterations by debris flows, bank erosion, or by construction. It also does not account for the presence of structures and their effects on flow.

The composite hazard map does not provide information on the frequency of debris floods or debris flows at specific locations or site-specific impact forces. Practitioners can determine this information using numerical modelling results for specific hazard scenarios (Appendix H).

Land managers should review the map periodically and revise if there are changed conditions or with new information. Changed conditions could include, but are not limited to, vegetation removal in the watershed, forest fire, large slope failure, mitigation works, or changes to topographic features on the fan. New information could be related to the magnitude and frequency of steep creek hazards and flow mobility and behaviour.

APPENDIX J
RISK ASSESSMENT METHODS

J.1. INTRODUCTION

This appendix describes the method and assumptions BGC used to assess debris-flow and debris-flood life-loss risk to individuals in buildings. This appendix answers the following questions:

- What is the probability of a debris flow or debris flood impacting an occupied building, and at what intensity[1]?
- What is the probability that a person is within a building at the time of impact?
- What is the probability that life-loss occurs given impact to an occupied building?

J.2. RISK ASSESSMENT FRAMEWORK

Life-loss risk can be evaluated for individual risk as described below, and for group risk. Understanding group risk is most applicable to support decisions where larger populations are exposed to hazard. This assessment entirely focused on individual risk, given the need of SLRD to make property-specific risk management decisions.

J.2.1. Individual Risk

Individual risk is the chance that a specific person will be killed by the hazard, expressed as the annual Probability of Death of an Individual (PDI). BGC calculated individual risk for a person inside a building. Individual risk typically applies to the individual most at risk, corresponding to a person spending the greatest proportion of time at home, such as a young child, stay-at-home person, or an elderly person. BGC calculated individual risk with Equation J-1 (Figure J-1):

$$PDI_j = \sum_{i=1}^{n} h_i S_{i,j} T_{i,j} V_{i,j} \qquad \text{Equation J-1}$$

Where:

- PDI_j is the annual probability of death of an individual from the geohazard at building (j) (years^{-1})
- h_i is the annual probability of a geohazard scenario (i) occurring (years^{-1})
- $S_{i,j}$ is the conditional probability that geohazard scenario (i) reaches building (j) (i.e., spatial probability of impact)
- $T_{i,j}$ is the conditional probability a person occupies building (j) during geohazard scenario (i) (i.e., temporal probability)
- $V_{i,j}$ is the conditional probability of fatality at building (j) given impact by the estimated geohazard scenario (i) intensity (i.e., vulnerability)
- n is the total number of geohazard scenarios considered.

[1] Intensity refers to the destructive potential of a geohazard.

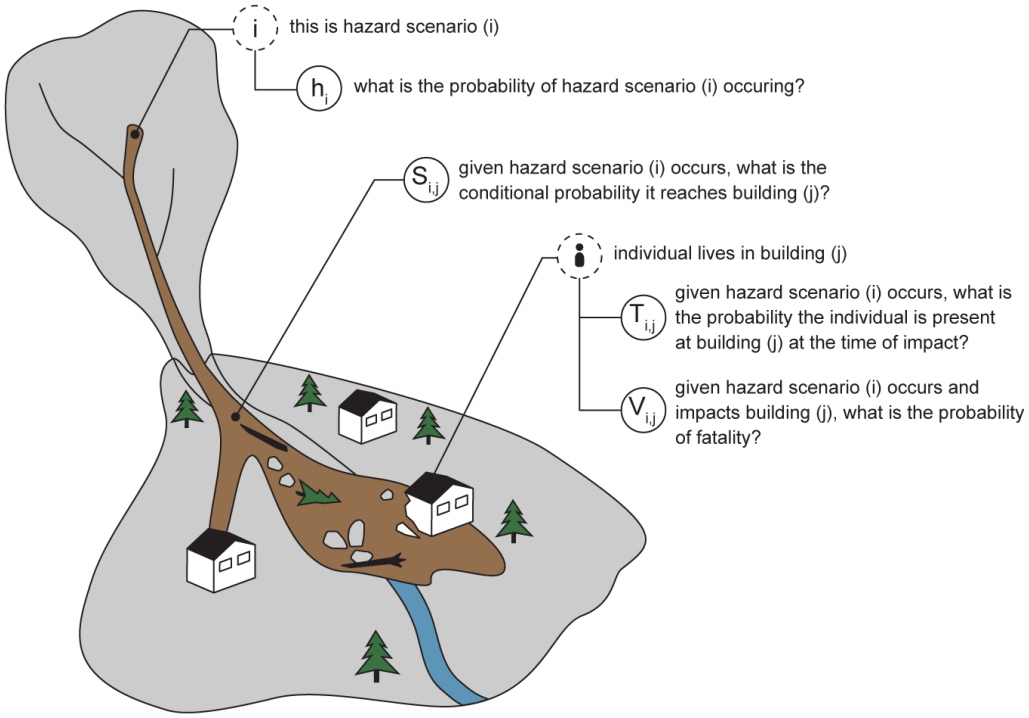

Figure J-1. Individual risk calculation variables.

J.2.2. Geohazard Scenario Probability (h)

The annual probability of a scenario is the probability of each assessed return period multiplied by a conditional probability. The return period probability is the difference between the probability of the lower-bound and upper-bound return periods (e.g., for the 20-year return period which represents a range from 10 to 30-year return periods, the probability is 1/10 – 1/30 = 0.067). The conditional probability is the relative likelihood of a sub-scenario occurring given a geohazard of a certain return period occurs. Conditional probabilities must sum to 1 for each return period. BGC determined geohazard scenario probabilities in the frequency-magnitude assessment (Appendix G).

J.2.3. Spatial Probability of Impact (S)

BGC used numerical modelling (Appendix H) to determine whether a scenario impacts an occupied building. BGC assumed a building is impacted (S = 1) if any model grid cell (2 m) with a non-zero flow depth intersects the building's footprint. BGC mapped building footprints based on field observations, BC Assessment data, lidar topography, and satellite and ortho (20 cm) imagery. BGC determined whether a building contained habitable space ("inhabited building", Drawing 02) based on information obtained during the field reconnaissance. For the purposes of the risk assessment, BGC assumed full occupation for buildings currently on evacuation order to evaluate risk to residents on those properties.

J.2.4. Temporal Probability of Impact (T)

The probability a person occupies a building depends on the building's primary use. All the buildings in the consultation zone are residential properties. For the individual risk calculation, BGC assumed an occupation rate of 90% (T = 0.9) for the most vulnerable person spending the greatest proportion of time at home, such as a young child, stay-at-home person, or an elderly person.

J.2.5. Vulnerability (V)

BGC assessed vulnerability by relating the debris-flow intensity index (I_{DF}) to building damage state (Jakob, Stein, & Ulmi, 2011), and building damage state to life loss vulnerability (Table J-1). I_{DF} describes the severity of debris-flow impact. BGC calculated I_{DF} with Equation J-2:

$$I_{DF} = dv^2 \qquad \text{Equation J-2}$$

Where:

- d is flow depth (m)
- v is velocity (m/s).

BGC exported I_{DF} values directly from HEC-RAS across the model domain (2 m grid cell size) for each scenario (Appendix H). At each occupied building, BGC assigned the maximum intensity grid cell intersecting a building footprint for each scenario then converted that value to a vulnerability using the best estimate in Table J-1. BGC used expert judgement to adjust building damage states at select buildings where the numerical modelling did not reflect the potential hazard intensity.

Table J-1. Life loss vulnerability criteria for persons within wood-frame buildings impacted by debris flows.

Debris-flow Intensity Index (m^3/s^2)	Building Damage State	Damage Description	Life Loss Vulnerability		
			Lower Bound	Best Estimate	Upper Bound
≤ 1	Minor	Slow flowing shallow and deep water with little or no debris. High likelihood of water damage, but structural damage is unlikely.	~0	~0	~0
1 to 3	Moderate	Mostly slow flow with minor debris. High likelihood of sedimentation and water damage. Potentially dangerous to people in buildings, or in areas with higher water depths.	0.01	0.02	0.04
3 to 10	Major	Potentially fast flowing but mostly shallow water with debris. Moderate likelihood of building damage and high likelihood of major sediment and/or water damage. Potentially dangerous to people on the first floor or in the basement of buildings without elevated concrete footings	0.05	0.2	0.4
10 to 30	Extensive	Fast flowing water and debris. High likelihood of structural building damage and severe sediment and water damage. Dangerous to people on the first floor or in the basement of buildings.	0.2	0.4	0.6
30 to 100	Severe	Fast flowing debris. High likelihood of severe structural building damage and severe sediment damage. Very dangerous to people in buildings irrespective of floor.	0.4	0.6	0.8
>100	Complete Destruction	Very fast flowing debris. Very high likelihood of complete building destruction for unreinforced and reinforced buildings, and extreme sediment damage. A person in the building will almost certainly be killed.	0.8	0.9	1

Notes: BGC selected life loss vulnerability estimates based on expert judgement paired with findings from a global literature review summarized by Jakob et al. (2012). Research is ongoing to further improve confidence in vulnerability estimates.

J.3. LIMITATIONS

BGC calculated risk for inhabited buildings. A person(s) outside of a building on other locations on the properties can be at risk of injury or fatality during a debris flow or debris flood due to the depth, speed, or force of the flows. BGC has not assessed economic risk as part of this scope.

BGC's risk assessment is based on the current understanding of steep creek hazards at the site, topography, layout of structures on the fan, and assumed building occupancy. Any changes to the fan surface (e.g., sedimentation and erosion from a debris flow, construction of mitigation measures, etc.), triggering conditions (e.g., forest fire, removal of vegetation in the watershed, large slope failure), or the location(s) and occupancy of buildings may change the risk.

APPENDIX K
MITIGATION COST ESTIMATE DETAILS

K.1. INTRODUCTION

This appendix contains the cost estimates of the mitigation options selected for further review at Jason and Mungye creeks. Unit costs are based on bid averages from similar projects across BC and Alberta between 2017 and 2022. BGC applied an increase factor to account for inflation and/or known increase in project actuals from bids to adjust the costs to a best estimate for 2022. Item subtotals are rounded to nearest $1,000. Subtotal and total costs are rounded to the nearest $10,000 to not give a sense of exactness, and these cost estimates may vary -50% to +100%. BGC estimated volumes, areas, and lengths using approximate geometries and layouts and are subject to change as part of future phases of design.

K.1.1. Flow diversion berms on individual properties

Table K-1 provides a cost estimate for a representative flow diversion berm on proposed by BGC on 1782, 1788, 1794, 1802 Reid Road. The costs are presented for a single berm and then multiplied by four to arrive at a total for all berms.

Table K-1. Cost estimate for representative individual property berms proposed at 1782, 1788, 1794, 1802 Reid Road.

Item	Description	Unit	Quantity	Cost per Unit	Item Total Cost
1	**Direct Costs**				
1.1	Clearing, grubbing, & disposal	m^2	970	$10	$9,000
1.2	Berm fill (cut & fill)	m^3	220	$25	$6,000
1.3	Berm fill (supply & placement)	m^3	990	$40	$40,000
1.4	Grouted riprap (supply & placements)	m^3	320	$500	$162,000
1.5	Class 500kg riprap (supply & placement)	m^3	220	$250	$ 55,000
1.6	Seeding, planting, site restoration	m^2	560	$5	$ 3,000
				SUBTOTAL DIRECT COSTS/ BERM	**$270,000**
2	**Indirect Costs**				
2.1	Contractor general	LS		15%	$41,000
2.2	Contingency (unlisted items)	LS		10%	$27,000
2.3	Engineering and permitting	LS		15%	$41,000
				SUBTOTAL INDIRECT COSTS/ BERM	**$110,000**
				TOTAL/ BERM	**$ 380,000**
				TOTAL ALL FOUR BERMS	**$1,520,000**

Notes:

1. LS refers to lump sum.

Table K-2. Cost estimate for the GRS wall (1781 Reid Road).

Item	Description	Unit	Quantity	Cost per Unit	Item Total Cost
1	**Direct Costs**				
2.1	Access construction	m	100	$250	$25,000
2.2	Clearing, grubbing, & disposal	m^2	850	$10	$8,000
2.3	Excavation and off-site disposal	m^3	320	$35	$11,000
2.4	GRS Wall	m^2	340	$300	$101,000
2.5	Class 1000kg riprap (supply & placement)	m^3	280	$300	$84,000
2.6	Seeding, planting, site restoration	m^2	1,060	$5	$5,000
				SUBTOTAL DIRECT COSTS	**$240,000**
2	**Indirect Costs**				
2.1	Contractor general	LS		15%	$36,000
2.2	Contingency (unlisted items)	LS		10%	$24,000
2.3	Engineering and permitting	LS		15%	$36,000
				SUBTOTAL INDIRECT COSTS	**$90,000**
				TOTAL	**$330,000**

K.1.2. Excavate channel and construct clear-span bridge

Table K-3. Cost estimates for the Jason Creek bridge placement, channel excavation, and erosion protection.

Item	Description	Unit	Quantity	Cost per Unit	Item Total Cost
Bridge Placement and Erosion Protection					
1	**Direct Costs**				
1.1	Grouted riprap (supply & placement)[1]	m^3	850	$500	$426,000
1.2	Bridge replacement[2]	m^2	260	$5,600	$1,432,000
				SUBTOTAL DIRECT COSTS	**$1,860,000**
2	**Indirect Costs**				
2.1	Contractor general	LS		15%	$279,000
2.2	Contingency (unlisted items)	LS		10%	$186,000
2.3	Engineering and permitting	LS		15%	$279,000
				SUBTOTAL INDIRECT COSTS	**$740,000**
				SUBTOTAL	**2,600,000**
Channel Excavation					
1	**Direct Costs**				
1.1	Access construction	m^3	250	$250	$62,000
1.2	Clearing, grubbing, & disposal	m^2	500	$10	$5,000
1.3	Excavation and off-site disposal	m^3	38,980	$35	$1,364,000
1.4	Seeding, planting, site restoration	m^2	500	$5	$2,000
				SUBTOTAL DIRECT COSTS	$1,430,000
2	**Indirect Costs**				
2.1	Contractor general	LS		15%	$215,000
2.2	Contingency (unlisted items)	LS		10%	$143,000
2.3	Engineering and permitting	LS		15%	$215,000
				SUBTOTAL INDIRECT COSTS	**$580,000**
				TOTAL	**$2,010,000**
				COMBINED TOTAL	**$4,610,000**

Notes:
1. Based on channel 10 m upstream and downstream of bridge.
2. Based on 32 m span, 8 m wide bridge.

K.1.3. Rock Slope Monitoring

Table K-4. Mitigation cost estimates for near-real time monitoring program

Item	Description	Unit	Quantity	Cost per Unit	Item Total Cost
1	**Monitoring Equipment**				
1.1	GNSS, Wire Extensometer, Tiltmeters & Weather Station	Total		$150,000	$150,000
1.2	Installation	Total		$100,000	$100,000
				SUBTOTAL DIRECT COSTS	**$250,000**
				TOTAL	**$ 250,000**
2	**Maintenance and Data Processing**				
2.1	Maintenance and Data Processing	/year		$70,000	$70,000/ year
				TOTAL ANNUAL COSTS	**$70,000/year**

K.1.4. Mungye Creek Box Culvert

Table K-5. Mitigation cost estimates for Mungye Creek culvert replacement.

Item	Description	Unit	Quantity	Cost per Unit	Item Total Cost
1	**Direct Costs**				
1.1	Concrete box culvert	each	1	$750,000	$750,000
				SUBTOTAL DIRECT COSTS	**$750,000**
2	**Indirect Costs**				
2.1	Contractor general	LS		15%	$113,000
2.2	Contingency (unlisted items)	LS		10%	$ 75,000
2.3	Engineering and permitting	LS		15%	$113,000
				SUBTOTAL INDIRECT COSTS	**$300,000**
				TOTAL	**$ 1,050,000**

PHOTOGRAPHS

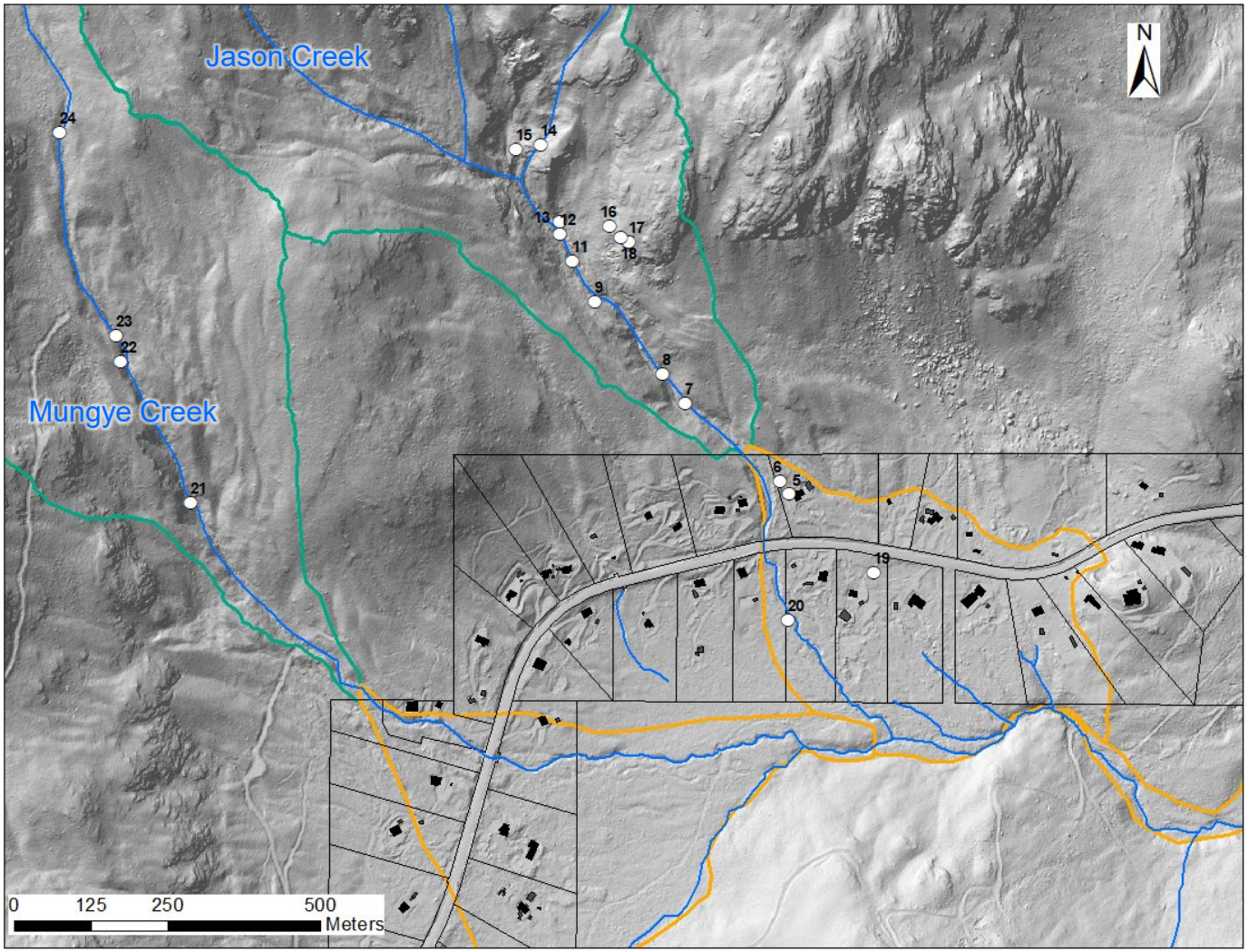

NOTES

1. THIS FIGURE SHOULD BE READ IN CONJUNCTION WITH BGC'S REPORT TITLED 'QUANTITATIVE LANDSLIDE HAZARD AND RISK ASSESSMENT – REID ROAD AREA, ELECTORAL AREA C' AND DATED JANUARY 2023.
2. BASE TOPOGRAPHIC DATA BASED ON LIDAR PROVIDED BY McELHANNEY AND DATED JULY 22, 2022.
3. BUILDINGS DIGITIZED BY BGC. BGC ASSESSED WHICH BUILDINGS WERE INHABITED BASED ON FIELD OBSERVATIONS, WHERE LANDOWNER PERMISSION TO ACCESS THE PROPERTY WAS PROVIDED. FOR OTHER BUILDINGS, BGC ASSESSED BASED ON SITE LAYOUT AND INTERPRETATION.
4. PHOTOS 1 TO 4 ARE NOT SHOWN AS THEY ARE FROM A HELICOPTER OVERFLIGHT. PHOTOS 25 TO 26 LOCATONS NOT SHOWN AS GPS POINT NOT LOGGED IN THE FIELD.

PREPARED BY: LCH	FIGURE TITLE: PHOTO LOCATION MAP		
CHECKED BY: SZ	CLIENT: SQUAMISH – LILLOOET REGIONAL DISTRICT		
APPROVED BY: LCH	SCALE: AS SHOWN	PROJECT NO: 1358010	FIGURE NO: PHOTOS

0 5 10 mm in ANSI A sized paper

BGC ENGINEERING INC.

Photo 1.

Jason Creek watershed. Helicopter overflight June 24, 2022.

(Note location not shown on Photo Location Map)

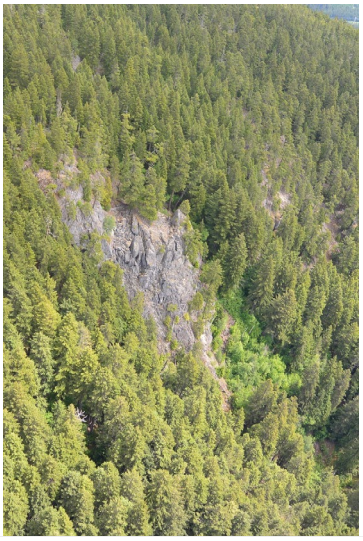

Photo 2.

Unstable rock mass in Jason Creek watershed. Helicopter overflight June 24, 2022.

(Note location not shown on Photo Location Map)

Photo 3.

Looking east to Jason Creek watershed and rockfall area east of watershed. Helicopter overflight June 24, 2022.

(Note location not shown on Photo Location Map)

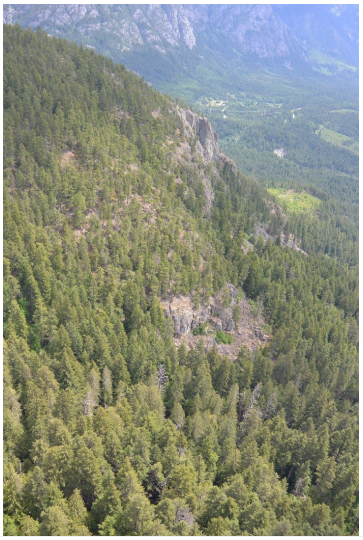

Photo 4.

Looking rockfall areas east of watershed. Helicopter overflight June 24, 2022.

(Note location not shown on Photo Location Map)

Photo 5.

Looking upstream at Jason Creek near fan apex. July 20, 2022.

Photo 6.

Looking downstream on Jason Creek near fan apex. July 20, 2022.

Photo 7.

Jason Creek mid section, both valley sides are moving inwards due to deep-seated landsliding. Photo: July 22, 2022.

Photo 8.

Jason Creek channel. Photo: July 20, 2022.

Photo 9.

Jason Creek channel. July 20, 2022.

Photo 10.
Jason Creek channel. July 20, 2022.

Photo 11.
Jason Creek channel. July 20, 2022.

Photo 12.
Fresh point source release on right bank sidewall.

Photo 13.

Fresh tension crack with 1.5 m displacement in Jason Creek watershed. July 20, 2022

Photo 14.

Tension crack formed upstream of 2021 headscarp. July 20, 2022

Photo 15.

Unstable slope on Jason Creek sidewall. Photo: July 20, 2022.

Photo 16.

Base of slope from Photo 16. Photo: July 22, 2022.

Photo 17.

Heavily dilated unstable rock masses on Jason Creek, toppling to the left towards the creek. Photo: July 22, 2022.

Photo 18.

Crack in rock in Jason Creek watershed. Photo: July 22, 2022.

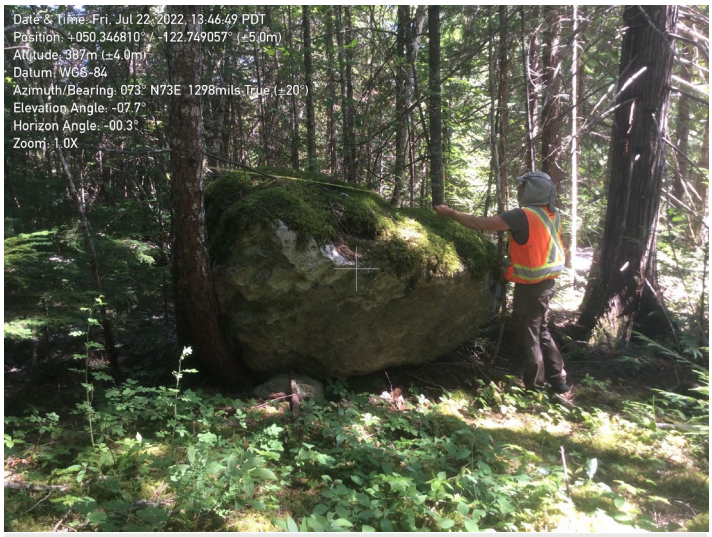

Photo 19.

Large blocks on the surface of Jason Creek fan. July 22, 2022

Photo 20.

Jason Creek downstream of Reid Road. Photo: July 22, 2022.

Photo 21.

Fault gouge exposed in Mungye Creek channel. Note knife in rock. July 21, 2022.

Photo 22.

Mungye Creek channel scattered with wood indicating no recent debris flow. Photo: July 21, 2022.

Photo 23.

Fault gouge exposed in Mungye Creek channel. July 21, 2022.

Photo 24.

Mungye Creek channel. July 21, 2022.

Photo 25.

Jason Creek fault with friable, heavily altered and clay-rich rock of the Gambier Group. Photo: July 22, 2022.

(Note location not shown on Photo Location Map)

Photo 26.

Jason Creek mid section, both valley sides are moving inwards due to deep-seated landsliding. Photo: July 22, 2022.

(Note location not shown on Photo Location Map)

DRAWINGS

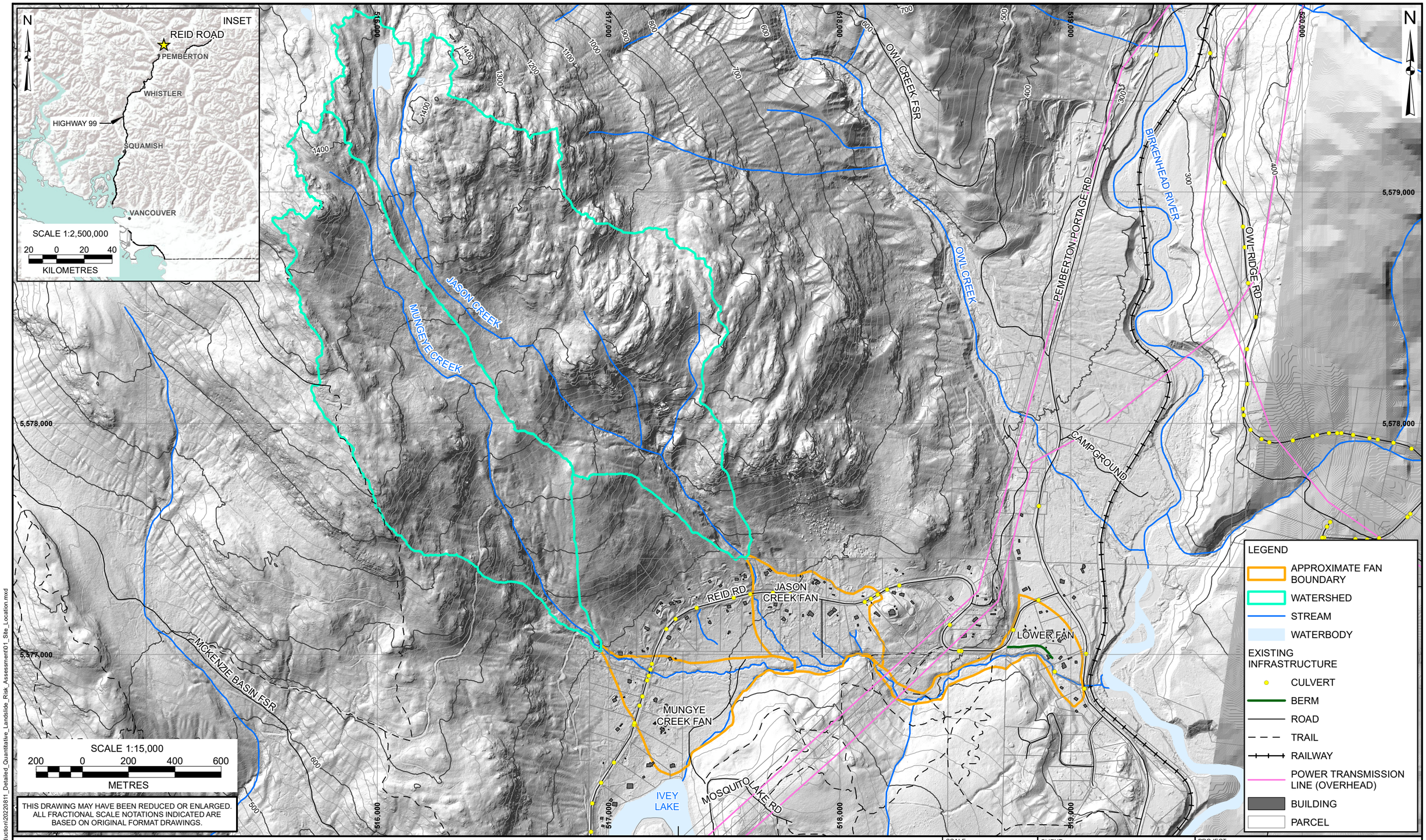

NOTES:
1. ALL DIMENSIONS ARE IN METRES UNLESS OTHERWISE NOTED.
2. THIS DRAWING MUST BE READ IN CONJUNCTION WITH BGC'S REPORT TITLED "QUANTITATIVE LANDSLIDE HAZARD AND RISK ASSESSMENT – REID ROAD AREA", AND DATED JANUARY 2023.
3. BASE TOPOGRAPHIC DATA BASED ON LIDAR PROVIDED BY McELHANNEY AND DATED JULY 22, 2022. CONTOUR INTERVAL IS 20 m.
4. BASE TOPOGRAPHIC MAPPING FROM CANVEC. CULVERTS FROM MOTI.STREAM LINES WERE MODIFIED BY BGC BASED ON LIDAR, AERIAL IMAGERY, AND FIELD OBSERVATIONS.
5. WATERSHED BOUNDARIES, FAN BOUNDARIES, AND BUILDINGS DIGITIZED BY BGC.
6. BERM EXTENTS DIGITIZED BY CORDILLERAN.
7. COORDINATE SYSTEM IS NAD 1983 UTM ZONE 10N. VERTICAL DATUM IS UNKNOWN.
8. UNLESS BGC AGREES OTHERWISE IN WRITING, THIS DRAWING SHALL NOT BE MODIFIED OR USED FOR ANY PURPOSE OTHER THAN THE PURPOSE FOR WHICH BGC GENERATED IT. BGC SHALL HAVE NO LIABILITY FOR ANY DAMAGES OR LOSS ARISING IN ANY WAY FROM ANY USE OR MODIFICATION OF THIS DOCUMENT NOT AUTHORIZED BY BGC. ANY USE OF OR RELIANCE UPON THIS DOCUMENT OR ITS CONTENT BY THIRD PARTIES SHALL BE AT SUCH THIRD PARTIES' SOLE RISK.

SCALE:	1:15,000
DATE:	JAN 2023
DRAWN:	CM
REVIEW:	HMS
APPROVED:	LCH

CLIENT: SQUAMISH - LILLOOET REGIONAL DISTRICT

BGC

PROJECT: **QUANTITATIVE LANDSLIDE HAZARD AND RISK ASSESSMENT – REID ROAD AREA**

TITLE: **OVERVIEW MAP**

PROJECT No.:	DWG No:
1358010	01

X:\Projects\1358\010\GIS\Production\20220811_Detailed_Quantitative_Landslide_Risk_Assessment\01_Site_Location.mxd

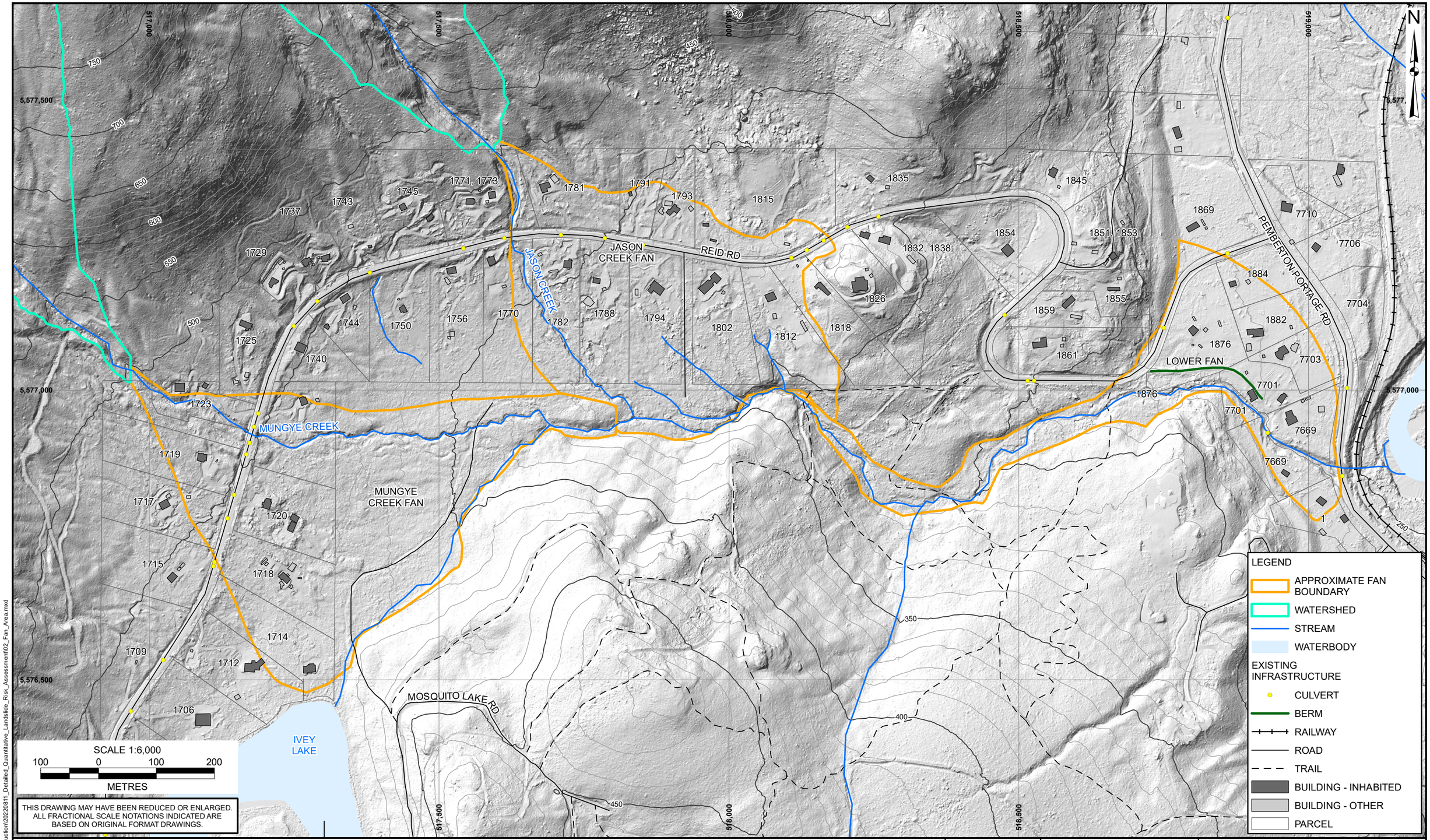

NOTES:
1. ALL DIMENSIONS ARE IN METRES UNLESS OTHERWISE NOTED.
2. THIS DRAWING MUST BE READ IN CONJUNCTION WITH BGC'S REPORT TITLED "QUANTITATIVE LANDSLIDE HAZARD AND RISK ASSESSMENT – REID ROAD AREA", AND DATED JANUARY 2023.
3. BASE TOPOGRAPHIC DATA BASED ON LIDAR PROVIDED BY McELHANNEY AND DATED JULY 22, 2022. CONTOUR INTERVAL IS 10 m.
4. BASE TOPOGRAPHIC MAPPING FROM CANVEC. CULVERTS FROM MOTI.STREAM LINES WERE MODIFIED BY BGC BASED ON LIDAR, AERIAL IMAGERY, AND FIELD OBSERVATIONS.
5. WATERSHED BOUNDARIES, FAN BOUNDARIES, AND BUILDINGS DIGITIZED BY BGC. BGC ASSESSED WHICH BUIDINGS ARE INHABITED BASED ON FIELD OBSERVATIONS WHERE ACCESS TO PROPERTIES WAS PROVIDED BY LANDOWNERS AND INTERPRETATION WHERE ACCESS WAS NOT PROVIDED.
6. COORDINATE SYSTEM IS NAD 1983 UTM ZONE 10N. VERTICAL DATUM IS UNKNOWN.
7. UNLESS BGC AGREES OTHERWISE IN WRITING, THIS DRAWING SHALL NOT BE MODIFIED OR USED FOR ANY PURPOSE OTHER THAN THE PURPOSE FOR WHICH BGC GENERATED IT. BGC SHALL HAVE NO LIABILITY FOR ANY DAMAGES OR LOSS ARISING IN ANY WAY FROM ANY USE OR MODIFICATION OF THIS DOCUMENT NOT AUTHORIZED BY BGC. ANY USE OF OR RELIANCE UPON THIS DOCUMENT OR ITS CONTENT BY THIRD PARTIES SHALL BE AT SUCH THIRD PARTIES' SOLE RISK.

SCALE:	1:6,000
DATE:	JAN 2023
DRAWN:	CM
REVIEW:	HMS
APPROVED:	LCH

CLIENT: SQUAMISH - LILLOOET REGIONAL DISTRICT

BGC

PROJECT: **QUANTITATIVE LANDSLIDE HAZARD AND RISK ASSESSMENT – REID ROAD AREA**

TITLE: **FAN AREA**

PROJECT No.:	DWG No:
1358010	02

X:\Projects\1358\010\GIS\Production\20220811_Detailed_Quantitative_Landslide_Risk_Assessment\02_Fan_Area.mxd

INSET 1

INSET 2

INTERPRETED POTENTIAL SOURCE AREAS FOR ROCK SLIDE-TRIGGERED DEBRIS FLOWS

1990, 2021 DEBRIS-FLOW HEADSCARP

SCALE 1:10,000
50 0 50 100 150
METRES

SCALE 1:7,500
50 0 50 100
METRES

SCALE 1:15,000
200 0 200 400 600
METRES

THIS DRAWING MAY HAVE BEEN REDUCED OR ENLARGED. ALL FRACTIONAL SCALE NOTATIONS INDICATED ARE BASED ON ORIGINAL FORMAT DRAWINGS.

JASON CREEK

MUNGYE CREEK

OWL CREEK

OWL CREEK FSR

BIRKENHEAD RIVER

OWL RIDGE ROAD

REID ROAD

JASON CREEK FAN

MUNGYE CREEK FAN

LOWER FAN

5,578,000

5,577,000

5,580,000

5,579,000

516,000

517,000

518,000

519,000

520,000

LEGEND

- STREAM
- APPROXIMATE FAN BOUNDARY
- WATERSHED

EXISTING INFRASTRUCTURE

- CULVERT
- GRAVEL ACCESS/LOGGING ROAD
- ROAD
- RAILWAY
- BUILDING
- PARCEL

GEOMORPHOLOGY

- ACTIVE HEADSCARP
- ANTI-SLOPE SCARP
- INACTIVE HEADSCARP
- LINEAMENT
- PALEOCHANNEL
- SLOPE CREST
- WATERSHED BREAK

GRABEN

- ACTIVE
- INACTIVE
- LANDSLIDE DEPOSIT
- ROCKFALL DEPOSIT

NOTES:
1. ALL DIMENSIONS ARE IN METRES UNLESS OTHERWISE NOTED.
2. THIS DRAWING MUST BE READ IN CONJUNCTION WITH BGC'S REPORT TITLED "QUANTITATIVE LANDSLIDE HAZARD AND RISK ASSESSMENT – REID ROAD AREA", AND DATED JANUARY 2023.
3. BASE TOPOGRAPHIC DATA BASED ON LIDAR PROVIDED BY McELHANNEY AND DATED JULY 22, 2022. CONTOUR INTERVAL IS 20 m.
4. BASE TOPOGRAPHIC MAPPING FROM CANVEC. STREAM LINES WERE MODIFIED BY BGC BASED ON LIDAR, AERIAL IMAGERY, AND FIELD OBSERVATIONS.
5. WATERSHED BOUNDARIES, FAN BOUNDARIES, AND BUILDINGS DIGITIZED BY BGC.
6. GEOMORPHOLOGICAL MAPPING COMPLETED BY BGC BASED ON LIDAR DATED JULY 2022 AT 1:2500 SCALE, FIELD OBSERVATIONS, AND SUPPLEMENTED WITH AERIAL IMAGERY. MAPPING COMPLETED WITHIN STUDY WATERSHEDS AND IMMEDIATELY ADJACENT AREAS ONLY.
7. CULVERT DATA PROVIDED BY MOTI. RAILWAY, ROADS, AND TRAILS ARE FROM CANVEC.
8. COORDINATE SYSTEM IS NAD 1983 UTM ZONE 10N. VERTICAL DATUM IS UNKNOWN.
9. UNLESS BGC AGREES OTHERWISE IN WRITING, THIS DRAWING SHALL NOT BE MODIFIED OR USED FOR ANY PURPOSE OTHER THAN THE PURPOSE FOR WHICH BGC GENERATED IT. BGC SHALL HAVE NO LIABILITY FOR ANY DAMAGES OR LOSS ARISING IN ANY WAY FROM ANY USE OR MODIFICATION OF THIS DOCUMENT NOT AUTHORIZED BY BGC. ANY USE OF OR RELIANCE UPON THIS DOCUMENT OR ITS CONTENT BY THIRD PARTIES SHALL BE AT SUCH THIRD PARTIES' SOLE RISK.

SCALE:	1:15,000
DATE:	JAN 2023
DRAWN:	CM
REVIEW:	HMS
APPROVED:	LCH

CLIENT: SQUAMISH - LILLOOET REGIONAL DISTRICT

BGC

PROJECT: QUANTITATIVE LANDSLIDE HAZARD AND RISK ASSESSMENT – REID ROAD AREA

TITLE: GEOMORPHOLOGIC MAP

PROJECT No.:	DWG No:
1358010	03

X:\Projects\1358\010\GIS\Production\20220811_Detailed_Quantitative_Landslide_Risk_Assessment\03_Geomorphological_Mapping.mxd

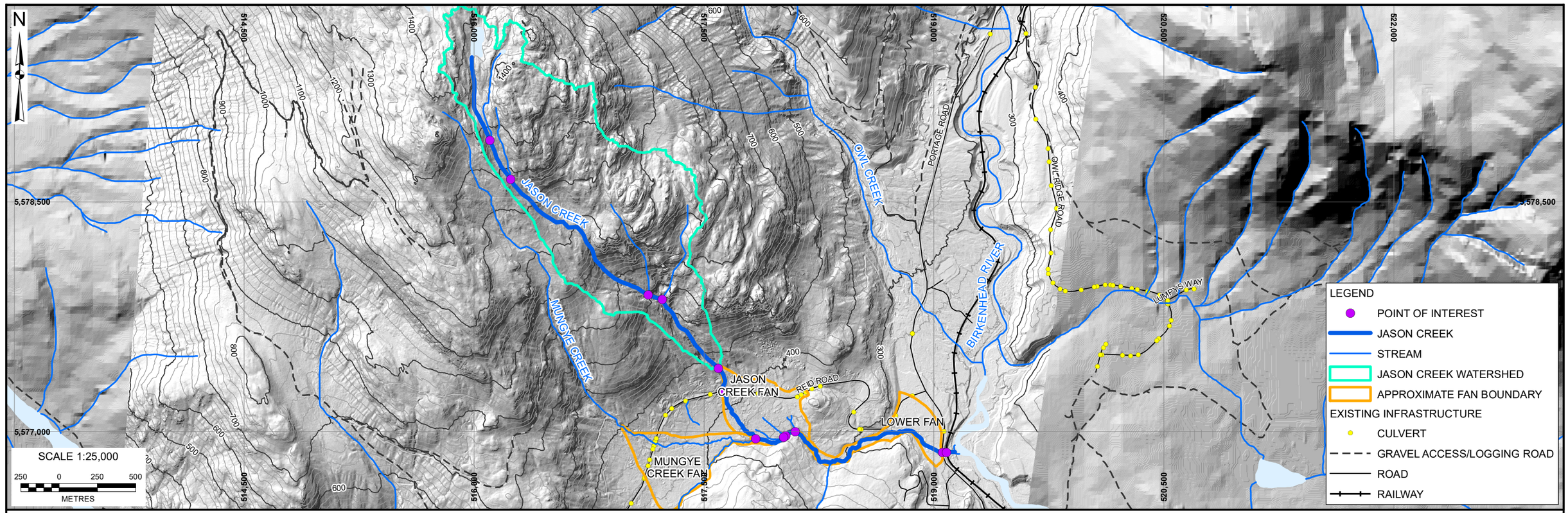

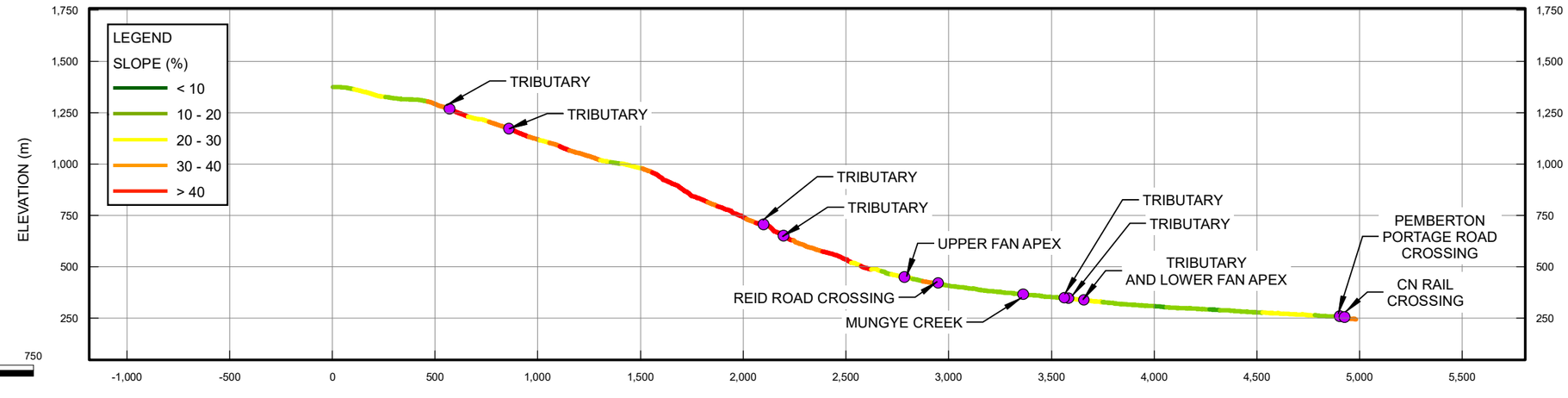

SCALE 1:25,000
250 0 250 500 750
METRES

THIS DRAWING MAY HAVE BEEN REDUCED OR ENLARGED. ALL FRACTIONAL SCALE NOTATIONS INDICATED ARE BASED ON ORIGINAL FORMAT DRAWINGS.

NOTES:
1. ALL DIMENSIONS ARE IN METRES UNLESS OTHERWISE NOTED.
2. THIS DRAWING MUST BE READ IN CONJUNCTION WITH BGC'S REPORT TITLED "QUANTITATIVE LANDSLIDE HAZARD AND RISK ASSESSMENT – REID ROAD AREA", AND DATED JANUARY 2023.
3. BASE TOPOGRAPHIC DATA BASED ON LIDAR PROVIDED BY McELHANNEY AND DATED JULY 22, 2022. CONTOUR INTERVAL IS 20 m.
4. BASE TOPOGRAPHIC MAPPING FROM CANVEC. STREAM LINES WERE MODIFIED BY BGC BASED ON LIDAR, AERIAL IMAGERY, AND FIELD OBSERVATIONS.
5. WATERSHED BOUNDARIES AND FAN BOUNDARIES DIGITIZED BY BGC.
6. CULVERT DATA PROVIDED BY MOTI. RAILWAY, ROADS, AND TRAILS ARE FROM CANVEC.
7. COORDINATE SYSTEM IS NAD 1983 UTM ZONE 10N. VERTICAL DATUM IS UNKNOWN.
8. UNLESS BGC AGREES OTHERWISE IN WRITING, THIS DRAWING SHALL NOT BE MODIFIED OR USED FOR ANY PURPOSE OTHER THAN THE PURPOSE FOR WHICH BGC GENERATED IT. BGC SHALL HAVE NO LIABILITY FOR ANY DAMAGES OR LOSS ARISING IN ANY WAY FROM ANY USE OR MODIFICATION OF THIS DOCUMENT NOT AUTHORIZED BY BGC. ANY USE OF OR RELIANCE UPON THIS DOCUMENT OR ITS CONTENT BY THIRD PARTIES SHALL BE AT SUCH THIRD PARTIES' SOLE RISK.

SCALE:	1:25,000
DATE:	JAN 2023
DRAWN:	CM
REVIEW:	HMS
APPROVED:	LCH

CLIENT: SQUAMISH - LILLOOET REGIONAL DISTRICT

BGC

PROJECT: **QUANTITATIVE LANDSLIDE HAZARD AND RISK ASSESSMENT – REID ROAD AREA**

TITLE: **CHANNEL PROFILE - JASON CREEK**

PROJECT No.:	DWG No:
1358010	04

X:\Projects\1358\010\GIS\Production\20220811_Detailed_Quantitative_Landslide_Risk_Assessment\04_Jason_Creek_Profile.mxd

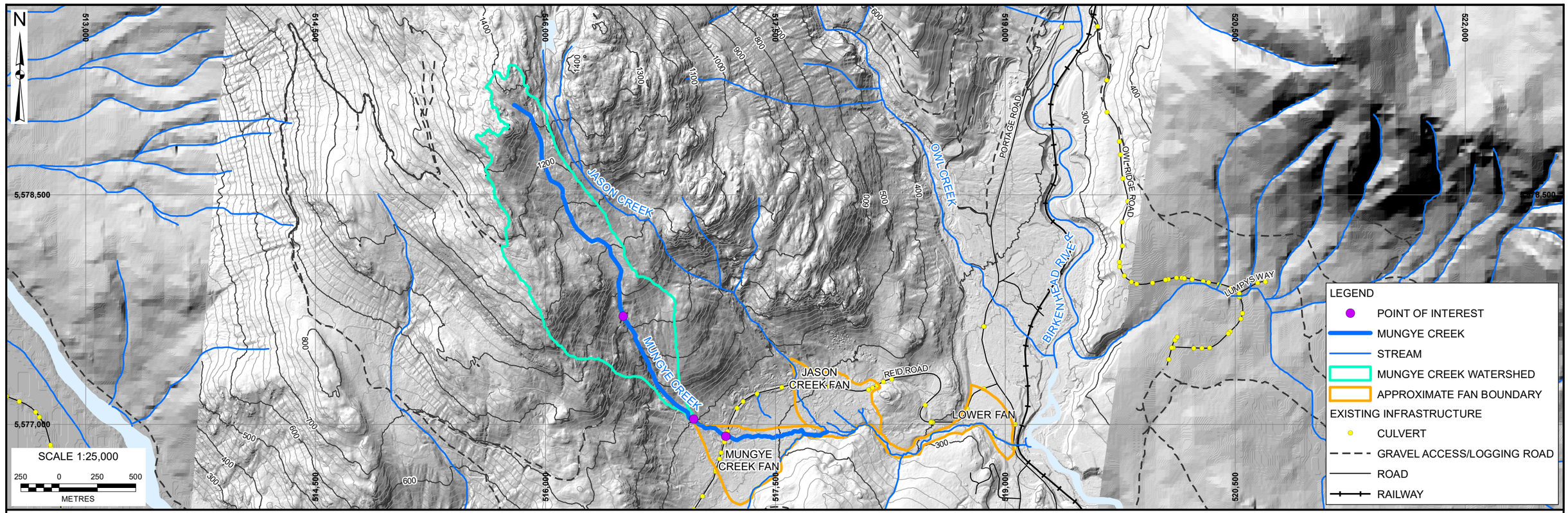

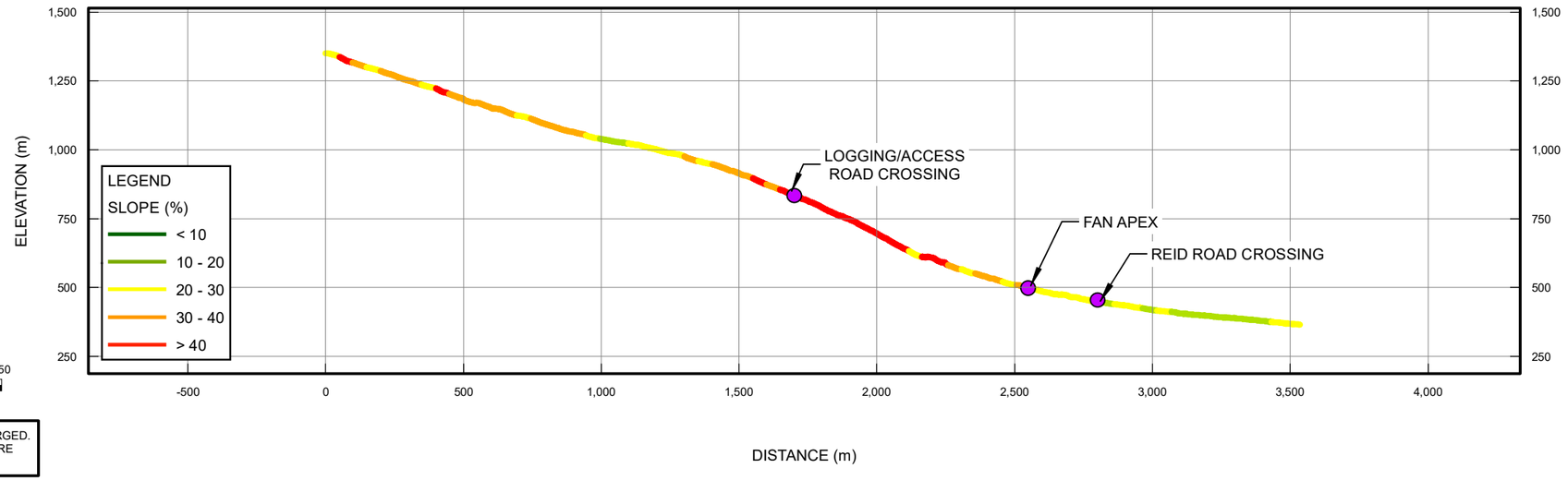

SCALE 1:20,000

250 0 250 500 750

METRES

THIS DRAWING MAY HAVE BEEN REDUCED OR ENLARGED. ALL FRACTIONAL SCALE NOTATIONS INDICATED ARE BASED ON ORIGINAL FORMAT DRAWINGS.

NOTES:

1. ALL DIMENSIONS ARE IN METRES UNLESS OTHERWISE NOTED.
2. THIS DRAWING MUST BE READ IN CONJUNCTION WITH BGC'S REPORT TITLED "QUANTITATIVE LANDSLIDE HAZARD AND RISK ASSESSMENT – REID ROAD AREA", AND DATED JANUARY 2023.
3. BASE TOPOGRAPHIC DATA BASED ON LIDAR PROVIDED BY McELHANNEY AND DATED JULY 22, 2022. CONTOUR INTERVAL IS 20 m.
4. BASE TOPOGRAPHIC MAPPING FROM CANVEC. STREAM LINES WERE MODIFIED BY BGC BASED ON LIDAR, AERIAL IMAGERY, AND FIELD OBSERVATIONS.
5. WATERSHED BOUNDARIES AND FAN BOUNDARIES DIGITIZED BY BGC.
6. CULVERT DATA PROVIDED BY MOTI. RAILWAY, ROADS, AND TRAILS ARE FROM CANVEC.
7. COORDINATE SYSTEM IS NAD 1983 UTM ZONE 10N. VERTICAL DATUM IS UNKNOWN.
8. UNLESS BGC AGREES OTHERWISE IN WRITING, THIS DRAWING SHALL NOT BE MODIFIED OR USED FOR ANY PURPOSE OTHER THAN THE PURPOSE FOR WHICH BGC GENERATED IT. BGC SHALL HAVE NO LIABILITY FOR ANY DAMAGES OR LOSS ARISING IN ANY WAY FROM ANY USE OR MODIFICATION OF THIS DOCUMENT NOT AUTHORIZED BY BGC. ANY USE OF OR RELIANCE UPON THIS DOCUMENT OR ITS CONTENT BY THIRD PARTIES SHALL BE AT SUCH THIRD PARTIES' SOLE RISK.

SCALE:	1:25,000
DATE:	JAN 2023
DRAWN:	CM
REVIEW:	HMS
APPROVED:	LCH

CLIENT: SQUAMISH - LILLOOET REGIONAL DISTRICT

BGC

PROJECT: **QUANTITATIVE LANDSLIDE HAZARD AND RISK ASSESSMENT – REID ROAD AREA**

TITLE: **CHANNEL PROFILE - MUNGYE CREEK**

PROJECT No.:	DWG No:
1358010	05

X:\Projects\1358\010\GIS\Production\20220811_Detailed_Quantitative_Landslide_Risk_Assessment\05_Mungye_Creek_Profile.mxd

N

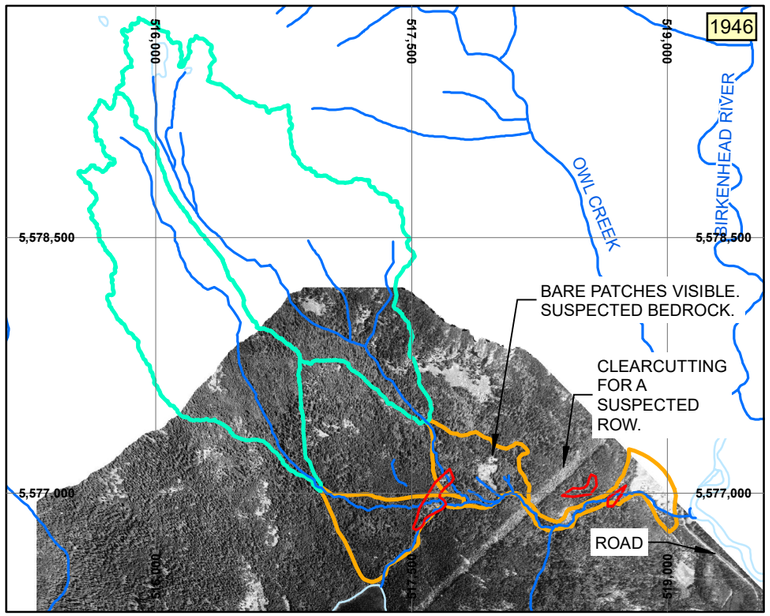

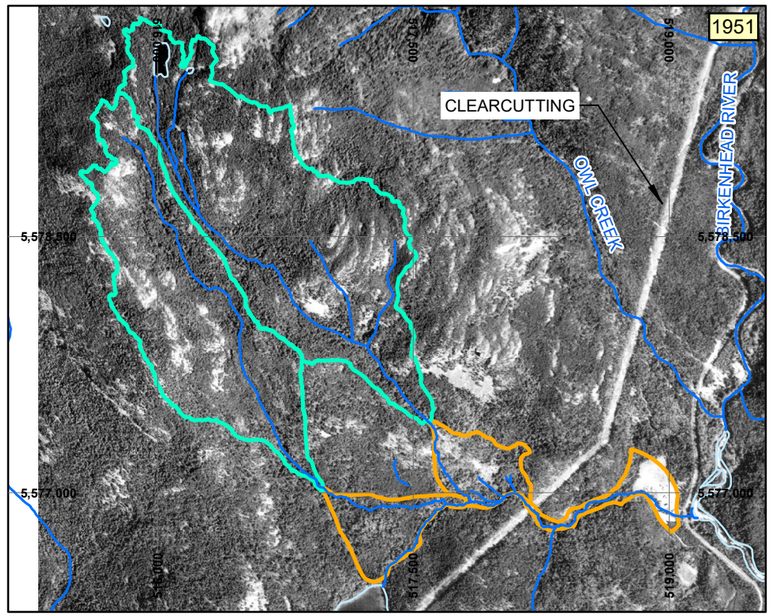

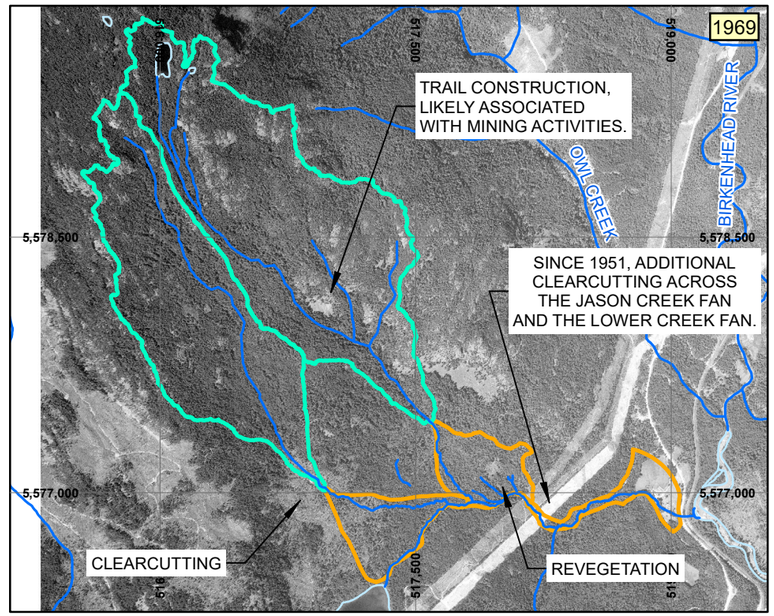

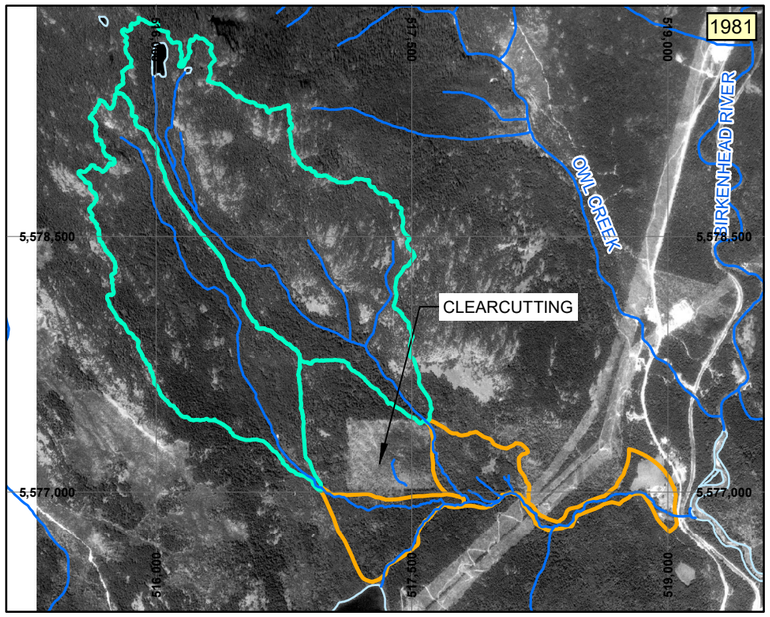

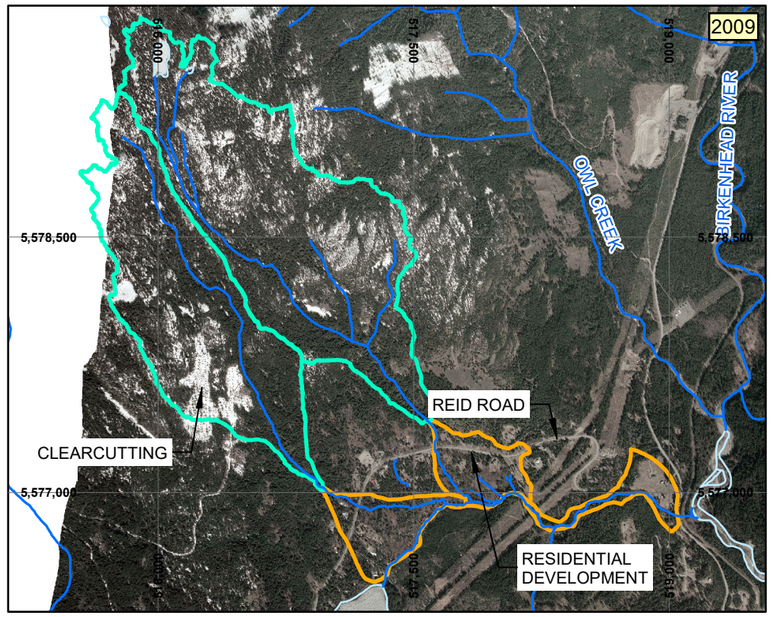

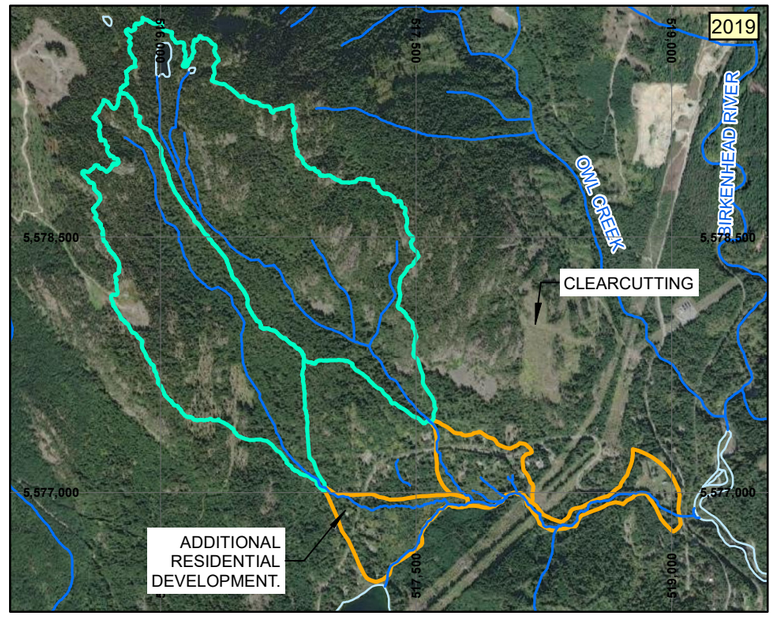

SCALE 1:35,000

500 0 500 1,000

METRES

THIS DRAWING MAY HAVE BEEN REDUCED OR ENLARGED. ALL FRACTIONAL SCALE NOTATIONS INDICATED ARE BASED ON ORIGINAL FORMAT DRAWINGS.

LEGEND

- STREAM
- WATERBODY
- WATERSHED
- APPROXIMATE FAN BOUNDARY
- DEBRIS DEPOSITION SUSPECTED

NOTES:

1. ALL DIMENSIONS ARE IN METRES UNLESS OTHERWISE NOTED.
2. THIS DRAWING MUST BE READ IN CONJUNCTION WITH BGC'S REPORT TITLED "QUANTITATIVE LANDSLIDE HAZARD AND RISK ASSESSMENT – REID ROAD AREA", AND DATED JANUARY 2023.
3. AIRPHOTOS FROM GEOBC, NATIONAL AIRPHOTO LIBRARY, AND ESRI WORLD IMAGERY (2019)
4. WATERSHED BOUNDARIES AND FAN BOUNDARIES DIGITIZED BY BGC.
5. STREAM LINES WERE MODIFIED BY BGC BASED ON LiDAR, AERIAL IMAGERY, AND FIELD OBSERVATIONS.
6. COORDINATE SYSTEM IS NAD 1983 UTM ZONE 11N. VERTICAL DATUM IS UNKNOWN.
7. UNLESS BGC AGREES OTHERWISE IN WRITING, THIS DRAWING SHALL NOT BE MODIFIED OR USED FOR ANY PURPOSE OTHER THAN THE PURPOSE FOR WHICH BGC GENERATED IT. BGC SHALL HAVE NO LIABILITY FOR ANY DAMAGES OR LOSS ARISING IN ANY WAY FROM ANY USE OR MODIFICATION OF THIS DOCUMENT NOT AUTHORIZED BY BGC. ANY USE OF OR RELIANCE UPON THIS DOCUMENT OR ITS CONTENT BY THIRD PARTIES SHALL BE AT SUCH THIRD PARTIES' SOLE RISK.

SCALE:	1:35,000
DATE:	JAN 2023
DRAWN:	CM
REVIEW:	HMS
APPROVED:	LCH

CLIENT: SQUAMISH - LILLOOET REGIONAL DISTRICT

BGC

PROJECT: **QUANTITATIVE LANDSLIDE HAZARD AND RISK ASSESSMENT – REID ROAD AREA**

TITLE: **AIR PHOTO COMPARISON**

PROJECT No.:	DWG No:
1358010	06

X:\Projects\1358\010\GIS\Production\20220811_Detailed_Quantitative_Landslide_Risk_Assessment\06_AirPhotoComparison.mxd

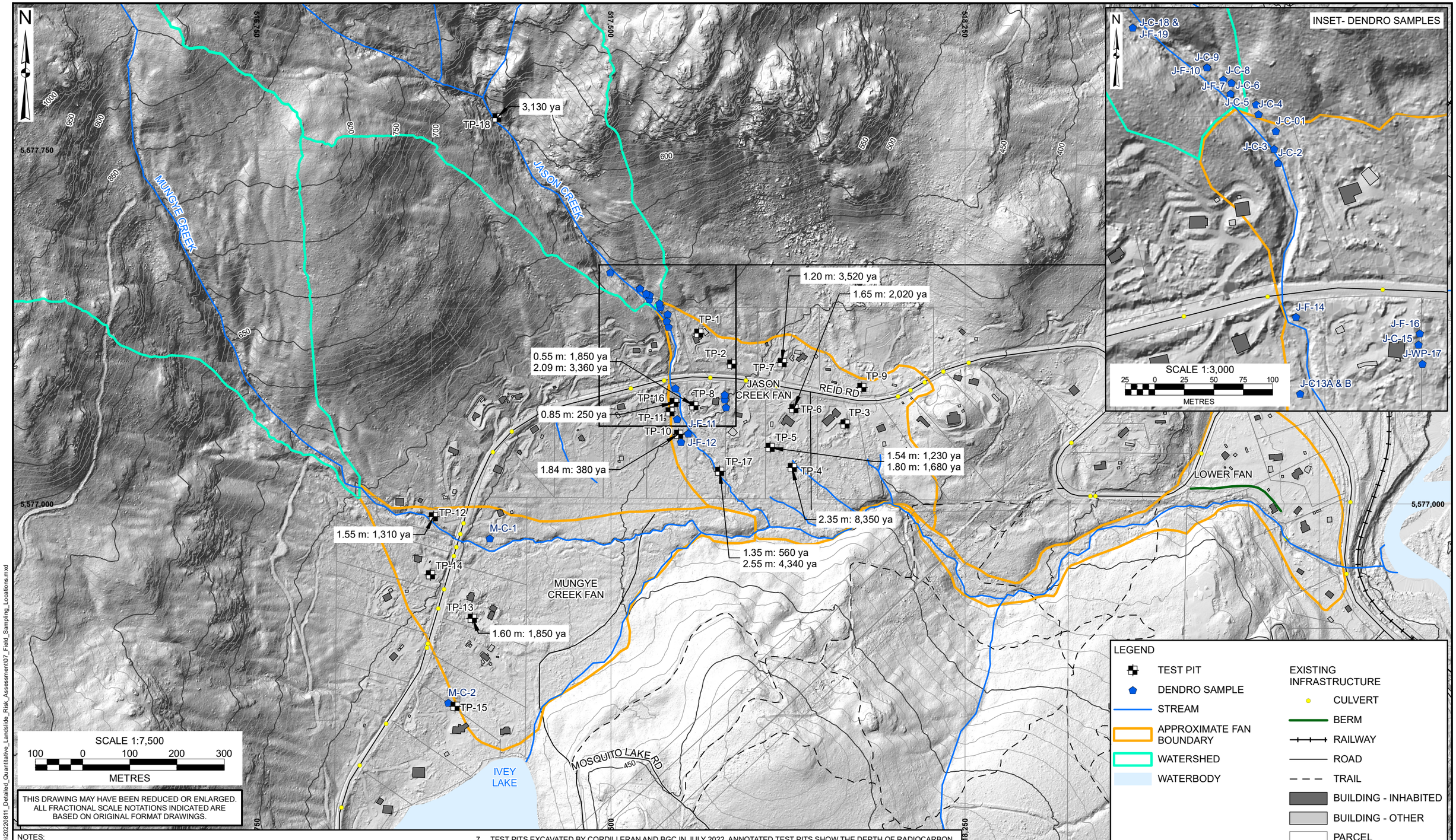

THIS DRAWING MAY HAVE BEEN REDUCED OR ENLARGED. ALL FRACTIONAL SCALE NOTATIONS INDICATED ARE BASED ON ORIGINAL FORMAT DRAWINGS.

NOTES:
1. ALL DIMENSIONS ARE IN METRES UNLESS OTHERWISE NOTED.
2. THIS DRAWING MUST BE READ IN CONJUNCTION WITH BGC'S REPORT TITLED "QUANTITATIVE LANDSLIDE HAZARD AND RISK ASSESSMENT – REID ROAD AREA", AND DATED JANUARY 2023.
3. BASE TOPOGRAPHIC DATA BASED ON LIDAR PROVIDED BY McELHANNEY AND DATED JULY 22, 2022. CONTOUR INTERVAL IS 10 m.
4. BASE TOPOGRAPHIC MAPPING FROM CANVEC. STREAM LINES WERE MODIFIED BY BGC BASED ON LIDAR, AERIAL IMAGERY, AND FIELD OBSERVATIONS. CULVERT DATA PROVIDED BY MOTI. RAILWAY, ROADS, AND TRAILS ARE FROM CANVEC.
5. WATERSHED BOUNDARIES, FAN BOUNDARIES, AND BUILDINGS DIGITIZED BY BGC.
6. DENDRO SAMPLES COLLECTED BY BGC AND CORDILLERAN IN JULY AND SEPTEMBER 2022. THE NAMING CONVENTION SHOWN AND RESULTS ARE PRESENTED IN BGC'S REPORT.
7. TEST PITS EXCAVATED BY CORDILLERAN AND BGC IN JULY 2022. ANNOTATED TEST PITS SHOW THE DEPTH OF RADIOCARBON DATING SAMPLES COLLECTED BY BGC AND ANALYZED BY BETA ANALYTICS. RADIOCARBON AGES ARE PRESENTED IN YEARS AGO "YA" FROM 2022. THE AGES ARE SUBJECT TO ERROR AND DO NOT DATE DEBRIS FLOWS. IN CASES OF UNDERLYING PALEOSOLS THE DATES INDICATE THE MAXIMUM AGE OF THE OVERLYING UNIT. SEE REPORT FOR FURTHER DETAILS.
8. COORDINATE SYSTEM IS NAD 1983 UTM ZONE 10N. VERTICAL DATUM IS UNKNOWN.
9. UNLESS BGC AGREES OTHERWISE IN WRITING, THIS DRAWING SHALL NOT BE MODIFIED OR USED FOR ANY PURPOSE OTHER THAN THE PURPOSE FOR WHICH BGC GENERATED IT. BGC SHALL HAVE NO LIABILITY FOR ANY DAMAGES OR LOSS ARISING IN ANY WAY FROM ANY USE OR MODIFICATION OF THIS DOCUMENT NOT AUTHORIZED BY BGC. ANY USE OF OR RELIANCE UPON THIS DOCUMENT OR ITS CONTENT BY THIRD PARTIES SHALL BE AT SUCH THIRD PARTIES' SOLE RISK.

SCALE:	1:7,500
DATE:	JAN 2023
DRAWN:	CM
REVIEW:	HMS
APPROVED:	LCH

CLIENT: SQUAMISH - LILLOOET REGIONAL DISTRICT

BGC

PROJECT: **QUANTITATIVE LANDSLIDE HAZARD AND RISK ASSESSMENT – REID ROAD AREA**

TITLE: **FIELD SAMPLING LOCATIONS**

PROJECT No.:	DWG No:
1358010	07

X:\Projects\1358\010\GIS\Production\20220811_Detailed_Quantitative_Landslide_Risk_Assessment\07_Field_Sampling_Locations.mxd

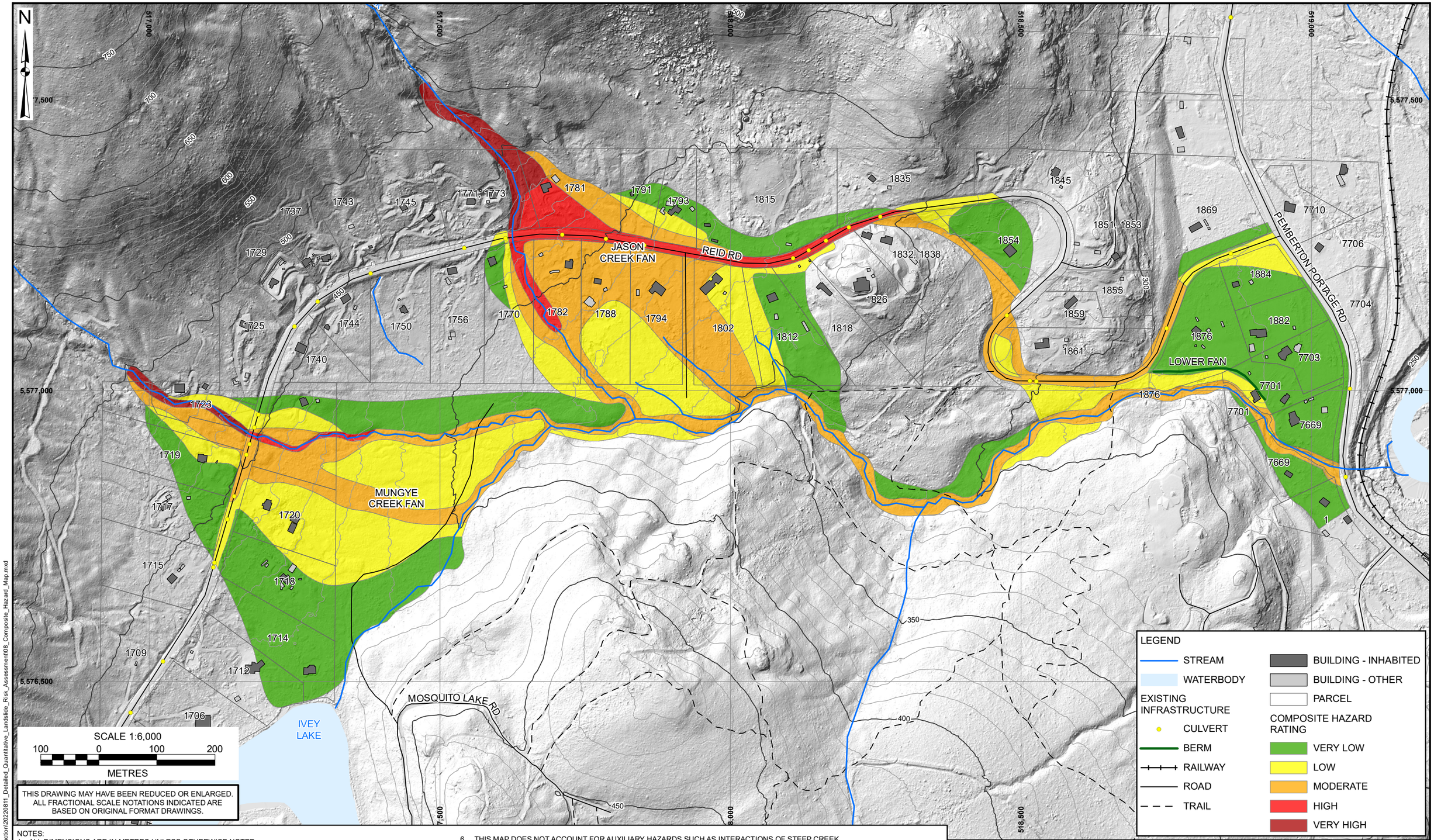

SCALE 1:6,000

100 0 100 200

METRES

THIS DRAWING MAY HAVE BEEN REDUCED OR ENLARGED. ALL FRACTIONAL SCALE NOTATIONS INDICATED ARE BASED ON ORIGINAL FORMAT DRAWINGS.

LEGEND

- STREAM
- WATERBODY

EXISTING INFRASTRUCTURE

- CULVERT
- BERM
- RAILWAY
- ROAD
- TRAIL
- BUILDING - INHABITED
- BUILDING - OTHER
- PARCEL

COMPOSITE HAZARD RATING

- VERY LOW
- LOW
- MODERATE
- HIGH
- VERY HIGH

NOTES:

1. ALL DIMENSIONS ARE IN METRES UNLESS OTHERWISE NOTED.
2. THIS DRAWING MUST BE READ IN CONJUNCTION WITH BGC'S REPORT TITLED "QUANTITATIVE LANDSLIDE HAZARD AND RISK ASSESSMENT – REID ROAD AREA", AND DATED JANUARY 2023.
3. BASE TOPOGRAPHIC DATA BASED ON LIDAR PROVIDED BY McELHANNEY AND DATED JULY 22, 2022. CONTOUR INTERVAL IS 10 m.
4. BASE TOPOGRAPHIC MAPPING FROM CANVEC. STREAM LINES WERE MODIFIED BY BGC BASED ON LIDAR, AERIAL IMAGERY, AND FIELD OBSERVATIONS. CULVERT DATA PROVIDED BY MOTI. RAILWAY, ROADS, AND TRAILS ARE FROM CANVEC. BUILDINGS DIGITIZED BY BGC.
5. COMPOSITE HAZARD RATINGS PORTRAYED ON THIS DRAWING ONLY REPRESENT HAZARDS ORIGINATING IN THE JASON AND MUNGYE CREEK WATERSHEDS.
6. THIS MAP DOES NOT ACCOUNT FOR AUXILIARY HAZARDS SUCH AS INTERACTIONS OF STEEP CREEK HAZARDS WITH HAZARDS ORIGINATING OUTSIDE THE STUDY WATERSHED (e.g., LANDSLIDES AND ROCKFALL). IT ALSO DOES NOT ACCOUNT FOR ANY HUMAN INTERFERENCE DURING THE RUNOFF EVENTS.
7. THIS MAP REPRESENTS A 'SNAPSHOT IN TIME'. FUTURE MODIFICATION OF THE LANDSCAPE WILL INFLUENCE FLOW BEHAVIOUR AND MAY WARRANT RE-MODELLING AND MAPPING OF HAZARD RATINGS.
8. COORDINATE SYSTEM IS NAD 1983 UTM ZONE 10N. VERTICAL DATUM IS UNKNOWN.
9. UNLESS BGC AGREES OTHERWISE IN WRITING, THIS DRAWING SHALL NOT BE MODIFIED OR USED FOR ANY PURPOSE OTHER THAN THE PURPOSE FOR WHICH BGC GENERATED IT. BGC SHALL HAVE NO LIABILITY FOR ANY DAMAGES OR LOSS ARISING IN ANY WAY FROM ANY USE OR MODIFICATION OF THIS DOCUMENT NOT AUTHORIZED BY BGC. ANY USE OF OR RELIANCE UPON THIS DOCUMENT OR ITS CONTENT BY THIRD PARTIES SHALL BE AT SUCH THIRD PARTIES' SOLE RISK.

SCALE:	1:6,000
DATE:	JAN 2023
DRAWN:	CM
REVIEW:	SZ
APPROVED:	LCH

CLIENT: SQUAMISH - LILLOOET REGIONAL DISTRICT

BGC

PROJECT: **QUANTITATIVE LANDSLIDE HAZARD AND RISK ASSESSMENT – REID ROAD AREA**

TITLE: **COMPOSITE HAZARD MAP**

PROJECT No.:	DWG No:
1358010	08

X:\Projects\1358\010\GIS\Production\20220811_Detailed_Quantitative_Landslide_Risk_Assessment\08_Composite_Hazard_Map.mxd

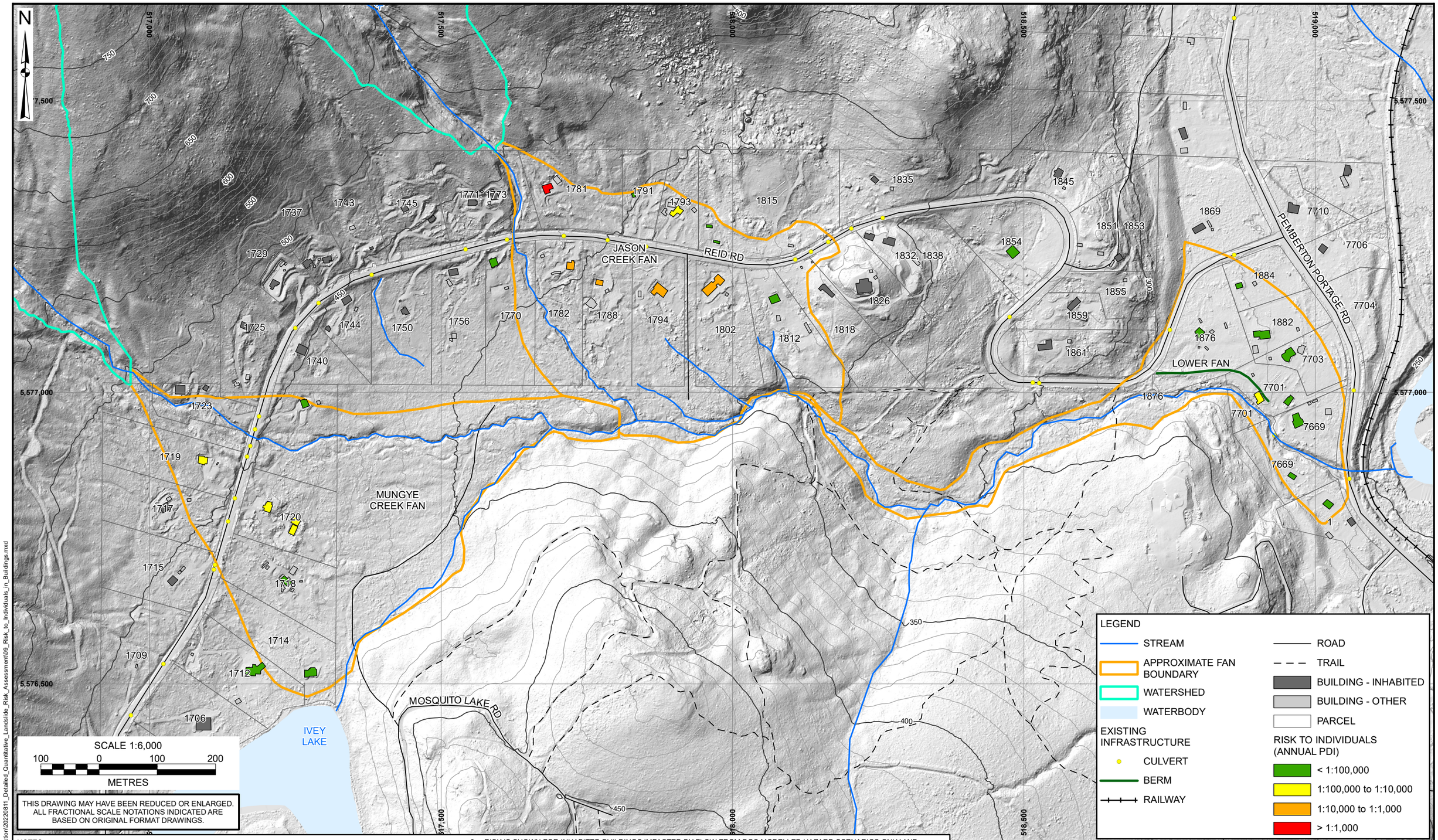

SCALE 1:6,000

100 0 100 200

METRES

THIS DRAWING MAY HAVE BEEN REDUCED OR ENLARGED. ALL FRACTIONAL SCALE NOTATIONS INDICATED ARE BASED ON ORIGINAL FORMAT DRAWINGS.

LEGEND

- STREAM
- APPROXIMATE FAN BOUNDARY
- WATERSHED
- WATERBODY

EXISTING INFRASTRUCTURE

- CULVERT
- BERM
- RAILWAY
- ROAD
- TRAIL
- BUILDING - INHABITED
- BUILDING - OTHER
- PARCEL

RISK TO INDIVIDUALS (ANNUAL PDI)

- < 1:100,000
- 1:100,000 to 1:10,000
- 1:10,000 to 1:1,000
- > 1:1,000

NOTES:

1. ALL DIMENSIONS ARE IN METRES UNLESS OTHERWISE NOTED.
2. THIS DRAWING MUST BE READ IN CONJUNCTION WITH BGC'S REPORT TITLED "QUANTITATIVE LANDSLIDE HAZARD AND RISK ASSESSMENT – REID ROAD AREA", AND DATED JANUARY 2023.
3. BASE TOPOGRAPHIC DATA BASED ON LIDAR PROVIDED BY McELHANNEY AND DATED JULY 22, 2022. CONTOUR INTERVAL IS 10 m.
4. BASE TOPOGRAPHIC MAPPING FROM CANVEC. STREAM LINES WERE MODIFIED BY BGC BASED ON LIDAR, AERIAL IMAGERY, AND FIELD OBSERVATIONS. CULVERT DATA PROVIDED BY MOTI. RAILWAY, ROADS, AND TRAILS ARE FROM CANVEC.
5. WATERSHED BOUNDARIES, FAN BOUNDARIES, AND BUILDINGS DIGITIZED BY BGC.
6. RISK IS SHOWN FOR INHABITED BUILDINGS IMPACTED BY FLOW FROM BGC MODELLED HAZARD SCENARIOS ONLY AND INFORMED BY PROFESSIONAL JUDGEMENT. IT DOES NOT INCLUDE RISK TO INDIVIDUALS OUTSIDE BUILDINGS OR FROM HAZARDS OUTSIDE THE JASON AND MUNGYE CREEK WATERSHEDS. SEE REPORT FOR DETAILS.
7. THIS MAP REPRESENTS A 'SNAPSHOT IN TIME'. THE OCCURENCE OF GEOHAZARD EVENTS OR MODIFICATION OF THE LANDSCAPE MAY WARRANT RE-ASSESSMENT OF RISK IN AFFECTED AREAS.
8. COORDINATE SYSTEM IS NAD 1983 UTM ZONE 10N. VERTICAL DATUM IS UNKNOWN.
9. UNLESS BGC AGREES OTHERWISE IN WRITING, THIS DRAWING SHALL NOT BE MODIFIED OR USED FOR ANY PURPOSE OTHER THAN THE PURPOSE FOR WHICH BGC GENERATED IT. BGC SHALL HAVE NO LIABILITY FOR ANY DAMAGES OR LOSS ARISING IN ANY WAY FROM ANY USE OR MODIFICATION OF THIS DOCUMENT NOT AUTHORIZED BY BGC. ANY USE OF OR RELIANCE UPON THIS DOCUMENT OR ITS CONTENT BY THIRD PARTIES SHALL BE AT SUCH THIRD PARTIES' SOLE RISK.

SCALE:	1:6,000
DATE:	JAN 2023
DRAWN:	CM
REVIEW:	SZ
APPROVED:	LCH

CLIENT: SQUAMISH - LILLOOET REGIONAL DISTRICT

BGC

PROJECT: **QUANTITATIVE LANDSLIDE HAZARD AND RISK ASSESSMENT – REID ROAD AREA**

TITLE: **RISK TO INDIVIDUALS IN BUILDINGS**

PROJECT No.:	DWG No:
1358010	09

X:\Projects\1358\010\GIS\Production\20220811_Detailed_Quantitative_Landslide_Risk_Assessment\09_Risk_to_Individuals_in_Buildings.mxd